



Medical University of Białystok
Faculty of Pharmacy with the Division of Laboratory Medicine

Aleksandra Maria Juszcak

Phytochemical analysis and biological activities
of *Jasione montana* L. (Campanulaceae)

Doctoral dissertation based on a series of scientific publications
in the field of medical sciences and health sciences
in the discipline of pharmaceutical sciences

Białystok, 2022

Supervisors

Dr. Michał Tomczyk
Department of Pharmacognosy
Faculty of Pharmacy with the Division of Laboratory Medicine
Medical University of Białystok, Poland

Prof. Dr. Sc. Marijana Zovko Končić
Department of Pharmacognosy
Faculty of Pharmacy and Biochemistry
University of Zagreb, Croatia

I would like to express grateful words of thanks to the Supervisors, Dr. Michał Tomczyk and Prof. Marijana Zovko Končić, as well as all the staff and PhD students of the Department of Pharmacognosy of the Medical University of Białystok for their generous kindness and help on the way to obtaining the degree

Table of contents

Chapter 1.	List of publications comprising the doctoral dissertation.....	5
Chapter 2.	Introduction. A review of the literature on the subject of dissertation.....	6
Chapter 3.	The objective of the work including the rationale for undertaken research with reference to publications comprising the doctoral dissertation.....	8
Chapter 4.	The achievement of scientific objectives, concise summary of research materials and methods, research results, summary and discussion with reference to publications comprising the doctoral dissertation and identification of prospects for further research in the subject.....	9
4.1.	Plant material.....	9
4.2.	Preparation of extracts and fractions.....	9
4.3.	Realization of scientific aims.....	9
4.3.1.	Analysis of the phytochemical profiles of <i>J. montana</i> extracts and fractions by means of LC–ESI–MS.....	9
4.3.2.	Isolation and identification of main flavonoids 9, 12 and 22.....	10
4.3.3.	Quantitative analysis of <i>J. montana</i> extracts and fractions by means of HPLC–PDA.....	10
4.3.4.	<i>In vitro</i> evaluation of the anticancer activity of <i>J. montana</i> extracts/fractions and their main compounds against human amelanotic melanoma C32 cell line.....	12
4.3.5.	Estimation of the effects of <i>J. montana</i> extracts/fractions and their major secondary metabolites on wound healing processes.....	17
4.3.6.	Statistical analysis.....	24
4.4.	Summary and discussion.....	24
4.5.	Abbreviations.....	27
Chapter 5.	Conclusion.....	29
Chapter 6.	References.....	30
Chapter 7.	Summary.....	32
Chapter 8.	Streszczenie w języku polski.....	33
Chapter 9.	Copies of publications comprising the doctoral dissertation.....	34
Publication I:	<i>In vitro</i> anticancer potential of <i>Jasione montana</i> and its main components against human amelanotic melanoma cells.....	34
Publication II:	Wound healing properties of <i>Jasione montana</i> extracts and their main secondary metabolites.....	74
Publication III:	Recent trends in the application of chromatographic techniques in the analysis of luteolin and its derivatives.....	91
Publication IV:	Skin cancer, including related pathways and therapy and the role of luteolin derivatives as potential therapeutics.....	130
Chapter 10.	Declarations of the author of the doctoral dissertation.....	171
Chapter 11.	Declarations of the co-authors of the doctoral dissertation.....	175
Chapter 12.	List of scientific accomplishments.....	191

Chapter 1. List of publications comprising the doctoral dissertation

Publication I

Juszczak A.M., Czarnomysy R., Strawa J.W., Zovko Končić M., Bielawski K., Tomczyk M.: *In vitro* anticancer potential of *Jasione montana* and its main components against human amelanotic melanoma cells. *International Journal of Molecular Sciences* Vol. 22, ID 3345, 2021, 25 pages.

DOI: 10.3390/ijms22073345

IF₂₀₂₀ = 5.923, MES score = 140; citation: Web of Science/SCOPUS = 3/3

Publication II

Juszczak A.M., Jakimiuk K., Czarnomysy R., Strawa J.W., Zovko Končić M., Bielawski K., Tomczyk M.: Wound healing properties of *Jasione montana* extracts and their main secondary metabolites. *Frontiers in Pharmacology* Vol. 13, ID 894233, 2022, 13 pages.

DOI: 10.3389/fphar.2022.894233

IF₂₀₂₀ = 5.810, MES score = 100; citation: Web of Science/SCOPUS = 0/0

Publication III

Juszczak A.M., Zovko Končić M., Tomczyk M.: Recent trends in the application of chromatographic techniques in the analysis of luteolin and its derivatives. *Biomolecules* Vol. 9, ID 731, 2019, 38 pages.

DOI: 10.3390/biom9110731

IF₂₀₁₉ = 4.879, MES score = 100; citation: Web of Science/SCOPUS = 18/21

Publication IV

Juszczak A.M., Wöelfle U., Zovko Končić M., Tomczyk M.: Skin cancer, including related pathways and therapy and the role of luteolin derivatives as potential therapeutics. *Medicinal Research Reviews* 2022, 40 pages.

DOI: 10.1002/med.21880

IF₂₀₂₀ = 12.944, MES score = 140; citation: Web of Science/SCOPUS = 0/0

Summarised scientometric data of publications **I–IV** included in a single-topic series:

Summary Impact Factor (IF)

= **29.556**

Summary number of MES scores

= **480 points**

Chapter 2. Introduction. A review of the literature on the subject of dissertation

Jasione montana L. (Sheep's bit scabious) (Figure 1) is usually a biennial, rarely annual, overwintering plant belonging to the Campanulaceae family. It is one of the 20 representatives of the genus *Jasione*. The valid taxonomic name of this species was first described by Carl von Linné [1]. It is a small perennial, usually 15–65 cm tall. It has a slender, shining white or yellowish-white tap root with numerous fibrous lateral branches. The aerial parts of the plant included green, erect or decumbent stalks. The alternate foliage morphology shows great variability according to the location. The lower parts have abundant branching and rich foliage, while the upper half lacks foliage and branching. The leaves are alternately arranged and single, villous, linear-oblong to linear-lanceolate and blunt-tipped. The flowers are surrounded by a series of bracts. Outer bracts are ovate to triangular, serrated or incised, while involucral bracts vary in terms of their outline, are narrow with deep incisions, in linear-oblong to lanceolate shapes, and are densely villous. The inflorescence is composed of 5–200 flowers with distinct pedicels that are typically irregularly arranged, narrow, ligulate with an acute apex, and are blue or, occasionally, pink or white in colour. The fruit of *J. montana* forms an oblong, acute capsule, while the brown or sometimes white seeds are ovoid-shaped and smooth [2,3].

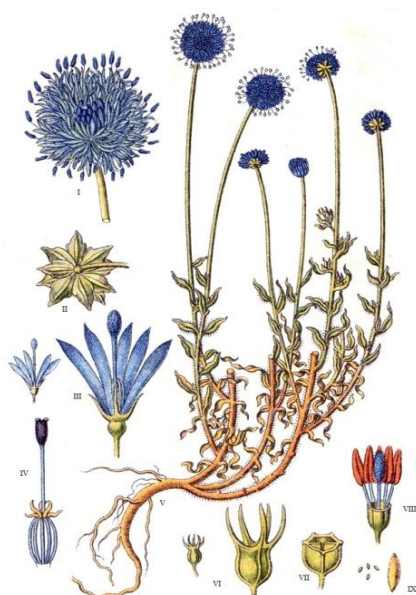


Figure 1. A depiction of the morphology of *Jasione montana* L. [i-flora.com, 2022]

The centre of distribution of *J. montana* is in Europe, including Poland. Moreover, its presence has also been noted in Morocco, Tunisia, Algeria, Russia and Turkey, and it has also been introduced to the north-eastern areas of the United States of America [3]. In Central and Eastern Europe, it can be found mainly in pine forests, on sandy terrain in forest and forest-steppe areas, cliffs, sand dunes, as well as wastelands and semi-natural communities. The plant does not have high environmental requirements. It is growing well on acidic, calcium-poor, well-drained soil of low fertility, both in sunny and semi-shady areas [2,4]. In addition, the plant can accumulate arsenic, and can thus serve as a natural indicator of soil pollution. The accumulation of other heavy metals, such as cadmium, lead, copper, chromium and zinc in the aboveground parts and roots of *J. montana* has also been proven [5,6].

In the earliest literature regarding *J. montana*, published in 1629, Sheep's bit scabious had already been recognized as a typically garden plant. There were also reports stating that this plant could have been used as feed for sheep (for this reason the name *Mountain Sheep's Scabious* occurs in old British literature). In addition, very limited literature sources identify *J. montana* as a milky plant [2]. From an ethnopharmacological point of view, interesting reports are provided by Belorussian folk medicine specifying *J. montana* as a plant with sedative effects in the case of

restless sleep in children [7]. So far, few literature sources report the presence of two flavonoid compounds characterized as 5,7,3',4'-tetrahydroxyflavone (luteolin), and luteolin 7-*O*- β -D-glucoside (cynaroside) in the aboveground parts of *J. montana*, at the full flowering phase [8]. Additionally, the presence of an anthocyanin derivative in the flowers, as well as delphinidin inulin, and unspecified flavonoid and alkaloid compounds in the vegetative organs were detected [2].

In modern medicine, drugs made from natural compounds and plant materials are important elements for the growth of the drug research and development industry. Among the classes of plant secondary metabolites studied thus far, flavonoids, including luteolin and its derivatives, are distinguished by multiple beneficial biological activities. Among others, they exhibit anti-inflammatory, immunomodulatory, antihypertensive and oxidative stress-modulating activity. In addition, by modulating signalling pathways at each stage of carcinogenesis, they may display therapeutic effects in various neoplasms, especially skin cancer [9], especially because the current state of knowledge supports the evidence of beneficial effects of combination therapies consisting of conventional anticancer drugs together with medicinal plants and their bioactive compounds [10–12]. The developments in phytochemistry, phytotherapy, as well as the discovery of new mechanisms of action, and new active ingredients is leading to breakthroughs in natural drug research. However, there is a need to develop plant matrix safety studies. At the moment, there are no sufficient publications regarding neither the presence of biologically active compounds in aboveground parts of *J. montana* nor the evaluation of their biological activity. Thus, this plant can be a promising source for obtaining biologically active compounds, especially polyphenolic compounds, with a wide range of pharmacological activities and possible therapeutic effects.

Chapter 3. The objective of the work including the rationale for undertaken research with reference to publications comprising the doctoral dissertation

The scientific aim of the doctoral dissertation was the detailed characterization of the chemical composition of the aboveground parts of *Jasione montana* L., including the preparation of selected extracts and fractions, undertaking attempts of isolation of active compounds and assessing their biological activity.

1. The characterization of the active components obtained from the aboveground parts of *J. montana* was carried out based on:
 - a. qualitative analysis of the water, water-methanol and methanol extracts and selected fractions from *J. montana* obtained by using multistage extraction with solvents of increasing polarity: diethyl ether, ethyl acetate and *n*-butanol by high-performance liquid chromatography (HPLC), including the LC–PDA–ESI–MS/TOF technique (**publication I**);
 - b. a multi-stage procedure for the isolation of polyphenolic compounds using low-pressure liquid chromatography (LPLC) with the use of various carriers: polyamide, Sephadex LH-20, and HPLC (**publication I**);
 - c. full structural characteristics of the isolated flavonoid compounds using chromatographic analysis of hydrolytic decay products (TLC) and spectral analyses: UV, nuclear magnetic resonance: ^1H and ^{13}C NMR, and final structural characterization obtained *via* mass spectrometry [electrospray ionization–mass spectrometry (ESI–MS)] (**publication I**);
 - d. description of a new analytical method with simultaneous determination of the quantitative content of flavonoid compounds in the abovementioned extracts and fractions obtained from *J. montana* by using the HPLC–PDA technique (**publication II**).
2. The evaluation of the anticancer activity of extracts and fractions from aerial *J. montana* and three isolated and identified flavonoid compounds in a C32 skin melanoma cells (CRL-1585) model was carried out based on (**publication I**):
 - a. evaluation of cytotoxic activity by measuring cell viability using the BD Horizon™ Fixable Viability Stain 520 by flow cytometry;
 - b. assessment of the induction of apoptosis in C32 cells using fluorescent staining of conjugated annexin V with fluorescein isothiocyanate and propidium iodide by flow cytometry;
 - c. evaluation of the mechanism of apoptosis by cytometric measurement of the change in mitochondrial membrane potential and the activity of selected caspases: -3, -8, -9 and -10;
 - d. evaluation of the influence on the phases of the cell cycle and the ability to induce/inhibit the process of autophagy.
3. The assessment of wound healing properties of extracts and fractions from *J. montana* and their isolated and identified flavonoid compounds was carried out based on (**publication II**):
 - a. spectrophotometric determination of the degree of inhibition of elastase in an *in vitro* model and assessment of antioxidant activity by means of the DPPH and FRAP methods;
 - b. measurement of collagen type-I biosynthesis, as well as evaluation of the selected pro-inflammatory cytokines secretion in a normal human dermal fibroblast cell line (PCS-201-012) model by flow cytometry;
 - c. evaluation of the potential to stimulate migration and proliferation of fibroblasts by bioimaging using a phase contrast microscope.
4. The comparison and description, based on global literature, of knowledge about the application of chromatographical techniques in the analysis of luteolin and its derivatives (**publication III**).
5. A review of studies describing luteolin and its derivatives as potential therapeutics in skin cancers, including related pathways and therapy (**publication IV**).

Chapter 4. The achievement of scientific objectives, concise summary of research materials and methods, research results, summary and discussion with reference to publications comprising the doctoral dissertation and identification of prospects for further research in the subject

The experimental methods applied during the research did not require the approval of the Bioethics Committee.

4.1. Plant material

The aerial parts of *J. montana* were collected from their natural environment in the Puszcza Knyszyńska area (N53°15'20.9"; E23°25'41.5") near the Supraśl region (Podlasie Province, Poland) in the period of June–August 2017 and 2018. The plant material was air-dried in ventilated premises with limited light conditions (**publication I and Supplementary material to publication II**). The species' identity was confirmed according to the scientific botanical literature and its morphological depiction [13]. A herbarium specimen with selected plant elements of *J. montana* (JM-15029) was deposited at the Department of Pharmacognosy at the Medical University of Białystok.

4.2. Preparation of extracts and fractions

To prepare the H₂O (**JM1**), 50% MeOH (**JM2**), and MeOH (**JM3**) extracts for further studies, the raw plant material (5 g per sample) was pulverized and subsequently extracted with 65 mL of the above-mentioned solvents by using a heating mantle and radiator (5 × 45 min). The extracts after filtration were dried to evaporation of the extraction solvents under reduced pressure at a controlled temperature of 40±2 °C. The residues of extracts were lyophilized using a freeze-drier after suspension in water. As a consequence, the extracts were obtained in the following amounts: **JM1** – 1293 mg; **JM2** – 1238 mg; and **JM3** – 858 mg. Furthermore, the plant material (130 g) was purified in a Soxhlet extractor with the following extraction solvents: extraction petrol (1.5 L × 8 h), and CHCl₃ (1.5 L × 8 h) according to the continuous extraction method, and finally extracted with MeOH (20 × 3 L) and 50% (v/v) MeOH (3 L) for 45 min each time. The MeOH extracts were aggregated, denuded of the extraction solvent, and their ballasts were eliminated through precipitation with water. The obtained water extract formed the basis of further exhaustive fractionations through liquid–liquid extraction with different solvents of increasing polarity: CHCl₃ (35 × 200 mL), Et₂O (**JM4**: 50 × 200 mL), EtOAc (**JM5**: 98 × 200 mL) and *n*-BuOH (**JM6**: 45 × 200 mL). All fractions were lyophilized using a freeze-drier after evaporation to dryness. The following amounts of the fractions were obtained: **JM4** – 8.5 g; **JM5** – 29 g and **JM6** – 38.5 g, and were used for further experiments. The CHCl₃ fraction obtained in one of the stages of the raw material purification process was not used for further analyzes (**publication I and II**).

4.3. Realization of scientific aims

4.3.1. Analysis of the phytochemical profiles of *J. montana* extracts and fractions by means of LC–ESI–MS

The first step in evaluating the general characteristics of the prepared extracts (**JM1–JM3**) and fractions (**JM4–JM6**) was the evaluation of the phytochemical analysis by means of the liquid chromatography–photodiode array detection–electrospray ionization–mass spectrometry (LC–PDA–ESI–MS/TOF) method. LC–ESI–MS analysis was performed (Kinetex XB-C18 reversed-phase chromatography column, 150 × 2.1 mm, 1.7 μm (Phenomenex, USA); UPW:MeCN:HCOOH). The compounds were analyzed in an MS detector in both positive and negative ionization modes. The data obtained by chromatographic separation allowed for the preliminary identification of 25 polyphenolic compounds, indicating at the same time the rich qualitative composition of the tested plant material (Table 1) (**Figures S1-S2 in Supplementary material to publication I**). As expected, the high content of free aglycones [peaks 22–25], with the

dominant peak belonging to **22** (luteolin), was correlated with the extraction of the raw material with MeOH (**JM3**), while **JM1** and **JM2** were rich in glycosides. It was observed that the 50% MeOH extractant (**JM2**) was more effective than H₂O (**JM1**). The dominant component in most of the extracts tested was **22**, while the second most represented compound was **12** (luteolin 7-*O*-glucoside). Its presence was also detected in glycoside-rich extracts **JM1**, **JM2**, **JM4**, and **JM5**. The composition of studied fractions (**JM4–JM6**) was symptomatic of the selectivity of the extraction process for specific groups of compounds. The analysis documented that in the **JM4** fraction, aglycones were predominate – mainly **22** and **23** (apigenin). In addition, **12**, as well as *p*-coumaric acid and its derivatives [peaks 3, 10] with a characteristic absorption maximum of 310 nm in the ultraviolet-visible (UV-VIS) spectrum, were also present. Moreover, **JM5** contained di- and triglycosides [peaks 9, 14, 15] with specific loss of fragments [M–162±H]^{+/-}, [M–146±H]^{+/-}, and [M–132±H]^{+/-}, which correspond to *O*-hexose, *O*-pentose and *O*-deoxyhexose, respectively. Furthermore, aglycones substituted with a linear glycoside molecule [peaks 9, 14] as well as unsubstituted compounds were shown in **JM5** [peak 15]. **JM6** contained a multicomponent mixture of flavonoid glycosides and was devoid of free aglycones (**publication I**).

Table 1. Qualitative analysis of extracts/fractions (**JM1–JM6**) from *Jasione montana* performed by means of the liquid chromatography–mass spectrometry (LC–MS) method.

Peak	Rt (min)	UV-VIS maxima (nm)	[M–H] ⁻ ions (m/z)	[M–H] ⁺ ions (m/z)	Identified compounds
1	4.60	260	191, 217, 235	86, 136, 276	unknown
2	14.53	260, 294	109 , 153, 277	93, 137 , 213, 248	unknown
3	19.29	256, 310sh	93 , 183	94 , 302	<i>p</i> -coumaroyl acid derivatives
4	20.79	268, 330	565, 771	302, 538, 773	unknown
5	21.61	272, 330	593	415, 432 , 595	flavonoid derivatives
6	22.53	268, 336	609	287, 449, 611	luteolin <i>O</i> -hex-hex
7	23.40	268, 338	563, 741	287, 449, 565, 743	luteolin <i>O</i> -hex-pent-hex
8	24.41	268, 340	609	287, 449, 611	luteolin <i>O</i> -hex-hex
9	25.59	268, 348	285, 579	287, 449, 581	luteolin 7- <i>O</i> -sambubioside (s)
10	25.87	310	119 , 162	91, 119, 147 , 165	<i>p</i> -coumaric acid (s)
11	26.11	268, 338	593	271, 433, 595	apigenin <i>O</i> -hex-hex
12	26.84	258, 266, 348	447 , 895	287, 449	luteolin 7- <i>O</i> -glucoside (s)
13	26.99	268, 326	593	287, 449, 595	luteolin <i>O</i> -hex-deoxyhex
14	27.46	250, 268, 336	285, 447, 609, 755	287, 449, 611, 757	luteolin <i>O</i> -hex-hex-deoxyhex
15	27.85	268, 330	269, 563	271, 418 , 565	apigenin <i>O</i> -deoxyhex- <i>O</i> -deoxyhex
16	28.76	268, 335	285, 447, 579 , 769	287, 449, 581, 771	luteolin <i>O</i> -hex-pent-feruloyl
17	29.27	268, 330	285, 431	286, 433	flavonoid derivatives
18	29.45	268, 336	285, 447	287, 449	luteolin <i>O</i> -hex
19	30.17	268, 284	431	301, 419 , 571	flavonoid derivatives
20	30.53	268, 300sh, 340	285, 447	287, 449	luteolin <i>O</i> -hex
21	32.36	270, 324	299, 461	331, 463	tricin <i>O</i> -pent
22	34.38	256, 266, 348	285	287	luteolin (s)
23	36.23	268, 295sh, 340	269	271	apigenin (s)
24	36.35	270, 300sh, 349	329	331	tricin (s)
25	36.54	268, 300sh, 344	299	301	chrysoeriol (s)

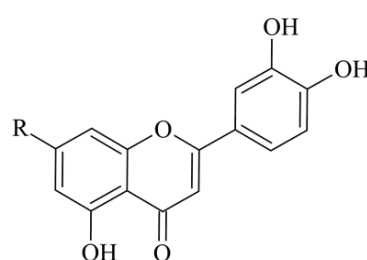
sh—peak shoulder; bold—most abundant; s—reference substance; hex—hexose, pent—pentose, deoxyhex—deoxyhexose.

4.3.2. Isolation and identification of main flavonoids **9**, **12** and **22**

Based on preliminary LC–ESI–MS phytochemical profiling, the presence of separable compounds belonging to the polyphenol group was detected in fractions **JM4–JM6**. Hence, the fractions were subjected to multistep and labor-intensive separation processes by means of low-pressure liquid chromatography (LPLC) using different stationary phases, polyamide and Sephadex

LH-20. The isolation procedures were inspected by means of the thin-layer chromatography (TLC) (TLC Cellulose, *n*-BuOH:CH₃COOH:H₂O, 4:1:5 (v/v/v); 1% Naturstoff reagent A) technique under UV light. As a result of chromatographic separation processes, three known substances: **9** (250 mg), **12** (1640 mg) and **22** (139 mg) were obtained. The full structural characterization of the isolated, chromatographically homogeneous substances was established through further spectral analyses (**publication I**).

The structures of the isolated compounds (**9**, **12**, **22**) were determined on the basis of chromatographic analysis and R_f values of acid hydrolysis products and analysis of recorded spectra of spectroscopic methods such as UV spectroscopy and nuclear magnetic resonance (¹H NMR, ¹³C NMR). The final characterization was confirmed by mass spectrometry (MS), including analysis of ion decay products (ESI) (**publication I**). The spectral data of the isolated compounds (**9**, **12** and **22**) were verified by comparison with those previously described in the literature. The isolated compounds were identified as luteolin 7-*O*-β-D-xylosyl-(1-2)-β-D-glucoside (luteolin 7-*O*-sambubioside, **9**), luteolin 7-*O*-β-D-glucoside (cynaroside, **12**) and 5,7,3',4'-tetrahydroxyflavone (luteolin, **22**) [14–16] (Figure 2) (**Figures S3-S8 in Supplementary material to publication I**).



Compd	R
22	OH
12	<i>O</i> -glu
9	<i>O</i> -glu- <i>O</i> -[2'-xyl]

Figure 2. Chemical structure of isolated compounds **9**, **12** and **22**.

4.3.3. Quantitative analysis of *J. montana* extracts and fractions by means of HPLC–PDA

Further studies focused also on the quantification of isolated secondary metabolites and the sum of their derivatives in extracts (**JM1–JM3**) and fractions (**JM4–JM6**) using high-performance liquid chromatography with a photodiode array detector (HPLC–PDA method). For this purpose, a new method was developed and validated. The parameters of the method for the two dominant compounds **12** and **22** ($\lambda_{\max} = 348$ nm) are presented in Table 2 (**Table S1 in Supplementary material to publication II**). The compounds were quantified by using calibration curves of the two reference substances.

Table 2. Regression data, the limit of detection (LOD) and limit of quantification (LOQ), accuracy and precision obtained during HPLC–PDA method validation.

Parameter	luteolin 7- <i>O</i> -glucoside (12)	luteolin (22)
Linear range [μg/mL]	25–1000	5–500
R ² (N=6)	0.9999	0.9999
Regression equation ^a	y = 22851x+106.69	y = 36173x-34.602
LOD [μg/mL]	19.4	4.6
LOQ [μg/mL]	59	14
Accuracy [%]	101.09±3.23	101.23±2.93
Intra-day precision (%CV) (N=6)	0.58	0.93
Inter-day precision (%CV) (N=9)	0.88	1.26

^a the value for y corresponds to the peak area and x to the concentration, respectively.

Table 3 shows the contents of the main phytoconstituents, compounds **9**, **12**, and **22**, as well as their derivatives. Each examined extract exhibits variations in quantitative content relative to the major compounds. Based on the results obtained, it can be determined that extracts **JM1–JM6** have a relatively limited phytochemical composition. Consequently, the determined dominant substances are present in substantial amounts. This formed the basis for their multistage isolation process. The predominant compounds found in **JM4** are **22** (72.13±3.86 mg/g dry fraction) and **12** (40.21±0.85 mg/g dry fraction), whereas **JM5** contains a substantial quantity of **12** (383.16±1.36 mg/g dry fraction) and other flavonoid derivatives (**publication II**).

Table 3. Quantification of major compounds in *J. montana* extracts (**JM1–JM3**) and fractions (**JM4–JM6**) by means of HPLC–PDA expressed as mg/g dry extract/fraction.

Compounds	JM1	JM2	JM3	JM4	JM5	JM6
9 [#]	10.30±0.03	6.57±0.03	BLQ	ND	BLQ	6.77±0.08
12	52.02±0.17	31.21±0.07	11.10±0.08	40.21±0.85	383.16±1.36	ND
22	5.78±0.11	7.82±0.02	8.18±0.09	72.13±3.86	ND	ND
luteolin derivatives ^{b#}	83.66±0.28	53.81±0.14	23.11±0.02	53.51±1	474.87±1.86	20.76±0.13

9—luteolin 7-*O*-sambubioside; **12**—luteolin 7-*O*-β-D-glucoside; **22**—luteolin; ^b excluding luteolin; [#] expressed as equivalent of luteolin 7-*O*-glucoside with standard deviation; BLQ—below the limit of qualification; ND—not detected.

4.3.4. *In vitro* evaluation of the anticancer activity of *J. montana* extracts/fractions and their main compounds against human amelanotic melanoma C32 cell line

According to a number of available studies, plant materials represent an important source of anticancer molecules due to their ability to inhibit tumor growth by means of cell cycle arrest and/or apoptosis induction [17]. However, research into the metabolic pathways of plant matrices and naturally derived compounds is deficient, therefore *in vitro* studies do not always correlate with the effect observed after internal administration. Therefore, it seemed appropriate to consider studies towards potential topical administration of the raw material and natural compounds. Based on the available literature and previous studies involving *in vitro* and *in vivo* models, luteolin and its derivatives have been suggested to have anticancer effects, including anti-melanoma properties (**publication IV**).

Taking these aspects into consideration, the anticancer activity of the *J. montana* extracts (**JM1–JM3**), their fractions (**JM4–JM6**) and isolated compounds (**9**, **12**, **22**) against a human amelanotic melanoma cell line C32 (CRL-1585) were investigated. The study was based on cell cycle arrest and apoptosis induction. Preliminary profiling of the cytotoxic potential of **JM1–JM6** and **9**, **12**, **22** was performed using a fixed viability staining assay *via* a flow cytometer (Table 4). The viability of the C32 cell was inhibited in a dose-dependent manner under the influence of the tested extracts and compounds (**Figures S9–S12 in Supplementary material in publication I**). The highest cytotoxic potential was observed for **22** (IC₅₀ = 95.1±7.2 μg/mL) and **JM4** (IC₅₀ = 119.7±3.2 μg/mL), but was slightly lower for **JM6** (IC₅₀ = 215.1±21.2 μg/mL). Notably, based on the content of compound **22** in **JM4**, it can be concluded that this compound is predominantly responsible for the observed effects of the **JM4** fraction on C32 cells (**publications I and II**). The observed activities of the **JM4** fraction and compounds **22** were comparable to vinblastine sulfate (VLB), which was used as a positive control (IC₅₀ = 148.5±7.7 μg/mL). While both **22** and **JM4** displayed notable degrees of cytotoxic activity in C32 cells in this study, their cytotoxic potential against a normal human dermal fibroblast cell line was much lower (**Figure S13 in Supplementary material in publication I**). On the other hand, other evaluated samples (**JM1–JM3**, **JM5–JM6**, compounds **9**, and **12**) showed no effect on the C32 cell survival rate (IC₅₀ > 300 μg/mL). Moreover, C32 cells treated with **22**, **JM4**, and VLB were visualized using phase-contrast microscopy to assess the morphological profile (Figure 3). Dose-dependent degradation of the cell membrane and a decrease in cell adhesion was observed. Additionally, it can be speculated that cell proliferation was inhibited or apoptosis induced, based on the observed reduction in cell numbers

in the treatment groups. Based on the results of the preliminary assessment of cytotoxic potential against cancer cells, samples with the highest toxic activity (**JM4**, **22**) were submitted for further elucidation of the mechanism of cell damage and the possible induction of apoptosis, as well as the ability to halt the cell cycle.

Table 4. Cytotoxic activity of **JM1–JM6** extracts and isolated compounds **9**, **12**, **22** against C32 human amelanotic melanoma cells. Mean values \pm SD from three independent experiments conducted in duplicate are presented. (IC₅₀ value in $\mu\text{g}/\text{mL}$).

Sample	IC ₅₀ [$\mu\text{g}/\text{mL}$]
JM1	> 300
JM2	> 300
JM3	> 300
JM4	119.7 \pm 3.2
JM5	> 300
JM6	215.1 \pm 21.2
9	> 300
12	> 300
22	95.1 \pm 7.2
VLB	148.5 \pm 7.7

VLB—vinblastine sulfate (positive control).

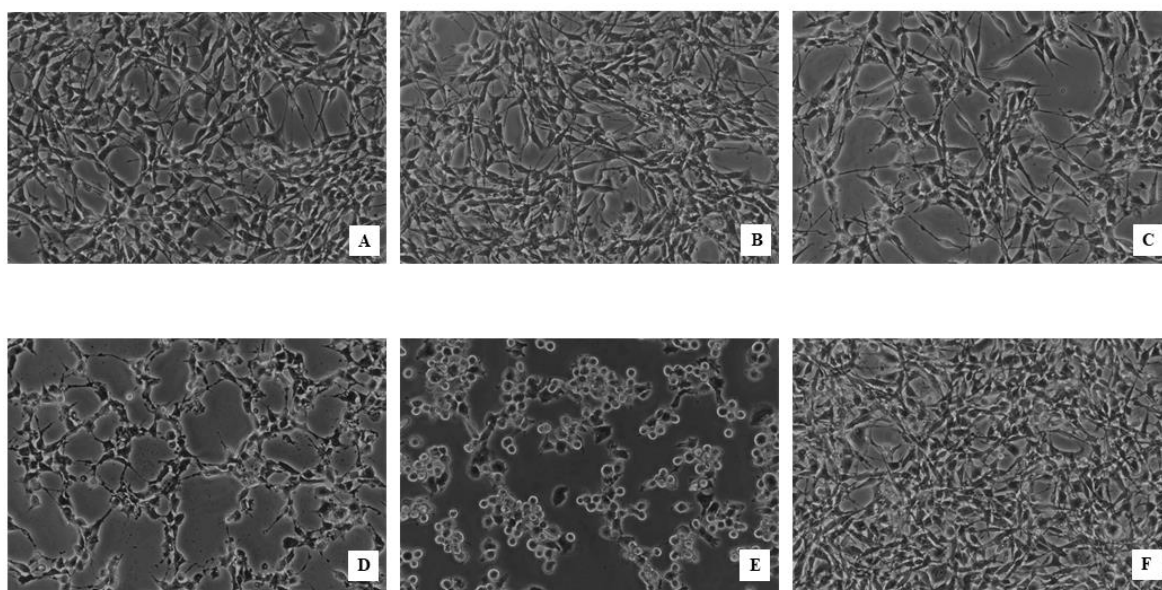


Figure 3. Morphological profile of C32 melanoma cells treated with **JM4** at concentrations of 25 $\mu\text{g}/\text{mL}$ (A), 50 $\mu\text{g}/\text{mL}$ (B) and 100 $\mu\text{g}/\text{mL}$ (C), **22** at a concentration of 25 $\mu\text{g}/\text{mL}$ (D), and vinblastine sulfate (VLB) at a concentration of 25 $\mu\text{g}/\text{mL}$ (E), compared with an untreated control (F) evaluated by means of phase contrast microscopy (magnification \times 200).

The fluorescent staining of conjugated annexin V with fluorescein isothiocyanate and propidium iodide (PI) was performed by means of a flow cytometer technique to establish the mode of programmed cell death induced by **JM4** and **22**. During apoptosis, annexin V has a close kinship with phosphatidylserine (PS) on the cell membrane, anticipatory of its externalization. Meanwhile, PI marks the integrity of the cell membrane and, consequently, the percentage of necrotic cells. Hence, this method allows for differentiation between viable cells, those undergoing early or late apoptosis, and necrotic cells [18]. Results demonstrated that **JM4** and **22** relevantly induced programmed death of C32 cells (Figure 4). The most significant proapoptotic effect was observed in the case of 100 $\mu\text{g}/\text{mL}$ **JM4** (44.2 \pm 1.0% viable cells and 51.5 \pm 1.7% apoptotic cells). Nevertheless, due to the fact that the percentage of necrotic cells increased in direct proportion to

the increase in **JM4** concentration ($4.3 \pm 2.6\%$ necrotic cells under the influence of $100 \mu\text{g/mL}$), a dose-dependent toxic effect could be attributed. VLB and **22** displayed comparable proapoptotic potential ($29.2 \pm 3.0\%$, and $27.4 \pm 1.0\%$ apoptotic cells, respectively); however, VLB was characterized by twofold higher necrotic potential.

Under cytometric examination of the effect on the induction of the autophagy process, it was observed that the highest dose-dependent activity was demonstrated after 24 hours of incubation with **JM4** ($100 \mu\text{g/mL}$) ($60.2 \pm 1.6\%$ non-autophagic cells and $38.6 \pm 1.6\%$ autophagic cells) (Figure 5). Admittedly, the potential of VLB at a concentration of $25 \mu\text{g/mL}$ was twofold higher ($22.4 \pm 0.6\%$ non-autophagic cells and $76.7 \pm 0.5\%$ autophagic cells). At the same time, it was observed that the effect after treatment with **JM4** was not compatible with its major component, **22**. Autophagy prevents the deposition of damaged cellular organelles through the regulation of intracellular homeostasis, and its levels are compatible with cellular stress leading to apoptosis of cancer cells [19]. Hence, the observed percentage of autophagic cells after treatment with **JM4** may suggest the induction of cellular stress and programmed cell death.

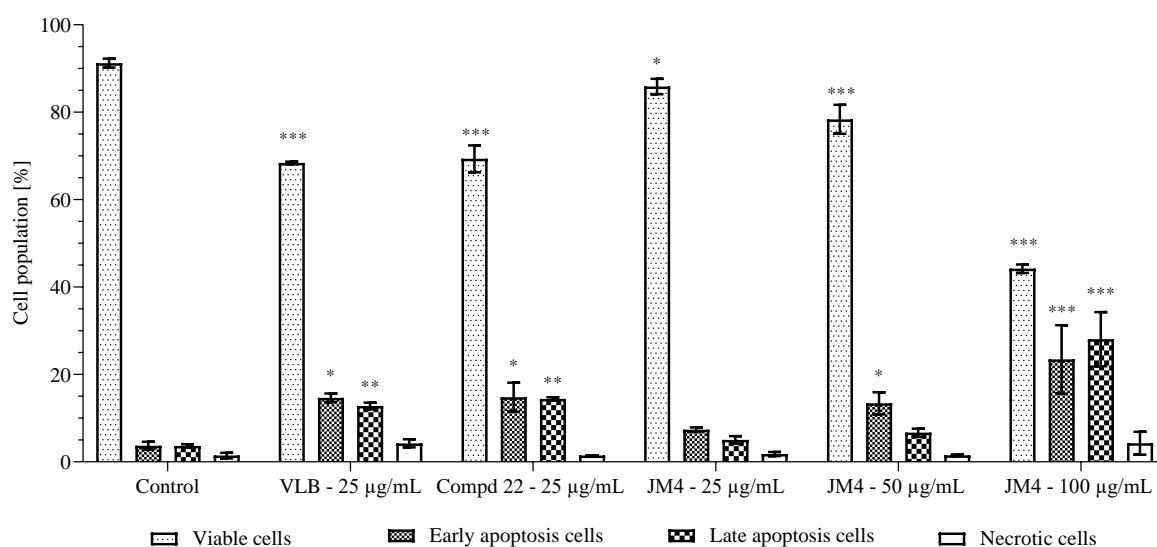


Figure 4. The percentage of C32 melanoma cells in the viable stage, early and late apoptosis, and necrotic stage, after treatment with **JM4** ($25, 50, 100 \mu\text{g/mL}$), **22** ($25 \mu\text{g/mL}$) and vinblastine sulfate (VLB) ($25 \mu\text{g/mL}$). Mean percentages from three independent experiments ($n = 3$) conducted in duplicate are presented. * $p < 0.05$ versus control group, ** $p < 0.01$ versus control group, *** $p < 0.001$ versus control group.

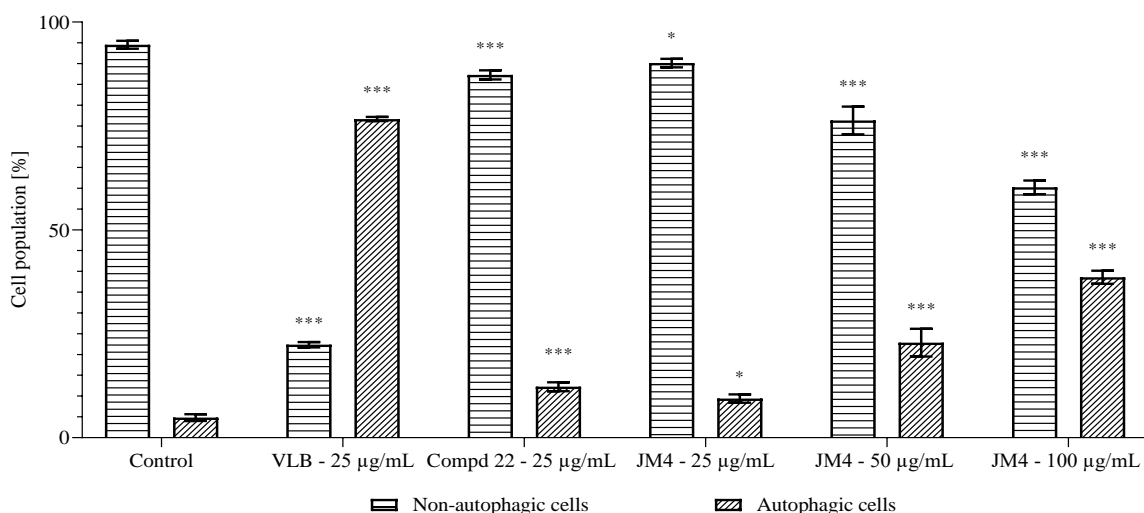


Figure 5. The percentage of non-autophagic and autophagic C32 melanoma cell population after incubation with **JM4** (25, 50, 100 µg/mL), **22** (25 µg/mL) and vinblastine sulfate (VLB) (25 µg/mL). Mean percentage values from three independent experiments (n = 3) conducted in duplicate are presented. * $p < 0.05$ versus control group, *** $p < 0.001$ versus control group.

Cell cycle arrest and apoptosis induction play an important role in the mechanism of activity and design of anticancer agents. Mitochondria and caspases activity, *inter alia*, are closely linked with programmed cell death. Cytometric analysis of the changes in C32 cell cycle progression caused by **JM4** and **22** are presented in Figure 6. It was observed that **JM4** at 100 µg/mL and **22** at 25 µg/mL led to an accumulation of cells in the G2/M phase (30.1±1.8% vs. 6.1±0.6% control, 14.6±1.5 % vs. 6.1±0.6 % control, respectively). Thereby, the potential of 25 µg/mL of VLB was only moderate compared to **JM4** and **22**. Moreover, the percentage of C32 cells in the G1 phase decreased after incubation with **JM4** (100 µg/mL) and **22** (25 µg/mL) (14.7± 2.4% vs. 73.0±0.9% control, 35.3±3.0% vs. 73.0±0.9% control, respectively). The demonstrated disruptions of the cell cycle were associated with inhibition of cell proliferation.

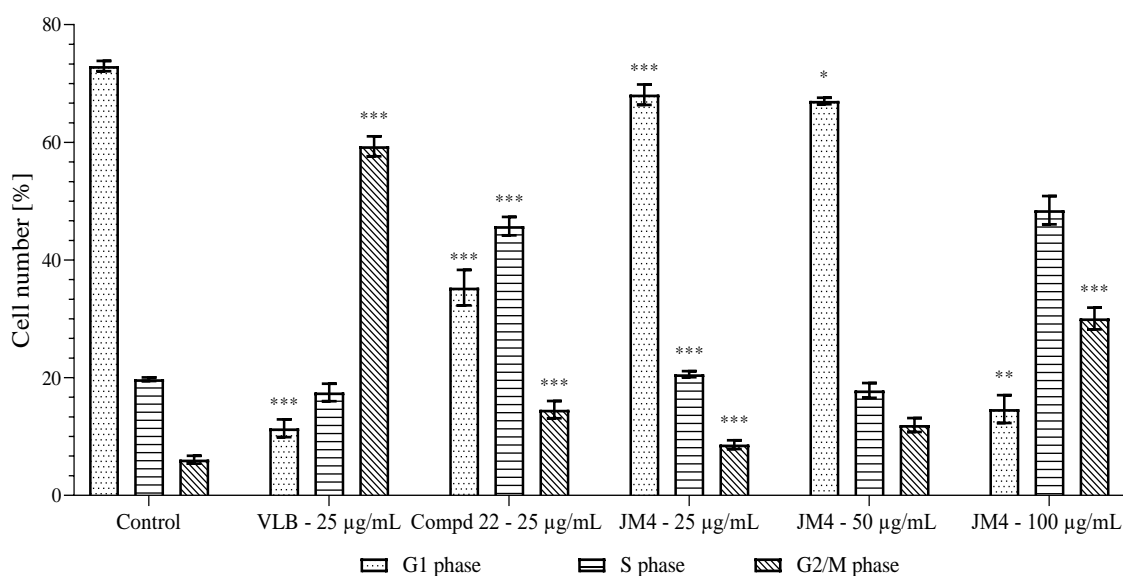


Figure 6. Percentage of accumulation C32 melanoma cells in the different cell cycle phases after 24 h of incubation with **JM4** (25, 50, 100 µg/mL), **22** (25 µg/mL) and vinblastine sulfate (VLB) (25 µg/mL). Mean percentage from three independent experiments (n = 3) done in duplicate are presented. * $p < 0.05$ versus control group, ** $p < 0.01$ versus control group, *** $p < 0.001$ versus control group.

Dysfunction of mitochondrial membrane integrity may affect the mitochondrial pathway in the apoptotic cell death process. The cytometric evaluation performed showed a significant decrease in dose-dependent mitochondrial membrane potential (MMP) under the influence of **JM4** and compound **22**, thus confirming the triggering of apoptosis (Figure 7). Notably, the reduction in MMP in the case of **22** at a concentration of 25 $\mu\text{g}/\text{mL}$ ($31.8\pm 0.7\%$) was similar to that caused by VLB, and in the case of **JM4** at a concentration of 100 $\mu\text{g}/\text{mL}$ ($74.5\pm 3.0\%$), it was twice as high as that recorded in the case of VLB ($34.1\pm 3.0\%$). Furthermore, in the untreated control group, reduced MMP was present in only $5.2\pm 0.1\%$ of cells. The obtained results are in accordance with the results from the annexin V binding assay. The correlation between reduced MMP and early stages of apoptosis is also linked to the appearance of cytochrome C and other proteins in the cytosol. These proteins play a crucial role in the activation of the intrinsic (mitochondrial) apoptotic pathway, closely related to caspase-9 and, therefore, caspase-3. Moreover, activation of apical caspases (caspase-8 and caspase-10) leads to initiation of the external apoptotic pathway as well as activation of the effector caspase, caspase-3, directly responsible for DNA damage-induced apoptosis [20,21]. Analysis of the changes in caspase expression presented in Table 5 showed a significant increase in the levels of all investigated caspases compared to the untreated control group under the influence of **JM4** and **22**. **JM4** (100 $\mu\text{g}/\text{mL}$) proved to be a potent inducer of apoptosis, exerting a significant effect on caspase-8, caspase-9 and caspase-10 activations ($41.8\pm 0.5\%$, $40.9\pm 2.4\%$, and $43.7\pm 1.1\%$, respectively), which was almost twice as effective as after VLB treatment. Additionally, the main component of **JM4**, **22** (25 $\mu\text{g}/\text{mL}$) showed a slightly weaker but equally adequate effect on caspase-8, caspase-9 and caspase-10 activation ($20.2\pm 1.5\%$, $16.6\pm 0.8\%$, and $15.4\pm 0.7\%$, respectively). The obtained results were consistent with the previous hypothesis of an intrinsic mitochondrial apoptotic pathway established by the results from the changes in MMP potential. Moreover, **JM4** (100 $\mu\text{g}/\text{mL}$) and **22** (25 $\mu\text{g}/\text{mL}$) affect the activity of the effector caspase, caspase-3 ($74.9\pm 4.0\%$, and $22.1\pm 1.9\%$, respectively). Therefore, it can be assumed that they induce external and intrinsic pathways of apoptosis and DNA degradation (**publication I**).

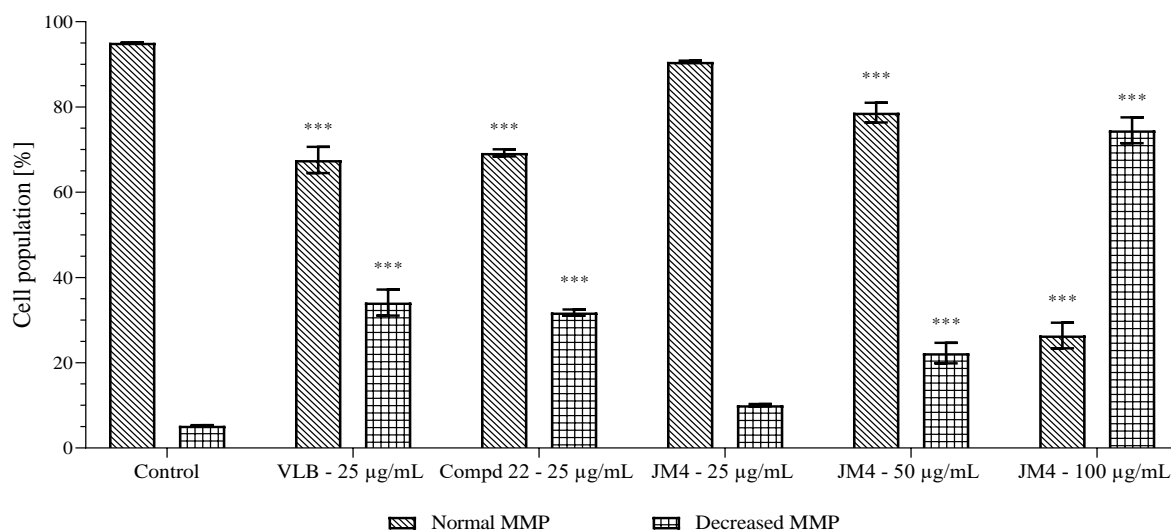


Figure 7. The percentage of C32 melanoma cells with normal and decreased mitochondrial membrane potential (MMP) after 24 h incubation with **JM4** (25, 50, 100 $\mu\text{g}/\text{mL}$), **22** (25 $\mu\text{g}/\text{mL}$) and vinblastine sulfate (VLB) (25 $\mu\text{g}/\text{mL}$). Mean percentage values from three independent experiments ($n = 3$) conducted in duplicate are presented. *** $p < 0.001$ versus control group.

Table 5. The percentage of C32 melanoma cells with active caspase-3 after 24 h incubation with **JM4** (25, 50, 100 µg/mL), **22** (25 µg/mL) and vinblastine sulfate (VLB) (25 µg/mL).

Samples	Cells with active caspases [%]			
	caspase-3	caspase-8	caspase-9	caspase-10
control	4.2±1.3	4.4±0.7	4.0±0.7	3.9±0.5
VLB	23.4±3.5	28.8±1.1	28.7±0.2	30.8±0.7
22	22.1±1.9	20.2±1.5	16.6±0.8	15.4±0.7
JM4 – 25 µg/mL	8.5±1.6	8.2±0.7	6.4±0.4	7.2±0.4
JM4 – 50 µg/mL	21.2±1.7	17.4±0.3	16.7±0.5	18.7±0.9
JM4 – 100 µg/mL	74.9±4.0	41.8±0.5	40.9±2.4	43.7±1.1

4.3.5. Estimation of the effects of *J. montana* extracts/fractions and their major secondary metabolites on wound healing processes

The wound healing process constitutes a series of dynamic, smoothly overlapping phases strictly related to the modulation of the release of various growth factors, extracellular matrix (ECM) signaling proteins, and cytokines; collagen depositing; and the control of oxidative stress, consequently resulting in restoration of anatomic continuity and tissue function [22,23]. Certain medicinal plants and their phytoconstituents may present an attractive therapeutic approach in the process of accelerating the restoration of the physical barrier of the skin [24]. Hence, the experiments conducted within the framework of this dissertation are intended to determine the effect of *J. montana* extracts (**JM1–JM3**), their fractions (**JM4–JM6**) and isolated compounds (**9**, **12**, **22**) on the wound healing process. The research presented herein focused mainly on investigating antioxidant potential, enzymatic inhibition against elastase, as well as the ability to accelerate the viability, migration and function of human dermal fibroblasts (PCS-201-012).

The antioxidant properties of *J. montana* extracts and their main components were established based on diverse mechanisms of action, including the 2,2-diphenyl-1-picrylhydrazyl (DPPH) free radical scavenging and ferric reducing antioxidant potential (FRAP) spectrophotometric assays. The radical scavenging activity by DPPH, expressed as IC₅₀ values, ranged from 848.47±4.4 µg/mL to 72.69±2.3 µg/mL for all extracts, and 10.65±0.7 µg/mL to 20.34±0.8 µg/mL for all compounds (Table 6). All of the tested compounds (**9**, **12**, and **22**) were comparably effective antiradical agents, while fractions **JM4** and **JM5**, with the highest content of these compounds (Table 3), showed the highest activity among the tested extracts/fractions. The obtained results were simultaneously comparable or stronger than the positive control, Trolox (IC₅₀ = 58.6±0.1 µg/mL). Similar findings were revealed in the reduction of metal ions in FRAP method (Table 6). The best reducing abilities were found in **JM5** (51.55±1.65 mM Fe²⁺/mL), followed by **JM4** (43.87±1.32 mM Fe²⁺/mL), while the lowest activity was observed in **JM6** in both the FRAP (10.63±0.92 mM Fe²⁺/mL) and DPPH assays (IC₅₀ = 848.47±4.4 µg/mL).

Elastin fibers, which are a component of the ECM, play an essential structural role and also benefit wound healing processes. Overproduction of one of the matrix metalloproteinases, elastase, leads to degradation of this protein and finally inhibition of skin re-epithelialization [25]. Performed spectrophotometric determinations of the inhibitory potential against elastase activity for crude extracts from *J. montana* and isolated compounds, carried out under the present doctoral research, showed that among all tested samples only a few exhibited moderate anti-elastase effects. The most active samples tested are classified from the strongest to the weakest elastase inhibitors as follows: **22**>**JM4**>**JM5**, with values of IC₅₀ = 39.93±1.06 µg/mL, 359.03±1.65 µg/mL, and 385.03±1.87 µg/mL, respectively. On the other hand, **JM1–JM3**, **JM6**, **9** and **12** showed no significant inhibitory activity (Table 7).

Table 6. Antiradical activity against DPPH radical (IC₅₀, µg/mL) and FRAP values (mM Fe²⁺ per mL) of **JM1–JM6** extracts and components (**9**, **12**, and **22**).

Sample	DPPH, IC ₅₀ (µg/mL) ^a	FRAP (mM Fe ²⁺ eq/mL) ^b
JM1	457.15±5.2	34.33±0.99
JM2	276.60±3.8	46.53±0.87
JM3	261.18±4.2	41.31±0.99
JM4	72.69±2.3	43.87±1.32
JM5	42.69±1.7	51.55±1.65
JM6	848.47±4.4	10.63±0.92
9	20.34±0.8	60.59±0.46
12	16.59±0.7	51.88±0.53
22	10.65±0.7	51.81±0.78

^a All data are represented as mean IC₅₀ values; ^b ability to reduce the Fe³⁺ complex to ferrous Fe²⁺.

Table 7. Elastase inhibitory activity of **JM1–JM6** extracts; compounds **9**, **12**, and **22**, and quercetin expressed as IC₅₀ (µg/mL).

Sample	IC ₅₀ (µg/mL)
JM1	> 600
JM2	> 600
JM3	> 600
JM4	359.03±1.65
JM5	385.03±1.87
JM6	> 600
9	> 200
12	> 200
22	39.93±1.06
PC	22.36±0.86

PC—positive control (quercetin).

Fibroblasts, one of the predominant cells in the wound closure process, may constitute a principal target in the commercial design of therapeutic preparations. To pre-determine the effects of the tested extracts and compounds on human dermal fibroblasts viability, a fixed viability staining assay was performed *via* a flow cytometer. As shown in Figure 8, the percentages of cell viability ranged from 94.9% to 104.6% compared to the control group. Most of the tested extracts and compounds at all tested concentrations (10–300 µg/mL) showed no noticeable toxicity. Nevertheless, **JM4** and **22** showed moderate dose-dependent cytotoxic potential. However, it was noted that there was no effect on cell viability in the presence of **JM4** at a concentration of 10–100 µg/mL and **22** (**Figure S13 in Supplementary material in publication I**).

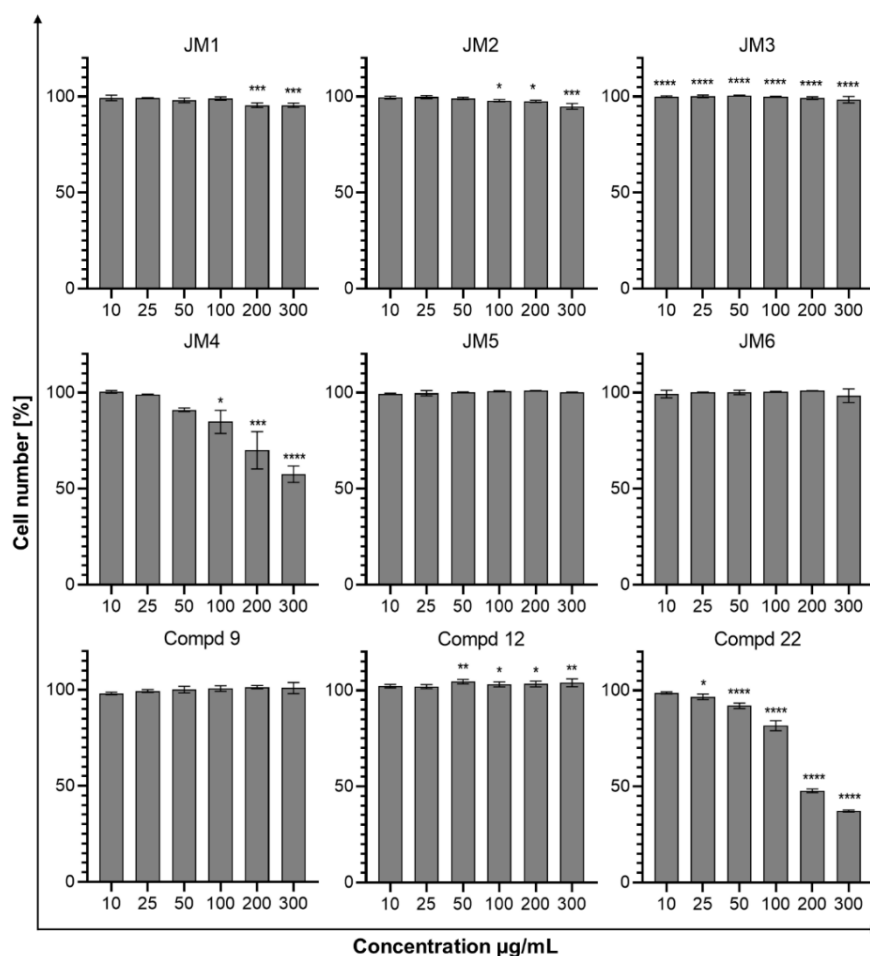


Figure 8. The percentage of viable HDF cells after 24 h of incubation with **JM1–JM6** extracts and their main components (**9**, **12**, **22**) (10–300 µg/mL) compared to the untreated control. Mean percentage from three independent experiments (n = 3) performed in duplicate. * $p < 0.05$ versus the control group, ** $p < 0.01$ versus the control group, *** $p < 0.001$ versus the control group, **** $p < 0.0001$ versus the control group.

The proliferation and migration of fibroblasts toward a temporary irruption plays a critical step during the re-epithelialization mechanism of restoring skin integrity [23]. The potency of either of these mechanisms has been examined by means of the *in vitro* scratch test, the preferred wound healing model applied in order to mimic cell migration during wound closure *in vivo* [26]. Considering the above-mentioned aspects, it has been demonstrated that *J. montana* extracts and their main metabolites can promote granulation tissue formation and, consequently, wound healing by inducing migration of fibroblasts as visualized using phase-contrast microscopy. Simultaneously, the tested samples showed no toxicity against the tested skin cells (Figure 9). Furthermore, among the tested samples, **9** and **JM1** (50 µg/mL) most firmly induced fibroblast growth and migration, and their influence was comparable to the healing-promoting potential of the positive control, allantoin (50 µg/mL). A slightly weaker effect was observed for the **JM5** fraction and its main compound, **12**, which likely determines the former's effects (Table 3). In contrast, a distinct trend was observed for **22** and **JM4**, which were capable of stimulating cells only at a low concentration (10 µg/mL). Above this concentration, a reduction in cell adhesion and loss of intercellular connections was observed. This observation coincides with the moderate cytotoxicity of these samples (Figure 8).

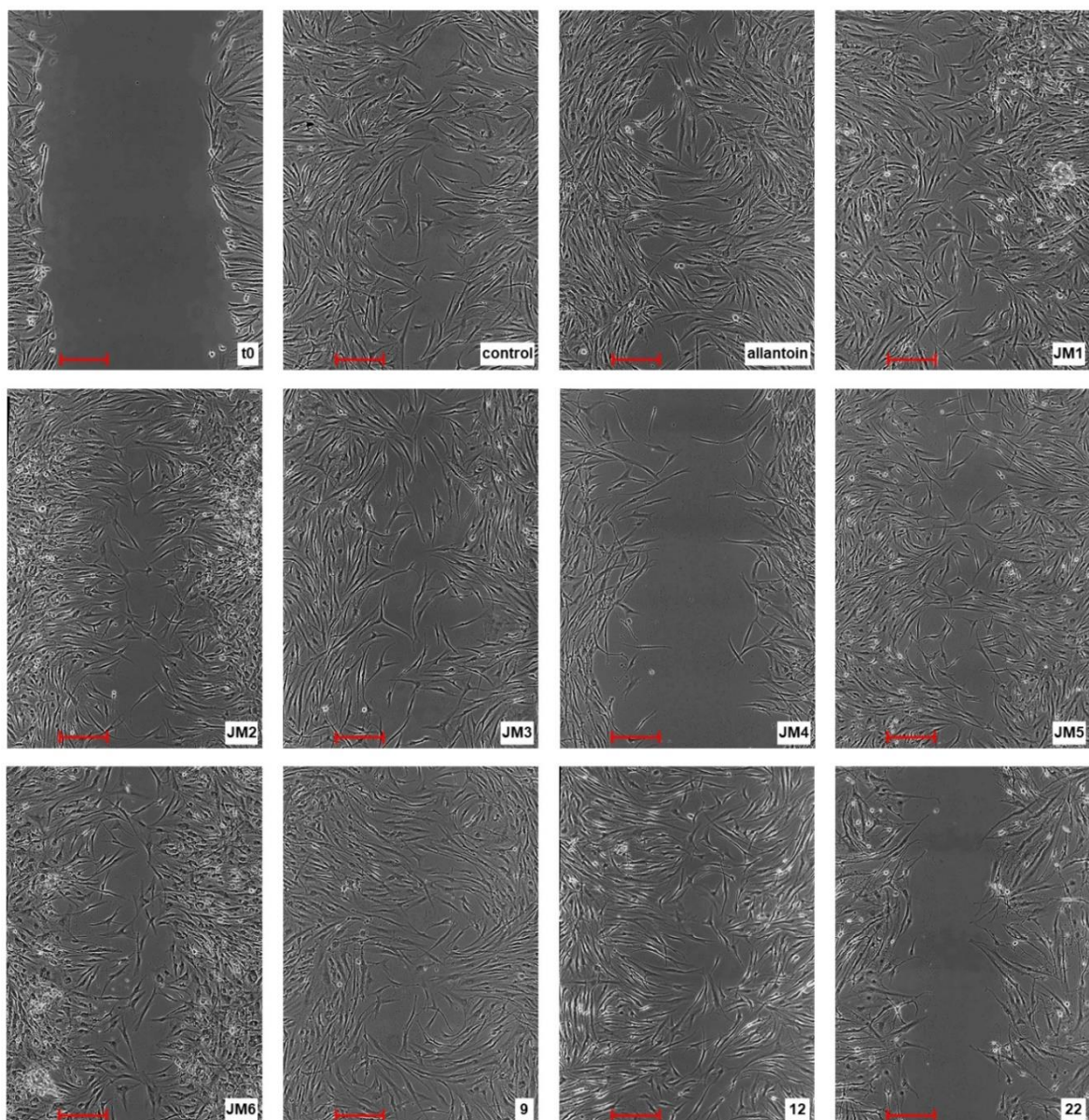


Figure 9. A representative image of the *in vitro* scratch migration assay in fibroblast cells immediately after wounding (t0), untreated (control) or treated with allantoin (50 $\mu\text{g}/\text{mL}$), extracts **JM1–JM6** (50 $\mu\text{g}/\text{mL}$), or compounds **9**, **12** (25 $\mu\text{g}/\text{mL}$) or **22** (10 $\mu\text{g}/\text{mL}$) after 24 h incubation, evaluated by means of phase contrast microscopy (magnification $\times 100$) (scale bar 250 μm).

Collagen is the major ECM protein produced by fibroblasts is as a significant protagonist of their survival, proliferation and function. Thus, from a clinical perspective, the deposition of collagen within the wound may constitute an exceedingly relevant aspect of healing and potentially contributes to the strengthening of the matrix [25]. The effect of *J. montana* extracts and isolated compounds on collagen type I content was evaluated in an *in vitro* model of human skin fibroblasts by means of a flow cytometry technique; however, the observed activity was restrained (Figure 10) (**Figure S1 in Supplementary material in publication II**). The highest increase in median fluorescence intensity (MFI) characterizing soluble collagen content in fibroblasts was observed for the highest tested concentrations (300 $\mu\text{g}/\text{mL}$) of **9** (MFI: 1763 ± 58 vs. 1507 ± 9.2 control) and **12** (MFI: 1717 ± 10.6 vs. 1507 ± 9.2 control); however, as already mentioned, they did not demonstrate an ability to reduce cell viability (Figure 8). Furthermore, the **JM3** extract slightly increased the soluble collagen content at a concentration of 25 $\mu\text{g}/\text{mL}$ (MFI: 2417 ± 45.2 vs. 2244 ± 7.1 control). However, this was not a dose-dependent effect; therefore, it is difficult to determine which dominant component (**12**, **9**) of this extract was responsible for its activity, or whether it was an

effect related to reciprocal inhibition with the other components (Table 3). Upon comparing the results obtained for the reference sample, allantoin at a concentration of 50 $\mu\text{g}/\text{mL}$, it became apparent that the majority of the investigated samples had more significant activity than allantoin (MFI: 1494 ± 2.8 vs. 1822 ± 62.2 control).

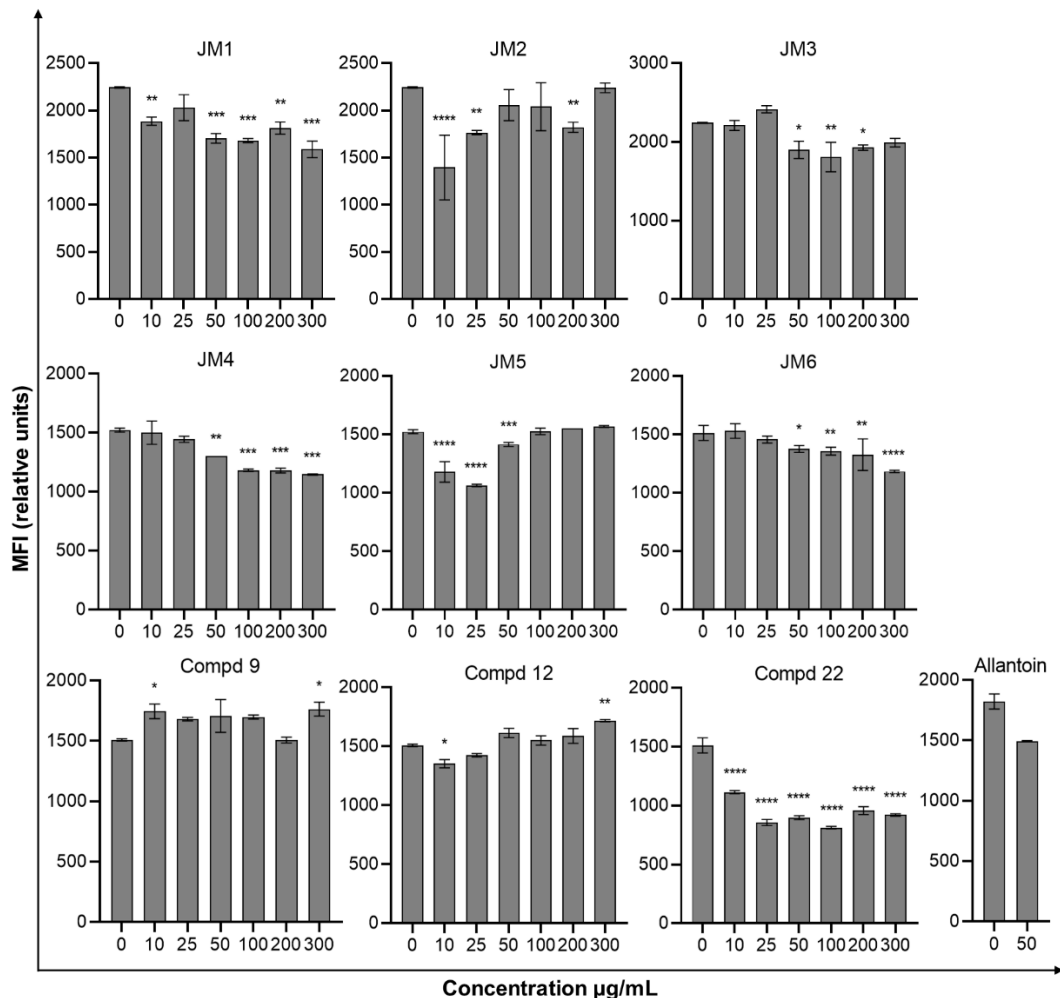


Figure 10. Effect of *J. montana* extracts (**JM1–JM6**) and their main compounds (**9**, **12**, and **22**) (10–300 $\mu\text{g}/\text{mL}$) and allantoin (50 $\mu\text{g}/\text{mL}$) on collagen type I content in fibroblast cells. Data are expressed as the percentage of the median fluorescence intensity compared with the control. Data are presented as the median fluorescence intensity (MFI) from three independent experiments ($n = 3$) performed in duplicate. * $p < 0.05$ versus the control group, ** $p < 0.01$ versus the control group, *** $p < 0.001$ versus the control group, **** $p < 0.0001$ versus the control group.

Inflammation is part of the normal wound healing process; however, in the absence of effective decontamination, this condition can be prolonged with elevated levels of proinflammatory cytokines, such as tumor necrosis factor- α (TNF- α) and its dependent interleukins (ILs) IL-6 and IL-8, as well as IL-1 β . This impedes the healing process by limiting proliferation, skin cell differentiation and collagen deposition at the wound site while synergistically increasing matrix metalloproteinase production [27]. Therefore, the levels of several inflammatory cytokines were evaluated in response to *J. montana* extracts and isolated compounds to assess the immune status of human fibroblast cells. All tested samples showed a complex effect on cytokine secretion that depended both on the cytokine considered and the concentration of the samples tested. The study showed that the tested extracts and compounds exhibited differential activity in modulating the expression levels of IL-1 β and IL-8 (Figure 11 and 13). Among the tested samples, the greatest ability to reduce the secretion of the labelled pro-inflammatory cytokine IL-1 β was observed in the case of the **JM4** at a concentration of 50 $\mu\text{g}/\text{mL}$ (0.5 ± 0.4 pg/mL vs. 13.4 ± 5.6 pg/mL control) and

its main component **22** at a concentration of 100 $\mu\text{g/mL}$ (1.7 ± 1.1 pg/mL vs. 13.4 ± 5.6 pg/mL control). Furthermore, the ability to reduce IL-1 β secretion was observed after treatment with **JM2**, **JM5** and **JM6**, but only at their higher concentrations (100-300 $\mu\text{g/mL}$). In contrast, the reference sample, allantoin, had a significant effect on stimulating pro-inflammatory IL-1 β levels (Figure 11). In the case of the proinflammatory IL-8, treatment with **JM2**, **JM4**, **JM5** and **22** resulted in a pronounced decrease in IL-8 expression. The most significant pro-inflammatory inhibitors proved to be **JM4** and **22** (300 $\mu\text{g/mL}$) undercutting cytokine expression at 154.0 ± 102.8 pg/mL vs. 8396.8 ± 2771.1 pg/mL control and 60.8 ± 8 pg/mL vs. 8396.8 ± 2771.1 pg/mL , respectively. Compared to the results obtained for allantoin (Figure 13) it can be observed that the decrease in IL-8 expression was weaker than for the most active samples tested. The highest increase in the expression level of IL-6, with both pro- and anti-inflammatory properties, appeared for extracts **JM1** (100 $\mu\text{g/mL}$), **JM2** (100 $\mu\text{g/mL}$), and **JM3** (100 $\mu\text{g/mL}$), fractions **JM5** (10 $\mu\text{g/mL}$), and **JM6** (50 $\mu\text{g/mL}$), as well as compounds **9** and **12** (100 $\mu\text{g/mL}$), while **JM4** and **22** induced a decrease in IL-6 below that of the untreated control in a dose-dependent manner (Figure 12). The observed up-regulation of IL-6 is comparable to the results obtained for the positive control. Considering the correlation between quantitative analysis (Table 3) and documented anti-inflammatory activity, it can be concluded that a high content of **22** also relevantly determines **JM4** activity, as well as, to a lesser extent, the activity of the other extracts/fractions (**publication II**).

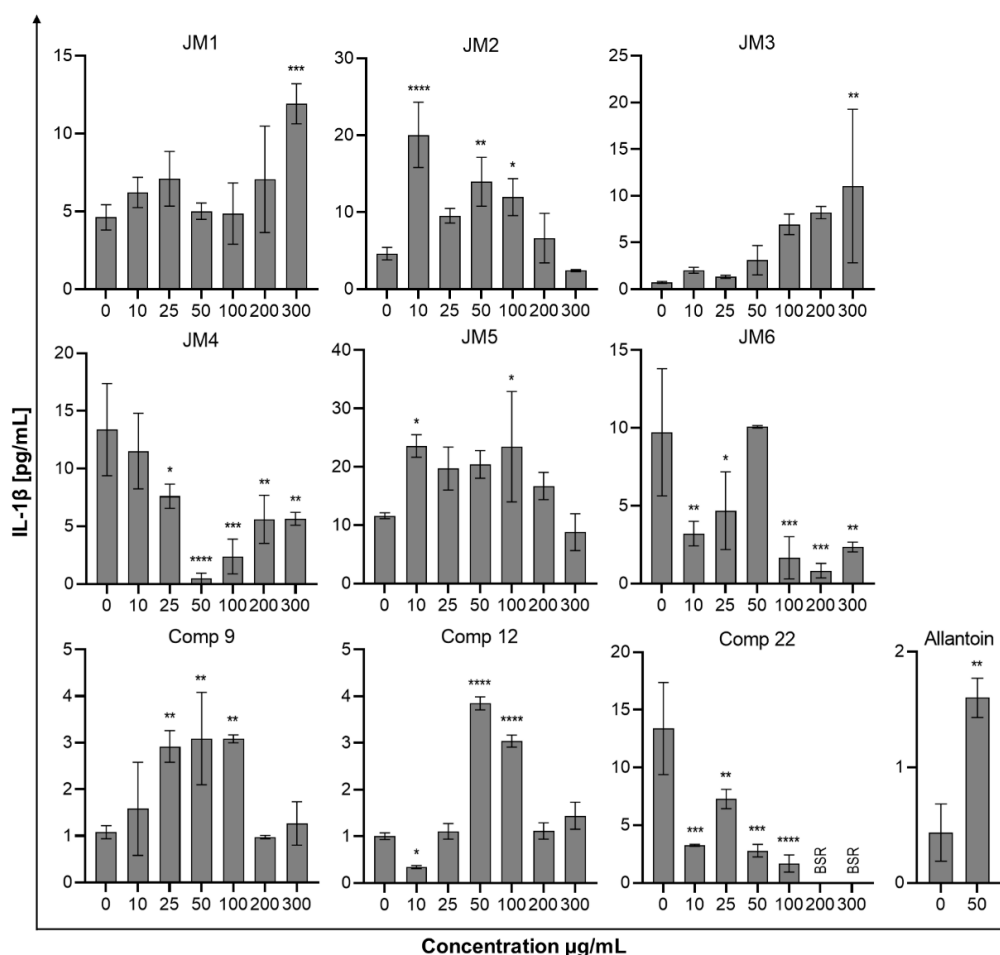


Figure 11. Effects of the *J. montana* extracts **JM1**–**JM6** and their main components (**9**, **12**, and **22**) (10–300 $\mu\text{g/mL}$) and allantoin (50 $\mu\text{g/mL}$) on IL-1 β production inhibition. Mean values from three independent experiments ($n = 3$) performed in duplicate are presented. * $p < 0.05$ versus the control group, ** $p < 0.01$ versus the control group, *** $p < 0.001$ versus the control group, **** $p < 0.0001$ versus the control group. BSR, below the standard range (values lower than the detection limit).

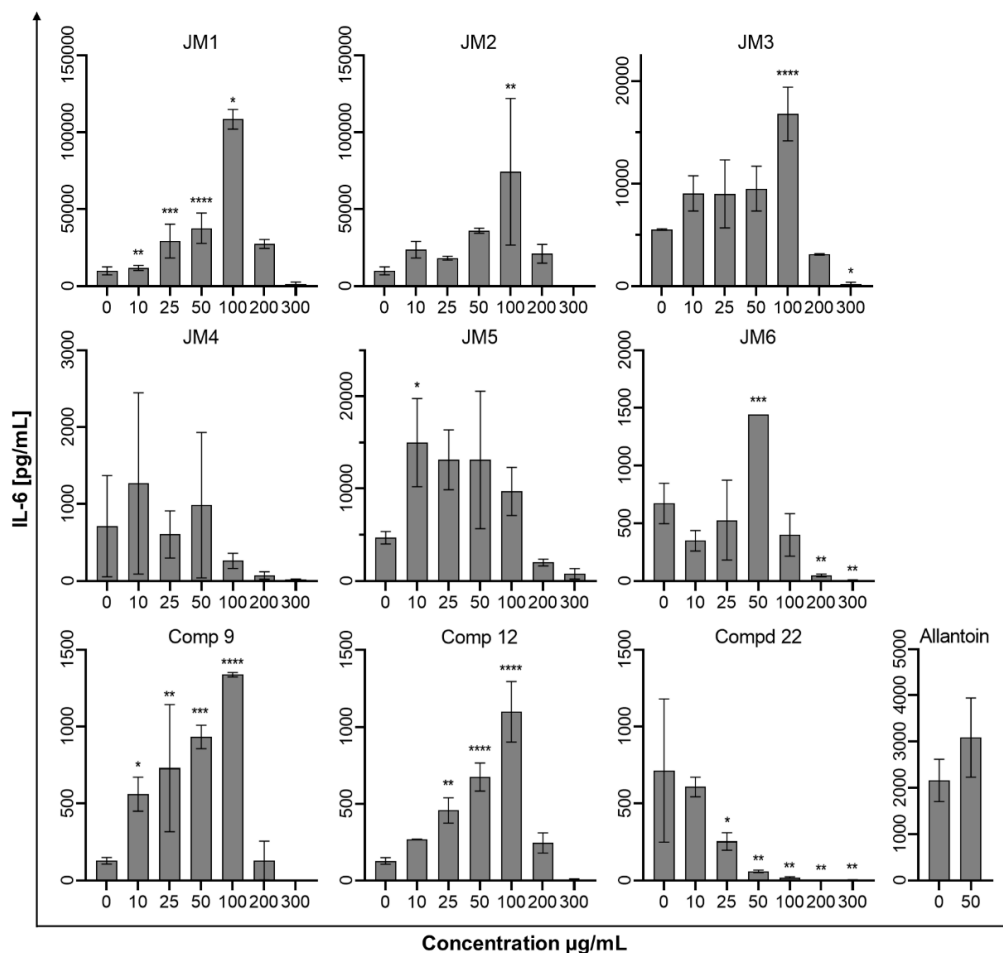


Figure 12. Effects of the *J. montana* extracts **JM1–JM6** and their main compounds (**9**, **12**, and **22**) (10–300 µg/mL) and allantoin (50 µg/mL) on the release of IL-6. Mean values from three independent experiments (n = 3) performed in duplicate are presented. * $p < 0.05$ versus the control group, ** $p < 0.01$ versus the control group, *** $p < 0.001$ versus the control group, **** $p < 0.0001$ versus the control group.

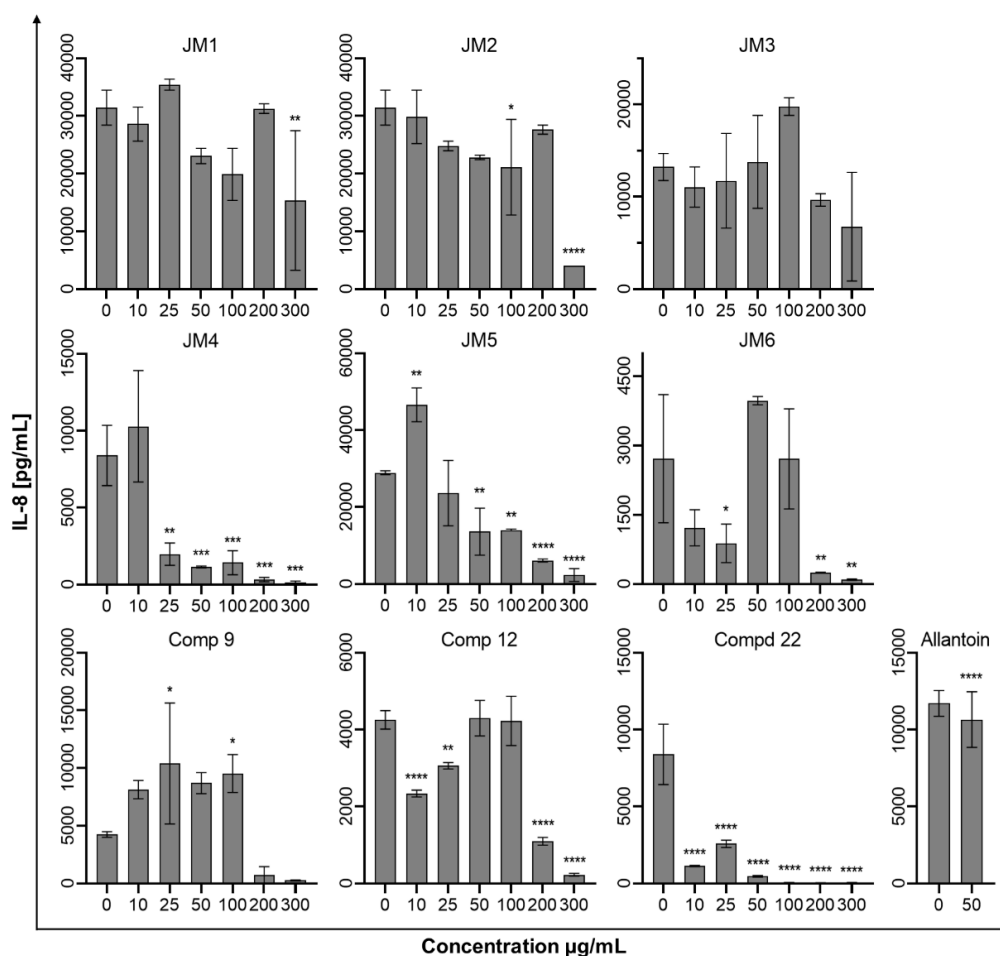


Figure 13. Effects of the *J. montana* extracts **JM1–JM6** and their main flavonoids (**9**, **12**, and **22**) (10–300 µg/mL) and allantoin (50 µg/mL) on IL-8 production inhibition. Mean values from three independent experiments ($n = 3$) performed in duplicate are presented. * $p < 0.05$ versus the control group, ** $p < 0.01$ versus the control group, *** $p < 0.001$ versus the control group, **** $p < 0.0001$ versus the control group.

4.3.6. Statistical analysis

All numerical data are expressed as the mean \pm standard deviation (SD) from at least three independent repeats. The GraphPad Prisma 8 software (GraphPad Software, San Diego, CA, USA) was used for statistical analysis. Statistical differences were assessed using one-way ANOVA followed by Dunnett's multiple comparisons test. Statistically significant values were considered under the condition of $p < 0.05$. The MS Excel 2019 software with the Data Analysis add-on was used for statistical analysis and determination of regression parameter calculations in quantification. The parameters were obtained using ANOVA with a confidence level of 95%.

4.4. Summary and discussion

Based on a review of the literature, it can be concluded that information describing the detailed chemical composition of the aboveground parts of *J. montana* are scarce. Previous reports indicate the presence of two flavonoid compounds, luteolin and cynaroside, in the aboveground parts of *J. montana* [8]. On the other hand, inulin, unspecified flavonoid compounds, alkaloids and an anthocyanin, derivative of delphinidin, were detected in vegetative organs [2]. Ethnopharmacological reports suggest the use of *J. montana* as a sedative in Belarusian traditional folk medicine [7]. Admittedly, the lack of available reports on their potential biological activity prompted a detailed phytochemical profiling and evaluation of the potential pharmacological activity of *J. montana* for the first time for this species.

In the first stage of the study, phytochemical analysis of secondary metabolites was performed. Detailed phytochemical profiling with LC–PDA–ESI–MS/TOF enabled the identification of 25 polyphenolic compounds, mainly flavonoids. The methanol extract (**JM3**), and the diethyl ether fraction (**JM4**) were dominated by free aglycones, predominately luteolin (**22**) and apigenin (**23**). In most of the extracts tested **22** was determined as the dominant component. Moreover, *p*-coumaric acid and its derivatives (**3**, **10**), as well as luteolin 7-*O*-glucoside (**12**) were also detected in **JM4**. The second most represented compound was **12**, and its presence was also detected in glycoside-rich extracts: water (**JM1**) and 50% methanol (**JM2**), as well as in the ethyl acetate fraction (**JM5**). **JM5** also contained diglycosides and triglycosides (**9**, **14**, **15**), and aglycones substituted with a linear glycoside moiety (**9**, **14**). The *n*-butanol fraction (**JM6**) contained a multicomponent mixture of flavonoid glycosides (**publication I**).

The next step of the analysis was an attempt to isolate and identify the processes of compounds belonging to the flavonoid group with potential pharmacological effects. The attempts undertaken to isolate flavonoid compounds led to three pure, homogeneous compounds. According to the detailed UV, TLC, NMR, MS analyses and available literature [14–16], the presence of compounds **12** and **22**, identified as luteolin 7-*O*- β -D-glucoside (cynaroside) and 5,7,3',4'-tetrahydroxyflavone (luteolin), respectively, was confirmed in *J. montana* [8]. Nonetheless, compound **9**, identified by means of the same spectral and spectrometric techniques as luteolin 7-*O*- β -D-xylosyl-(1-2)- β -D-glucoside (luteolin 7-*O*-sambubioside), was for the first time isolated and described within the aboveground parts of *J. montana* (**publication I**).

Chromatography is a powerful tool in the analysis of natural compounds, and its coupling with other analytical methods expands analytical capabilities while improving the accuracy, sensitivity and precision of natural compound determinations, especially in multi-ingredient plant extracts. The conducted review of the literature systematizes and shows that chromatographic techniques have been successfully applied in the analysis of luteolin derivatives. Combinations of large-scale chromatographic techniques with serially aligned detection modalities, such as LC–MS/MS or LC–NMR–MS, have proven particularly useful. The LC method is of predominant practical importance in this group of compounds. A fundamental element of the analysis in a chromatographic system that ensures its effectiveness is the correct and optimized selection of separation conditions. Proper selection of the sorbent stationary phase, its polarity, column diameter, the type of mobile phase used or type of elution are closely related to the efficiency and success of separation. In the analysis of luteolin and its derivatives, according to the available literature, separation is mainly performed using the reversed-phase (RP) system, using a mobile phase consisting of mixtures of acetonitrile and water or, less frequently, methanol and water, in both cases modified by the addition of formic acid or trifluoroacetic acid. In addition, the vast majority of reports document the use of gradient elution (**publication III**).

Based on the conducted review of the literature on the chromatographic techniques used in the determinations of luteolin and its derivatives, the new method of quantification of isolated compounds in *J. montana* extracts and fractions by means of the HPLC–PDA technique was developed and validated. According to the obtained HPLC analyses, luteolin (**22**) was determined as the dominant substance in the **JM4** fraction as well as the **JM1**, **JM2**, and **JM3** extracts, while only the **JM5** and **JM6** fractions did not contain **22**. In addition, **12** was present in most of the tested samples, and its highest amount was recorded in **JM5**. **9** was quantified only in **JM1**, **JM2** and **JM6** (**publication II**).

Continuing the research on the aboveground parts of *J. montana*, the biological activity of extracts and fractions **JM1–JM6** as well as isolated and identified compounds **9**, **12** and **22** was assessed. Firstly, by conducting an evaluation of the anticancer potential, it was shown that, among the tested samples, fraction **JM4** and its main component, compound **22**, decreased the viability of C32 melanoma cells by means of cytotoxic action. At the same time, after treatment with **JM4** and **22**, cell membrane degradation and reduction of melanoma cell population were observed, suggesting inhibition of their proliferation and induction of apoptotic processes. Further experiments were conducted to determine the impact of **JM4** and **22** on cell cycle and apoptotic cell death. It was confirmed that **JM4** and **22** led to cell death through both activations of the extrinsic and intrinsic (mitochondrial) apoptotic pathways. This ability, established by the documented reduction of MMP and the expression of caspase-9, correlated with the intrinsic

apoptotic pathway. Furthermore, increased caspase-8 and caspase-10 potential are indicative of an activated external apoptotic pathway. Both cell death pathways consequently lead to modulation of caspase-3 activity and direct DNA damage, which was also documented after incubation with **JM4** and **22**. Moreover, the isolated compound **22** and the **JM4** fraction had an effect on the number of autophagic cells and showed an increase in the accumulation of cells in the S and G2/M phases of the cell cycle. Cell cycle arrest and induction of apoptosis or autophagy inhibit neoplasm growth and are considered essential aspects of cancer therapy [28,29]. The anticancer effect of the **JM4** fraction can be partly explained by the significant presence of luteolin (**22**), confirmed by qualitative and quantitative analysis (**publication I**). The high antiproliferative activity of luteolin can be correlated with its structural features, especially the presence of the C2-C3 double bond and the oxo group at position C4 of the C ring, and the hydroxyl groups at C5 and C7 of ring A, as well as the catechol group containing two adjacent phenolic OH groups (3', 4'-di-OH) [30] (**publication IV**). However, taking into consideration differences between effects on mitochondrial potential, caspase activation and the apoptosis phase, a synergism of different phytochemical components such as compound **22** and its derivatives should be deliberated (**publication I**).

A review of previous studies, conducted within the framework of the present doctoral research, confirms the anticancer activity in the context of skin cancer in *in vitro* and *in vivo* models of luteolin and its derivatives. The presented effect is a result not only of the mentioned induction of apoptosis, cell cycle disruption or inhibition of proliferation, migration and angiogenesis, but also a multidimensional regulation of epigenetic layers, inhibition of a number of different pathways and expression of many key genes involved in tumor progression. The anticancer potential of this group of flavones correlates with the modulation of signaling proteins and genes involved in, *inter alia*, mutations of the mitogen-activated protein kinase (MAPK) and phosphoinositol-3-kinase (PI3K) oncogenic pathways [31,32]. Furthermore, luteolin and its derivatives also affect cancer cell proliferation and apoptosis through their pro-oxidant properties and ability to inhibit the process of melanogenesis related with the p53 protein [33,34]. Thus, melanogenesis is considered another target of therapy, more specifically eliminating malignant melanocytes. Luteolin and its derivatives, in addition to acting at the level of promotion and progression of carcinogenesis, are also involved in the stage of initiation of this process and the prevention of neoplastic lesions. A large body of evidence suggests that reduced photocarcinogenesis and prevention of skin cancer can be attributed to the antioxidant and anti-inflammatory properties through inhibiting, *inter alia*, further overexpression of the MAPK pathway, nuclear factor kappa-light-chain-enhancer of activated B (NF- κ B) and cyclooxygenase-2 (COX-2) [35] (**publication IV**).

On the other hand, in light of the high polyphenolic compound content, mainly in the form of flavonoids, the decision was made to evaluate the effect of the extracts (**JM1–JM3**) and their fractions (**JM4–JM6**) from *J. montana* as well as their main components (**9**, **12**, **22**) on the skin wound healing process. The fractions with the highest polyphenol content, including flavonoids (**JM4**, **JM5**), showed the highest antioxidant activity in DPPH and FRAP assays, which is supported by the available literature [36]. Furthermore, in an experiment conducted in an *in vitro* model evaluating the level of inhibition of elastase activity, most of the tested samples showed moderate activity. The highest percentage of elastase inhibition was established by compound **22** and the diethyl ether (**JM4**) and ethyl acetate (**JM5**) fractions, characterized by high content of **22**. The biological activity of the extracts and fractions can be correlated with their chemical composition. The chemical structure of the constituents, *e.g.* the *O*-glycosylation at the C7 position of the ring A of the luteolin structure in **9** and **12**, may strongly contribute to the biological activity [37]. The antioxidant properties, often related to the presence of polyphenolic substances, is repeatedly linked to enhanced fibroblast migration [38]. Within the frame of this work, the ability of the tested extracts and compounds to accelerate the proliferation and migration of human dermal fibroblasts in the *in vitro* scratch test was demonstrated. Due to their strong involvement in wound healing, fibroblasts are considered as an important therapeutic target in numerous skin diseases. In the performed experiments, the activity was strictly dependent on the type of dominant compound and, importantly, on its concentration. In addition, among the samples tested, compounds **9** and **12** promoted biosynthesis of collagen type I most strongly, with a concomitant lack of any cytotoxic effect. It was also noted that none of the samples tested had a destructive effect on collagen

content. Previous reports on *in vitro* and *in vivo* models confirm that flavonoids may not only lead to induced fibroblast proliferation, but also stimulate them to synthesize collagen and, presumably, assist in the formation of cross-links as collagen matures [39,40]. Finally, a multistep effect of *J. montana* extracts and fractions as well as their major constituents on the expression of cytokines IL-1 β , IL-6 and IL-8 involved in the immune response phases of wound healing was observed. **JM4** showed the most significant anti-inflammatory effect, as well as other luteolin-rich fractions, which correlates with available data from the literature [9] (**publication II**).

From the studies performed within the framework of the present doctoral dissertation, it appears that *Jasione montana*, rich in flavonoid compounds (mainly luteolin and its derivatives), exhibits significant cytotoxic and proapoptotic potential against melanoma cells. The plant extracts and their phytochemical components also influence the processes involved in wound healing, making it potentially useful for topical therapeutic application, for the development of new preparations with potential anticancer properties, as well as for stimulation of the wound healing process. However, this potential activity shown in *in vitro* models needs to be further clarified in order to understand the molecular mechanisms in each cell and to analyze the selectivity, efficacy, and pharmacological and toxicological properties. These are pivotal aspects in linking *in vitro* and *in vivo* laboratory studies with possible clinical trials. Additionally, there is a need to develop a suitable pharmaceutical formulation that ensures proper penetration, biochemical stability, bioavailability, and controlled release of the drug in the target tissue.

4.5. Abbreviations

CH ₃ COOH	acetic acid
CHCl ₃	chloroform
COX-2	cyclooxygenase-2
DPPH	2,2-diphenyl-1-picrylhydrazyl
ECM	extracellular matrix
ESI	electrospray ionization
Et ₂ O	diethyl ether
EtOAc	ethyl acetate
FRAP	ferric reducing antioxidant potential
H ₂ O	water
HCOOH	formic acid
HPLC	high-performance liquid chromatography
IC ₅₀	median inhibitory concentration
ILs	interleukins
JM1	water extract from <i>J. montana</i>
JM2	50% methanol extract from <i>J. montana</i>
JM3	methanol extract from <i>J. montana</i>
JM4	diethyl ether fraction from <i>J. montana</i>
JM5	ethyl acetate fraction from <i>J. montana</i>
JM6	<i>n</i> -butanol fraction from <i>J. montana</i>
LC	liquid chromatography
LOD	limit of detection
LOQ	limit of quantification
LPLC	low pressure liquid chromatography
MAPK	mitogen-activated protein kinase pathway
MeCN	acetonitrile
MeOH	methanol
MFI	median fluorescence intensity
MMP	mitochondrial membrane potential
MS	mass spectrometry
MS/MS	tandem mass spectrometry
<i>n</i> -BuOH	<i>n</i> -butanol
NF- κ B	nuclear factor kappa-light-chain-enhancer of activated B

NMR	nuclear magnetic resonance
PDA	photodiode array detection
PI	propidium iodide
PI3K	phosphoinositol-3-kinase pathway
PS	phosphatidylserine
RP	reversed-phase
SD	standard deviation
TLC	thin layer chromatography
TNF- α	tumor necrosis factor- α
UPW	ultra-pure water
UV-VIS	ultraviolet-visible spectroscopy
VLB	vinblastine sulfate

Chapter 5. Conclusion

- The qualitative and quantitative content of polyphenolic compounds in extracts and their fractions from the aboveground parts of *Jasione montana* L. (Campanulaceae) was described. Attempts to isolate flavonoid compounds led to the isolation and full structural characterization of three biologically active compounds, luteolin and its derivatives.
- Luteolin 7-*O*-sambubioside was isolated and described for the first time from the studied plant material.
- Extracts and their fractions obtained from the *J. montana* herb were shown to have significant cytotoxic and proapoptotic potential against cutaneous melanoma cells, both at the morphological and metabolic level. This type of activity can be attributed to the high content of polyphenolic compounds, especially flavone aglycone - luteolin.
- According to the results, extracts and fractions obtained from *J. montana* were shown to possess significant antioxidant, anti-inflammatory potential, moderate elastase inhibition and collagen biosynthesis activity. Additionally, by evaluating mechanisms focusing on multiple phases of the dynamic wound healing process, the ability to improve fibroblast viability and migration was also observed. Some of these activities can be attributed to the high content of main compounds, although the efficacy of some fractions suggests the presence of other biologically active compounds. These mechanisms focus on multiple phases of the dynamic wound healing process, making them major factors in promoting wound healing.
- The isolated substances, as well as the extracts and fractions from the aboveground parts of *J. montana*, may provide a potential strategy for the development of topical therapeutic formulations with potential anticancer and/or wound healing stimulating properties.
- Further studies are required, in particular using an *in vivo* model and in the human system to determine the level of safety and the exact cellular mechanism, distribution and effects on the skin after long-term exposure.

Chapter 6. References

1. Linné, C. *Spedies Plantarum*; 1 edition.; Impensis Laurentii Salvii: Holmiæ (Stockholm), Sweden, **1753**
2. Parnell, J.A.N. Biological flora of the British Isles. *J. Ecol.* **1985**, *73*, 341–358.
3. Parnell, J. Variation in *Jasione montana* L. (Campanulaceae) and related species in Europe and North Africa. *Watsonia* **1987**, *16*, 249–267.
4. Sales, F.; Hedge, I.C.; Preston, J.; Moeller, M. *Jasione* L. taxonomy and phylogeny. *Turk. J. Bot.* **2004**, *28*, 253–259.
5. Cai, Y.; Ma, L.Q. Metal tolerance, accumulation, and detoxification in plants with emphasis on arsenic in terrestrial plants. In *Biogeochemistry of Environmentally Important Trace Elements*; Eds.: Cai, Y., Braids, O.C. ACS Symposium Series: Washington, USA, **2002**.
6. García-Salgado, S.; García-Casillas, D.; Quijano-Nieto, M.A.; Bonilla-Simón, M.M. Arsenic and heavy metal uptake and accumulation in native plant species from soils polluted by mining activities. *Wat. Air Soil Poll.* **2012**, *223*, 559–572.
7. Trojanowska, A. Traditional belarussian herbal medicine in Michał Federowski's study: lud białoruski na Rusi Litewskiej. *Analecta* **2007**, *16*, 7.
8. Zapesochnaya, G.G.; Nikolaeva, V.G.; Ban'kovskii, A.I. The flavonoids of *Jasione montana* and *Melittis sarmatika*. *Chem. Nat. Compd.* **1972**, *8*, 112.
9. López-Lázaro, M. Distribution and biological activities of the flavonoid luteolin. *Mini Rev. Med. Chem.* **2009**, *9*, 31–59.
10. Chinembiri, T.N.; Du Plessis, L.H.; Gerber, M.; Hamman, J.H.; Du Plessis, J. Review of natural compounds for potential skin cancer treatment. *Molecules* **2014**, *19*, 11679–11721.
11. Chahar, M.K.; Sharma, N.; Dobhal, M.P.; Joshi, Y.C. Flavonoids: a versatile source of anticancer drugs. *Pharmacogn. Rev.* **2011**, *5*, 1–12.
12. Imran, M.; Rauf, A.; Abu-Izneid, T.; Nadeem, M.; Shariati, M.A.; Khan, I.A.; Imran, A.; Orhan, I.E.; Rizwan, M.; Atif, M.; et al. Luteolin, a flavonoid, as an anticancer agent: a review. *Biomed. Pharmacother.* **2019**, *112*, 108612.
13. Rutkowski, L. *Klucz Do Oznaczania Roślin Naczyniowych Polski Niżowej*; Wydawnictwo Naukowe PWN: Warsaw, Poland, **2006**.
14. Agrawal, P.K. *Carbon-13 NMR of Flavonoids*; Elsevier: Amsterdam, The Netherlands, **1989**.
15. Harborne, J.B. *The Flavonoids. Advances in Research Since 1986*; Chapman & Hall: London, UK, **1996**.
16. Markham, K.R.; Ternai, B.; Stanley, R.; Geiger, H.; Mabry, T.J. Carbon-13 NMR Studies of Flavonoids—III. *Tetrahedron* **1978**, *34*, 1389–1397.
17. Chan, K.T.; Meng, F.Y.; Li, Q.; Ho, C.Y.; Lam, T.S.; To, Y.; Lee, W.H.; Li, M.; Chu, K.H.; Toh, M. Cucurbitacin B induces apoptosis and S phase cell cycle arrest in BEL-7402 human hepatocellular carcinoma cells and is effective *via* oral administration. *Cancer Lett.* **2010**, *294*, 118–124.
18. Demchenko, A.P. Beyond annexin V: fluorescence response of cellular membranes to apoptosis. *Cytotechnology* **2013**, *65*, 157–172.
19. Bialik, S.; Dasari, S.K.; Kimchi, A. Autophagy-dependent cell death – where, how and why a cell eats itself to death. *J. Cell Sci.* **2018**, *131*, jcs215152.
20. Green, D.R.; Kroemer, G. The pathophysiology of mitochondrial cell death. *Science* **2004**, *305*, 626–629.
21. Denault, J.-B.; Salvesen, G. Caspases: keys in the ignition of cell death. *Chem. Rev.* **2003**, *102*, 4489–4500.
22. Addis, R.; Cruciani, S.; Santaniello, S.; Bellu, E.; Sarais, G.; Ventura, C.; Maioli, M.; Pintore, G. Fibroblast proliferation and migration in wound healing by phytochemicals: evidence for a novel synergic outcome. *Int. J. Med. Sci.* **2020**, *17*, 1030–1042.
23. Bainbridge, P. Wound healing and the role of fibroblasts. *J. Wound Care* **2013**, *22*, 407–412.
24. Marume, A.; Matope, G.; Katsande, S.; Khoza, S.; Mutingwende, I.; Mduluza, T.; Munodawafa-Taderera, T.; Ndhkala, A.R. Wound healing properties of selected plants used

- in ethnoveterinary medicine. *Front. Pharmacol.* **2017**, *8*, 544.
25. Tracy, L.E.; Minasian, R.A.; Caterson, E.J. Extracellular matrix and dermal fibroblast function in the healing wound. *Adv. Wound Care* **2016**, *5*, 119–136.
 26. Liang, C.-C.; Park, A.Y.; Guan, J.-L. *In vitro* scratch assay: a convenient and inexpensive method for analysis of cell migration *in vitro*. *Nat. Protoc.* **2007**, *2*, 329–333.
 27. Barrientos, S.; Stojadinovic, O.; Golinko, M.S.; Brem, H.; Tomic-Canic, M. Growth factors and cytokines in wound healing. *Wound Repair Regen.* **2008**, *16*, 585–601.
 28. Simões, M.C.F.; Sousa, J.J.S.; Pais, A.A.C.C. Skin cancer and new treatment perspectives: a review. *Cancer Lett.* **2015**, *357*, 8–42.
 29. Liu, H.; He, Z.; Simon, H.-U. Targeting autophagy as a potential therapeutic approach for melanoma therapy. *Semin. Cancer Biol.* **2013**, *23*, 352–360.
 30. Yáñez, J.; Vicente, V.; Alcaraz, M.; Castillo, J.; Benavente-García, O.; Canteras, M.; Lozano Teruel, J.A. Cytotoxicity and antiproliferative activities of several phenolic compounds against three melanocytes cell lines: relationship between structure and activity. *Nutr. Cancer* **2004**, *49*, 191–199.
 31. Penta, D.; Somashekar, B.S.; Meeran, S.M. Epigenetics of skin cancer: interventions by selected bioactive phytochemicals. *Photodermatol. Photoimmunol. Photomed.* **2018**, *34*, 42–49.
 32. Jiang, W.; Xia, T.; Liu, C.; Li, J.; Zhang, W.; Sun, C. Remodeling the epigenetic landscape of cancer-application potential of flavonoids in the prevention and treatment of cancer. *Front. Oncol.* **2021**, *11*, 705903.
 33. Kim, J.K.; Kang, K.A.; Ryu, Y.S.; Piao, M.J.; Han, X.; Oh, M.C.; Boo, S.J.; Jeong, S.U.; Jeong, Y.J.; Chae, S.; et al. Induction of endoplasmic reticulum stress *via* reactive oxygen species mediated by luteolin in melanoma cells. *Anticancer Res.* **2016**, *36*, 2281–2289.
 34. Bu, J.; Ma, P.C.; Chen, Z.Q.; Zhou, W.Q.; Fu, Y.J.; Li, L.J.; Li, C.R. Inhibition of MITF and tyrosinase by paeonol-stimulated JNK/SAPK to reduction of phosphorylated CREB. *Am. J. Chin. Med.* **2008**, *36*, 245–263.
 35. Horváthová, K.; Chalupa, I.; Šebová, L.; Tóthová, D.; Vachálková, A. Protective effect of quercetin and luteolin in human melanoma HMB-2 cells. *Mutat. Res. - Genet. Toxicol. Environ. Mutagen.* **2005**, *565*, 105–112.
 36. Sulaiman, M.; Tijani, I.H.; Abubakar, B.M.; Haruna, S.; Hindatu, Y.; Mohammed, J.N.; Idris, A. An overview of natural plant antioxidants: analysis and evaluation. *Adv. Biochem.* **2013**, *1*, 64–72.
 37. Jakimiuk, K.; Gesek, J.; Atanasov, A.G.; Tomczyk, M. Flavonoids as inhibitors of human neutrophil elastase. *J. Enzyme Inhib. Med. Chem.* **2021**, *36*, 1016–1028.
 38. Comino-Sanz, I.M.; López-Franco, M.D.; Castro, B.; Pancorbo-Hidalgo, P.L. The role of antioxidants on wound healing: a review of the current evidence. *J. Clin. Med.* **2021**, *10*, 3558.
 39. Bayrami, Z.; Hajiaghaee, R.; Khalighi-Sigaroodi, F.; Rahimi, R.; Farzaei, M.H.; Hodjat, M.; Baeeri, M.; Rahimifard, M.; Navaei-Nigjeh, M.; Abdollahi, M. Bio-guided fractionation and isolation of active component from *Tragopogon graminifolius* based on its wound healing property. *J. Ethnopharmacol.* **2018**, *226*, 48–55.
 40. Lodhi, S.; Jain, A.; Jain, A.P.; Pawar, R.S.; Singhai, A.K. Effects of flavonoids from *Martynia annua* and *Tephrosia purpurea* on cutaneous wound healing. *Avicenna J. Phytomed.* **2016**, *6*, 578–591.

Chapter 7. Summary

Sheep's bit scabious (*Jasione montana* L.) (bellflower, Campanulaceae), growing in sandy habitats in woodlands and forest-steppe areas, is a biennial stalk plant commonly found in Europe. Taking into account the scarce information on the phytochemical profile and pharmacological potential of *J. montana*, as well as low soil quality requirements, experimental work was undertaken to determine the chemical composition and biological activity of the *J. montana* herb. At the first stage of the study, a detailed qualitative analysis of the obtained extracts (**JM1–JM3**) and their fractions (**JM4–JM6**) was carried out using the LC–PDA–ESI–MS/TOF method, which resulted in the determination of the presence of 25 polyphenolic compounds – mainly flavonoids. Subsequently, an attempt was made to isolate compounds with potential pharmacological effects. As a result, three homogeneous, chromatographically pure compounds were obtained, and their full structural characterization was established based on the following spectral analyses: UV, ¹H and ¹³C NMR, and MS. The isolated compounds were identified as luteolin (compound **22**), luteolin 7-*O*-glucoside (compound **12**), as well as luteolin 7-*O*-sambubioside (compound **9**), which was isolated and described for the first time in the *J. montana* species. Based on a validated new method for quantification of the isolated compounds, compounds **22** and **12** were identified as the predominant compounds in **JM4**, while **22** and other flavonoid derivatives were found to be predominant in **JM4**. In subsequent steps, the biological activity of the extracts, fractions (**JM1–JM6**) and their main compounds (**9**, **12**, **22**) from *J. montana* were examined. Based on the results obtained in an *in vitro* model of C32 cutaneous melanoma cells, the **JM4** fraction and its predominant compound **22** were assigned strong cytotoxic activity, represented by IC₅₀ values of 119.7±3.2 µg/mL and 95.1±7.2 µg/mL, respectively. Moreover, the pro-apoptotic potential of the aforementioned fraction and its major component was established by cytometric determination of the apoptosis phase, mitochondrial membrane potential (MMP) and expression of caspase-3, -8, -9 and -10. The **JM4** fraction was able to significantly reduce MMP in C32 cells, which was consistent with a significant percentage of cells in the early and later apoptosis phase documented by annexin V staining. Furthermore, the determination of caspase-9 activity confirmed activation of the intrinsic (mitochondrial) apoptosis pathway. Based on the observed increased expression of caspase-8 and caspase-10 under the influence of **JM4** and its major component, **22**, their effect on the extrinsic apoptotic pathway was assessed. Final confirmation of the pro-apoptotic activity was obtained through the determination of caspase-3, directly leading to DNA degradation and cancer cell death. In the next stage, the effect of *J. montana* extracts, fractions and isolated compounds on the mechanisms involved in the skin repair process was evaluated. Among all tested samples, fractions **JM4** and **JM5**, which had the highest content of polyphenolic compounds, showed significant antioxidant potential in the DPPH and FRAP assays, as well as the highest elastase inhibition capacity. All tested extracts, fractions and isolated compounds were able to stimulate human skin fibroblast cell migration and proliferation in an *in vitro* "scratch" model. However, the effect on collagen synthesis was limited, and so a lack of collagen type I degradation was observed as concentration increased. Furthermore, anti-inflammatory potential was documented through the observed ability of compound **22** and fractions in which it was present, especially **JM4**, to modulate the expression of pro- and anti-inflammatory cytokines (IL-1β, IL-6 and IL-8), confirming the relationship between the content of flavonoid compounds and the activity of individual extracts/fractions. In conclusion, the research carried out for the purposes of the present dissertation suggests a potential application of the aboveground parts of *Jasione montana* in the development of new topical therapeutic preparations with potential anticancer and/or wound healing stimulating properties. However, further research on the molecular mechanism, selectivity, metabolism or toxicological properties of the plant material and compounds of natural origin in an *in vivo* model, as well as for the purposes of developing a suitable formulation, are necessary.

Chapter 8. Streszczenie w języku polskim

Jasieniec piaskowy (*Jasione montana* L.) (dzwonkowate, Campanulaceae), porastający siedliska piaszczyste terenów leśnych i leśno-stepowych, jest dwuletnią byliną powszechnie spotykaną na terenie Europy. Biorąc pod uwagę jedynie szczątkowe informacje o profilu fitochemicznym oraz potencjale farmakologicznym jasiońca piaskowego, jak również niskie wymagania glebowe, podjęto prace badawcze mające na celu ustalenie składu chemicznego oraz aktywności biologicznej ziela *J. montana*. W pierwszym etapie badań przeprowadzono szczegółową analizę jakościową otrzymanych wyciągów (**JM1–JM3**) i ich frakcji (**JM4–JM6**) metodą LC–PDA–ESI–MS/TOF, w wyniku której określono obecność 25 związków polifenolowych, głównie o charakterze połączeń flawonoidowych. Następnie podjęto się próby izolacji związków o potencjalnym aspekcie farmakologicznym, w wyniku której uzyskano trzy jednorodne, chromatograficznie czyste związki, których pełną charakterystykę strukturalną ustalono na podstawie następujących analiz spektralnych, UV, ¹H i ¹³C NMR, MS. Wyizolowane związki zidentyfikowano jako luteolinę (związek **22**), 7-*O*-glukozyd luteoliny (związek **12**), jak również 7-*O*-sambubiozyd luteoliny (związek **9**) wyizolowany i opisany po raz pierwszy w gatunku *J. montana*. Na podstawie zwalidowanej, nowej metody oznaczeń ilościowej zawartości wyizolowanych związków, zidentyfikowano związki **22** i **12** jako dominujące w **JM4**, zaś **22** i innych pochodnych flawonoidowych w **JM4**. W kolejnych etapach określono aktywność biologiczną wyciągów, frakcji (**JM1–JM6**) i ich głównych związków (**9**, **12**, **22**) z *J. montana*. Na podstawie wyników uzyskanych w badaniach w modelu *in vitro* nad komórkami czerniaka skóry C32, przypisano frakcji **JM4** oraz jej dominującemu związkowi **22** silną aktywność cytotoksyczną reprezentowaną przez wartości IC₅₀ równymi odpowiednio, 119,7±3,2 µg/mL oraz 95,1±7,2 µg/mL. Co więcej, ustalono potencjał proapoptyczny wspomnianej frakcji i jej głównego składnika, na podstawie cytometrycznego oznaczenia fazy apoptozy, aktywności potencjału mitochondrialnego MMP oraz ekspresji kaspazy-3, -8, -9 i -10. Frakcja **JM4** była zdolna do znaczącej redukcji MMP w komórkach C32, co było zgodne ze znaczącym odsetkiem komórek w fazie wczesnej i później apoptozy udokumentowanym w barwieniu aneksyną V. Ponadto, oznaczenie aktywności kaspazy-9 potwierdziło aktywację wewnętrznej (mitochondrialnej) ścieżki apoptozy. Na podstawie obserwowanej zwiększonej ekspresji kaspazy-8 i kaspazy-10 pod wpływem **JM4** i jej głównego składnika, **22**, oceniono ich wpływ na zewnętrzną drogę apoptozy. Ostateczne potwierdzenie aktywności proapoptycznej uzyskano na podstawie oznaczenia kaspazy-3, bezpośrednio prowadzącej do degradacji DNA i śmierci komórek nowotworowych. W kolejnym etapie oceniono, wpływ ekstraktów, frakcji *J. montana* oraz wyizolowanych związków na mechanizmy uczestniczące w procesie naprawczym skóry. Spośród wszystkich badanych próbek, frakcje (**JM4**, **JM5**), o najwyższej zawartości związków polifenolowych, cechowały się znaczącym potencjałem antyoksydacyjnym w teście DPPH oraz FRAP, jak również najwyższą zdolnością inhibicji elastazy. Wszystkie badane ekstrakty/frakcje oraz wyizolowane związki były zdolne do stymulacji migracji i proliferacji fibroblastów skóry ludzkiej w modelu „zadrapania” *in vitro*. Jednakże, wpływ na syntezę kolagenu był ograniczony, a jednocześnie nie zaobserwowano, wraz ze wzrostem stężenia, znacznej degradacji kolagenu. Ponadto, udokumentowano potencjał przeciwwzapalny poprzez obserwowaną zdolność związku **22** oraz frakcji o jego zawartości, zwłaszcza **JM4**, do modulacji ekspresji cytokin pro- i przeciwwzapalnych (IL-1β, IL-6 i IL-8), potwierdzając związek między zawartością związków flawonoidowych, a aktywnością poszczególnych ekstraktów/frakcji. Podsumowując, przeprowadzone w ramach prezentowanej rozprawy doktorskiej badania sugerują potencjalne zastosowanie nadziemnych części jasiońca piaskowego w opracowaniu nowych, miejscowych preparatów terapeutycznych o potencjalnych właściwościach przeciwnowotworowych i/lub stymulujących gojenie ran. Konieczne są jednak dalsze badania nad określeniem mechanizmu molekularnego, selektywności, metabolizmu, czy też właściwości toksykologicznych materiału roślinnego i związków pochodzenia naturalnego w modelu *in vivo*, jak również opracowanie odpowiedniej postaci preparatu.

Chapter 9. Copies of publications comprising the doctoral dissertation

Publication I

Juszczak A.M., Czarnomysy R., Strawa J.W., Zovko Končić M., Bielawski K., Tomczyk M.: *In vitro* anticancer potential of *Jasione montana* and its main components against human amelanotic melanoma cells. *International Journal of Molecular Sciences* Vol. 22, ID 3345, 2021, 25 pages. DOI: 10.3390/ijms22073345



Article

In Vitro Anticancer Potential of *Jasione montana* and Its Main Components Against Human Amelanotic Melanoma Cells

Aleksandra Maria Juszcak ¹, Robert Czarnomysy ², Jakub Władysław Strawa ¹, Marijana Zovko Končić ³, Krzysztof Bielawski ² and Michał Tomczyk ^{1,*}

- ¹ Department of Pharmacognosy, Faculty of Pharmacy with the Division of Laboratory Medicine, Medical University of Białystok, ul. Mickiewicza 2a, 15-230 Białystok, Poland; aleksandra.juszcak@umb.edu.pl (A.M.J.); jakub.strawa@umb.edu.pl (J.W.S.)
² Department of Synthesis and Technology of Drugs, Faculty of Pharmacy with the Division of Laboratory Medicine, Medical University of Białystok, ul. Kilińskiego 1, 15-089 Białystok, Poland; robert.czarnomysy@umb.edu.pl (R.C.); kbiel@umb.edu.pl (K.B.)
³ Department of Pharmacognosy, Faculty of Pharmacy and Biochemistry, University of Zagreb, Marulićev trg 20/II, 10000 Zagreb, Croatia; mzovko@pharma.hr
* Correspondence: michal.tomczyk@umb.edu.pl; Tel.: +48-85-748-56-94



Citation: Juszcak, A.M.; Czarnomysy, R.; Strawa, J.W.; Zovko Končić, M.; Bielawski, K.; Tomczyk, M. In Vitro Anticancer Potential of *Jasione montana* and Its Main Components Against Human Amelanotic Melanoma Cells. *Int. J. Mol. Sci.* **2021**, *22*, 3345. <https://doi.org/10.3390/ijms22073345>

Academic Editor: Gi-Young Kim

Received: 15 March 2021

Accepted: 23 March 2021

Published: 25 March 2021

Publisher's Note: MDPI stays neutral with regard to jurisdictional claims in published maps and institutional affiliations.



Copyright: © 2021 by the authors. Licensee MDPI, Basel, Switzerland. This article is an open access article distributed under the terms and conditions of the Creative Commons Attribution (CC BY) license (<https://creativecommons.org/licenses/by/4.0/>).

Abstract: *Jasione montana* L. (Campanulaceae) is used in traditional Belarusian herbal medicine for sleep disorders in children, but the chemical composition and biological activity have not been investigated. In this study, the activities of *J. montana* extracts, their fractions and main compounds were evaluated in amelanotic melanoma C32 (CRL-1585) cells and normal fibroblasts (PCS-201-012). The extracts and fractions were analyzed using liquid chromatography–photodiode array detection–electrospray ionization–mass spectrometry (LC–PDA–ESI–MS/TOF) to characterize 25 compounds. Further, three major and known constituents, luteolin (**22**) and its derivatives such as 7-*O*-glucoside (**12**) and 7-*O*-sambubioside (**9**) were isolated and identified. The cytotoxic activities against fibroblasts and the amelanotic melanoma cell line were determined using the fixable viability stain (FVS) assay. The influence of diethyl ether (Et₂O) fraction (**JM4**) and **22** on apoptosis induction was investigated using an annexin V binding assay. The obtained results showed significant cytotoxicity of **JM4** and **22** with IC₅₀ values of 119.7 ± 3.2 and 95.1 ± 7.2 µg/mL, respectively. The proapoptotic potential after **22** treatment in the C32 human amelanotic melanoma cell line was comparable to that of vinblastine sulfate (VLB), detecting 29.2 ± 3.0% apoptotic cells. Moreover, **22** displayed less necrotic potential against melanoma cells than VLB. In addition, the influences of **JM4** and **22** on the dysfunction of the mitochondrial membrane potential (MMP), cell cycle and activity of caspases 3, 8, 9, and 10 were established. The effects of **JM4** on MMP change (74.5 ± 3.0% of the cells showed a reduced MMP) corresponded to the results obtained from the annexin V binding assay and activation of caspase-9. **JM4** and **22** displayed a significant impact on caspase-9 (40.9 ± 2.4% of the cells contained active caspase-9 after **JM4** treatment and 16.6 ± 0.8% after incubation with **22**) and the intrinsic (mitochondrial) apoptotic pathway. Moreover, studies have shown that **JM4** and **22** affect the activation of external apoptosis pathways by inducing the caspase-8 and caspase-10 cascades. Thus, activation of caspase-3 and DNA damage via external and internal apoptotic pathways were observed after treatment with **JM4** and **22**. The obtained results suggest that *J. montana* extracts could be developed as new topical preparations with potential anticancer properties due to their promising cytotoxic and proapoptotic potential.

Keywords: *Jasione montana*; Campanulaceae; flavonoids; luteolin derivatives; fibroblasts; melanoma

1. Introduction

Skin cancers are the most common type of human cancer, with dramatically increasing incidence and mortality rates. The World Health Organization (WHO, Geneva, Switzerland) reports that globally, approximately 3 million skin cancers occur annually, of which less than

6% are melanomas [1]. Cutaneous malignant melanoma (CMM) developed by transformed melanocytes proliferating from the basal area of the epidermis, is the most aggressive form of diagnosed skin cancer [2,3]. Even though the incidence of melanoma is relatively low, its mortality is the highest among all skin cancers [4]. Although several new drugs have been developed over the last 10 years that have greatly improved the prognosis of patients with metastatic melanoma, many patients do not show a lasting response to these treatments [5]. Treatment with natural compounds and preparations based on plant materials have been increasingly used among patients with various neoplasms [6–8], and natural product-based treatments for melanoma are constantly being researched [9,10].

Jasione montana L., commonly known as Sheep's bit scabious, is one of 16 representatives of the genus *Jasione* L. (Campanulaceae). The presence of *J. montana* outside of Europe, the Scandinavian Peninsula, Great Britain, and Ireland has been established, inter alia, in Morocco, Tunisia, Algeria, Russia, and Turkey, as well as in the northeastern region of the United States. It is a biennial plant, or occasionally, an annual plant, mainly found in warmer, sunny or semiarid places in lowland and upland regions. The determining factors for the distribution of *J. montana* are the temperature and average precipitation per year [11,12]. *J. montana* has been recognized as a garden plant [11]. Ethnopharmacological reports regarding this traditional Belarusian herbal medicine state that *J. montana* is used to treat sleep disorders in children, although its biological activity has not yet been assessed [13]. The available scientific literature on *J. montana* is scarce, and little is known about its phytochemical composition. A previous study of the aerial parts of *J. montana* established the presence of the bioactive flavonoid luteolin [14]. Taking these aspects into consideration, a detailed phytochemical analysis and characterization of the *J. montana* aerial parts was undertaken. Furthermore, the activities of the extracts, their fractions and isolated compounds against a human amelanotic melanoma cell line were investigated.

2. Results

2.1. LC–ESI–MS Analysis of Extracts JM1–JM3 and Fractions JM4–JM6

The phytochemical analysis, based on liquid chromatography–photodiode array detection–electrospray ionization–mass spectrometry (LC–PDA–ESI–MS/TOF) technique, results of the extracts (H₂O, JM1; 50% MeOH, JM2; MeOH, JM3), and their fractions (Et₂O, JM4; EtOAc, JM5; *n*-BuOH, JM6) revealed 25 polyphenolic compounds. Extraction of the raw material with MeOH (JM3) resulted in a high content of free aglycones [peaks 22–25], among which luteolin (22) was the dominant peak. The second most represented compound was luteolin 7-*O*-glucoside (12). On the other hand, JM1 and JM2 were rich in glycosides, and the hydromethanolic extractant was the more efficient of the two solutions. The studied fractions (JM4–JM6) were characterized by the selectivity of the extraction process for specific groups of compounds. JM4 turned out to be rich in aglycones with a dominance of 22 as well as apigenin (23) and 12. Moreover, *p*-coumaric acid and its derivatives were also present in this fraction [peaks 3, 10]. An absorption maximum at 310 nm in the ultraviolet-visible (UV-VIS) spectrum is characteristic for these types of compounds. Compound 12 was also significantly dominated in the JM5 fraction. The presence of di- and triglycosides was also revealed [peaks 9, 14, 15]. These compound structures were suggested based on the loss of fragments $[M - 162 \pm H]^{+/-}$, $[M - 146 \pm H]^{+/-}$, and $[M - 132 \pm H]^{+/-}$, which correspond to *O*-hexose, *O*-pentose, and *O*-deoxyhexose, respectively. Moreover, aglycones substituted with a linear glycoside molecule [peaks 9, 14] as well as disubstituted compounds were present in the JM5 fraction [peak 15]. JM6 consisted of a mixture of flavonoid glycosides and was devoid of free aglycones. The LC–MS analysis is summarized in Table 1 and Supplementary Figures S1 and S2.

Table 1. Liquid chromatography–mass spectrometry (LC–MS) analysis of extracts/fractions (**JM1–JM6**) from *Jasione montana*.

Peak/Compound	Rt (min)	UV-VIS Maxima (nm)	[M–H] [–] Ions (m/z)	[M–H] ⁺ Ions (m/z)	Identified Compounds
1	4.60	260	191, 217, 235	86, 136, 276	Unknown
2	14.53	260, 294	109 , 153, 277	93, 137 , 213, 248	Unknown
3	19.29	256, 310 sh	93 , 183	94 , 302	<i>p</i> -coumaroyl acid derivatives
4	20.79	268, 330	565, 771	302, 538, 773	Unknown
5	21.61	272, 330	593	415, 432 , 595	Flavonoid derivatives
6	22.53	268, 336	609	287, 449, 611	Luteolin <i>O</i> -hex-hex
7	23.40	268, 338	563, 741	287, 449, 565, 743	Luteolin <i>O</i> -hex-pent-hex
8	24.41	268, 340	609	287, 449, 611	Luteolin <i>O</i> -hex-hex
9	25.59	268, 348	285, 579	287, 449, 581	Luteolin
10	25.87	310	119 , 162	91, 119, 147 , 165	7- <i>O</i> -sambubioside (s)
11	26.11	268, 338	593	271, 433, 595	<i>p</i> -coumaric acid (s)
12	26.84	258, 266, 348	447 , 895	287, 449	Apigenin <i>O</i> -hex-hex
13	26.99	268, 326	593	287, 449, 595	Luteolin 7- <i>O</i> -glucoside (s)
14	27.46	250, 268, 336	285, 447, 609, 755	287, 449, 611, 757	Luteolin <i>O</i> -hex-deoxyhex
15	27.85	268, 330	269, 563	271, 418 , 565	Apigenin
16	28.76	268, 335	285, 447, 579 , 769	287, 449, 581, 771	<i>O</i> -deoxyhex- <i>O</i> -deoxyhex
17	29.27	268, 330	285, 431	286, 433	Luteolin
18	29.45	268, 336	285, 447	287, 449	<i>O</i> -hex-pent-feruloyl
19	30.17	268, 284	431	301, 419 , 571	Flavonoid derivatives
20	30.53	268, 300 sh, 340	285, 447	287, 449	Luteolin <i>O</i> -hex
21	32.36	270, 324	299, 461	331, 463	Tricin <i>O</i> -pent
22	34.38	256, 266, 348	285	287	Luteolin (s)
23	36.23	268, 295 sh, 340	269	271	Apigenin (s)
24	36.35	270, 300 sh, 349	329	331	Tricin (s)
25	36.54	268, 300 sh, 344	299	301	Chrysoeriol (s)

sh—peak shoulder; bold—most abundant; s—reference substance; hex—hexose, pent—pentose, deoxyhex—deoxyhexose.

2.2. Identification of the Isolated Compounds **9**, **12** and **22**

As a result of exhaustive multistep chromatographic isolation processes, three chromatographically homogeneous known compounds (**9**, **12**, and **22**) were isolated from the obtained **JM4–JM6** fractions. The identification of those compounds was carried out on the basis of R_f values, products of acid hydrolysis and spectroscopic methods (ultraviolet (UV) spectroscopy, nuclear magnetic resonance (¹H NMR, ¹³C NMR), mass spectrometry (MS)). The spectral data of all compounds were identical to the available literature data. The spectral properties of compounds **9**, **12** and **22** were verified by comparison of its spectral data with those previously described in the literature. Isolated compounds were identified as luteolin 7-*O*-β-D-xylosyl-(1-2)-β-D-glucoside (luteolin 7-*O*-sambubioside, **9**), luteolin 7-*O*-β-D-glucoside (cynaroside, **12**) and luteolin (**22**) (Figure 1) [15–17] (Supplementary Figures S3–S8).

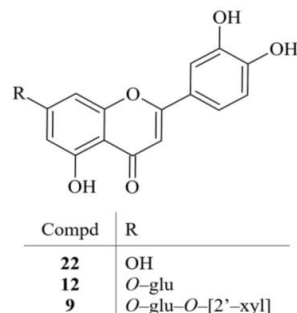


Figure 1. Chemical structures of isolated compounds **9**, **12** and **22**.

2.3. Cytotoxicity Assay

An MTT assay was performed separately for each sample for a preliminary assessment of the cytotoxic effects of **JM1–JM6** and compounds **9**, **12** and **22** on the viability of C32 and fibroblast cells. The MTT assay is among the most common methods for the evaluation of cell viability. However, several studies have shown inaccuracies that are inherent in the MTT method. Some studied plant extracts and polyphenols directly reduce the tetrazolium salt even in the absence of cells, which interferes with the MTT assay [18–20]. Additionally, the MTT assay has a limited operating range of compounds with a strong color that can be absorbed by the tested cells. Due to the imprecision of the MTT method, the fixable viability stain assay was chosen as an alternative to assess viability. C32 and fibroblast cells were treated with **JM1–JM6**, compounds **9**, **12**, **22** and vinblastine sulfate (VLB) at increasing concentrations (10–300 µg/mL) for 24 h. The results are presented in Table 2 and Supplementary Figures S9–S12. The morphological profile of C32 melanoma cells after 24 h of incubation with **JM4**, **22** and VLB is shown in Figure 2. We observed dose-dependent degradation of the cell membrane and a decrease in cell adhesion. Additionally, the number of cells in the treatment groups decreased compared with the untreated group, indicating inhibition of cell proliferation or induction of apoptosis. The highest activity was observed after treatment with compound **22** at a concentration of 25 µg/mL. The fixable viability stain study showed that C32 cell viability was inversely proportional to the applied concentration of all tested compounds. The cytotoxic potential is expressed as a median inhibitory concentration (IC₅₀) value, where the IC₅₀ value and cytotoxic activity value are inversely proportional. The tested extracts and compounds inhibited the viability of C32 cells in a dose-dependent manner. The IC₅₀ values for some of the extracts and compounds were either similar (**JM4** IC₅₀ = 119.7 µg/mL) to VLB (IC₅₀ = 148.5 µg/mL) or somewhat higher (e.g., **JM6** IC₅₀ = 215.7), while compound **22** had an IC₅₀ value (95.1 µg/mL) even lower than that of VLB. The IC₅₀ values of the other extracts were > 300 µg/mL. The viability of the fibroblast cells under the influence of **JM4** and **22** was higher than that of the C32 cells. In the case of fibroblasts, the IC₅₀ value for **JM4** was above 300 µg/mL, and that for compound **22** was 194.1 ± 4.4 µg/mL (Supplementary Figure S13).

Table 2. IC₅₀ of viability of CRL-1585 human amelanotic melanoma cells treated for 24 h with different concentrations of JM1–JM6 and isolated compounds 9, 12, 22 from *J. montana*. Mean values ± SD from three independent experiments done in duplicate are presented. (IC₅₀ value in µg/mL).

Sample	IC ₅₀ [µg/mL]
JM1	>300
JM2	>300
JM3	>300
JM4	119.7 ± 3.2
JM5	>300
JM6	215.7 ± 21.2
Compound 9	>300
Compound 12	>300
Compound 22	95.1 ± 7.2
VLB	148.5 ± 7.7

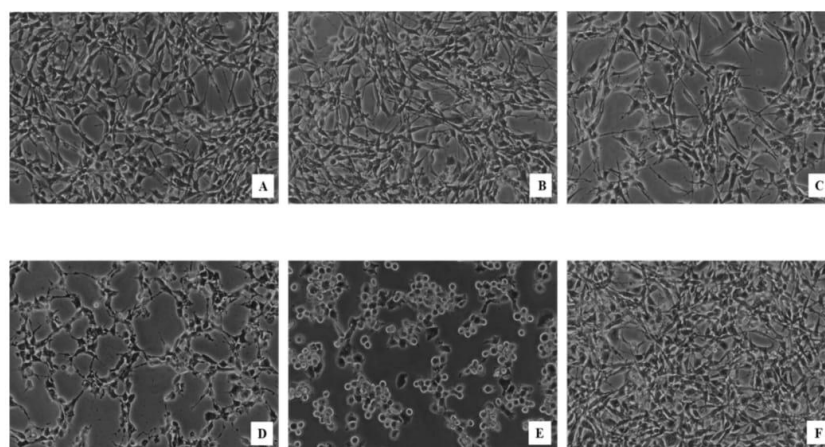


Figure 2. Morphological profile of C32 melanoma cells after 24 h of incubation with JM4 in concentration 25 µg/mL (A), 50 µg/mL (B) and 100 µg/mL (C), 22 at concentration 25 µg/mL (D), and vinblastine sulfate (VLB) at concentration 25 µg/mL (E), compared with untreated control (F) evaluated by phase contrast microscopy (magnification × 200).

The obtained results suggested that JM4 and compound 22 were the most active against human amelanotic melanoma C32 cells. Due to the high activity of the mentioned fraction and compound, JM4 and 22 were submitted for further study. Notably, based on the content of compound 22 in JM4, it can be concluded that this compound is dominantly responsible for the observed effects of the JM4 fraction on C32 cells.

2.4. Alteration of C32 Cell Cycle Progression by JM4 and 22

The results demonstrated the differences between the investigated JM4 and compound 22, their concentration and the control group with respect to the percentage of accumulated C32 cells in different cell cycle phases after 24 h incubation (Figures 3 and 4). JM4 at a concentration of 100 µg/mL led to the accumulation of C32 cells in the S and G2/M phases. Simultaneously, the population of C32 cells in G1 phase after treatment with JM4 was meaningfully reduced. The percentage of C32 cells in G2 phase increased from 6.1 ± 0.6% in the untreated control group to 30.1 ± 1.8% after treatment with JM4 (100 µg/mL). However, this result was significantly lower than that in the case of VLB (25 µg/mL). Additionally, the percentage of C32 cells in G1 phase in the untreated control group decreased from 73.0 ± 0.9% to 35.3 ± 3.0% after incubation with 22 (25 µg/mL), and the percentage of C32 cells in G2/M phase increased from 6.1 ± 0.6% to 14.6 ± 1.5% after treatment with 22 (25 µg/mL).

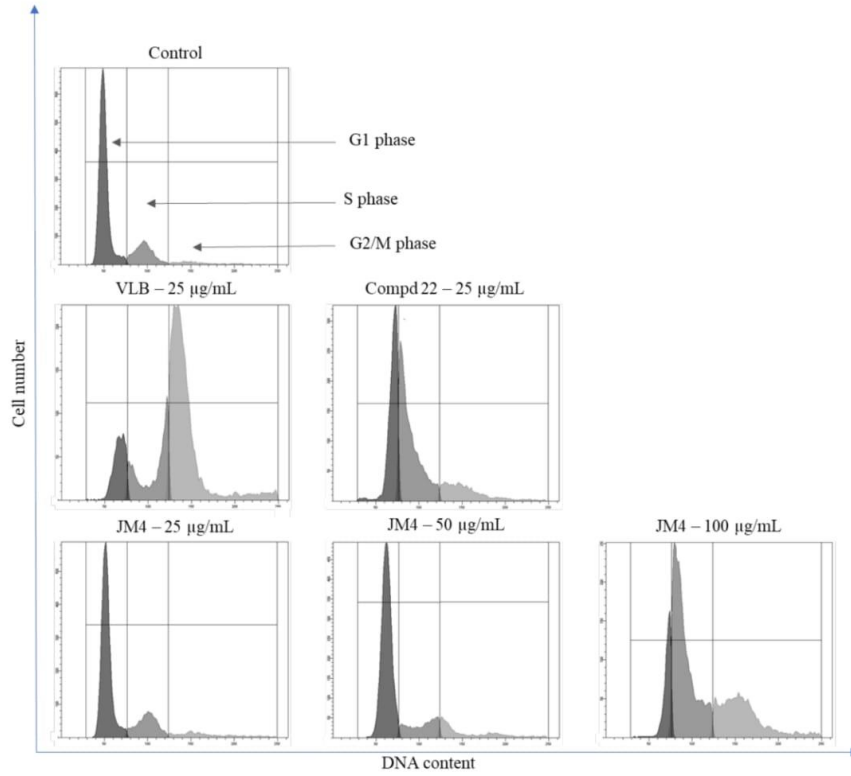


Figure 3. Flow cytometric analysis of cell cycle of C32 melanoma cells after 24 h of incubation with **JM4** (25, 50, 100 µg/mL), **22** (25 µg/mL) and vinblastine sulfate (VLB) (25 µg/mL) using propidium iodide (PI) staining.

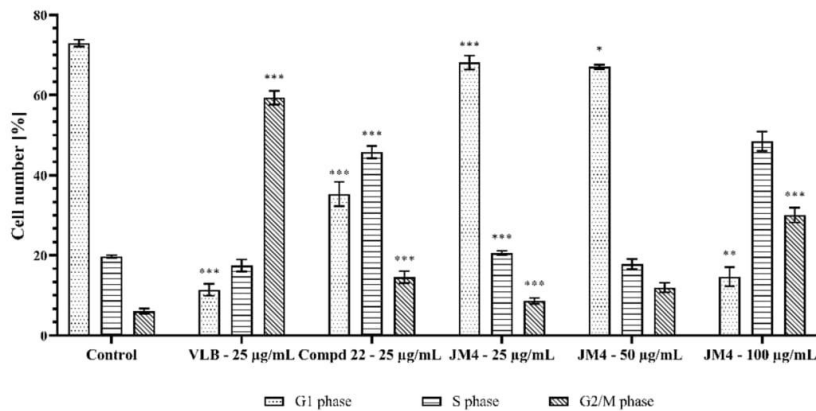


Figure 4. Percentage of accumulation C32 melanoma cells in the different cell cycle phases after 24 h of incubation with **JM4** (25, 50, 100 µg/mL), **22** (25 µg/mL) and vinblastine sulfate (VLB) (25 µg/mL). Mean percentage from three independent experiments ($n = 3$) done in duplicate are presented. * $p < 0.05$ versus control group, ** $p < 0.01$ versus control group, *** $p < 0.001$ versus control group.

The obtained results suggested that the effects on C32 cell cycle arrest in the S and G2/M phases was not caused by the main component of the **JM4** fraction, which is compound **22** (luteolin).

2.5. The **JM4** Fraction and Compound **22** Induce Apoptosis in Melanoma C32 Cells

During programmed cell death, annexin V has a high affinity for phosphatidylserine (PS) when it is exposed to the extracellular environment. Hence, this assay is based on the externalization of PS on the cell membrane. Additionally, propidium iodide (PI) was used to determine the number of necrotic cells, which confirms the integrity of the cell membrane [21,22]. The assay allows differentiability between viable cells (annexin V⁻/PI⁻) and early (annexin V⁻/PI⁺) and late (annexin V⁺/PI⁺) apoptotic cells, as well as necrotic cells (annexin V⁻/PI⁺).

An apoptosis study was performed to determine the mode of cell death provoked by **JM4** and **22**. The results are presented in Figures 5 and 6. This analysis demonstrated that both tested samples, **JM4** and **22**, significantly induced programmed death in C32 cells in comparison with the untreated control group, where $91.2 \pm 1.0\%$ viable cells and $7.3 \pm 1.3\%$ apoptotic cells were observed. Fraction **JM4** (100 $\mu\text{g}/\text{mL}$) displayed the most significant proapoptotic effect after 24 h of incubation, where we detected $44.2 \pm 1.0\%$ viable cells and $51.5 \pm 1.7\%$ apoptotic cells. Nevertheless, with increasing concentration, a significant increase in the percentage of necrotic cells ($4.3 \pm 2.6\%$ of necrotic cells after incubation with **JM4** (100 $\mu\text{g}/\text{mL}$)) was shown which may suggest the toxic activity of **JM4** at higher concentrations. Compound **22** (25 $\mu\text{g}/\text{mL}$) and VLB displayed similar proapoptotic effect after 24 h of incubation, where we detected $29.2 \pm 3.0\%$ apoptotic cells after treatment with **22**, and $27.4 \pm 1.0\%$ apoptotic cells after treatment with VLB. However, VLB exhibited two times higher necrotic potential ($4.2 \pm 1.0\%$ necrotic cells after incubation with VLB (25 $\mu\text{g}/\text{mL}$)).

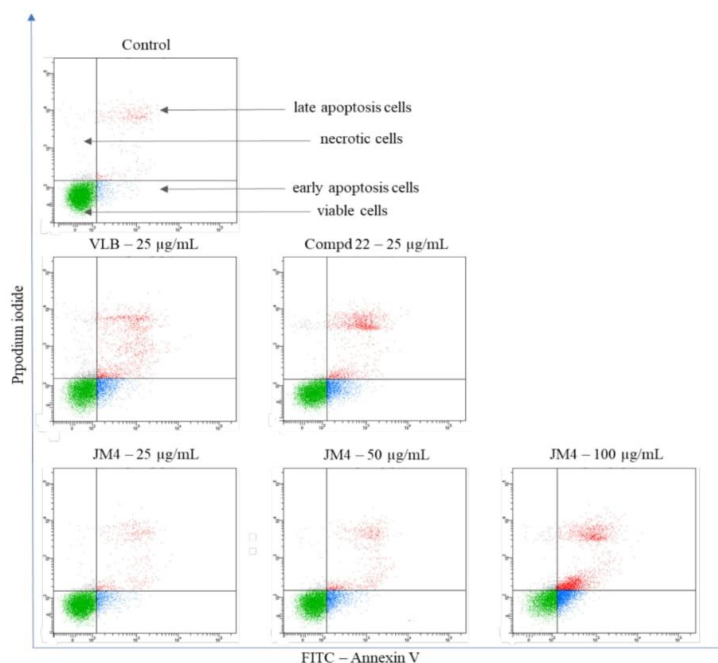


Figure 5. Flow cytometric analysis of C32 melanoma cells after incubation with **JM4** (25, 50, 100 $\mu\text{g}/\text{mL}$), **22** (25 $\mu\text{g}/\text{mL}$) and vinblastine sulfate (VLB) (25 $\mu\text{g}/\text{mL}$) for 24 h and subsequent staining with Annexin V and propidium iodide (PI).

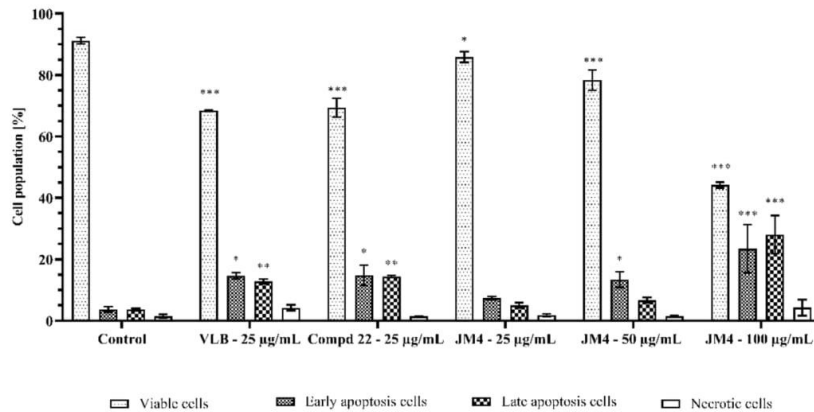


Figure 6. Percentage of viable C32 melanoma cells, early and late apoptosis cells, and necrotic cells, after 24 h of incubation with **JM4** (25, 50, 100 µg/mL), **22** (25 µg/mL) and vinblastine sulfate (VLB) (25 µg/mL). Mean percentages from three independent experiments ($n = 3$) done in duplicate are presented. * $p < 0.05$ versus control group, ** $p < 0.01$ versus control group, *** $p < 0.001$ versus control group.

2.6. Fraction **JM4** and Compound **22** Induce Autophagy

Autophagy contributes to the maintenance of internal cell homeostasis by preventing the accumulation of damaged cell organelles. The level of autophagy is directly proportional to the increase in cellular stress, which ultimately leads to programmed cell death [23,24].

The Autophagy Assay, Red was carried out via flow cytometry to detect the level of autophagy in C32 cells after 24 h of incubation with **JM4** and compound **22**. The results, expressed as the change in intensity of induced autophagy in C32 cells versus the untreated control group, differed according to treatment type (**JM4** vs. **22** vs. VLB) and concentrations (Figures 7 and 8). There were $94.5 \pm 1.0\%$ nonautophagic cells and $4.8 \pm 0.8\%$ autophagic cells in the untreated control group. The highest dose-dependent activity of the induced autophagy process among the investigated samples/concentrations was displayed after 24 h incubation with fraction **JM4** (100 µg/mL), where we observed $60.2 \pm 1.6\%$ nonautophagic cells and $38.6 \pm 1.6\%$ of autophagic cells, which was twofold lower than in case of VLB. Significant activation of autophagy was observed after 24 h treatment with VLB (25 µg/mL); $22.4 \pm 0.6\%$ nonautophagic cells and $76.7 \pm 0.5\%$ of autophagic cells. The significant dose-dependent increase in the percentage of autophagic cells after **JM4** treatment may suggest that **JM4** causes stress in cells and leads to the induction of programmed cell death.

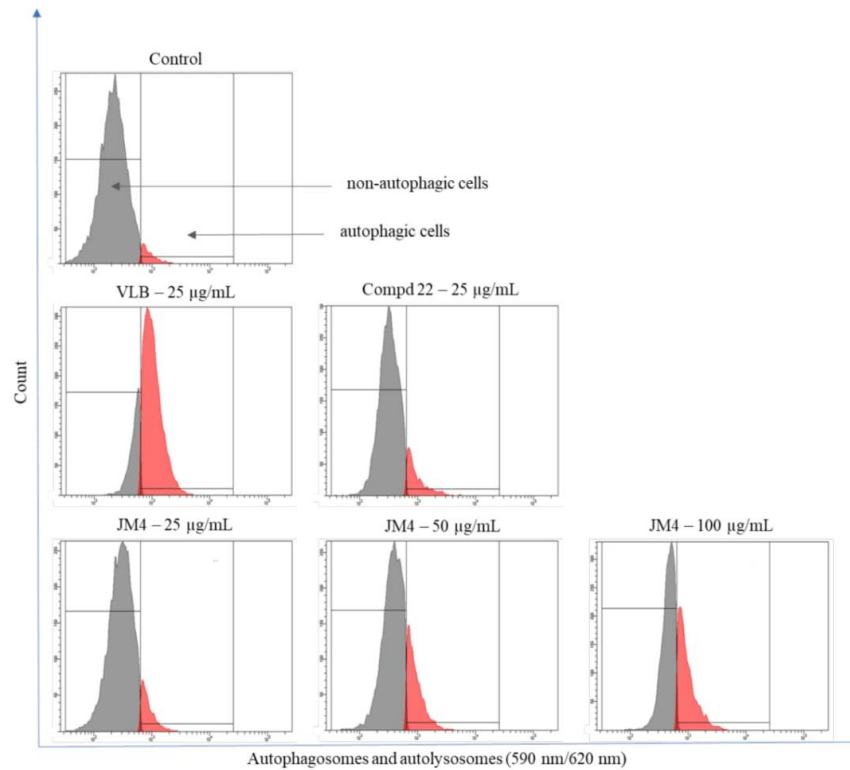


Figure 7. Autophagy induction in C32 melanoma cells measured by flow cytometry using Autophagy Probe (right—red histogram) compared to negative control cells (left—gray histogram) after 24 h incubation with **JM4** (25, 50, 100 µg/mL), **22** (25 µg/mL) and vinblastine sulfate (**VLB**) (25 µg/mL).

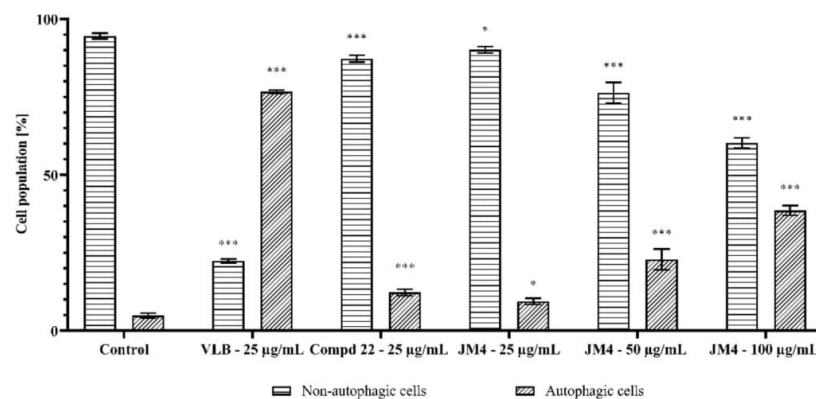


Figure 8. Percentage of nonautophagic and autophagic C32 melanoma cell population after 24 h incubation with **JM4** (25, 50, 100 µg/mL), **22** (25 µg/mL) and vinblastine sulfate (**VLB**) (25 µg/mL). Mean percentage values from three independent experiments ($n = 3$) done in duplicate are presented. * $p < 0.05$ versus control group, *** $p < 0.001$ versus control group.

2.7. The Impact of Fraction JM4 and Compound 22 on Mitochondrial Membrane Potential (MMP)

To evaluate the mechanism underlying intrinsic cellular apoptosis under the influence of JM4 and compound 22, staining with the fluorescent dye JC-1 was performed. Reduced mitochondrial membrane potential (MMP) is associated with the early stages of apoptosis as well as with the appearance of cytochrome C in the cytosol [25–27]. As shown in Figures 9 and 10, JM4 caused a significant dose-dependent reduction in the MMP at the highest dose. We observed that $74.5 \pm 3.0\%$ of the cells had a reduced MMP after 24 h incubation with JM4 (100 $\mu\text{g}/\text{mL}$), whereas the untreated control group had only a reduced MMP in $5.2 \pm 0.1\%$ of the cells. JM4 at a concentration of 100 $\mu\text{g}/\text{mL}$ led to a twofold higher percentage of cells with a reduced MMP than VLB ($34.1 \pm 3.0\%$). A weaker effect was displayed after 24 h of incubation with 22 (25 $\mu\text{g}/\text{mL}$), where we observed that $31.8 \pm 0.7\%$ of the cells had a reduced MMP. The obtained results are in accordance with the results from the annexin V binding assay.

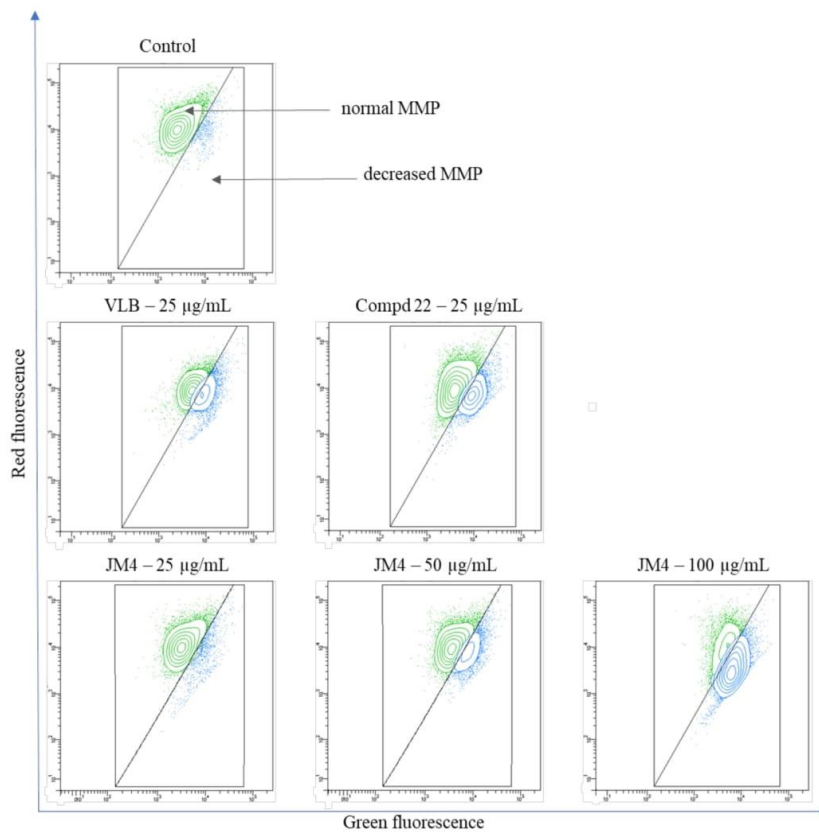


Figure 9. Fluorescence of C32 melanoma cells treated for 24 h with JM4 (25, 50, 100 $\mu\text{g}/\text{mL}$), 22 (25 $\mu\text{g}/\text{mL}$) and vinblastine sulfate (VLB) (25 $\mu\text{g}/\text{mL}$) incubated with mitochondrial membrane potential probe JC-1.

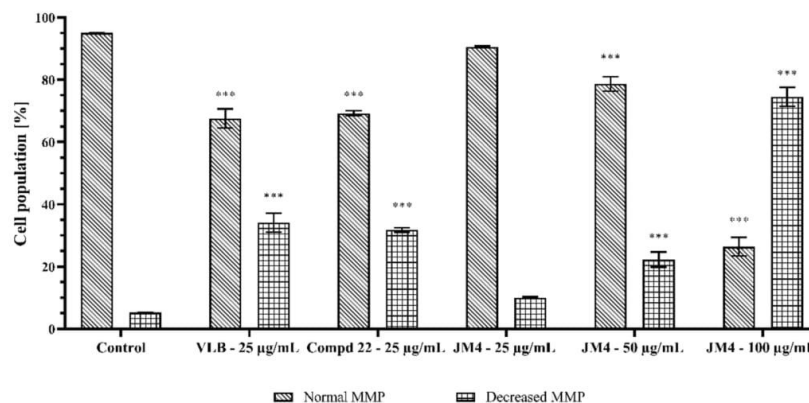


Figure 10. Percentage of C32 melanoma cells with normal and decreased mitochondrial membrane potential (MMP) after 24 h incubation with **JM4** (25, 50, 100 µg/mL), **22** (25 µg/mL) and vinblastine sulfate (VLB) (25 µg/mL). Mean percentage values from three independent experiments ($n = 3$) done in duplicate are presented. *** $p < 0.001$ versus control group.

2.8. Activation of Caspase-3, Caspase-8, Caspase-9, and Caspase-10

Caspases play a crucial role in the activation of the apoptotic process. Activation of apical caspases (caspase-8 and caspase-10) leads to initiation of the external apoptotic pathway as well as activation of the effector caspase, caspase-3. In addition, the intrinsic (mitochondrial) apoptotic pathway is closely related to the activity of caspase-9, which is stimulated by a reduction in the MMP and plays an equally important role in the activation of caspase-3. Caspase-3 instructs the cell directly through apoptosis and DNA damage [28–30]. The influence of **JM4** and compound **22** on the expression of caspases 3, 8, 9, and 10 in C32 cells is shown in Figures 11–18. The results proved that there was a significant increase in the levels of all caspases compared to the untreated control group after 24 h incubation with tested samples. The most significant effect of the activation of caspase-8, caspase-9, and caspase-10 was observed after incubation with **JM4** (100 µg/mL), where $41.8 \pm 0.5\%$ of cells had active caspase-8, $40.9 \pm 2.4\%$ of cells had active caspase-9, and $43.7 \pm 1.1\%$ of cells had active caspase-10. In all cases, the increases were almost twofold higher than after treatment with VLB. Compound **22** (25 µg/mL) displayed a slightly weaker impact on the activation of caspase-8, caspase-9, and caspase-10, with $20.2 \pm 1.5\%$, $16.6 \pm 0.8\%$, and $15.4 \pm 0.7\%$ of cells with the active respective caspase. According to these results, **JM4** and **22** induce the external and intrinsic apoptotic pathways as well as the activation of caspase-3, and **JM4** (100 µg/mL) is the strongest activator of caspase-3. After treatment with **JM4**, $74.9 \pm 4.0\%$ of the cells had active caspase-3, in comparison with $4.2 \pm 1.3\%$ of the cells in the untreated control group and $23.4 \pm 3.5\%$ of the cells after treatment with VLB. These results were consistent with the previous hypothesis of the intrinsic mitochondrial apoptotic pathway. The results showed that one of the molecular mechanisms leading to apoptosis caused by **JM4** is the activation of caspases in a dose-dependent manner. Our study confirmed that **JM4** was the strongest activator of all the tested caspases. Increasing the **JM4** concentration enhanced its cytotoxic properties and significantly increased the expression of caspase-3, which is responsible for DNA damage.

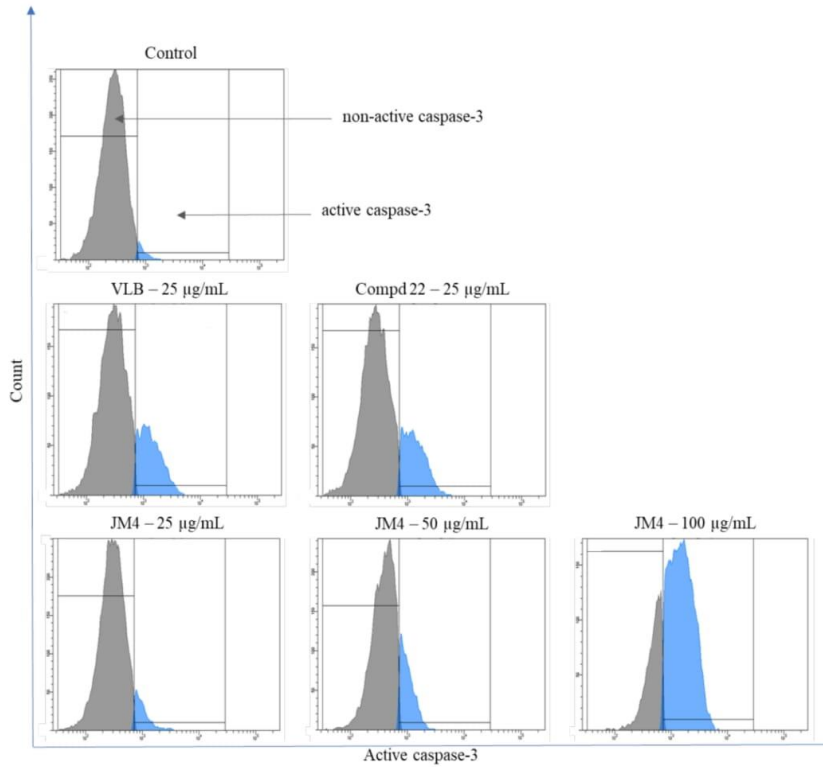


Figure 11. Flow cytometric analysis of populations C32 melanoma cells treated for 24 h with **JM4** (25, 50, 100 µg/mL), **22** (25 µg/mL) and vinblastine sulfate (VLB) (25 µg/mL) for active caspase-3.

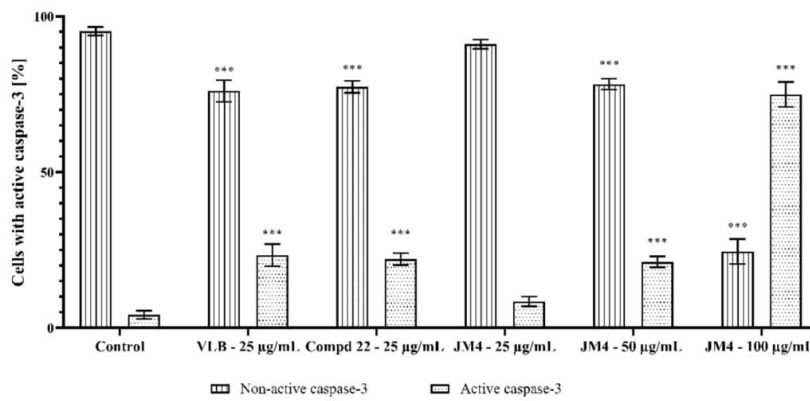


Figure 12. Percentage of C32 melanoma cells with nonactive and active caspase-3 after 24 h incubation with **JM4** (25, 50, 100 µg/mL), **22** (25 µg/mL) and vinblastine sulfate (VLB) (25 µg/mL). Mean percentage values from three independent experiments ($n = 3$) done in duplicate are presented. *** $p < 0.001$ versus control group.

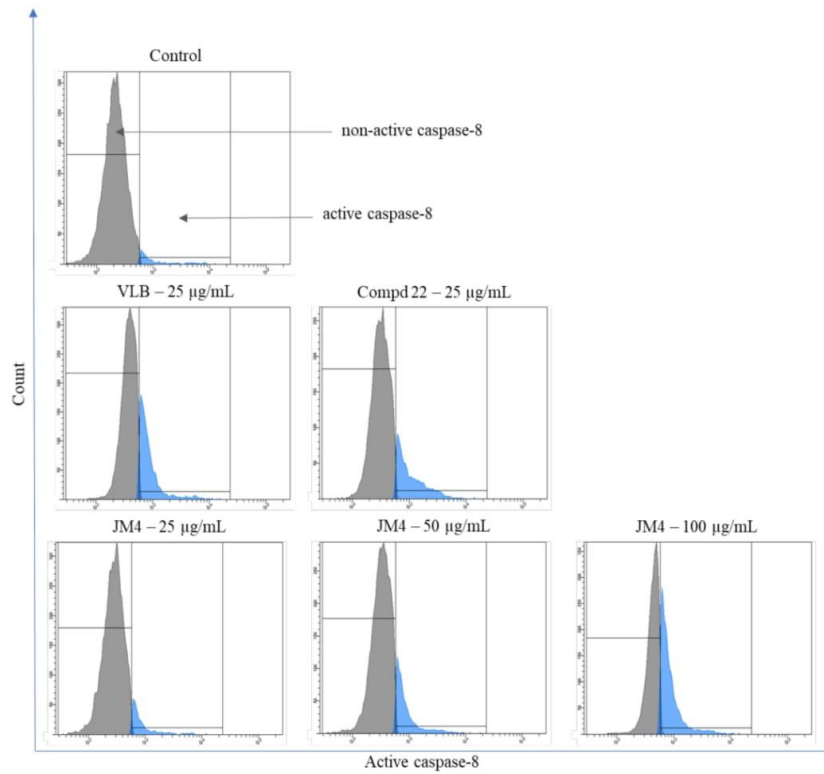


Figure 13. Flow cytometric analysis of populations C32 melanoma cells treated for 24 h with **JM4** (25, 50, 100 µg/mL), **22** (25 µg/mL) and vinblastine sulfate (VLB) (25 µg/mL) for active caspase-8.

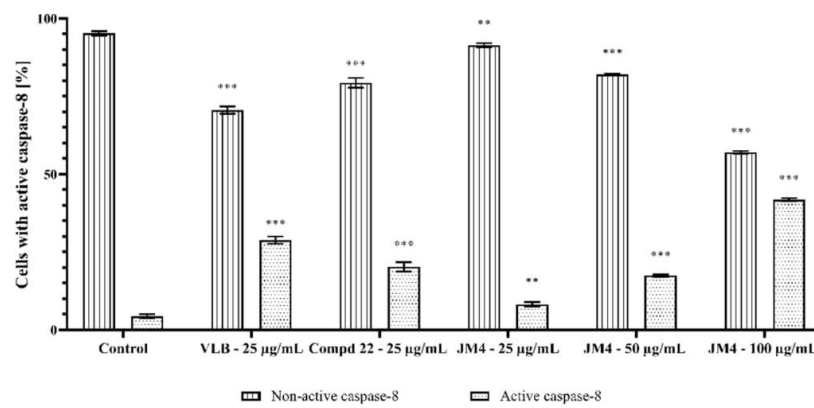


Figure 14. Percentage of C32 melanoma cells with nonactive and active caspase-8 after 24 h incubation with **JM4** (25, 50, 100 µg/mL), **22** (25 µg/mL) and vinblastine sulfate (VLB) (25 µg/mL). Mean percentage values from three independent experiments ($n = 3$) done in duplicate are presented. ** $p < 0.01$ versus control group, *** $p < 0.001$ versus control group.

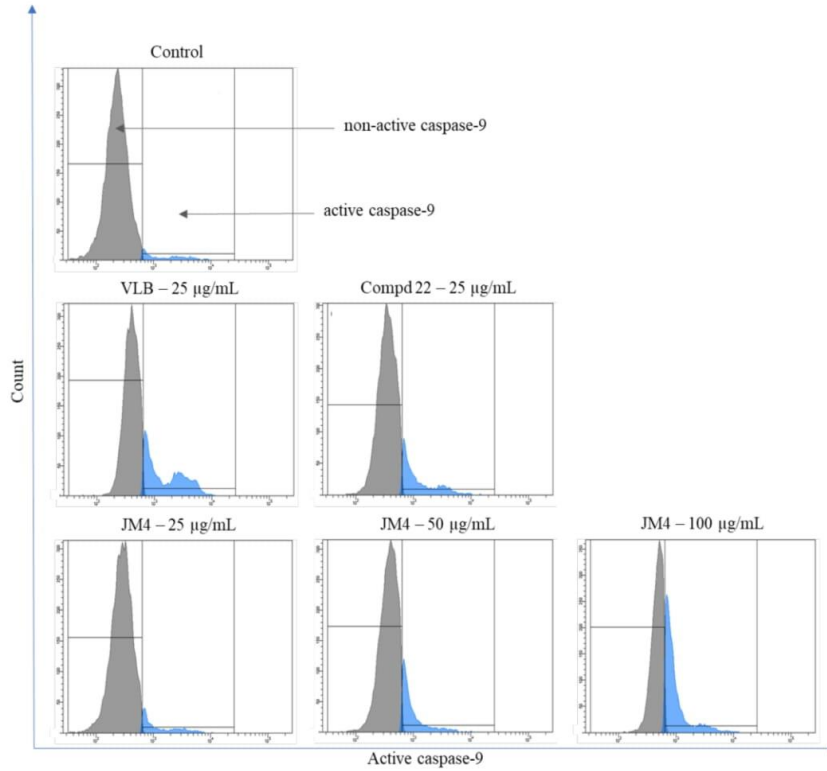


Figure 15. Flow cytometric analysis of populations C32 melanoma cells treated for 24 h with **JM4** (25, 50, 100 µg/mL), **22** (25 µg/mL) and vinblastine sulfate (VLB) (25 µg/mL) for active caspase-9.

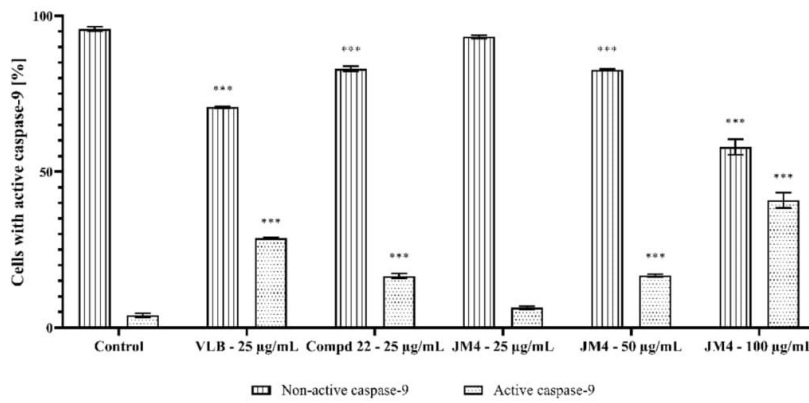


Figure 16. Percentage of C32 melanoma cells with nonactive and active caspase-9 after 24 h incubation with **JM4** (25, 50, 100 µg/mL), **22** (25 µg/mL) and vinblastine sulfate (VLB) (25 µg/mL). Mean percentage values from three independent experiments ($n = 3$) done in duplicate are presented. *** $p < 0.001$ versus control group.

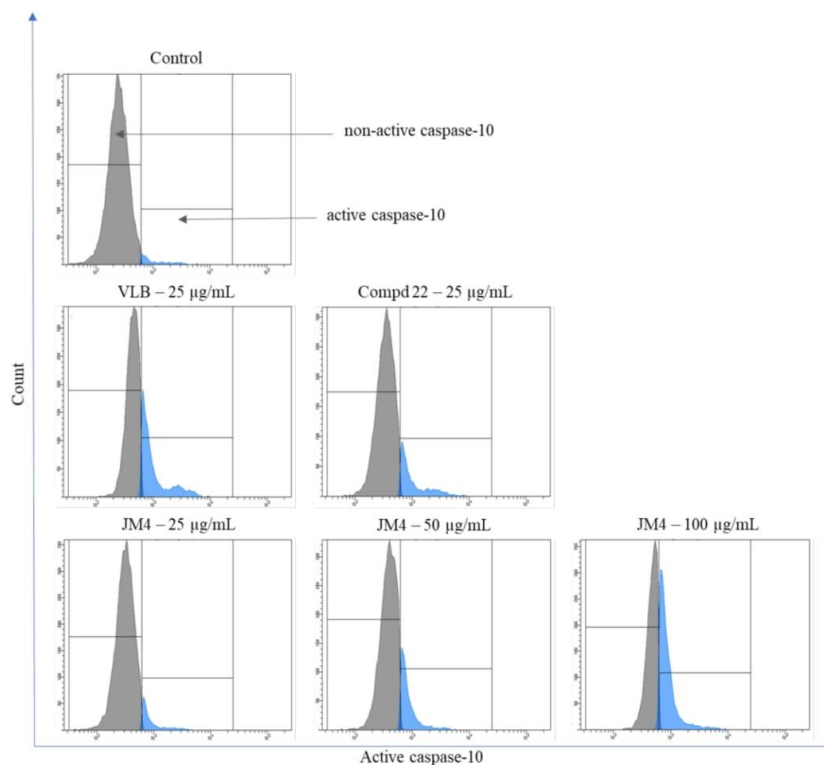


Figure 17. Flow cytometric analysis of populations C32 melanoma cells treated for 24 h with **JM4** (25, 50, 100 µg/mL), **22** (25 µg/mL) and vinblastine sulfate (VLB) (25 µg/mL) for active caspase-10.

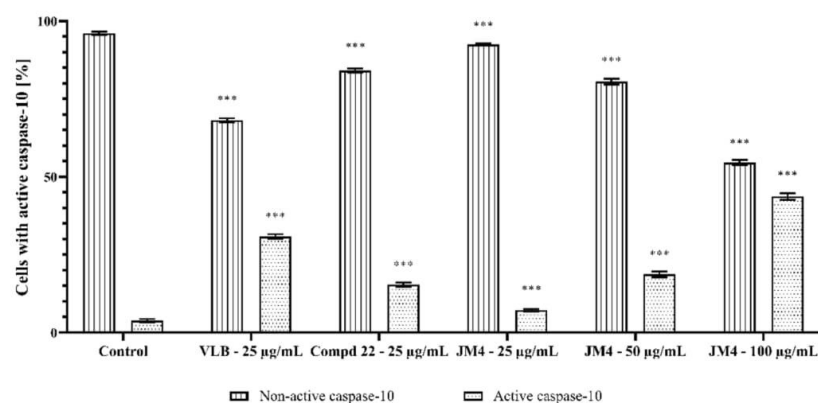


Figure 18. Percentage of C32 melanoma cells with nonactive and active caspase-10 after 24 h incubation with **JM4** (25, 50, 100 µg/mL), **22** (25 µg/mL) and vinblastine sulfate (VLB) (25 µg/mL). Mean percentage values from three independent experiments ($n = 3$) done in duplicate are presented. *** $p < 0.001$ versus control group.

3. Discussion

The extracts and fractions obtained from the aerial parts of *J. montana* were used in this study. Due to the lack of literature data on the phytochemical profile and biological prop-

erties of *J. montana* as well as traditional anticancer drugs from *J. montana*, we performed the isolation and identification of the main compounds from the fractions from *J. montana* and examined their activity against human amelanotic melanoma C32 cells. Pathological skin cells were selected for this research due to the awareness of problems resulting from unknown plant matrix metabolic pathways when used internally. Additionally, previous studies have suggested the anticancer potential of luteolin and its derivatives [6,31–33]. To the best of our knowledge, there are currently no reports in the literature on the effects of *J. montana* extracts and its main phytoconstituents on C32 cells.

The main phytochemicals belonging to the flavone group that were found and isolated from *J. montana* herbs include luteolin 7-*O*-sambubioside, luteolin 7-*O*-glucoside, and luteolin (**9**, **12**, and **22**, respectively). During the chromatographic study, it was found that the EtOAc fraction **JM4** contained luteolin (**22**) and luteolin 7-*O*-glucoside (**12**). **JM5** and the *n*-BuOH fraction **JM6** contained luteolin-7-*O*-sambubioside (**9**). These compounds were identified by comparison of the obtained UV spectral data as well as ¹H and ¹³C NMR data with the available literature data, thus confirming their presence in the aerial parts of *J. montana*. The presence of these compounds in the studied species had already been described for the first time [12]. However, compound **9** was isolated for the first time from *J. montana*.

Luteolin displays numerous health-related properties, such as anti-allergy, anti-inflammatory, antioxidant, anticancer activities and it was also reported as MAO-B inhibitors for the treatment of neurodegenerative diseases [34]. In traditional Chinese medicine, plants rich in luteolin have been used for the treatment of various disorders, such as inflammatory diseases, hypertension, and even malignant tumors [7,35]. Luteolin 7-*O*-glucoside (**12**) protects cells against apoptosis activated by hypoxia and buffers atopic dermatitis skin lesions in murine models [36].

The metabolic pathways of natural compounds and the complexity of the plant matrix have been insufficiently studied and pose a problem for internal administration. Hence, it seemed appropriate to undertake research towards only the potential external application of the raw material. Many anticancer compounds act by inhibiting tumor growth by arresting the cell cycle and/or inducing apoptosis [37]. The action of luteolin in the context of cancer, including melanoma, has been extensively described in review articles [8,31–33]. There are several suggested mechanisms by which luteolin may exert an inhibitory effect on human melanoma, including the induction of cell cycle arrest [38] or activation of apoptosis by increasing the level of intracellular reactive oxygen species (ROS) [39]. Additionally, the activity of luteolin was evaluated in an experimental *in vivo* metastasis model of hypoxia-induced epithelial–mesenchymal transition (EMT) inhibition through the regulation of β 3 integrin [4]. This result was confirmed by luteolin research in melanoma cells, during which attempts were made to determine the influence of luteolin on the programming of the cell cycle, proving the arrest of this process in the G2/M and G0/G1 phases of the cell cycle [3]. Luteolin activates caspase-3, caspase-8, caspase-9, and caspase-10, activates DNA fragmentation factor, reduces MMP, and induces cytochrome C release into the cytosol [32]. Additionally, research on CH27 human lung squamous carcinoma cells showed that luteolin causes DNA damage and cell cycle arrest in S phase [40]. The aforementioned anticancer effects and mechanisms of luteolin are only examples of the very broad spectrum of action of this flavonoid [32].

The cytotoxic properties of chemotherapeutic substances are often associated with the induction of apoptosis in cancer cells [41]. Our results demonstrated the cytotoxic potential of the tested samples in amelanotic melanoma C32 cells. These melanoma cells showed a reduction in cell viability in a dose-dependent manner. The calculated IC₅₀ value for all investigated extracts and fractions in the cytotoxic assays allowed us to observe differences in their activity. Luteolin (**22**) and fraction **JM4** showed the greatest cytotoxic potential that was comparable to that of VLB during the next steps of experiment. The presence of **22** in **JM4** was confirmed by LC–MS analysis, in which the presence of the ions 269 [M-H][−] and 271 [M-H]⁺ were found, which corresponded to the mass of the monoisotopic ion of

luteolin, as well as the LC peak of the standard substance that had the same retention time as luteolin. It is worth noting that the compound **22** was the dominant in the analyzed fraction **JM4**. However, **JM4** was identified as a mixture of other polyphenolic compounds (Supplementary Figure S2).

Said and co-authors set out to determine the antiproliferative potential of flavonoids isolated from *Ailanthus excelsa*, including **12** and **22** against the same amelanotic melanoma C32 cell line used in this study as well as large cell lung carcinoma COR-L23 cells and malignant melanoma A375 cells. The results showed that luteolin had strong antiproliferative effects, comparable to those of VLB in all tested cell lines [42]. The observed antiproliferative effects of luteolin indicate that it might play a significant role in the overall activity of **JM4**.

While both **22** and **JM4** displayed notable degrees of cytotoxic activity in C32 cells in this study, their cytotoxic potential against normal fibroblast cells was much lower. To further elucidate the mechanism of cell damage and the possible induction of apoptosis, the ability of the test compounds to arrest the cell cycle was investigated. Flow cytometry analysis showed a decrease in the number of cells in G1 phase, which was most clearly seen in the case of **JM4**. Additionally, both **JM4** and compound **22**, at concentrations of 100 and 25 µg/mL, respectively, showed an increase in the accumulation of cells in the S and G2/M phases. Similar results were obtained in A375 melanoma cells. It has been shown that luteolin can contribute to cell cycle arrest and the induction of apoptosis by arresting the cell cycle at the G2/M and G0/G1 phases [3]. Literature data have confirmed that many antitumor substances block the cell cycle in G2/M phase [43–45]. It should be emphasized that there was a significant increase in the number of cells in S phase, which is a significantly higher result than in the case of VLB. The demonstrated disruptions in the cell cycle were associated with the inhibition of cell proliferation.

Apart from cell cycle arrest, mitochondria and caspases play an essential role in the induction of apoptosis. At the cellular level, many factors mediate apoptosis. One is the dysfunction of mitochondrial membrane integrity that can result in apoptotic cell death. Reducing the MMP causes the release of cytochrome c and other proteins. These proteins play an important role in the activation of caspase-9 and hence caspase-3, which directly leads to cell death [46–48]. To show the effects of the mitochondrial pathway on the apoptosis process, flow cytometry analysis was conducted and showed a significant decrease in MMP under the influence of **JM4** and compound **22**, thus confirming that apoptosis was triggered. Notably, the reduction in MMP in the case of compound **22** was similar to that caused by VLB, and in the case of **JM4**, it was twice as high as that recorded in the positive control.

The relationship between the reduction in MMP and the induction of the intrinsic apoptotic pathway is based on the activation of pro-caspase-3. In the context of cellular apoptosis, caspase-8 and caspase-10, which are involved in the external apoptotic pathway, are equally important [49]. As discussed in the results section, **JM4** and compound **22** exerted a significant antiproliferative effect in C32 cells that was associated with caspase-8, caspase-9, and caspase-10, followed by caspase-3. In a recent paper, Danciu et al. showed that chamomile flower extract presents a proapoptotic effect against human melanoma A375 cells. The dominant components of the studied extract were the following flavonoids: apigenin glucoside, rutin, luteolin glucoside, and luteolin. The chamomile flower extract activated caspase-3 at a concentration of 60 µg/mL. However, this flavone complex did not show significant activity in terms of cell cycle distribution or induction of apoptotic phases. This nonsignificant effect of the extract may be caused by the synergistic action of all components of the extract [50]. A similar effect was observed in study on a rosemary extract and human melanoma A375 cells where the extract was subjected to an MTT test with the main pure compounds such as rosmarinic acid, luteolin, carnosol, apigenin, and scutellarin. The dominant compound, rosmarinic acid, showed a much weaker antiproliferative effect than the extract. The substances whose contents in the extract were lower (carnosol, apigenin and luteolin) turned out to be more effective. However, since the individual

substances were effective at concentrations well above those found in the rosemary extract, the results suggested that the cytotoxicity of the whole extract was due to the combination of activities of different substances [51].

Autophagy may have two functions: protumorigenic and antitumorigenic, depending on the type of cell, stage of cancer development and stimulator [24]. Most of the currently available chemotherapeutic agents exert their cytotoxic activity by promoting apoptosis. Previous reports have indicated that autophagy is essential in cancer therapy as well as apoptosis [52–55]. These assumptions are supported by studies on the effects of another natural polyphenol, curcumin, in melanoma A375 cells. Zhao et al. proved the relationship between the induction of cell proliferation and autophagy [56]. Our results led to similar conclusions by showing the activation of autophagy and apoptosis under the influence of **JM4** and compound **22**.

Thus, the induction of apoptosis in cancer cells treated with fraction **JM4** described in this study may be partly explained by the presence of luteolin (**22**). However, the conducted studies, which were aimed at demonstrating the induction of apoptosis in neoplastic cells under the influence of the tested fraction and pure compound, showed differences in the mitochondrial potential, caspase activation and the number of cells in the apoptotic phases between the samples used. This may be because the plant matrix of the fraction **JM4** is present and because of the possible synergism of the various phytochemical components such as compound **22** and its derivatives. Previous studies on luteolin (**22**) and its antitumor effects have confirmed its inhibitory effect against various types of cancer, including human lung carcinoma cells [40], oral squamous cancer cells [57], human esophageal adenocarcinoma cells [58], human colon cancer cells [59], human hepatoma cells [60], breast cancer, pancreatic cancer, prostate cancer, glioblastoma, and many others [7]. Hence, it is possible to hypothesize that *J. montana*, as a rich source of derivatives of luteolin, may be the basis for further research due to their potential antitumor activity.

4. Materials and Methods

4.1. Chemicals and Reagents

Methanol (MeOH) (CAS67-56-1), petroleum spirit (CAS8032-32-4), chloroform (CHCl₃) (CAS67-66-3), diethyl ether (Et₂O) (CAS60-29-7), ethyl acetate (EtOAc) (CAS141-78-6), *n*-butanol (*n*-BuOH) (CAS71-36-3), ethanol (EtOH) (CAS64-17-5), Sephadex LH-20, vinblastine sulfate (VLB) (CAS143-67-9), dimethyl sulfoxide (DMSO) (CAS67-68-5), and 3-(4,5-dimethylthiazol-2-yl)-2,5-diphenyl tetrazolium bromide (MTT) (CAS298-93-1) obtained from Sigma Aldrich Co. (St. Louis, MO, USA). Polyamide (CAS25038-54-4), chrysoeriol and *p*-coumaric acid were purchased from Carl ROTH (Karlsruhe, Germany). The human amelanotic melanoma cell line C32 (CRL-1585) and a normal human fibroblast cell line (PCS-201-012) were purchased from the American Type Culture Collection (ATCC; Manassas, VA, USA). Dulbecco's minimal essential medium (DMEM), fetal bovine serum (FBS), phosphate-buffered saline (PBS), glutamine, penicillin, and streptomycin were purchased from Corning (Corning, NY, USA). Propidium iodide (PI) (CAS 25535-16-4), stain buffer, and an FITC Annexin V Apoptosis Detection Kit II were obtained from BD Pharmingen (San Diego, CA, USA). Fixable Viability Stain 520 (FVS520) was from BD Horizon, San Diego, CA, USA and the DNase-free RNase A Solution was acquired from Promega, Madison, WI, USA. The Autophagy Assay, Red kit, FLICA Caspase-3/7 Assay Kit, FLICA Caspase-8 Assay Kit, FLICA Caspase-9 Assay Kit, and FLICA Caspase-10 Assay Kit were purchased from ImmunoChemistry Technologies (Bloomington, MN, USA). The JC-1 MitoScreen kit was from BD Biosciences Systems (San Jose, CA, USA). Ultra-pure water (UPW) for the preparation of the mobile phase for LC–PDA–ESI–MS/TOF analysis was performed on a POLWATER DL3-100 system (Labopol, Kraków, Poland). Acetonitrile (MeCN) (CAS75-05-08) was purchased from Fisher Chemical (Thermo Fisher Scientific, Leicestershire, UK), and both mobile phases were modified with the addition of formic acid (HCOOH) (CAS64-18-6) (Ph. Eur., Merck, Darmstadt, Germany). Apigenin (purity > 96%) and tricetin (purity > 96%) were isolated from the inflorescences of *Arctium tomentosum* [61] and *Cirsium palustre* flower

heads [62], respectively. Luteolin 7-*O*-sambubioside, luteolin 7-*O*-glucoside, and luteolin were isolated from *J. montana* as described below.

4.2. Plant Material

The aboveground parts of *J. montana* (2.0 kg) were collected from plants occurring in their natural habitat within the area of Puszcza Knyszyńska (N53°15′20.9″; E23°25′41.5″) in the region of Supraśl (Podlasie Province, Poland) within the period of June–August 2017 and 2018. The plant material was dried in a shaded and well-ventilated area. Samples of the collected plant material were identified based on the scientific botanical literature and its morphological features by one of the authors (M.T.). A plant voucher specimen (JM-15029) has been deposited in the Herbarium of the Department of Pharmacognosy at the Medical University of Białystok, Poland.

4.3. Preparation of Extracts JM1–JM3 and Fractions JM4–JM6

The raw plant material (5 g per sample) was powdered and subsequently extracted using a heating mantle and radiator (5 × 45 min). All extractions were carried out using 65 mL of one of the following solvents: H₂O (JM1), 50% MeOH (JM2), and MeOH (JM3). After filtration of the extracts, the solvents were evaporated under reduced pressure (BÜCHI System, Flawil, Switzerland) at a controlled temperature of 40 ± 2 °C. The remaining residues were suspended in water and lyophilized using a freeze-drier (Lyph-Lock, Labonco, Italy). The following amounts of the extracts were obtained: JM1, 1293 mg; JM2, 1238 mg; and JM3, 858 mg. Additionally, the plant material (130 g) was purified with a continuous extraction method using extraction petrol (1.5 L × 8 h), and then CHCl₃ (1.5 L × 8 h) in Soxhlet extractor. The purified raw material was exhaustively extracted with MeOH (20 × 3 L) and 50% (*v/v*) MeOH (3 L) for 45 min each time. After the obtained MeOH extracts were combined and evaporated to dryness, they were precipitated with water for elimination of the ballasts. The obtained water extract was exhaustively fractionated by liquid–liquid extraction with different solvents of increasing polarity: CHCl₃ (35 × 200 mL), Et₂O (JM4; 50 × 200 mL), EtOAc (JM5; 98 × 200 mL) and *n*-BuOH (JM6; 45 × 200 mL). All fractions were evaporated to dryness and finally lyophilized using a freeze-drier. The three fractions were obtained in the following amounts: JM4, 8.5 g; JM5, 29 g; and JM6, 38.5 g and were used for further experiments. The chloroform fraction (CHCl₃) was not investigated.

4.4. LC–ESI–MS Analysis of Extracts JM1–JM3 and Fractions JM4–JM6

To establish the phytochemical compositions of JM1–JM6, LC–PDA–ESI–MS/TOF analysis was performed on a 1260 Infinity chromatography system hyphenated to a 6230 TOF mass spectrometer and Dual Agilent Jet Stream ESI (Agilent Technologies, Santa Clara, CA, USA). The MS conditions were as follows: electrospray ionization (ESI) source in both positive and negative ionization mode, a gas flow of 12 L/min, a gas temperature of 325 °C, a nebulizer pressure of 45 psi, and capillary voltages of 4500 and 2500 V for positive and negative ion modes, respectively. The analysis was performed using a Kinetex XB-C18 column (150 × 2.1 mm, 1.7 µm; Phenomenex, Torrance, CA, USA). The mobile phases were UPW (solvent A) and MeCN (solvent B), both with 0.1% HCOOH. The gradient started with the elution of 5% solvent B over 1.5 min. Then, within 22 min, the concentration of solvent B reached 28%, in 35 min it reached 75%, and finally in 45 min it reached 95%, with a linear gradient. After 3 min of maintaining the 95% B concentration, in 49 min, the system returned to its initial conditions, and conditioning continued for 6 min. The total run time of the analysis was 55 min at 25 °C. The injection volume was 1.0 µL, and the flow rate was 0.1 mL/min.

4.5. Identification and Isolation of Main Compounds 9, 12 and 22 (JM7–JM9)

Fractions JM4–JM6 underwent labor-intensive isolation procedures with low pressure liquid chromatography (LPLC) to isolate the active compounds using various ad-

sorbents, such as polyamide and Sephadex LH-2. The fractionation process was controlled by thin layer chromatography (TLC) (TLC Cellulose, 20 × 20 cm, MERCK, *n*-BuOH:CH₃COOH:H₂O, 4:1:5 (*v/v/v*); upper layer, sprayed with 1% Naturstoff reagent A) analysis under UV light. Isolated, chromatographically homogeneous compounds **9** (250 mg), **12** (1640 mg), and **22** (139 mg) were subjected to spectral analyses to determine their full structural characteristics. Spectral measurements were performed using UV-VIS (SPECORD 200 Plus, Analytik Jena, Jena, Germany) with various complexing reagents and ¹H NMR and ¹³C NMR spectra were recorded (BRUKER Advance II 400, BRUKER, Billerica, MA, USA). The final characteristics of all isolated compounds were also confirmed by MS (Agilent, Santa Clara, CA, USA).

4.6. Biological Assays

4.6.1. Cell Culture

The human amelanotic melanoma cell line C32 (CRL-1585) and a normal human fibroblast cell line (PCS-201-012) were cultured in DMEM. DMEM was blended with 10% FBS, 10 µg/mL streptomycin, and 10 units/mol penicillin. The cells were cultured in 5% CO₂ and fully humidified at 37 °C. All tested compounds were used at a final DMSO concentration of not more than 0.5% (*v/v*). Cells cultured in drug-free DMEM were used as controls, and cells with the addition of only DMSO were used as solvent-controls; VLB was used as a positive control. The **JM4** fraction was analyzed at the following concentrations: 25, 50 and 100 µg/mL and compound **22** and VLB were analyzed at 25 µg/mL. For the cytotoxicity assay, all extracts and compounds were tested at the following concentrations: 10, 25, 50, 100, 200, and 300 µg/mL.

4.6.2. Cytotoxicity Assay

Cytotoxicity was evaluated by the MTT colorimetric assay previously described by Carmichael [63]. The MTT test is founded on the reduction of a yellow tetrazolium salt to purple formazan crystals by viable cells. C32 and fibroblast cells were seeded in 24-well plates at an initial density of 1 × 10⁵ cells per well. The cultured cells were grown at 37 °C for 24 h and incubated with **JM1–JM6** and compounds **9**, **12** and **22** at various concentrations for 24 h. Each sample was dissolved in DMSO (the DMSO concentration was no greater than 0.5%) and further diluted in serum-free DMEM to achieve different concentrations (10–300 µg/mL). After incubation, 10 µL of MTT solution (5 mg/mL) was added to all cultured cells and followed by an additional incubation for 4 h (fibroblast cell line) or 10 min (C32 cell line). Upon removal of the medium, 200 µL of DMSO was added to all wells to dissolve the insoluble formazan. The results were measured spectrophotometrically at 570 nm using an Evolution 201 reader (Thermo Scientific, Waltham, MA, USA).

4.6.3. Fixable Viability Stain Assay

This analysis was performed to estimate the level of viable cells after treatment with **JM1–JM6**, compounds **9**, **12**, **22** and VLB at concentrations ranging from 10 to 300 µg/mL. Cytotoxicity was evaluated by FVS520 via a flow cytometer (BD FACSCanto II flow cytometer, San Jose, CA, USA). In contrast to nonpermeable live cells, the permeable membranes of necrotic cells allow for the intracellular diffusion of FVS520 and the covalent binding of high concentrations of amines. Thus, necrotic cells contained a higher level of FVS520 and, consequently, increased fluorescence intensity than viable cells. After 24 h of incubation, C32 cells and fibroblasts were washed with PBS, trypsinized and resuspended in DMEM. The supernatant was removed, and 0.5 mL of Stain Buffer with the addition of 1 µL of FVS520 was added to each sample, which was vortexed immediately and kept for 10–15 min in the dark at room temperature. After incubation and the addition of 2 mL of PBS, the supernatant was removed, the cells were resuspended in 300 µL of PBS and then immediately subjected to analysis. The results were analyzed based on FACSDiva software (BD Biosciences Systems, San Jose, CA, USA). Based on the results of the cytotoxicity

analysis, further research in this project focused on the determination of the full anticancer mechanism of the most promising fraction **JM4** and compound **22**.

4.6.4. Cell Cycle Analysis

The allocation of cell cycle stage was analyzed on a FACSCanto II flow cytometer. C32 cells were cured with **JM4**, **22** and VLB for 24 h of incubation. Thereafter, the cells were harvested and adjusted with 1 mL of 70% EtOH and maintained at $-20\text{ }^{\circ}\text{C}$ for 24 h. Next, the cells were washed with PBS, treated with 50 $\mu\text{g}/\text{mL}$ DNase-free RNase A solution for 5 min at room temperature, stained with 100 $\mu\text{g}/\text{mL}$ PI for 30 min at $37\text{ }^{\circ}\text{C}$, and submitted to flow cytometry analysis. The results were analyzed with FACSDiva software.

4.6.5. Flow Cytometry Assessment of Annexin V Binding

Characterization of the mode of apoptosis induced by **JM4**, **22** and VLB was performed in C32 cells via flow cytometry using a FITC Annexin V Apoptosis Detection Kit II. All stages of programmed cell death could be identified by annexin V bound with high affinity to PS. PI is a standard flow cytometric viability explorer that stains cells that interfere with the cell membrane, and it can be used to distinguish necrotic cells from dead cells. After the C32 cells were incubated for 24 h with various concentrations of **JM4**, **22** and VLB, they were trypsinized and resuspended in binding buffer. After that, 5 μL of annexin V-FITC and 5 μL of PI were added and maintained for 15 min in the dark at room temperature. The results were analyzed using FACSDiva software.

4.6.6. Determination of the Level of Autophagy by Autophagy Assay, Red

An autophagy assay was carried out to detect the impact of **JM4**, compound **22**, and VLB on the autophagy process of C32 cells via flow cytometry using an Autophagy Assay, Red kit. The probe is a cell-permeable aliphatic molecule that brightly fluoresces after unjumbling autophosphates and autolysosomes into lipid membranes. Samples of C32 cells incubated for 24 h with **JM4**, **22**, and VLB were subjected to a rising procedure with PBS and then resuspended in PBS with the accessory of Autophagy Probe, Red solution, and maintained for 30 min at $37\text{ }^{\circ}\text{C}$ in the dark. After incubation, the cells were flushed again and resuspended in cellular assay buffer. The results were analyzed with FACSDiva software.

4.6.7. Analysis of Mitochondrial Membrane Potential (MMP)

Disorder of the MMP was determined by the lipophilic cationic probe 5,5',6,6'-tetrachloro-1,1',3,3'-tetrarhylbenzimidazol-carbocyanine iodide using a JC-1 MitoScreen kit. Samples of C32 cells after the 24 h incubation with **JM4**, compound **22**, and VLB, were subjected to a rising procedure with PBS, suspended in PBS with 10 $\mu\text{g}/\text{mL}$ JC-1 and maintained for 15 min at room temperature in the dark. After incubation, the cells were flushed again, resuspended in PBS, and immediately subjected to BD FACSCanto II flow cytometry analysis. The results were analyzed using FACSDiva.

4.6.8. Determination of Caspase-3, Caspase-8, Caspase-9, and Caspase-10 Activity

Determination of the caspase-3, caspase-8, caspase-9, and caspase-10 activity were carried out by the following kits: FLICA Caspase-3/7 Assay Kit, FLICA Caspase-8 Assay Kit, FLICA Caspase-9 Assay Kit, and FLICA Caspase-10 Assay Kit using a BD FACSCanto II flow cytometer. C32 cells were incubated with **JM4**, compound **22** and VLB for 24 h, washed twice with PBS, resuspended in buffer supplemented with 5 mL of FLICA reagent, and incubated. After 1 h, the cells were flushed with apoptosis wash buffer and resuspended in 100 mL of the same reagent with 10 mg/mL PI. The procedure of determining the activity of each caspase was carried out analogously. The results were analyzed with FACSDiva software.

4.6.9. Cell Morphological Analysis

Visualization of the nuclear morphology of C32 cells was evaluated using a phase contrast microscope (Nikon Eclipse Ti, Tokyo, Japan) at $200\times$ magnification. C32 cells

(2.5×10^5) were incubated with **JM4** at concentrations of 25, 50, and 100 $\mu\text{g}/\text{mL}$ and compound **22** and VLB at a concentration of 25 $\mu\text{g}/\text{mL}$ in 6-well plates for 24 h at 37 °C. After incubation, the cells were washed twice with PBS and observed under a phase contrast microscope.

4.6.10. Statistical Analysis

All numerical data are shown as the mean \pm standard deviation (SD) from at least three independent repeats. Statistical analysis was performed using GraphPad Prism 8 software (GraphPad Software, San Diego, CA, USA). Statistical differences were assessed using one-way ANOVA followed by Tukey's test. Values of $p < 0.05$ were considered statistically significant.

5. Conclusions

Summarizing, the results of conducted studies indicate that *J. montana* is a rich source of polyphenolic compounds, mainly luteolin and its derivatives demonstrated significant cytotoxic and proapoptotic potential. The obtained results have shown that *J. montana* may be an effective strategy to develop preparation with potential antimelanoma properties. However, further studies are required in the human system to determine cellular uptake, distribution, and the long-term effect of the isolated flavonoids in the skin.

Supplementary Materials: The following are available online at <https://www.mdpi.com/1422-0067/22/7/3345/s1>, Figure S1: The qualitative assessment of *J. montana* extracts (JM1–JM3). UV-VIS chromatogram ($\lambda = 280$ nm) obtained by LC–PDA–MS, Figure S2: The qualitative assessment of *J. montana* fractions (JM4–JM6). UV-VIS chromatogram ($\lambda = 280$ nm) obtained by LC–PDA–MS, Figure S3: ¹H NMR spectrum (400.15 MHz, DMSO-*d*₆) of compound 9, Figure S4: ¹³C NMR spectrum (400.15 MHz, DMSO-*d*₆) of compound 9, Figure S5: The MS spectrum of compound 9 in positive ion mode, Figure S6: ¹H NMR spectrum (400.15 MHz, DMSO-*d*₆) of compound 12, Figure S7: ¹³C NMR spectrum (400.15 MHz, DMSO-*d*₆) of compound 12, Figure S8: ¹H NMR spectrum (400.3 MHz, DMSO-*d*₆) of compound 22, Figure S9: Flow cytometric analysis of cytotoxicity of C32 melanoma cells after 24 h of incubation with DMSO and VLB (10, 25, 50, 100, 200, and 300 $\mu\text{g}/\text{mL}$) comparable with untreated control by the fixable viability stain assay, Figure S10: Flow cytometric analysis of cytotoxicity of C32 melanoma cells after 24 h of incubation with JM1–JM3 (10, 25, 50, 100, 200, and 300 $\mu\text{g}/\text{mL}$) comparable with untreated control by the fixable viability stain assay, Figure S11: Flow cytometric analysis of cytotoxicity of C32 melanoma cells after 24 h of incubation with JM4–JM6 (10, 25, 50, 100, 200, and 300 $\mu\text{g}/\text{mL}$) comparable with untreated control by the fixable viability stain assay, Figure S12: Flow cytometric analysis of cytotoxicity of C32 melanoma cells after 24 h of incubation with compound 9, 12, and 22 (10, 25, 50, 100, 200, and 300 $\mu\text{g}/\text{mL}$) comparable with untreated control by the fixable viability stain assay, Figure S13: Flow cytometric analysis of cytotoxicity of normal human fibroblasts cells after 24 h of incubation with DMSO, JM4, and compound 22 (10, 25, 50, 100, 200, and 300 $\mu\text{g}/\text{mL}$) comparable with untreated control by the fixable viability stain assay.

Author Contributions: Conceptualization, A.M.J. and M.T.; methodology, A.M.J., R.C., J.W.S. and M.Z.K.; formal analysis, K.B. and M.T.; investigation, A.M.J., R.C., J.W.S. and M.Z.K.; writing—original draft preparation, A.M.J., R.C., J.W.S., M.Z.K. and M.T.; writing—review and editing, K.B. and M.T.; visualization, A.M.J.; supervision, M.T.; project administration, A.M.J. and M.T. All authors have read and agreed to the published version of the manuscript.

Funding: The work was funded by the project N° POWR.03.02.00-00-I051/16 from European Union funds, POWER 2014-2020, grant No. 05/IMSD/G/2019.

Institutional Review Board Statement: Not applicable.

Informed Consent Statement: Not applicable.

Conflicts of Interest: The authors declare no conflict of interest.

Abbreviations

CHCl ₃	chloroform
CMM	cutaneous malignant melanoma
DMEM	Dulbecco's minimal essential medium
DMSO	dimethyl sulfoxide
ESI	electrospray ionization
Et ₂ O	diethyl ether
EtOAc	ethyl acetate
EtOH	ethanol
FBS	fetal bovine serum
HCOOH	formic acid
H ₂ O	water
IC ₅₀	median inhibitory concentration
LPLC	low pressure liquid chromatography
LC-PDA-ESI-MS/TOF	liquid chromatography-photodiode array detection-electrospray ionization-mass spectrometry
MeCN	acetonitrile
MeOH	methanol
MMP	mitochondrial membrane potential
MS	mass spectrometer
NMR	nuclear magnetic resonance
MTT	3-(4,5-dimethylthiazol-2-yl)-2,5-diphenyl tetrazolium bromide
<i>n</i> -BuOH	<i>n</i> -butanol
PBS	phosphate-buffered saline
PDA	photodiode array detection
PI	propidium iodide
PS	phosphatidylserine
ROS	reactive oxygen species
TLC	thin layer chromatography
UPW	ultra-pure water
UV	ultraviolet
UV-VIS	ultraviolet-visible spectroscopy
WHO	World Health Organization
VLB	vinblastine sulfate

References

- World Health Organization. Radiation: Ultraviolet (UV) Radiation and Skin Cancer. Available online: [https://www.who.int/news-room/q-a-detail/radiation-ultraviolet-\(uv\)-radiation-and-skin-cancer](https://www.who.int/news-room/q-a-detail/radiation-ultraviolet-(uv)-radiation-and-skin-cancer) (accessed on 28 January 2020).
- Majumder, D.; Debnath, M.; Libin Kumar, K.V.; Nath, P.; Debnath, R.; Sarkar, C.; Prasad, G.B.K.S.; Verma, Y.K.; Maiti, D. Metabolic profiling and investigations on crude extract of *Olea europaea* L. leaves as a potential therapeutic agent against skin cancer. *J. Funct. Foods* **2019**, *58*, 266–274. [CrossRef]
- George, V.C.; Kumar, D.R.N.; Suresh, P.K.; Kumar, S.; Kumar, R.A. Comparative studies to evaluate relative In Vitro potency of luteolin in inducing cell cycle arrest and apoptosis in HaCat and A375 cells. *Asian Pac. J. Cancer Prev.* **2013**, *14*, 631–637. [CrossRef] [PubMed]
- Ruan, J.S.; Liu, Y.P.; Zhang, L.; Yan, L.G.; Fan, F.T.; Shen, C.S.; Wang, A.Y.; Zheng, S.Z.; Wang, S.M.; Lu, Y. Luteolin reduces the invasive potential of malignant melanoma cells by targeting β 3 integrin and the epithelial-mesenchymal transition. *Acta Pharmacol. Sin.* **2012**, *33*, 1325–1331. [CrossRef]
- Davis, L.E.; Shalin, S.C.; Tackett, A.J. Current state of melanoma diagnosis and treatment. *Cancer Biol. Ther.* **2019**, *20*, 1366–1379. [CrossRef]
- Momtaz, S.; Niaz, K.; Maqbool, F.; Abdollahi, M.; Rastrelli, L.; Nabavi, S.M. STAT3 targeting by polyphenols: Novel therapeutic strategy for melanoma. *BioFactors* **2017**, *43*, 347–370. [CrossRef] [PubMed]
- Imran, M.; Rauf, A.; Abu-Izneid, T.; Nadeem, M.; Shariati, M.A.; Khan, I.A.; Imran, A.; Orhan, I.E.; Rizwan, M.; Atif, M.; et al. Luteolin, a flavonoid, as an anticancer agent: A review. *Biomed. Pharmacother.* **2019**, *112*, 108612. [CrossRef]
- Oliveira Júnior, R.; Ferraz, C.; Silva, M.; Lavor, É.; Rolim, L.; Lima, J.; Fleury, A.; Picot, L.; Quintans, J.; Quintans-Júnior, L.; et al. Flavonoids: Promising natural products for treatment of skin cancer (melanoma). In *Natural Products and Cancer Drug Discovery*; Badria, F.A., Ed.; IntechOpen: London, UK, 2017; pp. 161–2010. ISBN 978-953-51-3313-1.

9. Lelli, D.; Pedone, C.; Sahebkar, A. Curcumin and treatment of melanoma: The potential role of microRNAs. *Biomed. Pharmacother.* **2017**, *88*, 832–834. [[CrossRef](#)]
10. Yi, C.; Li, X.; Chen, S.; Liu, M.; Lu, W.; Ye, X. Natural product corynoline suppresses melanoma cell growth through inducing oxidative stress. *Phyther. Res.* **2020**, *34*, 2766–2777. [[CrossRef](#)]
11. Parnell, J.A.N. Biological flora of the British Isles. *Jasione montana* L. *J. Ecol.* **1985**, *73*, 341–358. [[CrossRef](#)]
12. Zapesochnaya, G.G.; Nikolaeva, V.G.; Ban'kovskii, A.I. The flavonoids of *Jasione montana* and *Melittis sarmatika*. *Chem. Nat. Compd.* **1972**, *8*, 112. [[CrossRef](#)]
13. Trojanowska, A. Traditional Belarussian herbal medicine in paper Michał Federowski's: Lud białoruski na Rusi Litewskiej. *Analecta* **2007**, *16*, 7–53.
14. Jabłonowska, M.; Mutryn, K.; Bazyłko, A.; Grochowski, D.; Strawa, J.; Tomczyk, M. Identification of antioxidant polyphenolics from *Jasione montana* based on a preliminary LC-MS profiling. *Planta Med. Inter. Open* **2017**, *4*, S1–S202. [[CrossRef](#)]
15. Agrawal, P.K. *Carbon-13 NMR of Flavonoids*; Elsevier: Amsterdam, The Netherlands, 1989; ISBN 9781483290744.
16. Harborne, J.B. *The Flavonoids. Advances in Research Since 1986*; Chapman & Hall: London, UK, 1996.
17. Markham, K.R.; Ternai, B.; Stanley, R.; Geiger, H.; Mabry, T.J. Carbon-13 NMR studies of flavonoids—III. *Tetrahedron* **1978**, *34*, 1389–1397. [[CrossRef](#)]
18. Bruggisser, R.; von Daeniken, K.; Jundt, G.; Schaffner, W.; Tullberg-Reinert, H. Interference of plant extracts, phytoestrogens and antioxidants with the MTT tetrazolium assay. *Planta Med.* **2002**, *68*, 445–448. [[CrossRef](#)]
19. Wang, P.; Henning, S.M.; Heber, D. Limitations of MTT and MTS-based assays for measurement of antiproliferative activity of green tea polyphenols. *PLoS ONE* **2010**, *5*, e10202. [[CrossRef](#)] [[PubMed](#)]
20. Wisman, K.N.; Perkins, A.A.; Jeffers, M.D.; Hagerman, A.E. Accurate assessment of the bioactivities of redox-active polyphenolics in cell culture. *J. Agric. Food Chem.* **2008**, *56*, 7831–7837. [[CrossRef](#)] [[PubMed](#)]
21. Demchenko, A.P. Beyond annexin V: Fluorescence response of cellular membranes to apoptosis. *Cytotechnology* **2013**, *65*, 157–172. [[CrossRef](#)] [[PubMed](#)]
22. Bielawski, K.; Czarnomysy, R.; Muszyńska, A.; Bielawska, A.; Popławska, B. Cytotoxicity and induction of apoptosis of human breast cancer cells by novel platinum(II) complexes. *Environ. Toxicol. Pharmacol.* **2012**, *35*, 254–264. [[CrossRef](#)] [[PubMed](#)]
23. D'Arcy, M.S. Cell death: A review of the major forms of apoptosis, necrosis and autophagy. *Cell Biol. Int.* **2019**, *43*, 582–592. [[CrossRef](#)] [[PubMed](#)]
24. Bialik, S.; Dasari, S.K.; Kimchi, A. Autophagy-dependent cell death—Where, how and why a cell eats itself to death. *J. Cell Sci.* **2018**, *131*, jcs215152. [[CrossRef](#)]
25. Ly, J.D.; Grubb, D.R.; Lawen, A. The mitochondrial membrane potential ($\Delta\psi_m$) in apoptosis; an update. *Apoptosis* **2003**, *8*, 115–128. [[CrossRef](#)]
26. Green, D.R.; Kroemer, G. The pathophysiology of mitochondrial cell death. *Science* **2004**, *305*, 626–629. [[CrossRef](#)]
27. Sánchez-Alcázar, J.A.; Ault, J.G.; Khodjakov, A.; Schneider, E. Increased mitochondrial cytochrome c levels and mitochondrial hyperpolarization precede camptothecin-induced apoptosis in Jurkat cells. *Cell Death Differ.* **2000**, *7*, 1090–1100. [[CrossRef](#)]
28. Denault, J.-B.; Salvesen, G. Caspases: Keys in the ignition of cell death. *Chem. Rev.* **2003**, *102*, 4489–4500. [[CrossRef](#)] [[PubMed](#)]
29. Porter, A.G.; Jänicke, R.U. Emerging roles of caspase-3 in apoptosis. *Cell Death Differ.* **1999**, *6*, 99–104. [[CrossRef](#)] [[PubMed](#)]
30. Russo, M.; Mupo, A.; Spagnuolo, C.; Russo, G.L. Exploring death receptor pathways as selective targets in cancer therapy. *Biochem. Pharmacol.* **2010**, *80*, 674–682. [[CrossRef](#)] [[PubMed](#)]
31. Amin, A.R.M.R.; Kucuk, O.; Khuri, F.R.; Shin, D.M. Perspectives for cancer prevention with natural compounds. *J. Clin. Oncol.* **2009**, *27*, 2712–2725. [[CrossRef](#)] [[PubMed](#)]
32. Seelinger, G.; Merfort, I.; Wölflle, U.; Schempp, C.M. Anti-carcinogenic effects of the flavonoid luteolin. *Molecules* **2008**, *13*, 2628–2651. [[CrossRef](#)] [[PubMed](#)]
33. Ombra, M.N.; Paliogiannis, P.; Stucci, L.S.; Colombino, M.; Casula, M.; Sini, M.C.; Manca, A.; Palomba, G.; Stanganelli, I.; Mandalà, M.; et al. Dietary compounds and cutaneous malignant melanoma: Recent advances from a biological perspective. *Nutr. Metab.* **2019**, *16*, 1–15. [[CrossRef](#)]
34. Carradori, S.; D'Ascenzio, M.; Chimenti, P.; Secci, D.; Bolasco, A. Selective MAO-B inhibitors: A lesson from natural products. *Mol. Divers.* **2014**, *18*, 219–243. [[CrossRef](#)] [[PubMed](#)]
35. Juszczak, A.M.; Zovko-Končić, M.; Tomczyk, M. Recent trends in the application of chromatographic techniques in the analysis of luteolin and its derivatives. *Biomolecules* **2019**, *9*, 731. [[CrossRef](#)] [[PubMed](#)]
36. Szekalska, M.; Sosnowska, K.; Tomczykowa, M.; Winnicka, K.; Kasacka, I.; Tomczyk, M. In vivo anti-inflammatory and anti-allergic activities of cynaroside evaluated by using hydrogel formulations. *Biomed. Pharmacother.* **2020**, *121*, 109681. [[CrossRef](#)]
37. Chan, K.T.; Meng, F.Y.; Li, Q.; Ho, C.Y.; Lam, T.S.; To, Y.; Lee, W.H.; Li, M.; Chu, K.H.; Toh, M. Cucurbitacin B induces apoptosis and S phase cell cycle arrest in BEL-7402 human hepatocellular carcinoma cells and is effective via oral administration. *Cancer Lett.* **2010**, *294*, 118–124. [[CrossRef](#)]
38. Lepley, D.M.; Li, B.; Birt, D.F.; Pelling, J.C. The chemopreventive flavonoid apigenin induces G2/M arrest in keratinocytes. *Carcinogenesis* **1996**, *17*, 2367–2375. [[CrossRef](#)] [[PubMed](#)]
39. Kim, J.K.; Kang, K.A.; Ryu, Y.S.; Piao, M.J.; Han, X.; Oh, M.C.; Boo, S.J.; Jeong, S.U.; Jeong, Y.J.; Chae, S.; et al. Induction of endoplasmic reticulum stress via reactive oxygen species mediated by luteolin in melanoma cells. *Anticancer Res.* **2016**, *36*, 2281–2289. [[PubMed](#)]

40. Leung, H.W.-C.; Wu, C.-H.; Lin, C.-H.; Lee, H.-Z. Luteolin induced DNA damage leading to human lung squamous carcinoma CH27 cell apoptosis. *Eur. J. Pharmacol.* **2005**, *508*, 77–83. [[CrossRef](#)] [[PubMed](#)]
41. Fecker, L.; Geilen, C.; Hossini, A.; Schwarz, C.; Fechner, H.; Bartlett, D.; Orfanos, C.; Eberle, J. Selective induction of apoptosis in melanoma cells by tyrosinase promoter-controlled CD95 ligand overexpression. *J. Invest. Dermatol.* **2005**, *124*, 221–228. [[CrossRef](#)]
42. Said, A.; Tundis, R.; Hawas, U.W.; El-Kousy, S.M.; Rashed, K.; Menichini, F.; Bonesi, M.; Huefner, A.; Loizzo, M.R.; Menichini, F. In Vitro antioxidant and antiproliferative activities of flavonoids from *Ailanthus excelsa* (Roxb.) (Simaroubaceae) leaves. *Z. Naturforsch C* **2010**, *65*, 180–186. [[CrossRef](#)] [[PubMed](#)]
43. Visanji, J.M.; Thompson, D.G.; Padfield, P.J. Induction of G2/M phase cell cycle arrest by carnosol and carnosic acid is associated with alteration of cyclin A and cyclin B1 levels. *Cancer Lett.* **2006**, *237*, 130–136. [[CrossRef](#)]
44. Choi, E.J.; Kim, G.-H. O-desmethylangolensin inhibits the proliferation of human breast cancer MCF-7 cells by inducing apoptosis and promoting cell cycle arrest. *Oncol. Lett.* **2013**, *6*, 1784–1788. [[CrossRef](#)]
45. Zhang, J.; Zhu, X.; Li, H.; Li, B.; Sun, L.; Xie, T.; Zhu, T.; Zhou, H.; Ye, Z. Piperine inhibits proliferation of human osteosarcoma cells via G2/M phase arrest and metastasis by suppressing MMP-2/-9 expression. *Int. Immunopharmacol.* **2015**, *24*, 50–58. [[CrossRef](#)] [[PubMed](#)]
46. Czarnomysy, R.; Surazyński, A.; Popławska, B.; Rysiak, E.; Pawłowska, N.; Czajkowska, A.; Bielawski, K.; Bielawska, A. Synergistic action of cisplatin and echistatin in MDA-MB-231 breast cancer cells. *Mol. Cell. Biochem.* **2016**, *427*, 1–10. [[CrossRef](#)] [[PubMed](#)]
47. Shoshan-Barmatz, V.; Krelin, Y.; Chen, Q. VDAC1 as a player in mitochondria-mediated apoptosis and target for modulating apoptosis. *Curr. Med. Chem.* **2017**, *24*, 4435–4446. [[CrossRef](#)]
48. Green, D.R.; Reed, J.C. Mitochondria and apoptosis. *Science* **1998**, *281*, 1309–1312. [[CrossRef](#)]
49. Czarnomysy, R.; Surazyński, A.; Muszyńska, A.; Gornowicz, A.; Bielawska, A.; Bielawski, K. A novel series of pyrazole-platinum(II) complexes as potential anti-cancer agents that induce cell cycle arrest and apoptosis in breast cancer cells. *J. Enzym. Inhib. Med. Chem.* **2018**, *33*, 1006–1023. [[CrossRef](#)] [[PubMed](#)]
50. Danciu, C.; Zupko, I.; Bor, A.; Schwiebs, A.; Radeke, H.; Hancianu, M.; Cioanca, O.; Alexa, E.; Oprean, C.; Bojin, F.; et al. Botanical therapeutics: Phytochemical screening and biological assessment of chamomile, parsley and celery extracts against A375 human melanoma and dendritic cells. *Int. J. Mol. Sci.* **2018**, *19*, 3624. [[CrossRef](#)] [[PubMed](#)]
51. Cattaneo, L.; Cicconi, R.; Mignogna, G.; Giorgi, A.; Mattei, M.; Graziani, G.; Ferracane, R.; Grosso, A.; Aducci, P.; Schinina, M.E.; et al. Anti-proliferative effect of *Rosmarinus officinalis* L. extract on human melanoma A375 cells. *PLoS ONE* **2015**, *10*, 1–18. [[CrossRef](#)] [[PubMed](#)]
52. Corazzari, M.; Fimia, G.M.; Lovat, P.; Piacentini, M. Why is autophagy important for melanoma? Molecular mechanisms and therapeutic implications. *Semin. Cancer Biol.* **2013**, *23*, 337–343. [[CrossRef](#)] [[PubMed](#)]
53. Liu, H.; He, Z.; Simon, H.-U. Targeting autophagy as a potential therapeutic approach for melanoma therapy. *Semin. Cancer Biol.* **2013**, *23*, 352–360. [[CrossRef](#)]
54. Thorburn, A.; Thamm, D.H.; Gustafson, D.L. Autophagy and cancer therapy. *Mol. Pharmacol.* **2014**, *85*, 830–838. [[CrossRef](#)]
55. Chu, Y.-L.; Raghu, R.; Lu, K.-H.; Liu, C.-T.; Lin, S.-H.; Lai, Y.-S.; Cheng, W.-C.; Lin, S.-H.; Sheen, L.-Y. Autophagy therapeutic potential of garlic in human cancer therapy. *J. Tradit. Complement. Med.* **2013**, *3*, 159–162. [[CrossRef](#)] [[PubMed](#)]
56. Zhao, G.; Han, X.; Zheng, S.; Li, Z.; Sha, Y.; Ni, J.; Sun, Z.; Qiao, S.; Song, Z. Curcumin induces autophagy, inhibits proliferation and invasion by downregulating AKT/mTOR signaling pathway in human melanoma cells. *Oncol. Rep.* **2016**, *35*, 1065–1074. [[CrossRef](#)] [[PubMed](#)]
57. Yang, S.-F.; Yang, W.-E.; Chang, H.-R.; Chu, S.-C.; Hsieh, Y.-S. Luteolin induces apoptosis in oral squamous cancer cells. *J. Dent. Res.* **2008**, *87*, 401–406. [[CrossRef](#)]
58. Zhang, Q.; Zhao, X.-H.; Wang, Z.-J. Flavones and flavonols exert cytotoxic effects on a human oesophageal adenocarcinoma cell line (OE33) by causing G2/M arrest and inducing apoptosis. *Food Chem. Toxicol.* **2008**, *46*, 2042–2053. [[CrossRef](#)] [[PubMed](#)]
59. Lim, D.Y.; Jeong, Y.; Tyner, A.L.; Park, J.H.Y. Induction of cell cycle arrest and apoptosis in HT-29 human colon cancer cells by the dietary compound luteolin. *Am. J. Physiol. Gastrointest. Liver Physiol.* **2007**, *292*, G66–G75. [[CrossRef](#)]
60. Selvendiran, K.; Koga, H.; Ueno, T.; Yoshida, T.; Maeyama, M.; Torimura, T.; Yano, H.; Kojiro, M.; Sata, M. Luteolin promotes degradation in signal transducer and activator of transcription 3 in human hepatoma cells: An implication for the antitumor potential of flavonoids. *Cancer Res.* **2006**, *66*, 4826–4834. [[CrossRef](#)]
61. Strawa, J.; Wajs-Bonikowska, A.; Jakimiuk, K.; Waluk, M.; Poslednik, M.; Nazaruk, J.; Tomczyk, M. Phytochemical examination of woolly burdock *Arctium tomentosum* leaves and flower heads. *Chem. Nat. Compd.* **2020**, *56*, 345–347. [[CrossRef](#)]
62. Nazaruk, J. Flavonoid compounds from *Cirsium palustre* (L.) Scop. flower heads. *Biochem. Syst. Ecol.* **2009**, *37*, 525–527. [[CrossRef](#)]
63. Carmichael, J.; DeGraff, W.; Gazdar, A.; Minna, J.; Mitchell, J. Evaluation of a tetrazolium-based semiautomated colorimetric assay: Assessment of radiosensitivity. *Cancer Res.* **1987**, *47*, 943–946.



SUPPLEMENTARY MATERIAL

***In vitro* anticancer potential of *Jasione montana* and its main components against human amelanotic melanoma cells**

Aleksandra Maria Juszcak, Robert Czarnomysy, Jakub Władysław Strawa, Marijana Zovko-Končić, Krzysztof Bielawski and Michał Tomczyk

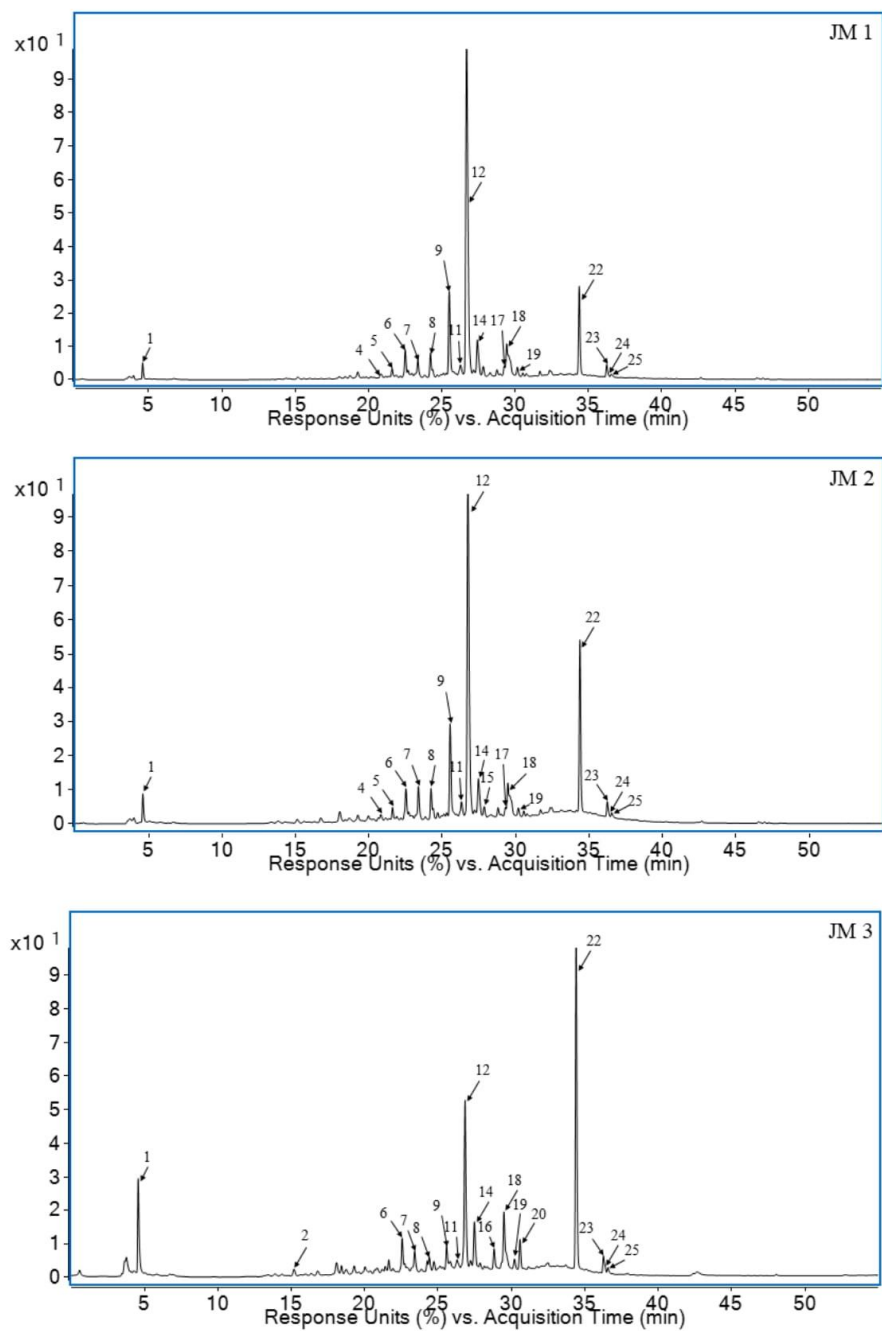


Figure S1. The qualitative assessment of *J. montana* extracts (JM1–JM3).
UV-VIS chromatogram ($\lambda=280$ nm) obtained by LC-PDA–MS.

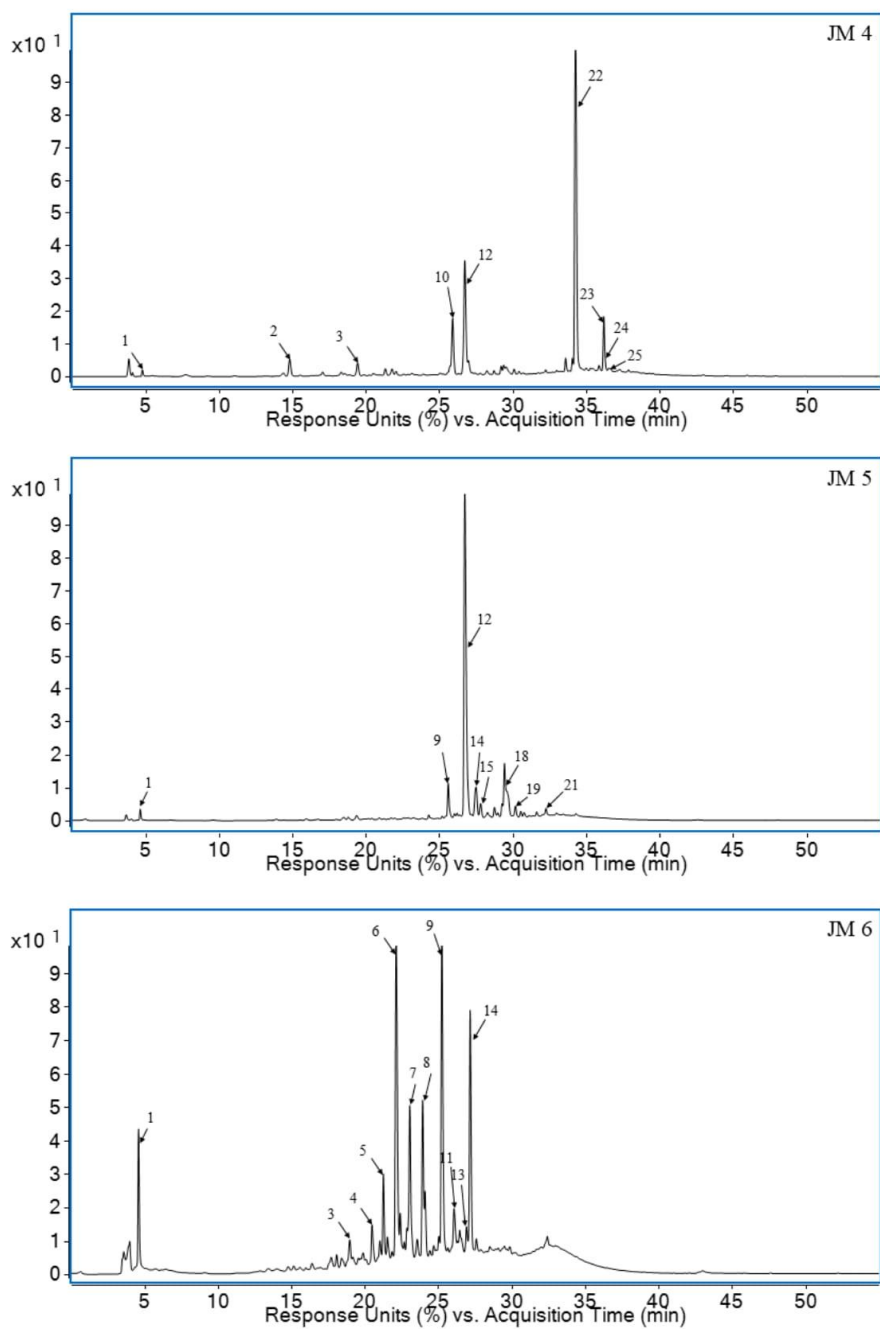


Figure S2. The qualitative assessment of *J. montana* fractions (JM4–JM6).
 UV-VIS chromatogram ($\lambda=280$ nm) obtained by LC-PDA–MS.

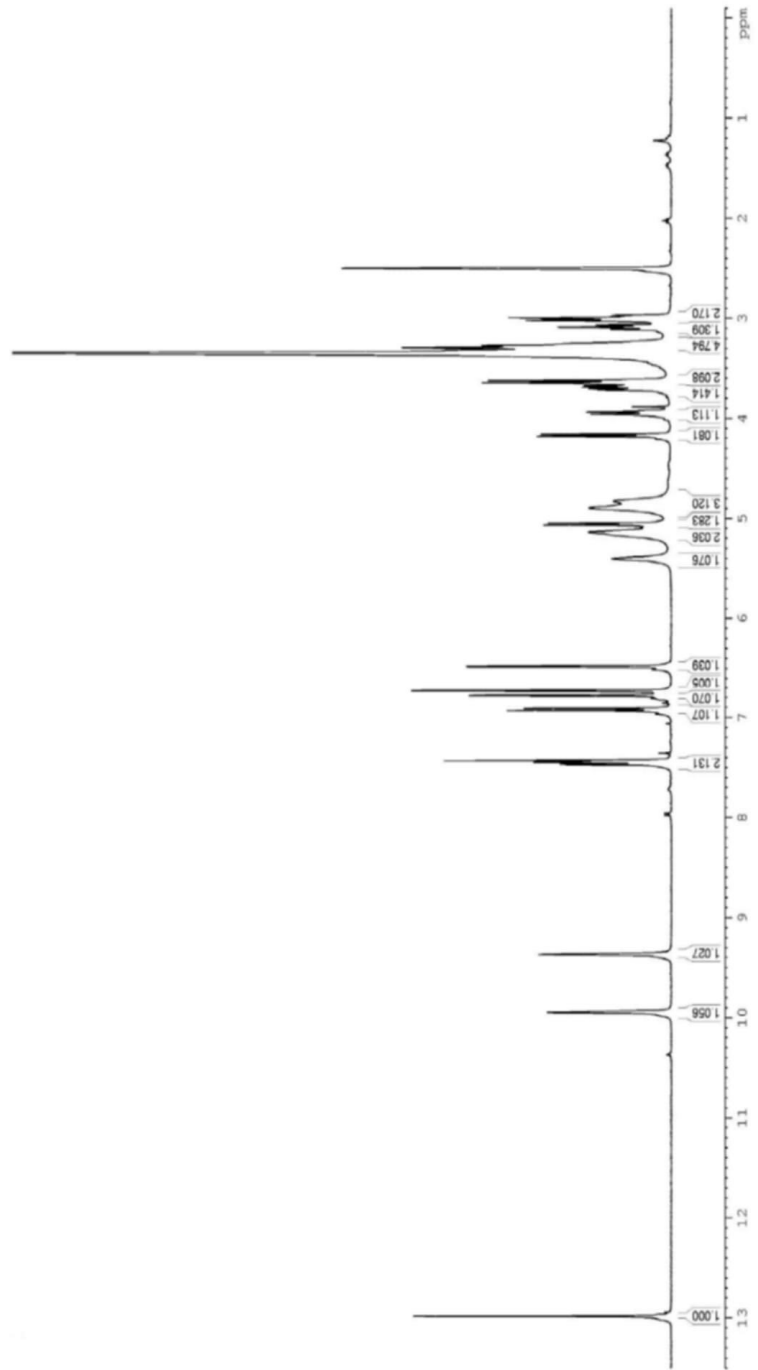


Figure S3. ¹H NMR spectrum (400.15 MHz, DMSO-*d*₆) of compound **9**.

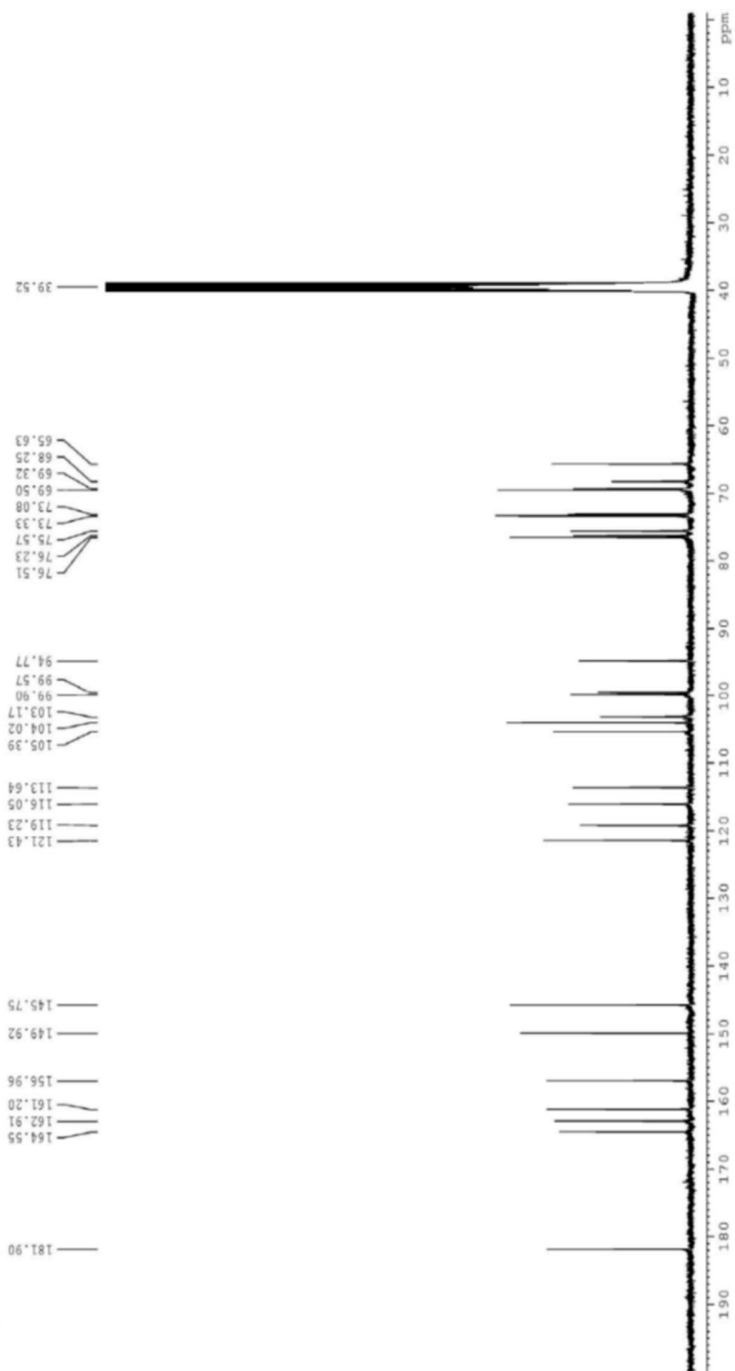


Figure S4. ^{13}C NMR spectrum (400.15 MHz, $\text{DMSO-}d_6$) of compound **9**.

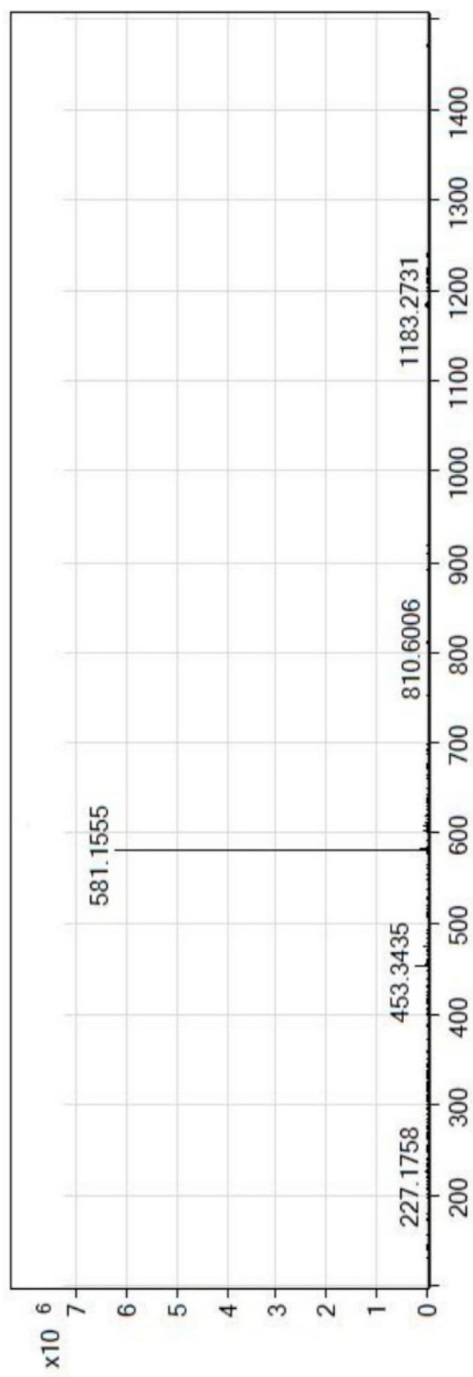


Figure S5. The MS spectrum of compound **9** in positive ion mode.

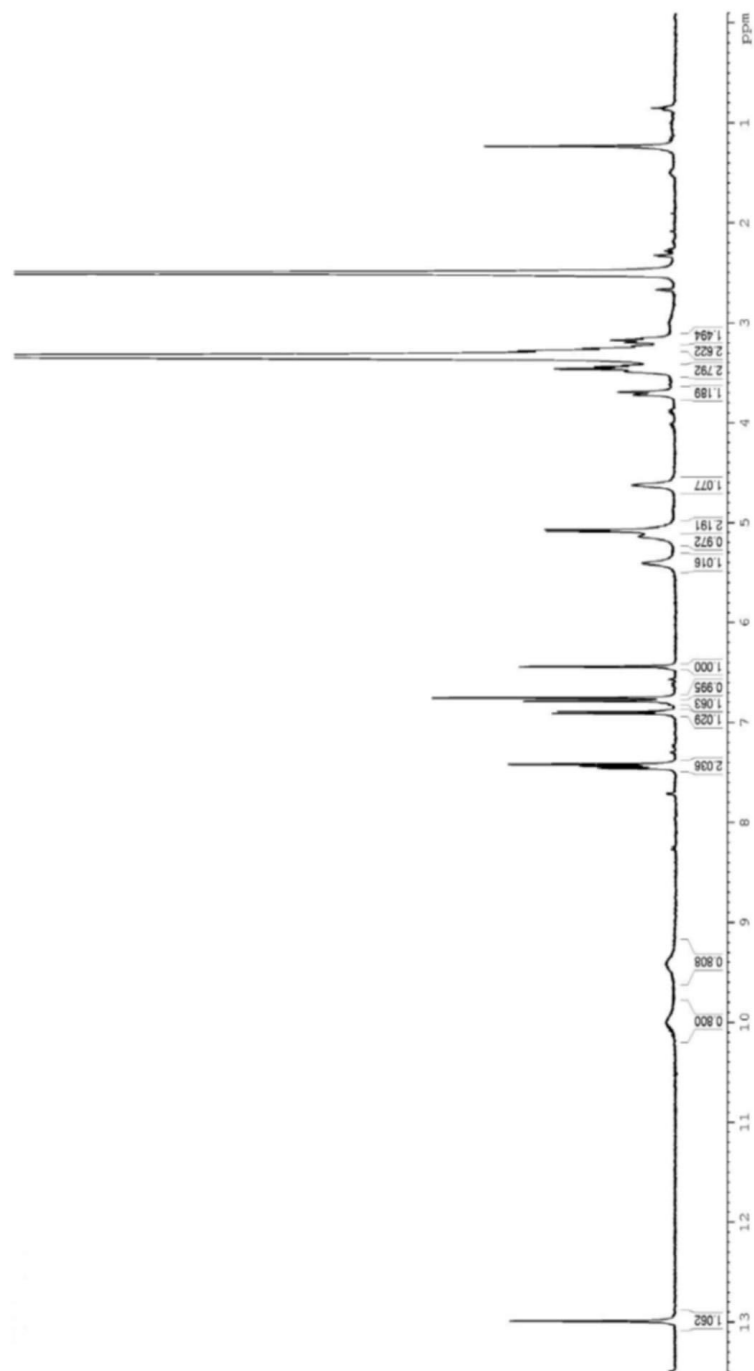


Figure S6. ¹H NMR spectrum (400.15 MHz, DMSO-*d*₆) of compound 12.

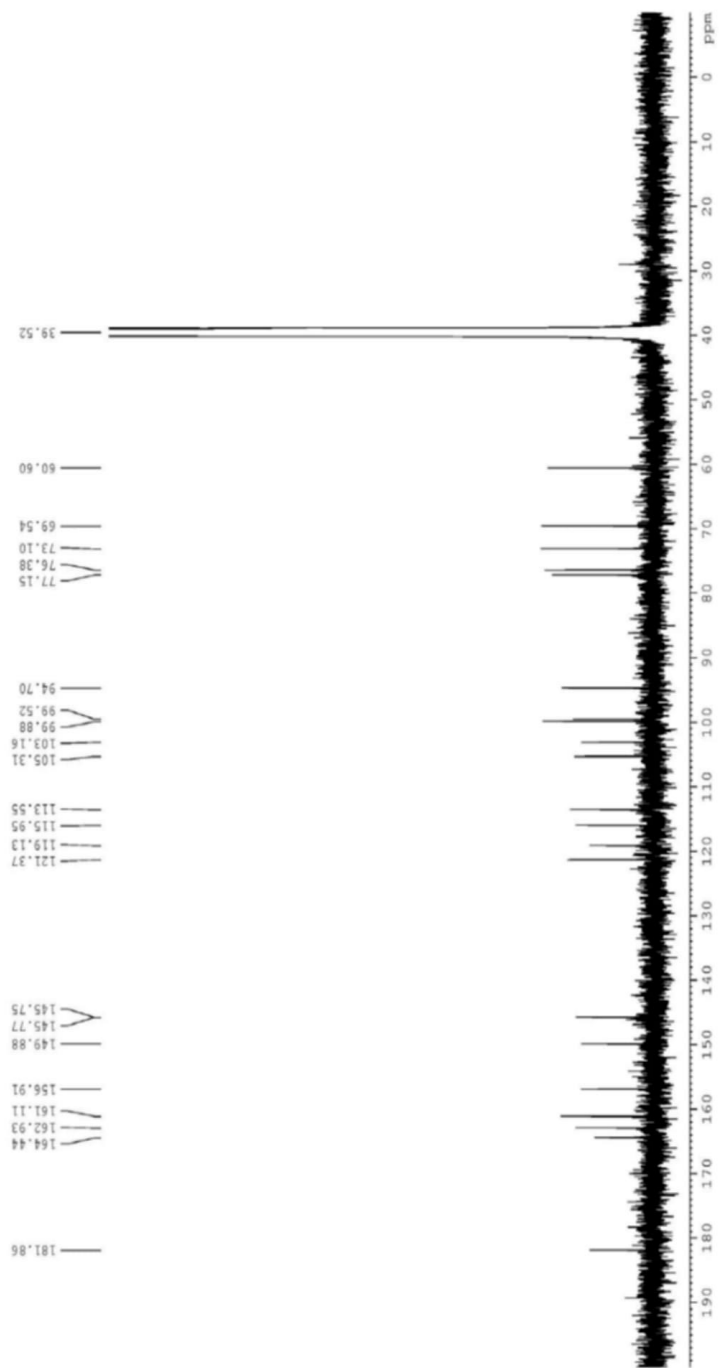


Figure S7. ^{13}C NMR spectrum (400.15 MHz, $\text{DMSO-}d_6$) of compound 12.

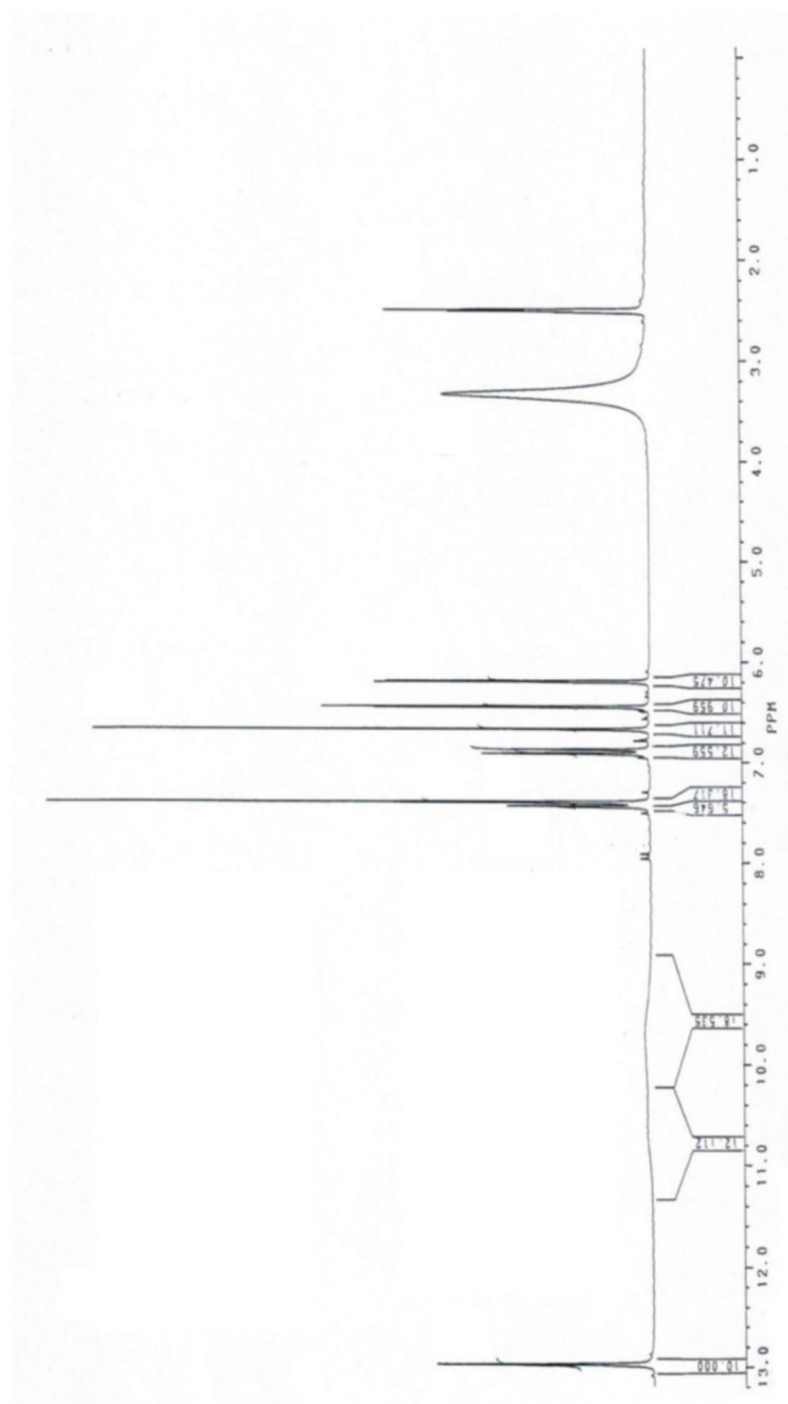


Figure S8. ¹H NMR spectrum (400.3 MHz, DMSO-*d*₆) of compound **22**.

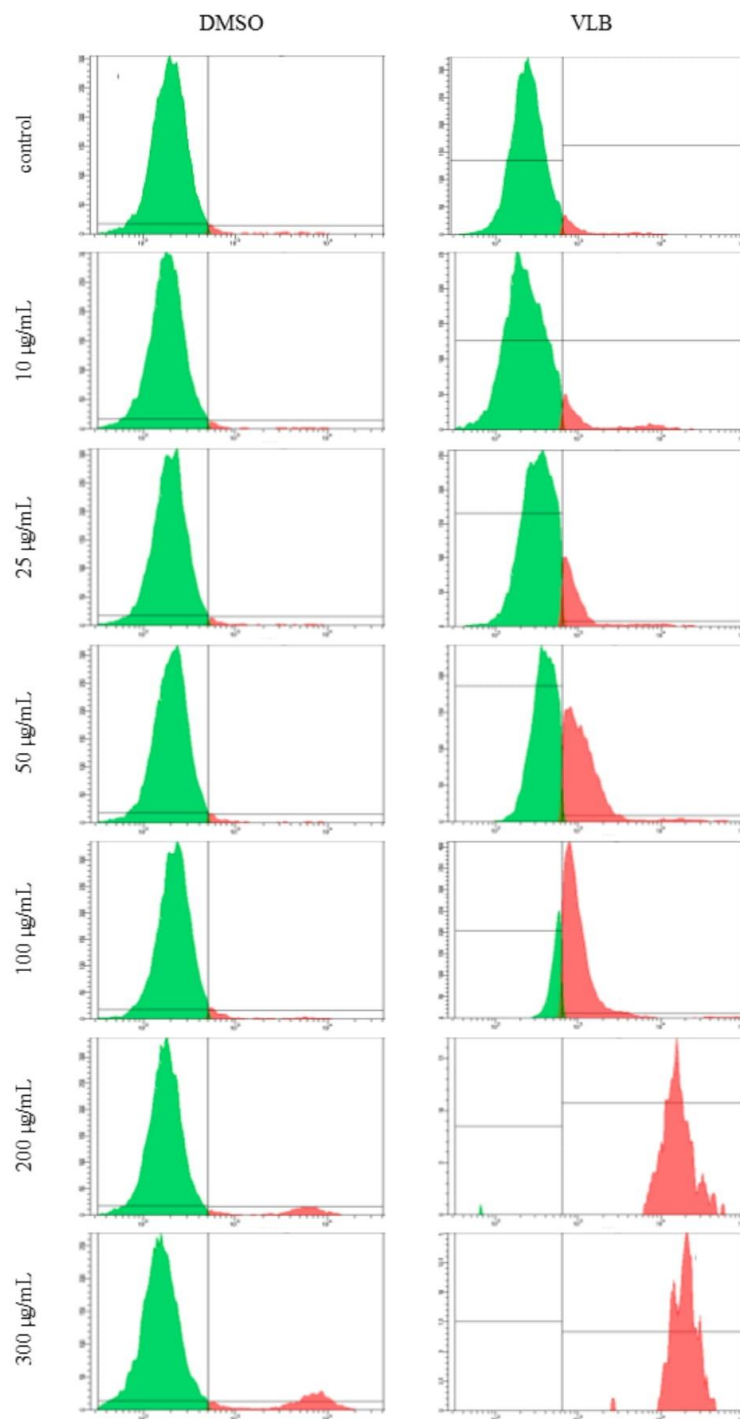


Figure S9. Flow cytometric analysis of cytotoxicity of C32 melanoma cells after 24 h of incubation with DMSO and VLB (10, 25, 50, 100, 200, and 300 µg/mL) comparable with untreated control by the Fixable Viability Stain assay.

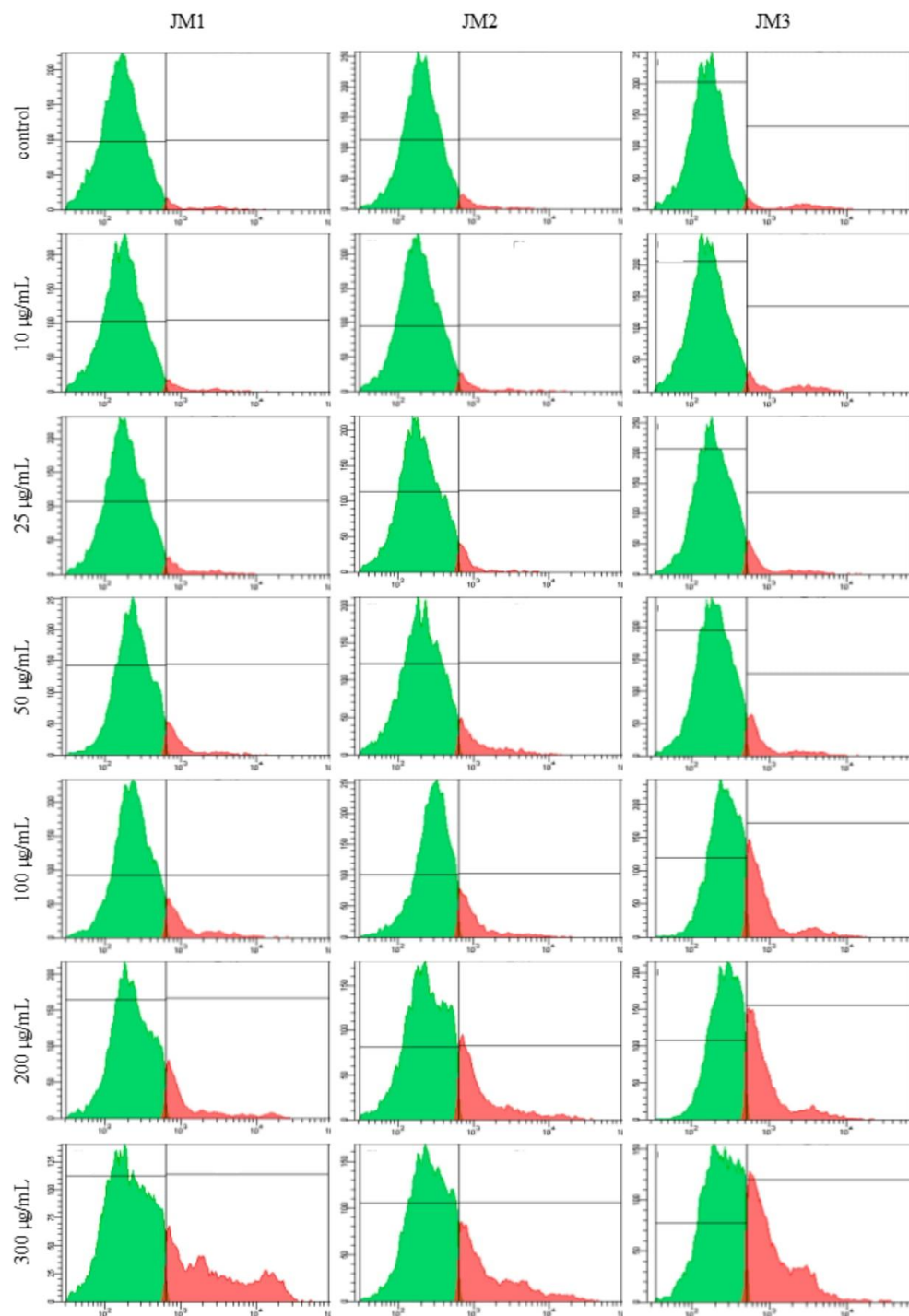


Figure S10. Flow cytometric analysis of cytotoxicity of C32 melanoma cells after 24 h of incubation with **JM1–JM3** (10, 25, 50, 100, 200, and 300 µg/mL) comparable with untreated control by the Fixable Viability Stain assay.

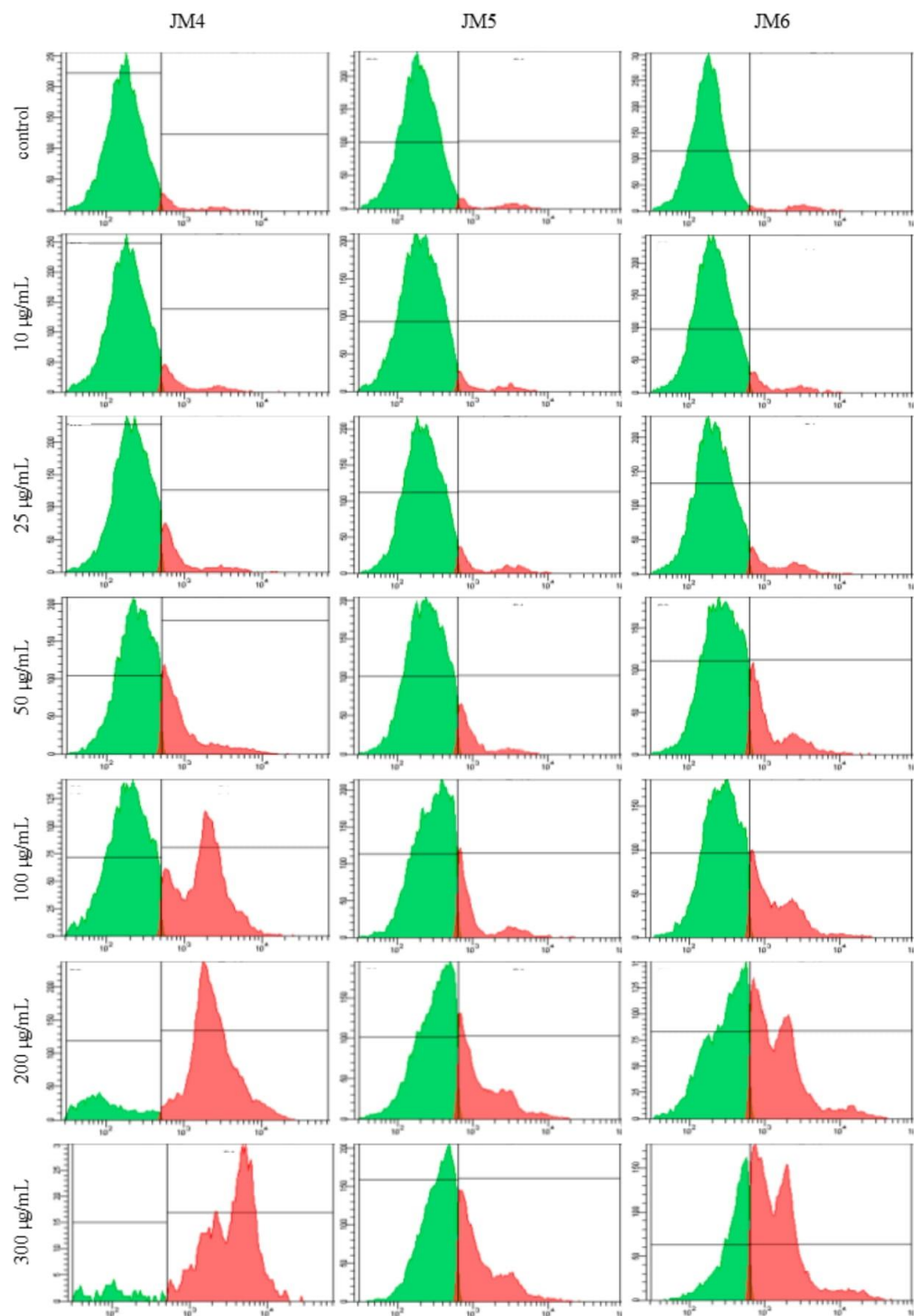


Figure S11. Flow cytometric analysis of cytotoxicity of C32 melanoma cells after 24 h of incubation with **JM4–JM6** (10, 25, 50, 100, 200, and 300 µg/mL) comparable with untreated control by the Fixable Viability Stain assay.

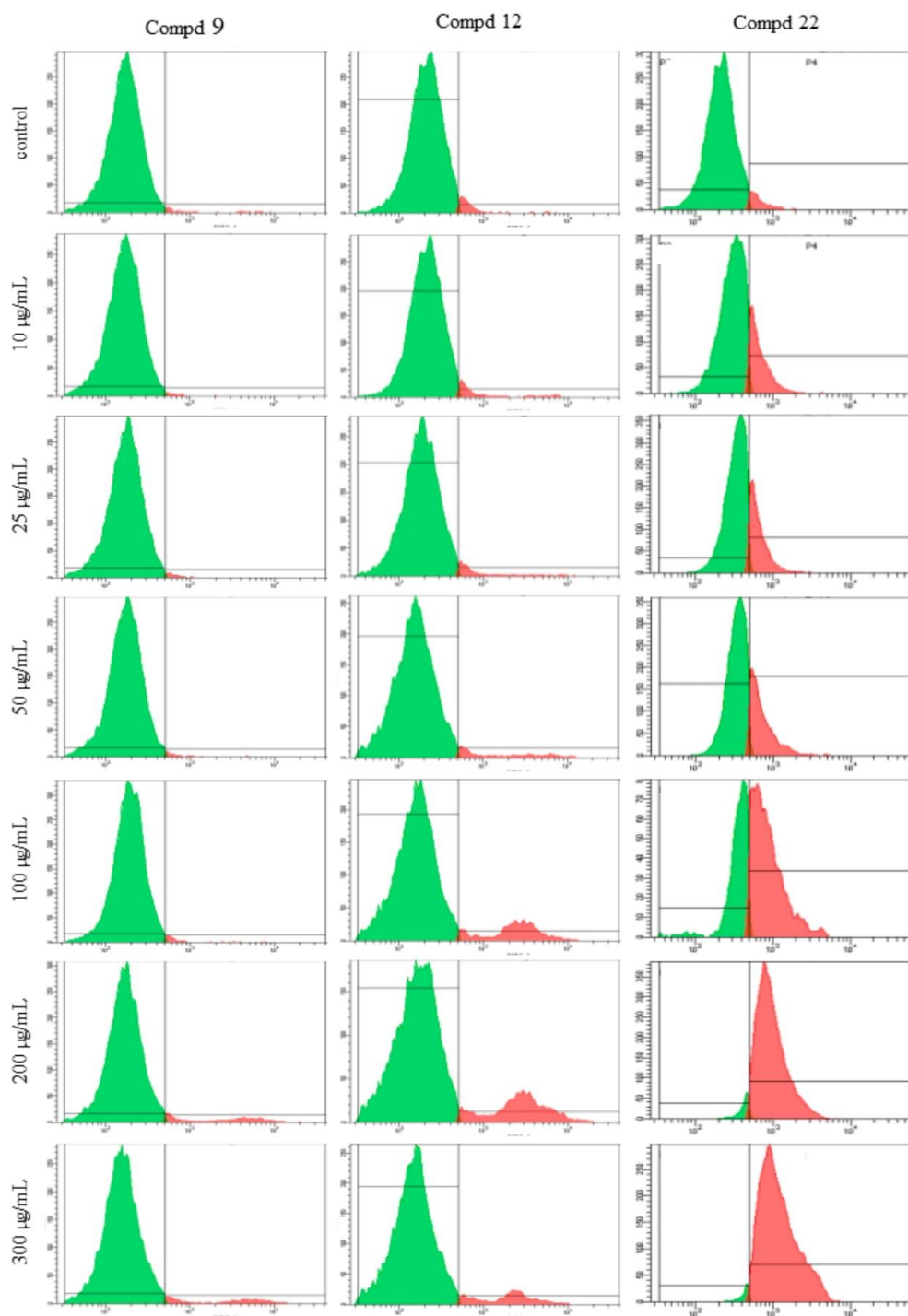


Figure S12. Flow cytometric analysis of cytotoxicity of C32 melanoma cells after 24 h of incubation with compound **9**, **12**, and **22** (10, 25, 50, 100, 200, and 300 $\mu\text{g/mL}$) comparable with untreated control by the Fixable Viability Stain assay.

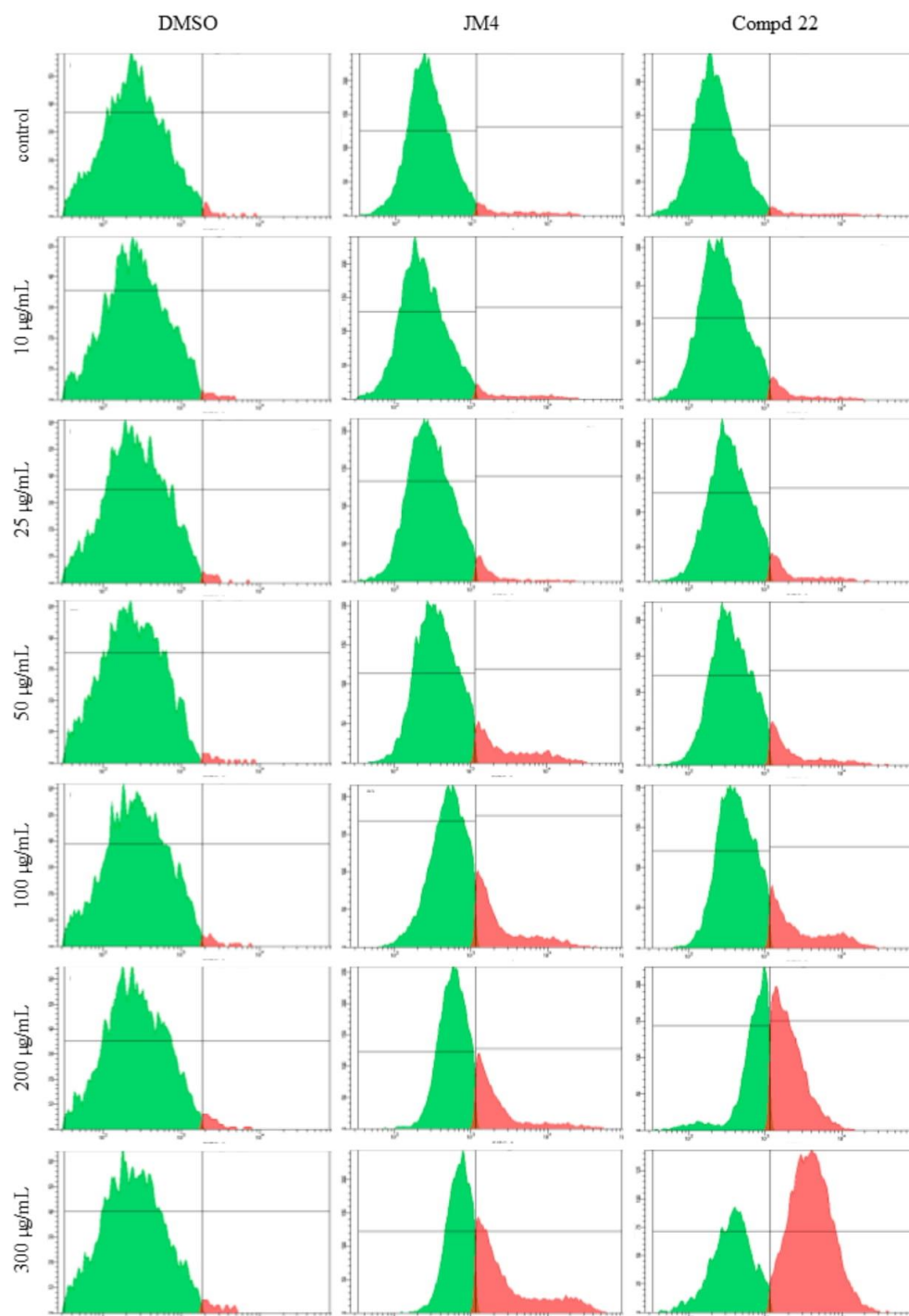


Figure S13. Flow cytometric analysis of cytotoxicity of normal human fibroblasts cells after 24 h of incubation with DMSO, **JM4**, and compound **22** (10, 25, 50, 100, 200, and 300 µg/mL) comparable with untreated control by the Fixable Viability Stain assay.

Publication II

Juszczak A.M., Jakimiuk K., Czarnomysy R., Strawa J.W., Zovko Končić M., Bielawski K., Tomczyk M.: Wound healing properties of *Jasione montana* extracts and their main secondary metabolites. *Frontiers in Pharmacology* Vol. 13, ID 894233, 2022, 13 pages.
DOI: 10.3389/fphar.2022.894233



Wound Healing Properties of *Jasione montana* Extracts and Their Main Secondary Metabolites

Aleksandra Maria Juszczyk¹, Katarzyna Jakimiuk¹, Robert Czarnomysy², Jakub Władysław Strawa¹, Marijana Zovko Končić³, Krzysztof Bielawski² and Michał Tomczyk^{1*}

¹Department of Pharmacognosy, Faculty of Pharmacy with the Division of Laboratory Medicine, Medical University of Białystok, Białystok, Poland, ²Department of Synthesis and Technology of Drugs, Faculty of Pharmacy with the Division of Laboratory Medicine, Medical University of Białystok, Białystok, Poland, ³Department of Pharmacognosy, Faculty of Pharmacy and Biochemistry, University of Zagreb, Zagreb, Croatia

OPEN ACCESS

Edited by:

Carlos L. Cespedes-Acuña,
Universidad del Bío-Bío, Chile

Reviewed by:

Carlos Areche,
University of Chile, Chile
Juan Rodrigo Salazar,
Universidad La Salle, Mexico

*Correspondence:

Michał Tomczyk
michal.tomczyk@umb.edu.pl

Specialty section:

This article was submitted to
Ethnopharmacology,
a section of the journal
Frontiers in Pharmacology

Received: 11 March 2022

Accepted: 21 April 2022

Published: 10 May 2022

Citation:

Juszczyk AM, Jakimiuk K,
Czarnomysy R, Strawa JW,
Zovko Končić M, Bielawski K and
Tomczyk M (2022) Wound Healing
Properties of *Jasione montana*
Extracts and Their Main
Secondary Metabolites.
Front. Pharmacol. 13:894233.
doi: 10.3389/fphar.2022.894233

The effects of different extracts obtained from *Jasione montana* L. (JM1–JM6) and their main metabolites on biological processes during wound healing were evaluated. The effect on wound closure in the scratch test was established, and collagen type I synthesis and anti-inflammatory effects were assessed by flow cytometry in a human dermal fibroblast model (PCS-201-012). Additionally, the antioxidant activity (DPPH and FRAP) and degree of inhibition of elastase participating in the proliferation processes of skin fibroblasts were determined in an *in vitro* model. The extracts and fractions were analyzed using high-performance liquid chromatography–photodiode array detection (HPLC–PDA) to quantitatively characterize their main polyphenolic compounds. The high antioxidant activity of the JM4–JM5 fractions correlated with the content of luteolin and its derivative 7-O-glucoside. Luteolin also showed the highest anti-elastase activity with an IC₅₀ value of 39.93 ± 1.06 µg/mL, and its substantial content in the JM4 fraction presumably determines its activity (359.03 ± 1.65 µg/mL). At lower concentrations (<50 µg/mL) of all extracts, cell proliferation and migration were significantly stimulated after 24 h of treatment. The stimulation of cell migration was comparable with that of allantoin, which was used as a positive control. However, most of the tested extracts showed limited capacity to affect collagen type I biosynthesis. Moreover, the tested samples exhibited a complex effect on cytokine secretion, and the strongest anti-inflammatory activity through the moderation of IL-1β, IL-6 and IL-8 was observed for JM4 and luteolin. Based on the obtained results of the quantitative analysis, the anti-inflammatory activity of JM4 may be due to the high content of luteolin. In summary, extracts from *J. montana*, which is flavonoid-rich, promote the viability and accelerate the migration of fibroblasts as well as moderate oxidant and inflammatory processes and elastase activity. Hence, they may be potentially useful for topical therapeutic applications to stimulate the wound healing process.

Keywords: *Jasione montana*, flavonoids, luteolin derivatives, fibroblasts, wound healing, antioxidant, enzyme inhibition

1 INTRODUCTION

The wound healing process is considered to be a series of dynamic overlapping reactions leading to proliferation, migration, matrix synthesis and contraction, as well as restoration of function and integrity to damaged tissues, resulting in the restoration of anatomic continuity. In general, the wound healing process consists of four distinct but smoothly overlapping phases, including hemostasis, the inflammatory phase, proliferation and remodeling of new tissue. Hemostasis occurs immediately after injury and is a form of protection of the vascular system and bridges invading cells. Transforming growth factor- β (TGF- β), which stimulates fibroblasts, and platelet-derived growth factor (PDGF) and vascular endothelial growth factor (VEGF), which are created by *inter alia* fibroblasts, are involved in promoting post-inflammatory wound healing cascades. In addition to VEGF, other important inflammatory cytokines regulated by tumor necrosis factor- α (TNF- α) are interleukin 6 (IL-6), with both pro- and anti-inflammatory properties, and interleukin 8 (IL-8) with chemotactic properties and downregulation of collagen expression by fibroblasts (Barrientos et al., 2008; Wedler et al., 2014). The proliferative phase, during which the aforementioned cytokines are still involved, is characterized by epithelialization, which leads to cell detachment, proliferation, migration and differentiation. The proliferation stage also includes angiogenesis in newly developed cells and tissue, formation of granulation tissue and deposition of collagen produced by proliferating fibroblasts (Gothai et al., 2016). The most common cells in the dermis particularly involved at each stage of the process are fibroblasts, which generate the proliferative phase of repair and are also involved in phases such as early inflammation and full epithelialization of the damaged tissue (Addis et al., 2020). The healing process is closely linked to the modulation of the secretion of many growth factors, extracellular matrix (ECM) signaling proteins, and cytokines; collagen deposition; and the control of oxidative stress (Bainbridge, 2013). ECM components such as collagen, fibrin, elastin, fibronectin, proteoglycans and others function as significant protagonists of the survival, proliferation and function of fibroblasts. The interaction between the ECM and these cells is a form of autocrine regulation that is essential in wound healing. Furthermore, matrix metalloproteinases (MMPs), such as collagenase and elastase, play an important role in regulating ECM degradation and deposition and thus affect tissue remodeling and repair (Tracy et al., 2016; Jakimiuk et al., 2021).

There is an association between wound healing processes and oxidative stress-regulating activity, and one of the main factors that play a fundamental role in wound healing is oxidation; hence, antioxidant polyphenolic substances of plant origin may be a particularly important aspect (Ustuner et al., 2019; Comino-Sanz et al., 2021; Monika et al., 2022). The presence of several polyphenolic compounds, mainly of a flavonoid nature, was revealed in the aerial parts of *Jasione montana* L. (Campanulaceae). To date, 5,7,3',4'-tetrahydroxyflavone (luteolin) (22), luteolin 7-O- β -D-glucoside (cynaroside) (12)

and luteolin 7-O- β -D-xylosyl-(1-2)- β -D-glucoside (luteolin 7-O-sambubioside) (9) have been isolated. Moreover, the anticancer effect of *J. montana* has been documented in an *in vitro* model of skin melanoma (Juszczak et al., 2021). As, from the pharmacological point of view, stimulation of proliferation, migration and differentiation of dermal fibroblasts, as well as anti-inflammatory or antioxidant effects, are critical aspects of the wound healing process, the aim of this study was to evaluate the effects of *J. montana* extracts and their main metabolites, such as luteolin, luteolin 7-O-glucoside and luteolin 7-O-sambubioside, on processes involved in wound healing.

2 MATERIALS AND METHODS

2.1 Plant Material and Preparation of Extracts JM1–JM3 and Fractions JM4–JM6

Aboveground parts of *J. montana* were collected and identified as reported previously by Juszczak and coauthors. The plant material was pretreated and then processed to obtain extracts JM1–JM3 and fractions JM4–JM6 following a previously described procedure (Juszczak et al., 2021).

2.2 Quantitative Analysis of Extracts JM1–JM3 and Fractions JM4–JM6 by HPLC–PDA

The quantification of selected secondary metabolites and the sum of their derivatives in extracts (JM1–JM3) and fractions (JM4–JM6) was performed in compliance with the International Council for Harmonisation of Technical Requirements for Pharmaceuticals for Human Use (ICH) recommendations (Okuda et al., 2014). Details of the optimization and validation high-performance liquid chromatography with a photodiode detector (HPLC–PDA) method are presented in the **Supplementary Table S1**.

2.3 DPPH Radical-Scavenging Assay

The antioxidant activity of the JM1–JM6 extracts and their main compounds (9, 12, and 22) against 2,2-diphenyl-1-picrylhydrazyl (DPPH) radicals was estimated according to the method previously described (Ciganović et al., 2019) with some modifications. All extracts (JM1–JM6) and main components of the tested extracts (9, 12, and 22) were isolated and identified as previously described (Juszczak et al., 2021). A total of 130 μ L of sample solution at various concentrations was mixed with 70 μ L of DPPH (0.2 mg/mL) in a 96-well plate. Then, the reaction mixture was incubated in the dark at room temperature. After 30 min, the absorbance was recorded at 517 nm using a microplate reader (BioTek Instruments microplate spectrophotometer EPOCH 2, Oxfordshire, United Kingdom). A blank solution was prepared by mixing methanol and DPPH solution. Trolox was used as a positive control. The experiment was performed in triplicate.

$$\text{RSA (\%)} = (C - S) / C \times 100\%$$

where C is the negative control and S is the sample. Concentration of the tested samples, which scavenges 50% of free radicals present in the solution (IC_{50}), was calculated.

2.4 Ferric Reducing Antioxidant Potential

Determination of the ferric reducing antioxidant potential (FRAP) was performed using a ferric reducing antioxidant power assay kit. Ten microliters of each sample (**JM1–JM6**, **9**, **12**, **22**) was mixed with 190 μ L of supplied reaction mix (FRAP assay buffer, $FeCl_3$ solution, FRAP probe). The absorbance was measured after 1 h of incubation at 37°C at 594 nm using a microplate reader. A blank solution contained 10 μ L of MeOH instead of extract/compound solution. For further calculations, the ferrous standard curve was evaluated. The values are given as mM ferrous equivalents. All tests were executed in triplicate.

2.5 Elastase Inhibitory Activity

The measurement of elastase inhibition was modified slightly according to a previous method (Wittenauer et al., 2015). The procedure was performed in 100 mM Tris buffer (pH = 8.0). Briefly, 100 μ L of extracts (**JM1–JM6**) (100–600 μ g/mL) or compounds (**9**, **12**, and **22**) (10–200 μ g/mL) and 100 μ L of Tris buffer were mixed with 25 μ L of porcine pancreatic elastase solution (0.05 mg/mL). Then, the mixtures were preincubated at 25°C for 5 min, and 70 μ L of AAAPVN (0.4 mg/mL) was added. After another 15 min of incubation, the release of *p*-nitroaniline was monitored at 410 nm using a microplate reader. A blank solution was prepared by using buffer instead of sample solution. Quercetin was employed as a positive control. The calculations were performed as follows:

$$EI_{inh}(\%) = (C - S) / C \times 100\%$$

where C is the negative control and S is the sample.

2.6 Cell Culture

The normal human dermal fibroblast cell line (PCS-201-012) was cultured in DMEM blended with 10% fetal bovine serum (FBS), 10 μ g/mL streptomycin, and 10 units/mol penicillin. The cells were cultured in 5% CO_2 and fully humidified at 37°C. All tested compounds were dissolved at a final vehicle (DMSO) concentration of not more than 0.5% (*v/v*). Cells cultured in drug-free DMEM were used as controls, and cells treated with DMSO alone were used as solvent controls. All extracts (**JM1–JM6**) and the main components of the tested extracts (**9**, **12**, and **22**) were analyzed at the following concentrations: 10, 25, 50, 100, 200, and 300 μ g/mL.

2.6.1 Proliferation and Migration Assay

The *in vitro* wound healing activity of *J. montana* extracts and isolated compounds was determined by a scratch assay, which is a model of a wound in which monolayer skin cells, including fibroblasts, react to the disruption of contact between cells and stimulate proliferation and migration by modulating the concentration of growth factors and cytokines at the edge wounds (Liang et al., 2007). For this purpose, fibroblast cells were seeded at a density of 2.5×10^5 in 6-well cell culture dishes and incubated for 24 h at 37°C. After incubation, a linear scratch

was made with a universal sterile 200 μ L pipette tip. Cells were incubated with the tested extracts (**JM1–JM6**) and compounds (**9**, **12**, and **22**) at concentrations of 10, 25, 50, 100, 200 and 300 μ g/mL for 24 h at 37°C. Allantoin, a plant-derived commercialized drug, was used as the positive control at a concentration of 50 μ g/mL to judge the rate of cell migration (Sarkhail et al., 2020). After incubation, the migrated cells were washed twice with PBS and observed under a phase contrast microscope. The progress of migration, proliferation and closing of the wound before and after treatment with the tested samples was monitored by imaging with a phase contrast microscope (Nikon Eclipse Ti, Tokyo, Japan) at $\times 100$ magnification and NIS-Elements 3.0 imaging software (Nikon Instruments Inc., Melville, NY, United States).

2.6.2 Biosynthesis of Collagen Type I

The effect of the tested extracts and fractions (**JM1–JM6**), as well as their main compounds (**9**, **12**, and **22**) on collagen type I biosynthesis was determined using a method of cytometric staining of the surface anti-collagen type I according to the manufacturer's protocols. Fibroblasts were incubated for 24 h at 37°C with the test samples at concentrations of 10, 25, 50, 100, 200, and 300 μ g/mL. Allantoin (50 μ g/mL) was used as a positive control. After incubation, fibroblasts were washed with PBS, trypsinized, resuspended in DMEM and centrifuged (1,200 rpm, 10 min, 4°C). The supernatant was removed, and the cells were washed with 2 mL of stain buffer. Then, the cells were incubated for 30 min on ice with 100 μ L of stain buffer and 1 μ L of antibody. After complete incubation, 2 mL of stain buffer was added. After consecutive centrifugation (1,200 rpm, 10 min, 4°C), the supernatant was removed, the cells were resuspended in 300 μ L of buffer and then immediately subjected to analysis on a flow cytometer (BD FACSCanto II flow cytometer, San Jose, CA, United States) calibrated with BD Cytometer Setup and Tracking beads (BD Biosciences, San Diego, CA, United States). The median fluorescence intensity was calculated using FACSDiva software (BD Biosciences Systems, San Jose, CA, United States) and analyzed by FCS Express 7 software (DeNovo Software, Pasadena, CA, United States).

2.6.3 Flow Cytometric Analysis of Inflammatory Cytokines

The effect of the tested extracts and fractions (**JM1–JM6**) as well as **9**, **12**, and **22** on cytokine (IL-1 β , IL-6, IL-8, IL-10, IL-12p70 and TNF) secretion was determined using the Cytometric Bead Array (CBA) Human Inflammatory Cytokine Kit according to the manufacturer's protocols. After 24 h of incubation with the test samples at concentrations of 10, 25, 50, 100, 200, and 300 μ g/mL, fibroblast cells were washed with PBS, trypsinized, resuspended in DMEM and centrifuged (1,200 rpm, 10 min, 4°C). The supernatant was then replaced with 50 μ L of assay diluent with the addition of 50 μ L of assay beads and 50 μ L of PE-labeled antibodies (detection reagent) from the human inflammatory cytokine kit. Incubation was performed for 3 h at room temperature without daylight, after which the fibroblast cells were washed and centrifuged (1,200 rpm, 5 min, 4°C). The cell pellet was resuspended in 300 μ L of wash buffer and then immediately subjected to analysis by FCAP Array v3 software on

TABLE 1 | Quantification of major compounds (compounds **9**, **12** and **22**) in *J. montana* extracts (**JM1–JM3**) and fractions (**JM4–JM6**) by HPLC–PDA.

Compounds	JM1	JM2	mg/g dry Extract/fraction			
			JM3	JM4	JM5	JM6
9 ^p	10.30 ± 0.03	6.57 ± 0.03	BLQ	nd	BLQ	6.77 ± 0.08
12	52.02 ± 0.17	31.21 ± 0.07	11.10 ± 0.08	40.21 ± 0.85	383.16 ± 1.36	nd
22	5.78 ± 0.11	7.82 ± 0.02	8.18 ± 0.09	72.13 ± 3.86	nd	nd
luteolin derivatives ^{a,b}	83.66 ± 0.28	53.81 ± 0.14	23.11 ± 0.02	53.51 ± 1	474.87 ± 1.86	20.76 ± 0.13

9 – luteolin 7-O-sambubioside; **12** – luteolin 7-O-β-D-glucoside; **22** – luteolin.

^aExcluding luteolin.

^bExpressed as equivalent of luteolin 7-O-glucoside with standard deviation; BLQ, below the limit of qualification; nd, not detected.

a BD FACSCanto II flow cytometer (both from BD Biosciences Systems, San Jose, CA, United States) calibrated with BD Cytometer Setup and Tracking beads (BD Biosciences, San Diego, CA, United States).

2.7 Statistical Analysis

All numerical data are expressed as the mean ± standard deviation (SD) from at least three independent repeats. GraphPad Prisma eight software (GraphPad Software, San Diego, CA, United States) was used for statistical analysis. Statistical differences were assessed using one-way ANOVA followed by Dunnett's multiple comparisons test. Statistically significant values were considered under the condition of $p < 0.05$. MS Excel 2019 software with the Data Analysis add-on was used for statistical analysis and determination of linear regression parameters. The parameters were obtained using ANOVA with a confidence level of 95%.

3 RESULTS

3.1 Quantitative Analysis of Extracts JM1–JM3 and Fractions JM4–JM6 by HPLC–PDA

The main components of the aerial parts of *J. montana* were successfully identified by LC–MS analysis in a previous report (Juszczak et al., 2021). The extracts from *J. montana* were quantified by HPLC–PDA by preparing the calibration curves of the four reference substances. **Table 1** presents the contents of major components, luteolin 7-O-sambubioside (**9**), luteolin 7-O-glucoside (**12**), and luteolin (**22**), as well as their derivatives in the extracts (**JM1–JM3**) and the fractions (**JM4–JM6**). Each investigated extract has variations in quantitative content with regard to the main compounds. The phytochemical composition of **JM1–JM6** is relatively limited, however, the dominant compounds in the studied extracts are present in significant amounts. The dominant compounds present in **JM4** are **22** (72.13 ± 3.86 mg/g dry fraction) and **12** (40.21 ± 0.85 mg/g dry fraction), while **JM5** contains a significant amount of **12** (383.16 ± 1.36 mg/g dry fraction), and other flavonoid derivatives. The high content of dominant constituents in these fractions was the basis for the attempt to isolation process of compounds **9**, **12**, and **22** (Juszczak et al., 2021).

TABLE 2 | Antiradical activity against DPPH radical (IC₅₀, μg/mL) of **JM1–JM6** extracts and compounds (**9**, **12**, and **22**), FRAP values (mM Fe²⁺ per mL).

Sample	DPPH, IC ₅₀ (μg/mL) ^a	FRAP (mM Fe ²⁺ eq/mL) ^b
JM1	457.15 ± 5.2	34.33 ± 0.99
JM2	276.60 ± 3.8	46.53 ± 0.87
JM3	261.18 ± 4.2	41.31 ± 0.99
JM4	72.69 ± 2.3	43.87 ± 1.32
JM5	42.69 ± 1.7	51.55 ± 1.65
JM6	848.47 ± 4.4	10.63 ± 0.92
Compound 9	20.34 ± 0.8	60.59 ± 0.46
Compound 12	16.59 ± 0.7	51.88 ± 0.53
Compound 22	10.65 ± 0.7	51.81 ± 0.78

^aAll data are represented as the mean IC₅₀ values.

^bAbility to reduce the Fe²⁺ complex to ferrous Fe²⁺.

3.2 Antioxidant Activity of *J. montana* Extracts and Isolated Compounds

The effects of *J. montana* extracts and isolated compounds on antioxidant activity are given in **Table 2**. The analysis of antioxidant potential by the DPPH and FRAP methods confirmed that the highest activity for extracts and fractions are connected with increasing polyphenolic compound content (Sulaiman et al., 2013). Based on the results obtained, the tested plant had high antioxidant activity in the presence of compounds **22** (DPPH: IC₅₀ = 10.6 ± 0.7 μg/mL, FRAP: 60.59 ± 0.5 mM Fe²⁺/mL) and **12** (DPPH: IC₅₀ = 16.6 ± 0.7 μg/mL, FRAP: 51.9 ± 0.5 mM Fe²⁺/mL). As stated by the quantitative HPLC analysis, the highest contents of **22** and **12** were prevalent in the **JM4** and **JM5** fractions, which is consistent with their free radical-scavenging potential, with IC₅₀ values of 72.7 ± 2.3 and 42.7 ± 1.7 mM Fe²⁺/mL and reducing powers of 43.87 ± 1.32 and 51.55 ± 1.65 mM Fe²⁺/mL, respectively. Moreover, all tested compounds (**9**, **12**, and **22**) possessed stronger antiradical potential in the DPPH method than a positive control, Trolox (IC₅₀ = 58.6 ± 0.1 μg/mL).

3.3 Elastase Inhibition Activity of *J. montana* Extracts

Inhibition of elastase activity for crude extracts from *J. montana* was performed. The effect of their anti-elastase potential expressed as IC₅₀ values is summarized in **Table 3**. Among all tested samples, only three (**JM4**, **JM5**, and **22**) exhibited moderate anti-elastase effects. Compound **22** (IC₅₀ = 39.93 ± 1.06 μg/mL)

TABLE 3 | Elastase inhibitory activity of **JM1–JM6** extracts; compounds **9**, **12**, and **22**; and quercetin expressed as IC₅₀ (µg/mL).

Sample	IC ₅₀ (µg/mL)
JM1	na
JM2	na
JM3	na
JM4	359.03 ± 1.65
JM5	385.03 ± 1.87
JM6	na
Compound 9	na
Compound 12	na
Compound 22	39.93 ± 1.06
Quercetin	22.36 ± 0.86

na, not active; PC, positive control (quercetin).

showed the highest activity, followed by **JM4** (IC₅₀ = 359.03 ± 1.65 µg/mL) and **JM5** (IC₅₀ = 385.03 µg/mL). On the other hand, **JM1–JM3**, **JM6**, **9** and **12** showed no significant inhibitory activity.

3.4 Scratch Wound Healing of Fibroblast Cells by the Influence of *J. montana* Extracts

To assess the *in vitro* wound healing effect of *J. montana*, fibroblast migration concerning the closure of the uncovered scratched area by the scratch assay was monitored. Data obtained from an *in vitro* scratch model using fibroblast cells showed that *J. montana* extracts and isolated compounds significantly enhanced fibroblast cell migration toward an induced temporary interruption at most of the tested concentrations to varying extents compared with the migration of cells into the wounded area incubated in medium free from tested samples 24 h after wounding (**Figure 1**). Wound closure was stimulated in a concentration range of 10–300 µg/mL, with the tested fractions, extracts and compounds being less effective at higher concentrations. For the **JM1–JM3** extracts, **JM5–JM6** fractions and compounds **9** and **12**, the cell migration into the injured area was significantly increased up to a concentration of 100 µg/mL. However, above this concentration, significantly less stimulation of fibroblasts, as well as a reduction in cell adhesion and loss of intercellular connections, was observed (data not shown). **JM1** and **9** (50 µg/mL) proved to be most effective in the scratch test, and cell migration to the wound area after 24 h of incubation was comparable with the healing-promoting activity visualized for allantoin (50 µg/mL). Both treatments returned cells to a confluent or near confluent state within 24 h, comparable with the untreated control cells. In contrast, a distinct trend was observed for **22** and **JM4**, which were capable of stimulating cells only at a low concentration (10 µg/mL). This observation coincides with the higher cytotoxicity of these samples presented in the previous report (Juszczak et al., 2021).

3.5 Collagen Type I Biosynthesis

In the further evaluation of the wound healing properties, we examined the intracellular expression of the anti-collagen type I antibody fluorescein conjugation specific for collagen type I

under the influence of *J. montana* extracts and their main compounds in fibroblast cells. The results are expressed as the median fluorescence intensity (MFI) and are shown in **Figure 2** and **Supplementary Figure S1**. Most of the tested extracts showed limited capacity to affect collagen biosynthesis. After treatment with **JM3** at a concentration of 25 µg/mL, only a slight increase in collagen content was observed in fibroblast cells (MFI: 2,417 ± 45.2 vs. 2,244 ± 7.1 control). The observed effect was not dose dependent. The pure isolated compounds showed higher activity than the extracts. Compounds **9** and **12** at the highest tested concentrations significantly increased the soluble collagen content in fibroblast cells compared with untreated control cells. The highest expression of collagen antigen was observed after treatment with **9** at a concentration of 300 µg/mL (MFI: 1763 ± 58 vs. 1,507 ± 9.2 control). Slightly weaker expression was recorded after incubation with **12**, achieving a stimulatory effect on collagen production at a concentration of 300 µg/mL (MFI: 1717 ± 10.6 vs 1,507 ± 9.2 control). Comparing the results obtained for the reference sample, allantoin, it is clear that most of the tested samples had higher activity than the positive control. Moreover, allantoin at a concentration of 50 µg/mL induced downregulation of collagen antigen expression in fibroblast cells (MFI: 1,494 ± 2.8 vs. 1822 ± 62.2 control).

3.6 Effect of *J. montana* Extracts on Cytokine Secretion

To assess the immune status of human fibroblast cells in response to *J. montana* extracts and their major compounds, the levels of representative cytokines in cellular supernatants were examined by flow cytometry. All tested samples showed a complex effect on cytokine secretion that depended on the cytokine considered as well as the concentration of the samples tested. As shown in **Figures 3, 5**, the expression levels of interleukin 1β (IL-1β) and IL-8 gradually decreased for some extracts and compounds. The highest decrease in the secretion of the labeled pro-inflammatory cytokine IL-1β occurred for all tested concentrations of the **JM4** fraction (10–300 µg/mL) and **22**. After incubation with 50 µg/mL of **JM4**, a decrease in IL-1β to 0.5 ± 0.4 pg/mL vs 13.4 ± 5.6 pg/mL control, and under the influence of 100 µg/mL of **22** 1.7 ± 1.1 pg/mL vs 13.4 ± 5.6 pg/mL control. At the same time, at concentrations of 200–300 µg/mL of **22**, a strong reduction in IL-1β expression below the sensitivity of the method was observed. Furthermore, at higher concentrations (100–300 µg/mL), the **JM2** extract and **JM5** and **JM6** fractions showed a significant reduction in IL-1β release. In the case of the proinflammatory IL-8, a decrease in its expression was most pronounced after treatment with **JM2**, **JM4**, **JM5**, and **22**. The **JM4** fraction and **22** (300 µg/mL) appeared again to be the most significant inhibitors of proinflammatory cytokine expression (154 ± 102.8 pg/mL vs 8,396.8 ± 2,771.1 pg/mL control and 60.8 ± 8 pg/mL vs 8,396.8 ± 2,771.1 pg/mL, respectively). Based on the quantitative analysis results, the anti-inflammatory activity of **JM4** may be due to the high content of **22** (**Table 1**). Nevertheless, the other extracts mentioned above showed anti-inflammatory activity in a dose-dependent manner.

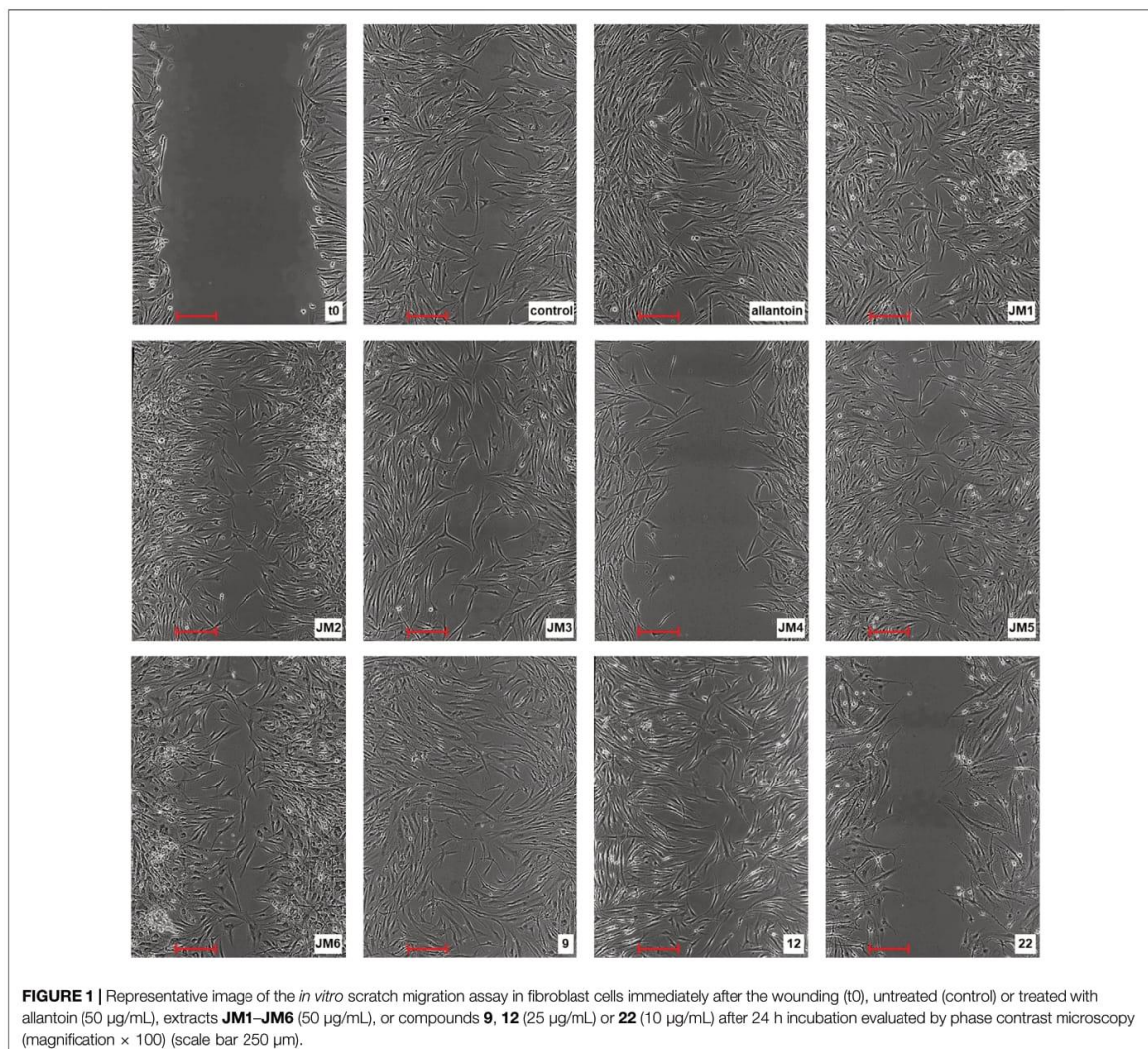


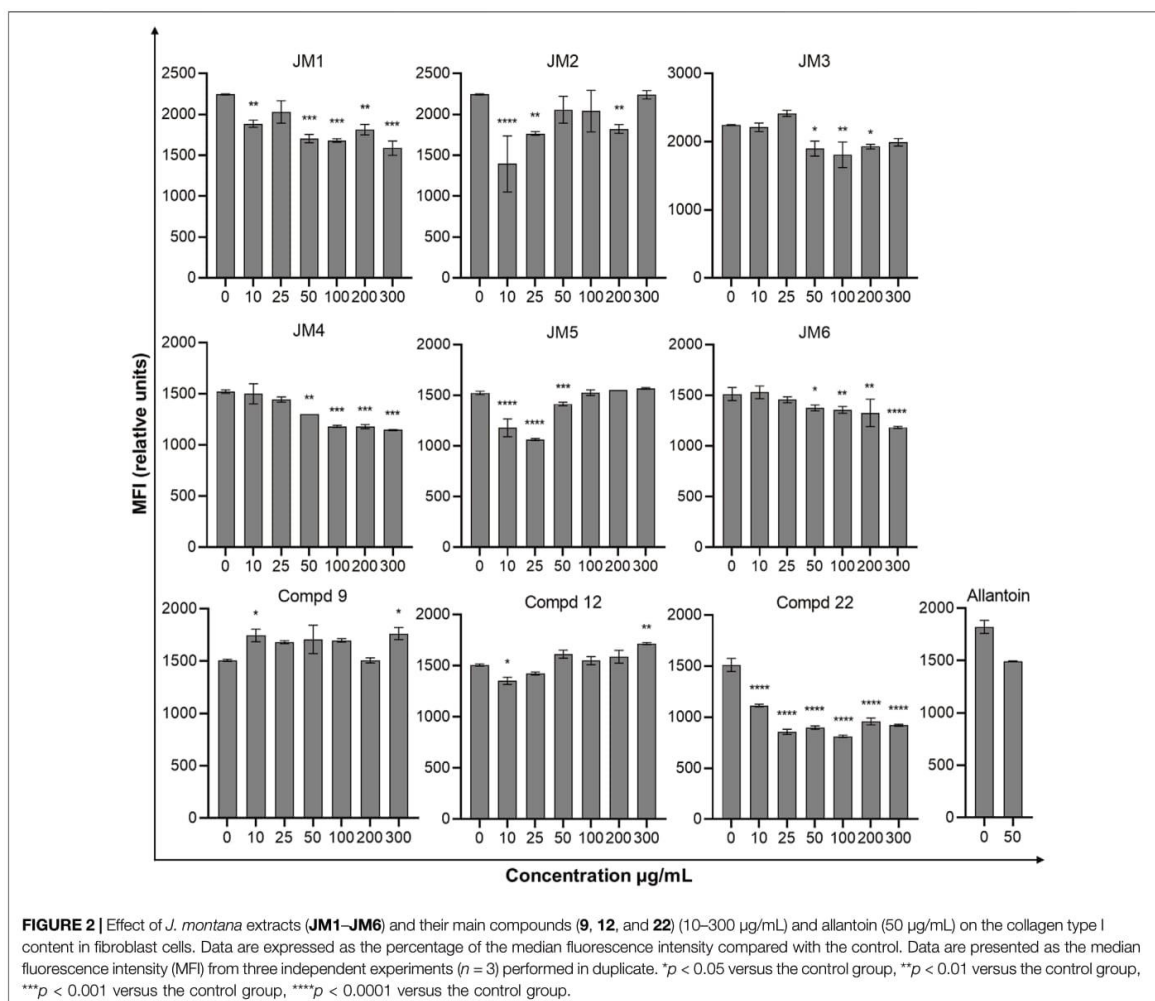
FIGURE 1 | Representative image of the *in vitro* scratch migration assay in fibroblast cells immediately after the wounding (t0), untreated (control) or treated with allantoin (50 µg/mL), extracts **JM1–JM6** (50 µg/mL), or compounds **9**, **12** (25 µg/mL) or **22** (10 µg/mL) after 24 h incubation evaluated by phase contrast microscopy (magnification $\times 100$) (scale bar 250 µm).

Moreover, extracts such as **JM1**, **JM3**, **JM6**, and compounds **9** and **12** resulted in reduced IL-8 levels in the higher ranges of tested concentrations (100–300 µg/mL). However, there was a significant increase in the aforementioned proinflammatory cytokine levels after treatment with lower concentrations of **9** (10–100 µg/mL). The highest increase in IL-6 secretion occurred for **JM1** (100 µg/mL), **JM2** (100 µg/mL), **JM3** (100 µg/mL), **JM5** (10 µg/mL), **JM6** (50 µg/mL), **9** and **12** (100 µg/mL) (**Figure 4**). However, at higher concentrations (300 µg/mL) of the tested samples, there was a drastic decrease in the level of this cytokine. **JM4** and **22** induced a dose-dependent decrease in IL-6 expression levels below that of the untreated control. Compared with the results obtained for the reference sample, allantoin, a decrease in IL-8 expression and upregulation of IL-6 can be observed, but the effect was weaker than for the most active

samples tested. However, a significant effect of allantoin on the stimulation of proinflammatory IL-1 β levels was observed. Cytokine values lower than the detection limit (IL-10, IL-12p70, and TNF) were considered undetectable and are not shown. The most pronounced effects were observed for the most highly expressed cytokines.

4 DISCUSSION

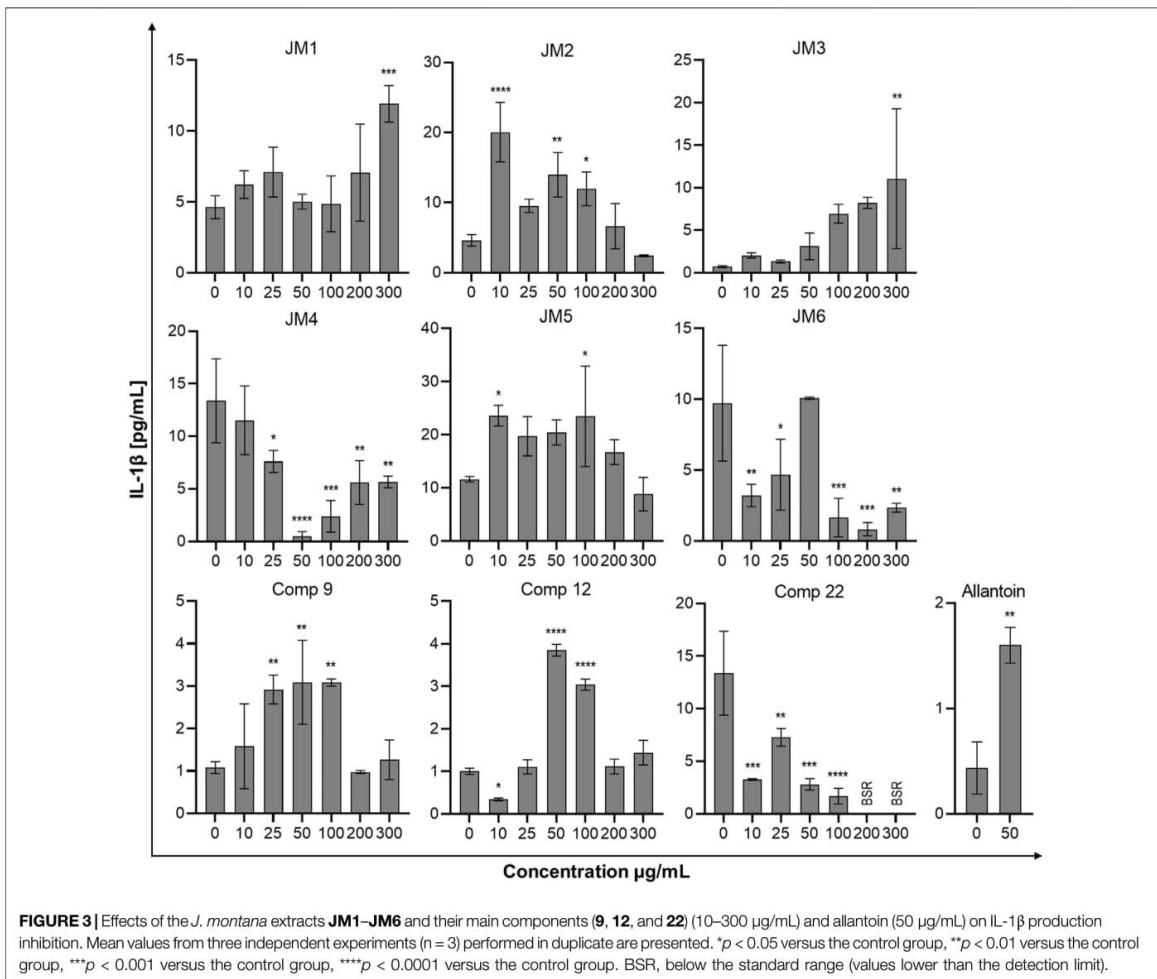
Repair of disrupted skin structure is a complex process leading to the restoration of tissue function in a series of overlapping phases (Soib et al., 2020). Changes at each stage of normal wound healing can result in a delay or inability to repair the disrupted structure (Süntar et al., 2012). In the case of diseases such as obesity and



diabetes, the incidences of which are increasing rapidly, patients are at a high risk of developing chronic wounds due to the delay, impairment and uncoordinated healing process (Muniandy et al., 2018). Moreover, impaired repair processes, such as skin and underlying tissue injuries, are encountered in cardiovascular diseases and disorders during cancer therapy (Martinengo et al., 2019). Therefore, to restore the regularity of the wound healing process, the use of substances capable of accelerating the restoration of the physical barrier, as well as protection against unfavorable factors causing wound pathology, may be necessary. The role of certain medicinal plants and phytoconstituents in the wound healing process may represent an attractive approach to their therapeutic properties (Marume et al., 2017; Ustuner et al., 2019). Moreover, the World Health Organization (WHO) defines recommendations for the use of medicinal plant treatment due to their safety and efficacy (World Health Organization, 2013). Previous reports identify *J. montana* as a raw material rich in

polyphenolic substances, mainly flavonoids (Juszczak et al., 2021), which are well known for their significant antioxidant properties. Hence, the potential of extracts and fractions from *J. montana* in stimulating wound healing, as well as various biological activities, such as antioxidant and anti-inflammatory properties, was investigated.

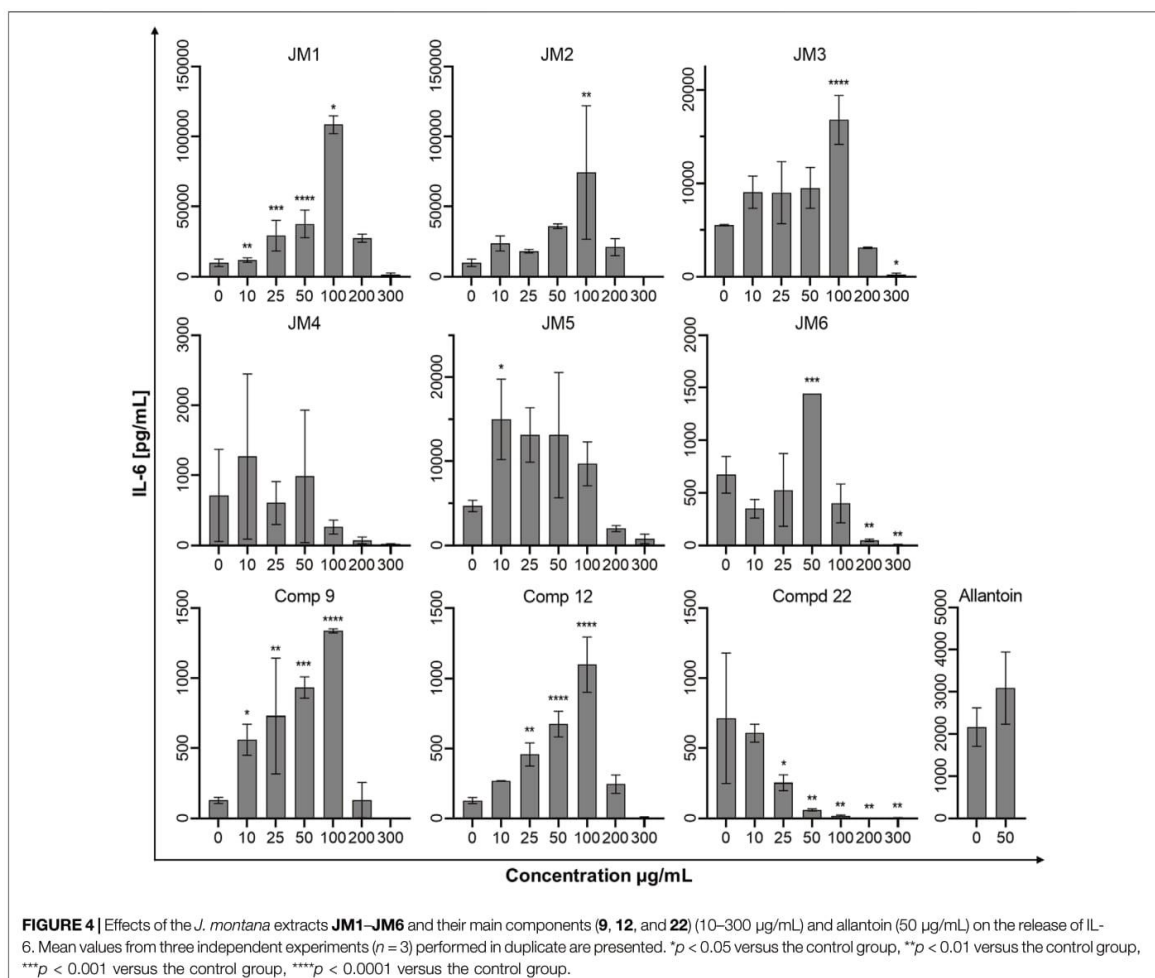
The need to measure antioxidant potential is well-reported; such measurements are conducted for significant comparison of food or cosmeceutical products for delivery of quality determination for regulatory cases and health-promoting issues. Overproduction of reactive oxygen species (ROS) caused by skin damage can induce apoptotic changes, damage living tissues, delay or completely stop the healing process due to damage to cell membranes and destruction of proteins, lipids and ECM elements (Ustuner et al., 2019). In the current work, the antioxidant properties of *J. montana* and its main components were established using two different chemical methods, including



the DPPH free radical scavenging and FRAP assay. In the DPPH assay, **9** (luteolin 7-*O*-sambubioside), **12** (luteolin 7-*O*-glucoside), **22** (luteolin) and the fractions with their highest content (**Table 1**), **JM4** and **JM5**, exhibited the strongest ability to scavenge the radicals. Similar findings were revealed in the FRAP method. The best reducing abilities were found in **JM5**, followed by **JM4**, while the lowest activity was observed in **JM6** in both the FRAP and DPPH assays. In accordance with the assays performed, the best antioxidant abilities were found in **JM4**, **JM5** and compounds **9**, **12**, and **22**. The observations could clearly be explained by the higher concentration of the total phenolic compounds in the fractions and extracts. These conclusions are supported by previously reported studies and available literature data (Mainka et al., 2021).

Fibroblasts, alongside keratinocytes, are the predominant cells in the wound closure mechanism and constitute a major target in the commercial design of therapeutic preparations (Ustuner et al., 2019). Their proliferation and migration to the wound site play a

key role during the re-epithelialization process of restoring skin integrity, generating new granulation dermis and new collagen structures to support other cells (Bainbridge, 2013). The strength of both of these proliferation phase mechanisms has been assessed using the preferred wound healing model of the *in vitro* scratch test, a useful method for mimicking cell migration during wound closure *in vivo* (Liang et al., 2007). The present study shows that *J. montana* extracts and their major metabolites can promote wound closure and granulation tissue formation by inducing fibroblast cell migration in the scratch assay, a critical step in the proliferation phase, and they simultaneously lack cytotoxic effects as established in a previous study (Juszczak et al., 2021). Furthermore, among the tested samples, **9** and **JM1** most strongly stimulated fibroblast growth and migration (**Figure 1**). A similar stimulating effect was observed for the **JM5** fraction and its main compound, **12**, probably determining its effects of action (**Table 1**). The stimulation of fibroblast migration has been repeatedly linked



with antioxidant properties (Comino-Sanz et al., 2021); however, only the **JM5** fraction and compounds **9** and **12** partially support the initial hypothesis. Interestingly, fraction **JM4** and its main component probably responsible for its action, **22** (Table 1), show toxicity at the higher concentrations tested despite their high antioxidant properties (Juszczak et al., 2021) as well as moderate fibroblast migration to the wound at lower concentrations. The activity of the *Lavandula stoechas* extract containing luteolin derivatives (54.49 ± 5.02 mg/L), demonstrated by Addis and coauthors, exhibited slight stimulation of the migration and proliferation of fibroblast activity that decreased with increasing incubation time and tested concentration (Addis et al., 2020). On the other hand, Bayrami and coauthors reported a lack of toxicity of luteolin, which was more effective than *Tragopogon graminifolius* extract rich in this flavone, on stimulating cell proliferation in the 3-(4,5-dimethylthiazol-2-yl)-2,5-diphenyl-2H-tetrazolium bromide (MTT) assay and migration in the scratch assay. Moreover, luteolin-induced cell

accumulation in the S-phase of the cell cycle was demonstrated, confirming its role in cell proliferation (Bayrami et al., 2018). However, the authors tested luteolin at a concentration of 0.1 µg/mL, which was many times lower than the concentration used in the present study. At the same time, the luteolin-rich fraction from *T. graminifolius* was tested at a concentration of 50 µg/mL, which can be assumed to be in agreement with our reports on the stimulating effect of **JM4** at lower concentrations. Chen et al. (2021) demonstrated that systemic administration of luteolin promotes re-epithelialization of wounds with a well-organized arrangement of fibroblasts. Furthermore, the activity of *Calendula officinalis* extracts, of which luteolin and their derivatives are among the flavonoid components, was reported to stimulate fibroblasts to overgrow the wound (Fronza et al., 2009; Srivastava et al., 2010; Wedler et al., 2014). Nevertheless, according to our data, at higher concentrations, the **JM4** fraction and **22** confer antiproliferative and cytotoxic effects. In both cases, it is probably caused by the high concentration of **22**

(Table 1). Moreover, our data about the activity of another predominant constituent, **12**, are in good agreement with those confirmed by the findings of Ustner and coauthors on a *Thymus sipyleus* extract with a significant cynaroside content (0.46 ± 0.01 mg/100 mg extract). The authors simultaneously showed stimulation of proliferation under the influence of the mentioned extracts, as determined by the MTT assay (Ustner et al., 2019). On the other hand, Karatoprak and coauthors proved that the butanol fraction from *Alchemilla mollis* with a high content of luteolin 7-*O*-glucoside (23.04 ± 0.22 mg/g extract) has at the same time a strong antioxidant potential and toxic activity on L929 fibroblast cells in the sulforhodamine B (SRB) assay. The authors suggest antioxidant as well as toxic effects of luteolin 7-*O*-glucoside (Karatoprak et al., 2017). However, according to Juszczak et al. (2021) and coauthors, this derivative did not show strong cytotoxicity against dermal fibroblast cells and additionally stimulated their migration in the scratch assay (Figure 1).

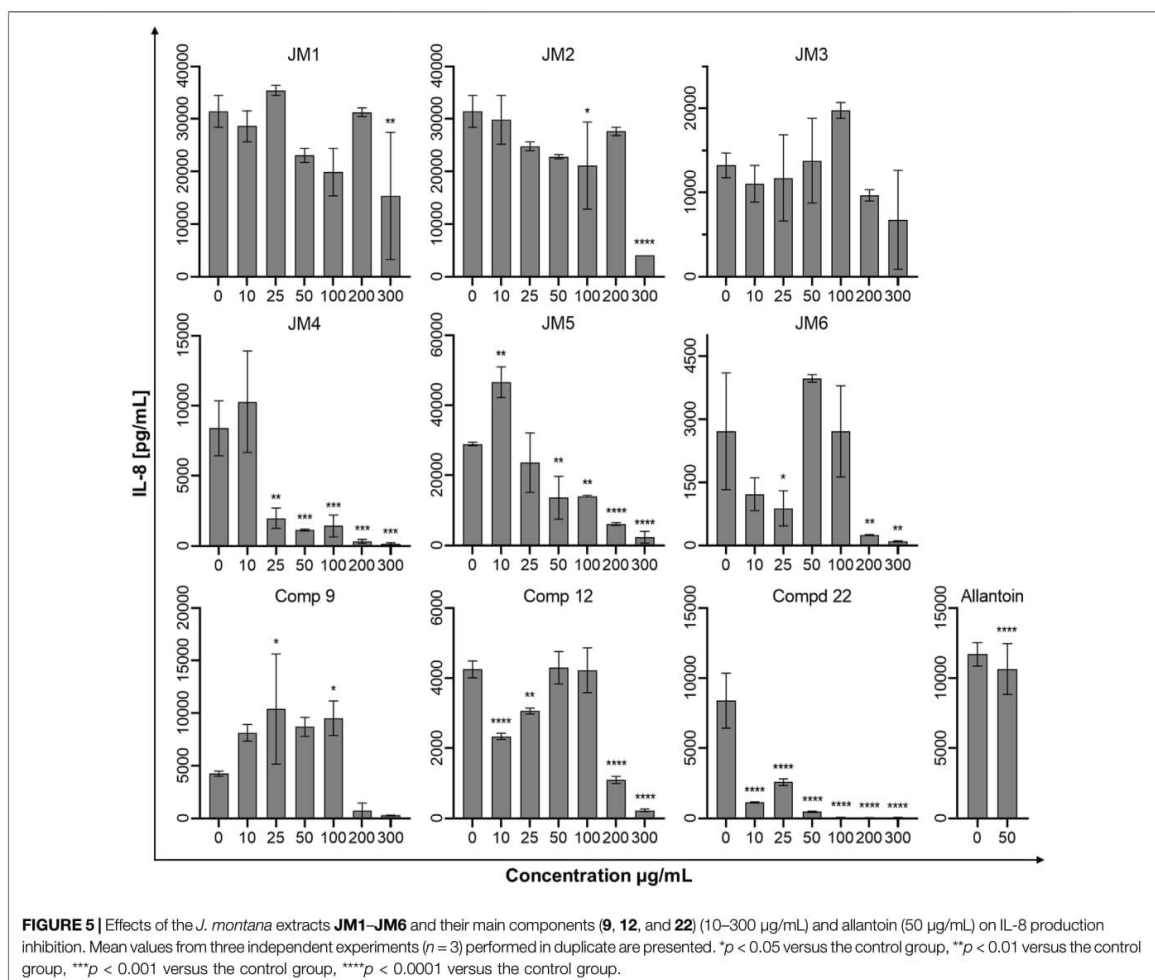
According to previously performed LC-MS analysis, *J. montana* extracts are present rich in polyphenolic compounds (Juszczak et al., 2021), which have been repeatedly proven to modulate processes closely related to wound healing. In addition to their antioxidant properties, which are associated with repair processes, *p*-coumaric acid as well as apigenin are able to stimulate migration and differentiation of fibroblasts in an *in vitro* and *in vivo* models. Moreover, the anti-inflammatory potential of apigenin through inhibition of TNF- α , IL-6 and IL-1 β has been demonstrated (Carvalho et al., 2021; Melguizo-Rodríguez et al., 2021). However, taking into account the complex plant matrix and various phytochemical compositions as well as the fact that the major compounds which are luteolin and its derivatives, present in significant amounts, it cannot be unequivocally stated that other compounds determined in the tested extracts displayed influence on the observed biological effect of *J. montana* extracts or fractions.

From a clinical perspective, the deposition in the wound of collagen produced by fibroblasts, the main protein of the ECM, may be the most important phase of healing and ultimately contributes to the strengthening of the matrix (Lodhi and Singhai, 2013; Tracy et al., 2016). The effect of flavonoid compounds on the stimulation of collagen synthesis in skin fibroblast cultures has already been reported (Ibrahim et al., 2018; Shedoeva et al., 2019). Hence, the effect of *J. montana* extracts on the content of collagen type I in an *in vitro* model of human skin fibroblasts was investigated. However, the observed activity of stimulating collagen type I synthesis for most of the tested samples was limited. The highest activity was observed for compounds **9** and **12**, while, as already mentioned, they did not show the ability to reduce cell viability. In addition, the **JM3** extract slightly increased the content of soluble collagen in the supernatant at a dose of 25 μ g/mL. However, it was not a dose-dependent effect; therefore, it is difficult to state which component is responsible for its activity, **12**, **9** or the synergy of the actions of both tested luteolin derivatives (Table 1). Previous reports confirm the hypothesized activity attributed to luteolin glucoside, the presence of which has been reported in extracts from *T. sipyleus*, to alter hydroxyproline levels used as

a biomarker for collagen content determinations (Ustuner et al., 2019). However, the effect of stimulating collagen synthesis decreased with increasing concentrations of the administered *T. sipyleus* extract, unlike the results shown in the present study (**12** and **JM5** activity). This fact can be explained by the presence of a second unidentified dominant compound in the mentioned extracts from *T. sipyleus*. Increased content of cross-linked collagen in wounds was also observed by hydroxyproline determination in an *in vivo* model of diabetic mice after topical administration of *Martynia annua* and *Tephrosia purpurea* extracts containing luteolin and was confirmed by histopathological studies. This confirms that flavonoids can lead to the stimulation of collagen synthesis and probably participate in the formation of cross-links as collagen matures (Lodhi et al., 2016). However, our study showed a decrease in collagen content in fibroblast cells after the lowest dose (10 μ g/mL) of **22** (luteolin).

Impairment of wound healing leads, *inter alia*, to the overproduction of MMPs and, consequently, to the degradation of the ECM, such as collagen or elastin, and the inhibition of skin re-epithelialization (Wu et al., 2016; Chen et al., 2021). Under physiological conditions, elastin fibers, which contribute to the maintenance of skin elasticity and flexibility, intertwine with the rigid collagen fibers of the ECM. In addition to its important structural role, elastin also has a beneficial effect on wound healing and regeneration (Tracy et al., 2016). In this study, two extracts (**JM4** and **JM5**) and one compound (**22**) were most active elastase inhibitors. However, **JM1**–**JM3**, **JM6**, and compounds **9** and **12** were not active on elastase. When all results were evaluated together, the obtained enzyme inhibitory results may be linked to the chemical composition of the tested extracts and the chemical structure of the compounds. The contradictory results were also observed in the literature, and these phenomena could be explained by the complex nature and possible interactions of phytochemicals in **JM1**–**JM6** (Table 1), as well as *O*-glycosylation at position C7 of the A-ring of the luteolin structure in **9** and **12** (Jakimiuk et al., 2021). Following that, the noticed enzyme inhibitory abilities of **JM4** and **JM5** could be related to the presence of **22**.

The mechanism of chronic wound healing, in addition to the overproduction of MMPs, is also associated with the activation of the prolonged immune response. Inflammation is part of the normal wound healing process; however, in the absence of effective decontamination, this condition can be prolonged with elevated levels of proinflammatory cytokines such as TNF- α and its dependent IL-6 and chemokine IL-8 as well as cytokine IL-1 β , impeding the healing itself by limiting proliferation, skin cell differentiation and collagen deposition at the wound site (Ibrahim et al., 2018; Sarkhail et al., 2020). TNF- α and IL-1 β levels are elevated in chronic wounds and have a similar response inhibiting ECM synthesis while synergistically increasing MMP production (Barrientos et al., 2008). The modulation of inflammation of the wound healing process may occur through the reduction of pro-inflammatory mediators IL-6 and IL-8 induced by TNF- α secreted from



activated fibroblasts and thus may represent an effective therapeutic approach for the regulation of wound healing progression (Bainbridge, 2013; Sarkhail et al., 2020). Therefore, *J. montana* extracts and pure isolated compounds were evaluated to determine whether they have any effect on the production of several inflammatory cytokines. Our findings suggest that fractions from *J. montana* have varying degrees of *in vitro* anti-inflammatory effects on human skin fibroblasts by modulating the levels of IL-1 β , IL-6 and IL-8 (Figures 3–5). Furthermore, the inhibition of inflammatory mediator levels was not due to an overall cytotoxic effect, as described in a previous study (Juszczak et al., 2021), except for high concentrations of **22** and the luteolin-rich fraction **JM4** with antiproliferative and cytotoxic potential, which may be related to the activation of caspases (Juszczak et al., 2021). Many well-known anti-inflammatory molecules may inhibit the activity of the enzymes belonging to caspase-family. For example, numerous non-steroidal anti-inflammatory drugs (NSAIDs), such as

propionic acid derivatives (tenbufen, indoprofen, and iaprofenic acid), acetic acid derivatives (ketorolac, felbinac and tolmetin), as well as others such as ebsele and flunixin are potent multi-caspase inhibitors. Furthermore, it seems that the inhibition occurs at physiologically relevant concentrations *in vitro* and *in vivo*, as well as that it is cyclooxygenase-independent (Smith et al., 2017). *In vitro* and docking studies show that other anti-inflammatory drugs, such as colchicine, and the corticosteroid drugs, dexamethasone and methylprednisolone, also suppress the caspase-1 activity (Ben-Chetrit, 2018; Caruso et al., 2022). Numerous natural phenols such as anthranoids (chrysophanol) (Kim et al., 2010), and flavonoids (icariin and taxifolin) (Zu et al., 2019; Zhan et al., 2021) may also influence caspase activity. Thus, the study of small molecules as caspase inhibitors represents a developing area of research on new anti-inflammatory drugs. Previous studies have reported the anti-inflammatory effects of luteolin and its derivatives (López-Lázaro, 2009; Aziz et al., 2018). Karatoprak

and coauthors suggested that the inhibitory effect of *A. mollis* extracts on TNF- α secretion, which in addition to initiating and propagating inflammation upregulates the already mentioned pro-inflammatory cytokines, is linked to the presence of luteolin 7-*O*-glucoside (Karatoprak et al., 2017). Furthermore, Ustuner and coauthors also attributed the anti-inflammatory effect of the *T. sipyleus* extracts to the presence of luteolin-7-*O*-glucoside (Ustuner et al., 2019). In an *in silico* study, the transcription factors Src, MAPK pathway and SOCS3 were found to be the main targets of the anti-inflammatory effect of luteolin 7-*O*-glucoside (Aziz et al., 2018). Wedler and coauthors suggested that a luteolin derivative probably responsible for the action of *Phyllostachys edulis* extract exerts moderate anti-inflammatory activity by inhibiting TNF- α -induced production of the proinflammatory cytokine IL-6 and the chemokine IL-8 in an *in vitro* model of HaCaT cells (Wedler et al., 2014). Moreover, our data on the anti-inflammatory activity of **22** and the **JM4** fraction are in good agreement with data from *in vitro* and *in vivo* studies during which inhibition of TNF- α and IL-6 secretion was observed (Yang et al., 2018) and from clinical studies reporting that luteolin has excellent therapeutic activity against inflammation-related disorders (Ustuner et al., 2019).

In conclusion, extracts from the aerial parts of *J. montana* have been shown to have high antioxidant activity, promote viability and accelerate the migration of fibroblasts. These mechanisms focus on multiple phases of the dynamic wound healing process, making them, along with the described anti-inflammatory, anti-elastase and stimulating collagen synthesis activities, the main factors in wound healing. Hence, the aboveground parts of *J. montana*, rich in flavonoid compounds, may be potentially useful for topical therapeutic application to stimulate the wound healing process.

REFERENCES

- Addis, R., Cruciani, S., Santaniello, S., Bellu, E., Sarais, G., Ventura, C., et al. (2020). Fibroblast Proliferation and Migration in Wound Healing by Phytochemicals: Evidence for a Novel Synergic Outcome. *Int. J. Med. Sci.* 17, 1030–1042. doi:10.7150/ijms.43986
- Aziz, N., Kim, M. Y., and Cho, J. Y. (2018). Anti-inflammatory Effects of Luteolin: A Review of *In Vitro*, *In Vivo*, and *In Silico* Studies. *J. Ethnopharmacol.* 225, 342–358. doi:10.1016/j.jep.2018.05.019
- Bainbridge, P. (2013). Wound Healing and the Role of Fibroblasts. *J. Wound Care* 22, 407–412. doi:10.12968/jowc.2013.22.8.407
- Barrientos, S., Stojadinovic, O., Golinko, M. S., Brem, H., and Tomic-Canic, M. (2008). Growth Factors and Cytokines in Wound Healing. *Wound Repair Regen.* 16, 585–601. doi:10.1111/j.1524-475X.2008.00410.x
- Bayrami, Z., Hajiaghachee, R., Khalighi-Sigaroodi, F., Rahimi, R., Farzaei, M. H., Hodjat, M., et al. (2018). Bio-guided Fractionation and Isolation of Active Component from *Tragopogon Graminifolius* Based on its Wound Healing Property. *J. Ethnopharmacol.* 226, 48–55. doi:10.1016/j.jep.2018.08.002
- Ben-Chetrit, E. (2019). "Colchicine," in *Textbook of Autoinflammation*. Editors P. J. Hashkes, R. M. Laxer, and A. Simon (Cham, Switzerland: Springer), 729–749. doi:10.1007/978-3-319-98605-0_40
- Caruso, F., Pedersen, J. Z., Incerpi, S., Kaur, S., Belli, S., Florea, R. M., et al. (2022). Mechanism of Caspase-1 Inhibition by Four Anti-inflammatory Drugs Used in COVID-19 Treatment. *Int. J. Mol. Sci.* 23, 1849. doi:10.3390/ijms23031849
- Carvalho, M. T. B., Araújo-Filho, H. G., Barreto, A. S., Quintans-Júnior, L. J., Quintans, J. S. S., and Barreto, R. S. S. (2021). Wound Healing Properties of

DATA AVAILABILITY STATEMENT

The original contributions presented in the study are included in the article/**Supplementary Material**, further inquiries can be directed to the corresponding author.

AUTHOR CONTRIBUTIONS

AJ and MT performed the conceptualization and the project administration. AJ, KJ, RC, and JS were responsible for the methodology and experiments. MZK, KB, and MT were responsible for formal analysis, writing—review and editing. AJ, KJ, RC, and JS contributed to the investigation. AJ, KJ, RC, JS, MZK, and MT prepared the original draft. AJ contributed to data analysis and visualization. MT supervised and completed the final manuscript. All authors have read and agreed to the published version of the manuscript.

FUNDING

The work was funded by project No. POWR.03.02.00-00-I051/16 from European Union funds, POWER 2014–2020, Grant No. 02/IMSD/G/2021.

SUPPLEMENTARY MATERIAL

The Supplementary Material for this article can be found online at: <https://www.frontiersin.org/articles/10.3389/fphar.2022.894233/full#supplementary-material>

- Flavonoids: A Systematic Review Highlighting the Mechanisms of Action. *Phytomedicine* 90, 153636. doi:10.1016/j.phymed.2021.153636
- Chen, L. Y., Cheng, H. L., Kuan, Y. H., Liang, T. J., Chao, Y. Y., and Lin, H. C. (2021). Therapeutic Potential of Luteolin on Impaired Wound Healing in Streptozotocin-Induced Rats. *Biomedicines* 9, 1–13. doi:10.3390/biomedicines9070761
- Ciganović, P., Jakimiuk, K., Tomczyk, M., and Zovko Končić, M. (2019). Glycerolic Licorice Extracts as Active Cosmeceutical Ingredients: Extraction Optimization, Chemical Characterization, and Biological Activity. *Antioxidants* 8, 445. doi:10.3390/antiox8100445
- Comino-Sanz, I. M., López-Franco, M. D., Castro, B., and Pancorbo-Hidalgo, P. L. (2021). The Role of Antioxidants on Wound Healing: A Review of the Current Evidence. *J. Clin. Med.* 10, 3558. doi:10.3390/jcm10163558
- Fronza, M., Heinzmann, B., Hamburger, M., Laufer, S., and Merfort, I. (2009). Determination of the Wound Healing Effect of *Calendula* Extracts Using the Scratch Assay with 3T3 Fibroblasts. *J. Ethnopharmacol.* 126, 463–467. doi:10.1016/j.jep.2009.09.014
- Gothai, S., Arulselvan, P., Tan, W. S., and Fakurazi, S. (2016). Wound Healing Properties of Ethyl Acetate Fraction of *Moringa Oleifera* in Normal Human Dermal Fibroblasts. *J. Intercult. Ethnopharmacol.* 5, 1–6. doi:10.5455/jice.20160201055629
- Ibrahim, N. I., Wong, S. K., Mohamed, I. N., Mohamed, N., Chin, K. Y., Ima-Nirwana, S., et al. (2018). Wound Healing Properties of Selected Natural Products. *Int. J. Environ. Res. Public Health* 15, 2360. doi:10.3390/ijerph15112360
- Jakimiuk, K., Gesek, J., Atanasov, A. G., and Tomczyk, M. (2021). Flavonoids as Inhibitors of Human Neutrophil Elastase. *J. Enzyme Inhib. Med. Chem.* 36, 1016–1028. doi:10.1080/14756366.2021.1927006

- Juszczak, A. M., Czarnomysy, R., Strawa, J. W., Zovko Končić, M., Bielawski, K., and Tomczyk, M. (2021). *In Vitro* anticancer Potential of *Jasione montana* and its Main Components against Human Amelanotic Melanoma Cells. *Int. J. Mol. Sci.* 22, 3345. doi:10.3390/ijms22073345
- Kim, S. J., Kim, M. C., Lee, B. J., Park, D. H., Hong, S. H., and Um, J. Y. (2010). Anti-Inflammatory Activity of Chrysophanol through the Suppression of NF-kappaB/caspase-1 Activation *In Vitro* and *In Vivo*. *Molecules* 15, 6436–6451. doi:10.3390/molecules15096436
- Liang, C. C., Park, A. Y., and Guan, J. L. (2007). *In Vitro* scratch Assay: a Convenient and Inexpensive Method for Analysis of Cell Migration *In Vitro*. *Nat. Protoc.* 2, 329–333. doi:10.1038/nprot.2007.30
- Lodhi, S., Jain, A., Jain, A. P., Pawar, R. S., and Singhai, A. K. (2016). Effects of Flavonoids from *Martynia Annuua* and *Tephrosia Purpurea* on Cutaneous Wound Healing. *Avicenna J. Phytomed.* 6, 578–591. doi:10.22038/ajp.2016.6760
- Lodhi, S., and Singhai, A. K. (2013). Wound Healing Effect of Flavonoid Rich Fraction and Luteolin Isolated from *Martynia Annuua* Linn. On Streptozotocin Induced Diabetic Rats. *Asian pac. J. Trop. Med.* 6, 253–259. doi:10.1016/S1995-7645(13)60053-X
- López-Lázaro, M. (2009). Distribution and Biological Activities of the Flavonoid Luteolin. *Mini Rev. Med. Chem.* 9, 31–59. doi:10.2174/138955709787001712
- Mainka, M., Czerwińska, M. E., Osińska, E., Zająca, M., and Bazyłko, A. (2021). Screening of Antioxidative Properties and Inhibition of Inflammation-Linked Enzymes by Aqueous and Ethanol Extracts of Plants Traditionally Used in Wound Healing in Poland. *Antioxidants (Basel)* 10, 698. doi:10.3390/antiox10050698
- Martinengo, L., Olsson, M., Bajpai, R., Soljak, M., Upton, Z., Schmidchen, A., et al. (2019). Prevalence of Chronic Wounds in the General Population: Systematic Review and Meta-Analysis of Observational Studies. *Ann. Epidemiol.* 29, 8–15. doi:10.1016/j.annepidem.2018.10.005
- Marume, A., Matope, G., Katsande, S., Khoza, S., Mutingwende, I., Mduluzi, T., et al. (2017). Wound Healing Properties of Selected Plants Used in Ethnoveterinary Medicine. *Front. Pharmacol.* 8, 544. doi:10.3389/fphar.2017.00544
- Melguizo-Rodríguez, L., de Luna-Bertos, E., Ramos-Torrecillas, J., Illescas-Montesa, R., Costela-Ruiz, V. J., and García-Martínez, O. (2021). Potential Effects of Phenolic Compounds that Can Be Found in Olive Oil on Wound Healing. *Foods* 10, 1642. doi:10.3390/foods10071642
- Monika, P., Chandraprabha, M. N., Rangarajan, A., Waiker, P. V., and Chidambara Murthy, K. N. (2021). Challenges in Healing Wound: Role of Complementary and Alternative Medicine. *Front. Nutr.* 8, 791899. doi:10.3389/fnut.2021.791899
- Muniandy, K., Gothai, S., Tan, W. S., Kumar, S. S., Mohd Esa, N., Chandramohan, G., et al. (2018). *In Vitro* Wound Healing Potential of Stem Extract of *Alternanthera Sessilis*. *Evid. Based Complement. Altern. Med.* 2018, 1–13. doi:10.1155/2018/3142073
- Okuda, M., Kaihara, S., Murakami, T., Koide, D., and Ohe, K. (2014). *Wiley StatsRef: Statistics Reference Online*. Chichester: John Wiley & Sons, 71–77.
- Sarkhail, P., Navidpour, L., Rahimifard, M., Hosseini, N. M., and Souri, E. (2020). Bioassay-guided Fractionation and Identification of Wound Healing Active Compound from *Pistacia Vera* L. Hull Extract. *J. Ethnopharmacol.* 248, 112335. doi:10.1016/j.jep.2019.112335
- Şeker Karatoprak, G., İlğün, S., and Koşar, M. (2017). Phenolic Composition, Anti-inflammatory, Antioxidant, and Antimicrobial Activities of *Alchemilla Mollis* (Buser) Rothm. *Chem. Biodivers.* 14, e1700150. doi:10.1002/cbdv.201700150
- Shedoeva, A., Leavesley, D., Upton, Z., and Fan, C. (2019). Wound Healing and the Use of Medicinal Plants. *Evid. Based Complement. Altern. Med.* 2019, 2684108. doi:10.1155/2019/2684108
- Smith, C. E., Soti, S., Jones, T. A., Nakagawa, A., Xue, D., and Yin, H. (2017). Non-steroidal Anti-inflammatory Drugs Are Caspase Inhibitors. *Cell. Chem. Biol.* 24, 281–292. doi:10.1016/j.chembiol.2017.02.003
- Soib, H. H., Ismail, H. F., Husin, F., Abu Bakar, M. H., Yaakob, H., and Sarmidi, M. R. (2020). Bioassay-guided Different Extraction Techniques of *Carica Papaya* (Linn.) Leaves on *In Vitro* Wound-Healing Activities. *Molecules* 25, 515. doi:10.3390/molecules25030517
- Srivastava, J. K., Shankar, E., and Gupta, S. (2010). Chamomile: A Herbal Medicine of the Past with Bright Future. *Mol. Med. Rep.* 3, 895–901. doi:10.3892/mmr.2010.377
- Sulaiman, M., Tijani, I. H., Abubakar, B. M., Haruna, S., Hindatu, Y., Mohammed, J. N., et al. (2013). An Overview of Natural Plant Antioxidants: Analysis and Evaluation. *Ab* 1, 64–72. doi:10.11648/j.ab.20130104.12
- Süntar, I., Akkol, E. K., Nahar, L., and Sarker, S. D. (2012). Wound Healing and Antioxidant Properties: Do They Coexist in Plants? *Free Radicals Antioxidants* 2, 1–7. doi:10.5530/ax.2012.2.2.1
- Tracy, L. E., Minasian, R. A., and Caterson, E. J. (2016). Extracellular Matrix and Dermal Fibroblast Function in the Healing Wound. *Adv. Wound Care (New Rochelle)* 5, 119–136. doi:10.1089/wound.2014.0561
- Ustuner, O., Anlas, C., Bakirel, T., Ustun-Alkan, F., Diren Sigirci, B., Ak, S., et al. (2019). *In Vitro* evaluation of Antioxidant, Anti-inflammatory, Antimicrobial and Wound Healing Potential of *Thymus Sipylyeus* Boiss. Subsp. *Rosulans* (Borbas) Jalas. *Molecules* 24, 1–21. doi:10.3390/molecules24183353
- Wedler, J., Daubitz, T., Schlotterbeck, G., and Butterweck, V. (2014). *In Vitro* anti-inflammatory and Wound-Healing Potential of a Phyllostachys Edulis Leaf Extract-Identification of Isoorientin as an Active Compound. *Planta Med.* 80, 1678–1684. doi:10.1055/s-0034-1383195
- Wittenauer, J., Mäcke, S., Sußmann, D., Schweiggert-Weisz, U., and Carle, R. (2015). Inhibitory Effects of Polyphenols from Grape Pomace Extract on Collagenase and Elastase Activity. *Fitoterapia* 101, 179–187. doi:10.1016/j.fitote.2015.01.005
- World Health Organization (2013). Traditional Medicine Strategy: 2014–2023. Available at: <https://www.who.int/publications/i/item/9789241506096> (Accessed February 2, 2022).
- Wu, X., Yang, L., Zheng, Z., Li, Z., Shi, J., Li, Y., et al. (2016). Src Promotes Cutaneous Wound Healing by Regulating MMP-2 through the ERK Pathway. *Int. J. Mol. Med.* 37, 639–648. doi:10.3892/ijmm.2016.2472
- Yang, S. C., Chen, P. J., Chang, S. H., Weng, Y. T., Chang, F. R., Chang, K. Y., et al. (2018). Luteolin Attenuates Neutrophilic Oxidative Stress and Inflammatory Arthritis by Inhibiting Raf1 Activity. *Biochem. Pharmacol.* 154, 384–396. doi:10.1016/j.bcp.2018.06.003
- Zhan, Z. Y., Wu, M., Shang, Y., Jiang, M., Liu, J., Qiao, C. Y., et al. (2021). Taxifolin Ameliorate High-Fat-Diet Feeding Plus Acute Ethanol Binge-Induced Steatohepatitis through Inhibiting Inflammatory Caspase-1-dependent Pyroptosis. *Food Funct.* 12, 362–372. doi:10.1039/D0FO02653K
- Zu, Y., Mu, Y., Li, Q., Zhang, S. T., and Yan, H. J. (2019). Icaritin Alleviates Osteoarthritis by Inhibiting NLRP3-Mediated Pyroptosis. *J. Orthop. Surg. Res.* 14, 307. doi:10.1186/s13018-019-1307-6

Conflict of Interest: The authors declare that the research was conducted in the absence of any commercial or financial relationships that could be construed as a potential conflict of interest.

Publisher's Note: All claims expressed in this article are solely those of the authors and do not necessarily represent those of their affiliated organizations, or those of the publisher, the editors and the reviewers. Any product that may be evaluated in this article, or claim that may be made by its manufacturer, is not guaranteed or endorsed by the publisher.

Copyright © 2022 Juszczak, Jakimiuk, Czarnomysy, Strawa, Zovko Končić, Bielawski and Tomczyk. This is an open-access article distributed under the terms of the Creative Commons Attribution License (CC BY). The use, distribution or reproduction in other forums is permitted, provided the original author(s) and the copyright owner(s) are credited and that the original publication in this journal is cited, in accordance with accepted academic practice. No use, distribution or reproduction is permitted which does not comply with these terms.

Wound healing properties of *Jasione montana* extracts and their main secondary metabolites

Aleksandra Maria Juszcak¹, Katarzyna Jakimiuk¹, Robert Czarnomysy², Jakub Władysław Strawa¹, Marijana Zovko Končić³, Krzysztof Bielawski², and Michał Tomczyk^{1*}

- ¹ Department of Pharmacognosy, Faculty of Pharmacy with the Division of Laboratory Medicine, Medical University of Białystok, ul. Mickiewicza 2a, 15-230 Białystok, Poland
- ² Department of Synthesis and Technology of Drugs, Faculty of Pharmacy with the Division of Laboratory Medicine, Medical University of Białystok, ul. Kilińskiego 1, 15-089 Białystok, Poland
- ³ Department of Pharmacognosy, Faculty of Pharmacy and Biochemistry, University of Zagreb, Marulićev trg 20/II, 10000 Zagreb, Croatia

*** Correspondence:**

Michał Tomczyk
michal.tomczyk@umb.edu.pl

Keywords: *Jasione montana*, Campanulaceae, flavonoids, luteolin derivatives, fibroblasts, wound healing, antioxidant, enzyme inhibition

1 Plant material

The aboveground parts of *J. montana* were collected from plants occurring in their natural habitat within the area of Puszcza Knyszyńska (N53°15'20.9"; E23°25'41.5") in the region of Supraśl (Podlasie Province, Poland) within the period of June–August 2017 and 2018. Samples of the collected plant material were identified based on the scientific botanical literature, available the Royal Botanic Gardens database (<https://powo.science.kew.org/>) and its morphological features by one of the authors (M.T.) (Rutkowski, 2006). A plant voucher specimen (JM-15029) has been deposited in the Herbarium of the Department of Pharmacognosy at the Medical University of Białystok, Poland.

2 Chemicals

2,2-diphenyl-1-picrylhydrazyl (DPPH) (CAS1898-66-4), methanol (MeOH) (CAS67-56-1), trolox (CAS53188-07-1), Ferric Reducing Antioxidant Power Assay Kit (MAK369), Tris buffer (CAS77-86-1), elastase from porcine pancreas type I (PPE) (CAS39445-21-1), quercetin (CAS 849061-97-8), dimethyl sulfoxide (DMSO) (CAS67-68-5), allantoin (CAS97-59-6), formic acid (HCOOH) (CAS64-18-6) were purchased from Sigma Aldrich Co. (St. Louis, MO, USA). N-Succ-Ala-Ala-Ala-p-nitroanilide (AAAPVN) (CAS52299-14-6) was purchased from Serva Electrophoresis (Heidelberg, Germany). The normal human dermal fibroblast cell line (PCS-201-012) was purchased from the American Type Culture Collection (ATCC; Manassas, VA, USA). Dulbecco's minimal essential medium (DMEM), fetal bovine serum (FBS), phosphate-buffered saline (PBS), trypsin EDTA, glutamine, penicillin, and streptomycin were acquired from Corning (Corning, NY, USA). Stain Buffer was acquired from BD Pharmingen (San Diego, CA, USA). Anti-Collagen Type I (RABBIT) antibody fluorescein conjugated was purchased from the Rockland Immunochemicals, Inc. (Pottstown, PA, USA). Cytometric Bead Array (CBA) Human Inflammatory Cytokines Kit was obtained from BD Biosciences (San Jose, CA, USA). Luteolin (CAS491703) and luteolin 7-*O*-glucoside (CAS5373115) used

as standards for quantification analysis were purchased from Chemat (Gdańsk, Poland). Acetonitrile (MeCN) (CAS75-05-08) was purchased from Fisher Chemical (Thermo Fisher Scientific, Leicestershire, UK). Water (UPW) type I (18.2 MΩxcm resistivities at 25°C) was obtained using a deionizer POLWATER DL3-100 (Labopol, Kraków, Poland).

3 HPLC–PDA condition

To establish the quantitative content of the main compounds of **JM1–JM6**, HPLC–PDA analysis was performed on a 1260 Infinity chromatography system (Agilent Technologies, Santa Clara, CA, USA). The analysis was performed using a Kinetex XB-C18 column (150 × 2.1 mm, 1.7 μm; Phenomenex, Torrance, CA, USA) secured by pre-column and thermostated at 25°C. Compounds were eluted at flow rate 0.1 mL/min with UPW and MeCN acidified with HCOOH (0.1%) in 3 steps of a linear gradient (22 min - 28% B, 35 min - 75% B, 45 min - 95% B) after 1.5 min of initial conditions (5% B). The analysis was completed with a 3 min cleaning of the column (95% B), and a 6 min equilibration before next injection. Chromatogram UV were recorded at 348 nm wavelengths matching the value of the maximum absorption of the selected standards.

3.1 Preparation of calibration curves

Exactly weighed standard substances were dissolved, filtered through a 0.2 μm PVDF syringe filter to give a final concentration of 1 mg/ml (*m/v*). In the next step, stock solutions were used to create a mixture of patterns. The working range of the curves from 6 concentration levels was then obtained by the multiple dilution method with the mobile phase. Then, were immediately used to determine the standard curve.

3.2 Preparation of samples solution

Accurately weighed samples were dissolved, then centrifuged and filtered through a 0.2 μm PVDF syringe filter into a volumetric flask to give a final 5 mg/mL and 2 mg/mL concentration of extracts and fractions, respectively.

4 Method Validation

4.1.1 Selectivity

Three solutions were made for tested extracts to exclude the occurrence of co-elution. Analysis with the use of a PDA detector at three selected wavelengths was used. The analysis of the obtained UV chromatograms made it possible to exclude the possibility of elution of the compounds at the same time.

4.1.2 Linearity

Standard solutions at six concentration levels were analyzed in triplicate. Calibration curves were generated using linear regression on the plots of peak area of each standard versus injected content to the column. Linear regression parameters for the standard curve were determined using ANOVA. Statistical significance has been confirmed. Calculations were made using MS Excel 2019 with a Data Analysis add-on.

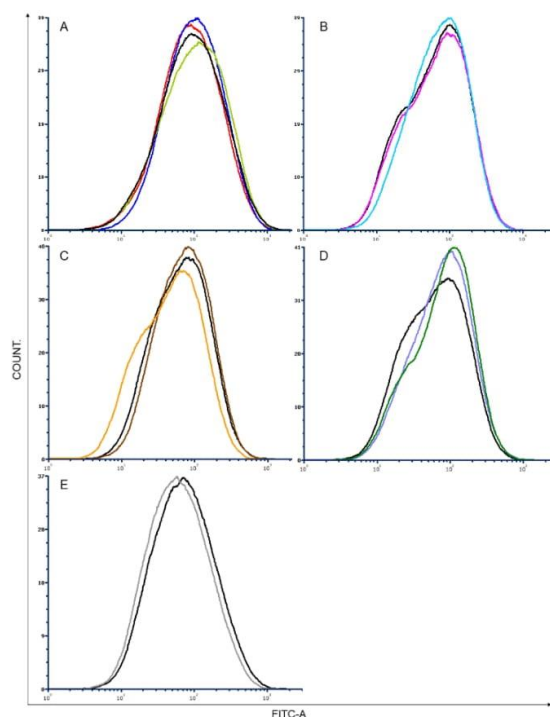
4.1.3 Limits of Detection (LOD) and Quantification (LOQ)

In accordance with the International Council for Harmonisation of Technical Requirements for Pharmaceuticals for Human Use (ICH) recommendations the detection limit and limit of quantification based on the standard deviation (σ) of the response and the slope (S). Repeating for ICH, we assumed $LOD = 3.3\sigma/S$ and $LOQ = 10\sigma/S$. The parameters are summarized in Supplementary Table S1.

Supplementary Table S1. Regression data, the limit of detection (LOD) and limit of quantification (LOQ), accuracy and precision obtained during HPLC–PDA method validation.

Parameter	luteolin 7-O-glucoside (12)	luteolin (22)
Linear range [$\mu\text{g/mL}$]	25–1000	5–500
R^2 (N=6)	0.9999	0.9999
Regression equation ^a	$y = 22851x+106.69$	$y = 36173x-34.602$
LOD [$\mu\text{g/mL}$]	19.4	4.6
LOQ [$\mu\text{g/mL}$]	59	14
Accuracy [%]	101.09 \pm 3.23	101.23 \pm 2.93
Intraday precision (%CV) (N=6)	0.58	0.93
Interday precision (%CV) (N=9)	0.88	1.26

^a the value for y corresponds to the peak area and x to the concentration, respectively



Supplementary Figure S2. Expression of Collagen Type 1 antibody in fibroblast cells after 24 h incubation with *J. montana* extracts (**JM1–JM6**) and their main compounds (**9**, **12**, **22**) (10–300 $\mu\text{g/mL}$) analysis by FCS Express 7 software (DeNovo Software, Pasadena, CA, USA). Representative histograms were derived from flow cytometric analysis of 10.000 cells and show control cells (black line), (A) **JM1**-treated cells (red line), **JM2**-treated cells (blue line) and **JM3**-treated cells (light green line), (B) **JM4**-treated cells (pink line) and **JM5**-treated cells (light blue line), (C) **JM6**-treated cells (brown line) and **22**-treated cells (orange line), (D) **12**-treated cells (purple line) and **9**-treated cells (dark green line) and (E) cells treated with positive control allantoin (gray line).

5 References

Rutkowski, L. (2006). *Klucz do oznaczania roślin naczyniowych Polski niżowej*. Warsaw: Wydawnictwo Naukowe PWN.

Publication III

Juszczak A.M., Zovko Končić M., Tomczyk M.: Recent trends in the application of chromatographic techniques in the analysis of luteolin and its derivatives. *Biomolecules* Vol. 9, ID 731, 2019, 38 pages.

DOI: 10.3390/biom9110731

Review

Recent Trends in the Application of Chromatographic Techniques in the Analysis of Luteolin and Its Derivatives

Aleksandra Maria Juszcak ¹, Marijana Zovko-Končić ² and Michał Tomczyk ^{1,*}

¹ Department of Pharmacognosy, Faculty of Pharmacy, Medical University of Białystok, ul. Mickiewicza 2a, 15-230 Białystok, Poland; aleksandra.juszcak@umb.edu.pl

² Department of Pharmacognosy, University of Zagreb, Faculty of Pharmacy and Biochemistry, A. Kovačića 1, 10000 Zagreb, Croatia; mzovko@pharma.hr

* Correspondence: michal.tomczyk@umb.edu.pl; Tel.: +48-85-748-5694

Received: 1 October 2019; Accepted: 8 November 2019; Published: 12 November 2019

Abstract: Luteolin is a flavonoid often found in various medicinal plants that exhibits multiple biological effects such as antioxidant, anti-inflammatory and immunomodulatory activity. Commercially available medicinal plants and their preparations containing luteolin are often used in the treatment of hypertension, inflammatory diseases, and even cancer. However, to establish the quality of such preparations, appropriate analytical methods should be used. Therefore, the present paper provides the first comprehensive review of the current analytical methods that were developed and validated for the quantitative determination of luteolin and its C- and O-derivatives including orientin, isoorientin, luteolin 7-O-glucoside and others. It provides a systematic overview of chromatographic analytical techniques including thin layer chromatography (TLC), high performance thin layer chromatography (HPTLC), liquid chromatography (LC), high performance liquid chromatography (HPLC), gas chromatography (GC) and counter-current chromatography (CCC), as well as the conditions used in the determination of luteolin and its derivatives in plant material.

Keywords: luteolin; hyphenated techniques; chromatography

1. Introduction

Luteolin (Figure 1) is a yellow dye commonly found in fresh plants. It is a flavonoid of the flavone type that is distributed widely throughout the plant kingdom. Similar to other derivatives of 2-phenylbenzo- γ -pyrone, its basic skeleton has a characteristic C₆-C₃-C₆ system, containing two benzene rings and a bridge with a C2-C3 double carbon bond and an attached oxygen atom [1–4]. Structure-activity studies have demonstrated that the pharmacological effects of luteolin and other flavonoids are strongly related to the presence of hydroxyl groups at the C5, C7, C3' and C4' carbons as well as to the presence of the double bond in the C2-C3 position [3,5]. The presence of the -OH group at position C3' distinguishes luteolin from apigenin, and the lack of this group at the C3 carbon is an element that places luteolin in the flavone group [6].

Luteolin exhibits multiple biological effects such as antioxidant, anti-inflammatory and immunomodulatory activity. Plants rich in luteolin are often used in traditional medicine for treatment of various diseases such as hypertension, inflammatory disorders, and even cancer [7].

Because luteolin bears four hydroxyl groups (at the C5, C7, C3' and C4' positions), many derivatives of luteolin can be created. Various types of functional groups and/or sugar molecules can be attached to those positions, creating a huge number of different but structurally similar molecules. The most common are methyl derivatives, as well as C- and -O-glycosides [8,9].

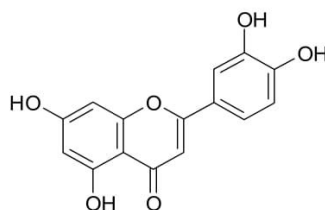


Figure 1. Chemical structure of luteolin.

Orientin, an 8-C-glucoside derivative of luteolin, displays an array of health-related biological properties, such as antioxidant, anti-ageing, antiviral, antibacterial, anti-inflammatory, vasodilatation, cardioprotective, radiation protective, neuroprotective, antidepressant-like, anti-adipogenesis, and antinociceptive effects. It may be found in different medicinal plants such as *Ocimum sanctum* (holy basil), *Phyllostachys nigra* (bamboo leaves), *Passiflora* sp. (passion flower), *Linum usitatissimum* (flax), *Euterpe oleracea* (Acai palm) and many others [10]. Another luteolin derivative, isoorientin (luteolin-6-C-glucoside) acts as an antioxidant, photoprotective [11], skin lightening [12], hepatoprotective [13] and anti-inflammatory agent [14]. *O*-glucosides of luteolin also display biological activities. For example, luteolin 7-*O*-glucoside alleviates skin lesions in murine models of atopic dermatitis [15] and protects cells against apoptosis induced by hypoxia/reoxygenation [16].

An increasing number of herbal preparations on the market contain luteolin and its derivatives, either as single-ingredient products or in mixtures with other phytochemicals, e.g., in form of medicinal plants extracts. To establish the quality of such products, it is important to use appropriate analytical methods. However, there is a lack of quality reviews of the available methods for quantification of luteolin derivatives, and the information on their comparison is lacking. Therefore, the aim of this article is to systematize knowledge and information in the field of chromatographic analytical techniques used for quantification of luteolin and its derivatives. The presented review is the first description of this type and provides a systematic overview of chromatographic analytical techniques including thin layer chromatography (TLC), high performance thin layer chromatography (HPTLC), liquid chromatography (LC), high performance liquid chromatography (HPLC), gas chromatography (GC) and counter-current chromatography (CCC), as well as the conditions used to assess luteolin and its derivatives.

2. Chromatographic Techniques for the Analysis of Luteolin Derivatives

Chromatography occupies a leading position among other instrumental methods in the analysis of chemical compounds. As a physicochemical method of separation and analysis of mixtures of chemical compounds, it allows detection and identification as well as quantitative determination of the test substance with high accuracy. The coupling of chromatography with other methods of analysis contributes to a more accurate detection and expansion of analytical capabilities, especially for complex mixtures of organic compounds [2,17,18].

Chromatographic techniques are based on the interaction of the mixture components with the mobile and stationary phases of the chromatographic system. This results in the division of the mixture components between the two phases. In addition, the interaction of the mobile and stationary phases is also important in the separation process [17,18]. According to the aggregation state of the mobile phase, chromatographic techniques are divided into gas, liquid and supercritical chromatography. Another criterion for classification of chromatographic techniques is the type of stationary phase. If the stationary phase is a liquid, the chromatography technique is referred to as partition chromatography. In the case of a solid, the technique is referred to as adsorption chromatography. Another example of the classification of chromatographic methods is their division depending on the chromatographic processing method. This classification allows distinguishing column chromatography and planar techniques, which include TLC and paper chromatography

[17,19]. Many different chromatographic techniques are used in the analysis of luteolin derivatives. These include TLC, HPTLC, LC, HPLC, GC and CCC [19].

2.1. Thin Layer Chromatography in the Analysis of Luteolin Derivatives

Thin layer chromatography (TLC) is a rather simple but relatively popular method used in the analysis of flavonoids since 1960 [20]. It is a variation of LC that is carried out on a plane and is therefore referred to as planar chromatography. Despite the dynamic development of other chromatography techniques, TLC has not lost its importance in phytochemical analysis [18]. Its values are still recognized as is the basic tool in the qualitative analysis of natural products, and as such, it is still recommended by most modern Pharmacopoeias. In addition, the TLC technique is currently being improved, and the scope of its application is widening, while the results are becoming comparable to those obtained by GC or HPLC [20–22]. The stages of chromatographic analysis consist of placing the sample on the stationary phase and developing the chromatogram, followed by its visualization. In the final step, qualitative and/or quantitative determinations of the tested components are made [18,22,23]. General guidelines for flavonoid separation on TLC plates are presented in Table 1.

The main advantage of TLC is that it is a relatively simple and inexpensive technique that allows for rapid qualitative and quantitative analysis of the tested compounds. Samples analyzed with this method usually do not require pre-treatment, such as purification or concentration. In addition, several dozens of samples can be analyzed simultaneously on one plate. A large amount of the diluted sample can be applied to the stationary phase because the solvent evaporates during the application to the plate. Furthermore, due to the evaporation of the solvent phase after the development of the chromatogram, the detection method does not depend on the type of mobile phase used for separation. In TLC, it is possible not only to compare the analyzed components with the standards, but also to differentiate between substances bearing specific functional groups using the appropriate reagents for detection [18].

Thin layer chromatography and column chromatography (CC) are interchangeable techniques that may be combined, which significantly reduces costs and analysis time [22]. To achieve this, the same adsorbents are ideally used for both TLC and CC [18,22,24]. Nevertheless, other solvent systems may also be used. Elution in CC may be carried out in one mobile phase, or its composition may be changed during chromatography (mobile phase gradient), thereby increasing the elution force. In this case, the TLC mobile phase should be changed accordingly [18,24].

Table 1. Recommended combinations of solvents / adsorbents for identification. of different flavonoid types by thin layer chromatography (TLC).

Flavonoid type	Adsorbent type / Mobile phase		
	Cellulose	Polyamide	Silica gel
Polar flavonoid aglycones, e.g. flavones	BuOH:AcOH:H ₂ O (3:1:1 v/v/v) ^a	MeOH:AcOH:H ₂ O (18:1:1 v/v/v)	To:Py:FA (36:9:5 v/v/v)
	CHCl ₃ :AcOH:H ₂ O (30:15:2 v/v/v) ^b		
Non-polar flavonoid aglycones, e.g. methylated flavones	10–30% AcOH	---	CHCl ₃ :MEOH (15:1 to 3:1 v/v)
Flavonoid glycosides	BuOH:AcOH:H ₂ O (3:1:1 v/v/v) ^a	H ₂ O:MeOH:MEK:methyl acetylacetone (13:3:3:1 v/v/v)	EtOAc:Py:H ₂ O:MeOH (80:20:10:5 v/v/v/v) (especially flavone C-glycosides)
	BuOH:AcOH:H ₂ O (4:1:5 v/v/v) ^a		

Abbreviations: AcOH, acetic acid; BuOH, butanol; CHCl₃, chloroform; EtOAc, ethyl acetate; FA, formic acid; MeOH, methanol; MEK, methyl ethyl ketone; Py, pyridine; To, toluene. ^a The mobile phase is thoroughly mixed in the separating funnel and the upper phase is used. ^b The mobile phase is thoroughly mixed in the separating funnel and the excess water is discarded.

Table 2. Thin layer chromatography in the analysis of luteolin derivatives.

Luteolin derivative	Stationary phase	Mobile phase	Detection	Analyzed species	Ref.
Luteolin	silica gel 60 F ₂₅₄	Hx:EtOAc:AcOH (31:14:5 v/v/v); To:DI:AcOH (90:25:4 v/v/v)	FBS; UV, 254, 366 nm	<i>Artemisia annua</i>	[25]
Luteolin 7-rutinoside	silica gel 60 RP-18 F ₂₅₄ S	FA:H ₂ O:MeOH (5.5:47.25:47.25 v/v/v)	NP/PEG, aniline phthalate; UV, 254, 366 nm	<i>Ligustrum vulgare</i>	[26]
Luteolin 7-rhamnoside	silica gel cellulose	EtOAc:FA:AcOH:H ₂ O (100:11:11:23 v/v/v/v) 30% AcOH	MS, NMR		
Luteolin 3'-glucoside	polyamide	CHCl ₃ :MeOH:MEK:AcAc (9:4:2:1 v/v/v/v); To:MeOH:MEK:BuOH (300:150:150:3 v/v/v/v)	NP/PEG; UV, 366 nm	<i>Phlomis persica</i> <i>Ph. elliptica</i>	[27]
Luteolin 6,8-dihexoside	silica gel 60 F ₂₅₄	MeOH:H ₂ O (15:5 v/v); CHCl ₃ :MeOH (15:5 v/v); 15% AcOH	NP/PEG; UV, 366 nm		
Luteolin 7-rutinoside	silica gel	EtOAc:FA:H ₂ O (18:1:1 v/v/v)	NP/PEG; UV, 366 nm	<i>Carduus acanthoides</i>	[28]
Luteolin 7-glucoside	polyamide plates	EtOAc:FA:AcOH:H ₂ O (100:10:10:13 v/v/v/v)	NP/PEG; UV, 366 nm		
Luteolin					
Luteolin 7,4'-diglucoside					
Luteolin 6-hydroxy-7-glucoside					
Luteolin 4'-glucoside	silica gel 60 F ₂₅₄	EtOAc:Ac:FA (8:1:1 v/v/v); EtOAc:H ₂ O:AcOH:FA (10:3:1:1 v/v/v/v)	NP; UV, IR, NMR	<i>Leontopodium alpinum</i>	[29]
Luteolin 3'-glucoside					
Luteolin 7-glucoside					
Luteolin	silica gel 60 F ₂₅₄	To:EtO:AcOH (60:40:10 v/v/v); EtOAc:AcOH:FA:H ₂ O (100:11:1:26 v/v/v/v)	NP/PEG; UV, 366 nm	<i>Matricaria recutita</i> , <i>Achillea millefolium</i> , <i>Thymus vulgaris</i> , <i>Salvia officinalis</i>	[30]
Luteolin 7-glucoside					

Abbreviations: AcAc, acetylacetone; Ace, acetone; AcOH, acetic acid; BuOH, butanol; CHCl₃, chloroform; DI, 1,4-dioxane; EtO, diethyl ether; EtOAc, ethyl acetate; FA, formic acid; FBS, Fast Blue B Salt; Hx, hexane; MeOH, methanol; MEK, methyl ethyl ketone; NP, 1% methanolic diphenylboric acid-β-ethylamino ester - natural product reagents; PEG, 5% ethanolic polyethylene glycol 4000; To, toluene; UV, ultraviolet spectroscopy; MS, mass spectrometry; NMR, nuclear magnetic resonance; IR, infrared.

Table 3. High performance thin layer chromatography in the analysis of luteolin derivatives.

Luteolin derivative	Stationary phase	Mobile phase	Detection	Analyzed species	Ref
	HPTLC silica gel 60 F ₂₅₄	Hx:EtOAc:AcOH (31:14:5 v/v/v); To:DI:AcOH (90:25:4 v/v/v)	FBS; UV, 254, 366 nm	<i>Artemisia annua</i>	[25]
	HPTLC diol F ₂₅₄ S	CHCl ₃ :Hx:EtOAc (34:4 v/v/v)	2% AlCl ₃ ; UV, 366 nm		
	HPTLC silica gel 60 RP-18W	BuOH:MeOH:H ₂ O (300:50:50 v/v/v); 15% AcOH	NPR/PEG; UV, 366 nm	<i>Oxytropis glabra</i>	[31]
	HPTLC silica gel 60 F ₂₅₄	EtOAc:MeOH:FA:H ₂ O (20:3:1:2 v/v/v/v)	MeOH:H ₂ SO ₄ (95:5 v/v); UV, 254, 366 nm	<i>Asparagus racemosus</i> , <i>Withania somnifera</i> , <i>Vitex negundo</i> , <i>Plumbago zeylenica</i> , <i>Butea monosperma</i> , <i>Tephrosia purpurea</i>	[32]
Luteolin	HPTLC silica gel 60 F ₂₅₄	To:EtOAc:FA (10:9:1 v/v/v)	UV, 254 nm	<i>Cardiospermum halicacabum</i>	[33]
	HPTLC silica gel 60 F ₂₅₄	DCM:MeOH (70:30 v/v)	UV, 254 nm; NMR	<i>Satureja montana</i>	[34]
	HPTLC silica gel G ₆₀ F ₂₅₄	To:EtOAc:FA (6:4:1 v/v/v)	UV, 349 nm	<i>Hygrophila spinosa</i>	[35]
	HPTLC silica gel 60 F ₂₅₄	EtOAc:MeOH:H ₂ O:AcOH (3:1:1:1 v/v/v/v)	UV, 254, 366 nm	<i>Foeniculum vulgare</i> , <i>Cuminum cyminum</i> , <i>Apium graveolens</i> , <i>Petroselinum crispum</i> , <i>Anethum graveolens</i> , <i>Anmmi majus</i>	[36]
	HPTLC silica gel 60 F ₂₅₄	To:EtOAc:FA (3:3:0.8 v/v/v)	MeOH:H ₂ SO ₄ (90:10 v/v); UV, 254 nm	<i>Saraca asoca</i>	[37]
	HPTLC silica gel 60 F ₂₅₄	To:EtOAc:FA (6:4:0.3 v/v/v)	NP/PEG; UV, 366 nm	<i>Premna mucronata</i>	[38]
	HPTLC silica gel G ₆₀ F ₂₅₄	To:EtOAc:FA (10:9:1 v/v/v)	UV, 254, 366 nm	<i>Anisochilus carnosus</i>	[39]

Table 3. Cont.

	HPTLC silica gel 60	nHx:EtOAc:FA (30:20:1.5 v/v/v)	NP/PEG; UV, 349 nm	<i>Satureja hortensis</i>	[40]
	HPTLC silica gel 60 F ₂₅₄	nHx:EtOAc:AcOH (5:3:1 v/v/v)	UV	Propolis	[41]
	HPTLC silica gel 60 GF ₂₅₄	To:EtOAc:FA:MeOH (3:3:0.8:0.2 v/v/v/v)	UV, 254, 365 nm	<i>Eclipta alba</i>	[42]
	HPTLC silica gel 60 F ₂₅₄	To:EtOAc:FA (5:3:1 v/v/v)	NP; UV, 366, 254 nm	<i>Vitis vinifera</i>	[43]
Luteolin 6-glucoside	HPTLC silica gel 60 F ₂₅₄	EtOAc:FA:AcOH:H ₂ O (100:11:11:27 v/v/v/v)	NP/PEG; UV, 366 nm	<i>Clinacanthus nutans</i>	[44]
	HPTLC silica gel 60 F ₂₅₄	EtOAc:FA:H ₂ O (82:9:9 v/v/v)	NP/PEG; UV, 366 nm	<i>Passiflora alata</i> , <i>P. edulis</i>	[45]
Luteolin 8-glucoside	Nano-DUASIL silica gel 60	THF:To:FA:H ₂ O (16:8:2:1 v/v/v/v)	UV, 350 nm	<i>Phyllanthus pubescens</i>	[46]
	HPTLC silica gel 60 F ₂₅₄	EtOAc:FA:AcOH:H ₂ O (100:11:11:26 v/v/v/v)	NP/PEG; UV, 366 nm	<i>Equisetum arvense</i>	[47]
Luteolin glucoside	HPTLC silica gel 60 F ₂₅₄	EtOAc:AcOH:FA:H ₂ O (10:1:1:1:2.6 v/v/v/v/v)	UV, 254, 366 nm	<i>Aerva javanica</i>	[48]
	NP-HPTLC silica gel	EtOAc:FA:AcOH:H ₂ O (100:11:11:27 v/v/v/v/v)	H ₂ O solution of 4% Al ₂ (SO ₄); UV, 365 nm	<i>Apis mellifera</i> , honey	[49]
Luteolin		To:EtOAc:AcOH (50:45:5 v/v/v)			
	HPTLC silica gel 60 F ₂₅₄	To:EtFo:FA (6:4:1 v/v/v)		<i>Potentilla grandiflora</i> , <i>P. recta</i> ,	
	modified HPTLC silica gel 60 F ₂₅₄ with CN, NH ₂	To:EtFo:FA (7:5:1 v/v/v)	NP; UV, 254, 366 nm	<i>P. anserina</i> , <i>P. fruticosa</i> , <i>P. rupestris</i> ,	[50]
Luteolin 7-glucoside	HPTLC diol F ₂₅₄	EtOAc:MEK:DIPE:FA (3:10:4:1 v/v/v/v)		<i>P. thuringiaca</i>	
	HPTLC silica gel 60	EtOAc:DCM:AcOH:FA:H ₂ O (100:25:10:10:11 v/v)	NP; UV, 366 nm	<i>Lavandula stoechas</i>	[51]
Luteolin 7-glucoside	HPTLC silica gel 60 F ₂₅₄	EtOAc:AcOH:FA:H ₂ O (100:11:11:26 v/v/v/v)	NP/PEG; UV, 254, 366 nm	<i>Stachys sylvatica</i> , <i>S. recta</i>	[52]

Table 3. Cont.

Luteolin 7-rutinoside	HPTLC NH ₂ HPTLC RP-18W	Acc:AcOH (85:15 v/v) H ₂ O:MeOH (60:40 v/v)	MeOH:AlCl ₃ (98:2 v/v), bis-diazodized sulfanilamide; UV-VIS, 365 nm IR, MS, NMR	<i>Mentha piperita</i> [53]
Luteolin 7-glucoside	HPTLC silica gel 60	Et:Ac:H ₂ O:FA (55:25:10:10 v/v/v/v)	NP/PEG; UV, 365 nm	<i>Mentha piperita</i> , <i>Melissa officinalis</i> , <i>Salvia officinalis</i> [54]
Luteolin 7-rutinoside	HPTLC NH ₂	Acc:AcOH (85:15 v/v)		
Luteolin 7-glucoside	HPTLC NH ₂	Acc:FA (85:15 v/v)	MeOH:AlCl ₃ (98:2 v/v), NP/PEG; UV, 365 nm	<i>Thymus vulgaris</i> , <i>Th. serpyllum</i> , <i>Majonana hortensis</i> , <i>Mentha piperita</i> [55]
Luteolin 7-glucuronide	HPTLC silica gel 60	DIPE:Ac:H ₂ O:FA (50:30:10:10 v/v/v/v)		<i>Rosmarinus officinalis</i> [56]
Luteolin acetyl hexuronide	HPTLC silica gel 60	pre-develop: CHCl ₃ :MeOH (1:1 v/v); nHx:EtOAc:FA (20:19:1 v/v/v)	NP: white light, 254, 366, 330 nm; PEG: 254, 297, 340, 366, 430 nm; paraifin-nHx: 254, 320, 360, 366, 400 nm; ESI-MS/MS	<i>Salvia officinalis</i> [57]
Luteolin 3',7-diglucoside	HPTLC silica gel 60 F ₂₅₄			
Luteolin 4'-glucoside	HPTLC silica gel 60 F ₂₅₄	EtOAc:MeOH:AcOH:FA:H ₂ O (30:1:2:1:3 v/v/v/v/v)	NP; UV, 366 nm	<i>Colocasia esculenta</i> [58]
Luteolin 7-glucoside	HPTLC RP C ₁₈	FA:MeOH:H ₂ O (0.5:6.65:2.85 v/v/v)	ESI-MS/MS, 254, 366 nm	<i>Cyclanthera pedata</i> [59]
Luteolin 8-glucoside	HPTLC silica gel F ₂₅₄	To:EtOAc:FA (6:5:1 v/v/v)		

Abbreviations: Ace, acetone; AcOH, acetic acid; AlCl₃, aluminium trichloride; Al₂(SO₄)₃, aluminium sulfate; BuOH, butanol; CHCl₃, chloroform; DCM, dichloromethane; DI, 1,4-dioxane; DIPE, diisopropyl ether; ESI-MS/MS, electrospray ionization combined with tandem mass spectrometry; Et₂O, ethyl formate; EtOAc, ethyl acetate; Et, ether; FA, formic acid; Hx, hexane; MeOH, methanol; MEK, methyl ethyl ketone; nHx, n-hexane; NP, 1% methanolic diphenylboric acid-β-ethylamino ester - natural product reagents; neurotransmitters; PEG, 5% ethanolic polyethylene glycol 4000; THF, tetrahydrofuran; To, toluene; UV-VIS, ultraviolet-visible spectroscopy; ESI-MS, electrospray ionization combined with mass spectrometry.

The type and quality of the stationary phase greatly affect the separation of mixture components. Thus, the selection of an appropriate adsorbent is very important. However, most TLC analyses are carried out in a normal phase system where hydrophilic (polar) adsorbents are used [18,23,24]. Reversed phase systems with lipophilic (non-polar) stationary phases are common and have little significance in the analysis of flavonoids [20]. Currently, the most commonly used stationary phase for the analysis of flavonoids is silica gel [20]. However, the use polyamide coated chromatography plates, in both normal and reversed phase systems, is not uncommon [24].

Detection of flavonoids on TLC plates is most often conducted under ultraviolet (UV) light at wavelengths of 254 or 366 nm. Luteolin derivatives also display fluorescence, which can be enhanced using the appropriate derivatization reagents, e.g., with the so-called NP/PEG reagent. The most frequent procedure consists of spraying the plate with 1% methanolic diphenylboric acid- β -ethylamino ester (natural product reagents, NP), followed by 5% ethanolic polyethylene glycol 4000 (PEG) solution [20]. A densitometer may also be used for the qualitative analysis of the substance. The analysis is performed by comparing the retardation factor (Rf) and absorption spectrum of the test substance and the standard. Analytes can also be identified by extracting the separated substances from the plate. Then, the analysis is carried out using Fourier transform infrared mass spectrometry (MS), UV spectrometry, Raman spectrometry or other techniques [23]. Even though TLC separation of luteolin derivatives (Table 2) can be performed in different types of stationary phases such as a polyamide phase [26,28], it is most frequently performed on silica gel plates that are often coated with a fluorescent indicator [27,29] (F₂₅₄ plates) for preliminary detection. Such an approach has been used in case of analysis of luteolin 3'-O-glucoside, luteolin 6,8-C-dihexoside and luteolin 7-O-rutinoside in *Phlomis* sp. [27]. However, subsequent analysis with NP/PEG is the standard procedure for TLC analysis of luteolin [26–29], and it is almost always performed regardless of additional types of detection such as detection of flavonoids in *Ligustrum vulgare* with aniline phthalate [26]. Typically, the mobile phase for luteolin derivative separation consists of a mixture of aprotic organic solvents such as ethyl acetate (EtOAc) [26,28] or acetone (Ace) [29] and H₂O with a significant amount of formic (FA) and/or acetic acid (AcOH) to avoid tailing of the separated zones [26–29].

Thin layer chromatography is often used as a complementary method to other chromatographic techniques. For example, analysis of the butanol (BuOH) fraction of the methanol (MeOH) extract from the leaves of the common privet (*Ligustrum vulgare*) conducted by Mučaji et al. [26] allowed isolation of two luteolin derivatives from the plant. TLC was carried out, among other techniques, on polyamide plates, and the optimal mobile phase was found. TLC was used for analysis of individual fractions obtained in column chromatography with or without acid hydrolysis of compounds. MS detection and nuclear magnetic resonance (NMR) spectra were also used [26]. Furthermore, TLC was used together with high performance liquid chromatography combined with mass spectrometry and pulsed amperometric detection (HPLC-PAD-MS) for analysis of luteolin and other phenolic compounds in *Leontopodium alpinum*. In addition to NP/PEG, UV, infrared (IR) and NMR analyses were used for identification of these compounds [29].

Compared to other chromatographic techniques, HPTLC results in reduced time and costs of analysis and provides much greater efficiency of separation. It is suitable even for the analysis of crude extracts similar to TLC, and a relatively small amount of solvent is used to analyze several samples, making this method environmentally friendly [60]. In the analysis of luteolin derivatives (Table 3), HPTLC silica gel 60 is almost exclusively used as the stationary phase [45,47,49,51], while HPTLC NH₂ plates are rarely used, e.g., for separation of flavonoids in some Lamiaceae species such as *Mentha piperita* [53] and *Thymus* sp. [55]. In addition to NP/PEG (e.g., [52,57]), other detection systems may be employed for visualization of luteolin derivatives, such as bis-diazotized sulfanilamide [53] or aqueous solutions of Al³⁺ ions for flavonoids in *M. piperita* [53], honey [49] or *Thymus* sp. [55]. Similar to TLC, mixtures of organic solvents, H₂O, and FA are most often used as the mobile phase [44,45,47–49,51,52].

High performance thin layer chromatography may also be used as a complimentary method to other chromatographic techniques. Chelyn et al. [44] used the HPTLC technique in the analysis of the

ethanol (EtOH) extract of *Clinacanthus nutans* leaves. The analysis revealed the presence of, among others, luteolin 8-C-glucoside (orientin) and luteolin 6-C-glucoside (isoorientin) in the raw material. Their detection was conducted by comparing R_f coefficients using derivatization reagents and 366 nm UV light. In this work, the characteristic fluorescent bands after derivatization provided important clues for the identification of the major flavone present in the samples, while high performance liquid chromatography combined with ultraviolet spectrometry or a diode array detector (HPLC-UV/DAD) technique was employed for the simultaneous detection and quantification of these compounds [44].

2.2. High Performance Liquid Chromatography in the Analysis of Luteolin Derivatives

Among the many chromatographic methods, adsorptive chromatography, in which the mobile phase is liquid and the stationary phase is solid, is of the greatest practical importance. For example, this method has a much wider application than GC because it allows the analysis of substances in the form of liquids and soluble solids. Furthermore, it is also suitable for analysis of thermolabile substances because it is usually performed at low temperatures, and such samples are not degraded [61]. Due to the long analysis time, high mobile phase consumption and low efficiency, traditional CC is currently used mainly for preparative purposes. However, improved methods, such as HPLC and especially liquid chromatography combined with mass spectrometry (LC-MS), are increasingly used for analysis of natural compounds including luteolin derivatives [62].

High performance liquid chromatography has been performed since 1960. It is a dynamically developing method with a wide range of uses and has been proven to be very useful in phytochemical analysis. The principle of operation consists of pumping the mobile phase from the tank (or tanks) through the stationary phase-filled column. Eluents are previously filtered and degassed. Some systems are additionally equipped with thermostats that regulate the temperature of the column. If the chromatographic system is properly selected and applied, then the individual components are separated and detected. Strengthened signals are transmitted to the computer, where the obtained data are registered and properly processed [19]. The separation is based on competition of the molecules of the eluent and the substance being analyzed for the space on the adsorbent surface in the column [63,64].

When choosing a column, one should be guided by the size of the sample, time of analysis and expected effect of the separation. Although columns with different diameters are available, those with a diameter of 4.6 mm are by far the most common. However, due to better detection of the components separated in smaller diameter columns, these columns are increasingly being used for separation and analysis [19,63,65]. In addition, improved separation can be achieved using a column filled with smaller particles. In addition to 5 μm particles, which are most common, particles of 3 μm in diameter or even smaller can be used. For example (Table 4), this approach was chosen when separating luteolin 2''-O-feruloylhexosyl-6-C-hexoside and luteolin 6-C-glucoside from *Arenaria montana* [66,67] and isoorientin in *Achillea millefolium* [68,69], as well as separating luteolin 6-C-hexosyl-8-C-pentoside, luteolin 2''-O-deoxyhexosyl-6-C-glucoside and luteolin 6-C-glucoside in *Cymbopogon citratus* [70,71]. Particles less than 2 μm in diameter were used for ultra-performance liquid chromatography (UPLC) analysis of luteolin derivatives and other flavonoids in *Lactuca sativa* [72,73] and date palm (*Phoenix dactylifera*) [74].

Stationary phases with different polarity may be used in HPLC. In the normal phase system, polar column fillings are used, and most often the filling is silica gel. However, silica gel can adsorb water, which leads to the loss of the original separating properties of the column and thus to impaired reproducibility of the obtained results [19,65]. Therefore, the gel is often modified with the aim of enabling better separation of mixture components. This is performed mainly by bonding alkyl chains (or alkyl chains bearing other functional groups) to functional groups on the gel surface. Silica gels optimized in this way are referred to as the associated phase [2,65]. In the so-called reversed phase (RP) system, non-polar associated phases are used. Such systems are especially useful in the analysis of insoluble or poorly water-soluble compounds, as well as in the analysis of polar compounds, provided that a mobile phase with high water content is used. Typically, an octadecylsilane (ODS) phase, composed of 18 carbon atoms (RP-18), is employed. Such fillers can have different properties

depending on the silica gel type and/or production method [19,65]. According to the available literature, the analysis of luteolin derivatives (Table 4) was performed exclusively with RP systems, and the RP-18 system was the most frequently used system, as exemplified in the separation of six luteolin derivatives in *Securigera securidaca* [75] or as many as ten derivatives in *Capsicum annuum* [76]. Stationary phases composed of 8 carbon atoms (RP-8) were rarely used. Examples include the separation of flavonoids in *Coriandrum sativum* [77] and *Achillea millefolium* [68,69].

The selection of an appropriate mobile phase is extremely important for chromatographic separation. The type of analyte, mixture composition, stationary phase and detector used should be taken into account. Mixtures of up to three components are most commonly used. In the reverse system, mixtures of MeOH/H₂O or acetonitrile (ACN)/H₂O are routinely used. As the amount of organic solvent increases, the retention time for non-polar substances decreases, while the addition of H₂O extends their retention times. As a rule of thumb, systems containing ACN/H₂O eluents are more efficient than those containing MeOH/H₂O [19]. In the normal phase system, however, the base solvent is a non-polar eluent, and its polarity is appropriately modified by the addition of another solvent of higher polarity, e.g., chloroform (CHCl₃) [65]. According to the available literature, virtually all mobile phases used for analysis of luteolin derivatives consisted either of ACN/H₂O, e.g., [26,66,67,78] or, less often, MeOH/H₂O mixtures [72,79–81]. Additionally, a modifier such as FA, e.g., [79,82–84], AcOH, e.g., [44,78,85–87], or trifluoroacetic acid (TFA) [88] was added to avoid peak tailing [89]. Analyses performed without acidic modifiers are rare [90].

In the chromatography process, the elution can be carried out in two ways. The first method is isocratic elution, which involves running with the same composition of mobile phase during the analysis. This means that a constant elution force is maintained throughout the entire separation period. In this case, even a slight change in the composition of the mobile phase may affect the results of the analysis. Isocratic elution is only rarely used for analysis of flavonoids. In the case of luteolin derivatives, this method was used only for analysis of luteolin 7-rhamnosyl- (1-6)-galactoside in *Filago germanica* [91], luteolin 7-rhamnosyl(1-6)galactoside in *Galactites elegans* [90], and various luteolin derivatives in *Apium graveolens* [80]. If the composition of the eluent changes during the division of the mixture, then the gradient elution can be described. The gradient can be linear or specifically programmed. With a change in the composition of the eluent, its elution force increases. For this reason, this method is used particularly for the separation of mixtures composed of substances of different polarity [2,64]. The vast majority of papers describing the separation of luteolin derivatives in plant mixtures use a gradient approach. Examples include the separation of luteolin 8-C-glucoside, luteolin 6-C-glucoside, luteolin 4'-O-glucoside and luteolin 7-O-glucoside from *Chrysanthemum trifurcatum* [92], thirteen luteolin derivatives from *Cymbopogon citratus* [70,71] and many others.

By far, the most common method for detection of luteolin derivatives is using diode array detectors (DADs) (also called photodiode array detectors, PDA), which were used in as many as 46 instances (e.g., for the analysis of luteolin derivatives and other flavonoids in *Cymbopogon citratus* [79], *Dianthus versicolor* [88], *Clinacanthus nutans* [44], *Thymus alternans* and others [93]). More often than not, however, DADs were combined with other detectors for additional structure determination or confirmation, with or without prior isolation. Examples of DADs combined with other detection methods for analysis of luteolin derivatives in plants include the use of tandem mass spectrometry (MS/MS) and NMR for *Ligustrum vulgare* [26], diode array detectors combined with electrospray ionization and mass spectrometry (DAD-ESI-MS) for *Phoenix dactylifera* [94] and *Nerium indicum* [95], electrospray ionization combined with tandem mass spectrometry (ESI-MS/MS) for *Achillea moschata* [96], electrospray ionization combined with time of flight mass spectrometry (ESI-TOF-MS) and electrospray ionization combined with ion trap and tandem mass spectrometry (ESI-IT-MS/MS) for *Aloysia citrodora* and many others.

Table 4. High performance liquid chromatography/ultra performance liquid chromatography in the analysis of luteolin derivatives.

Luteolin derivative	Stationary phase/column	Mobile phase	Conditions	Detection	Analyzed species	Ref.
	ODS	0.2% PA:H ₂ O (A), MeOH (B)	injection volume: 20 µL; flow rate: 1.0 mL/min	DAD, 360 nm	Honey	[97]
	ODS C ₁₈	0.2% PA:H ₂ O (58:41 v/v)	injection volume: 50 µL; flow rate: 1.0 mL/min	UV, 350 nm	<i>Chrysanthemum morifolium</i>	[98]
	Kinetex C ₁₈	ACN (A), 0.05% TFA:H ₂ O (B)	flow rate: 0.8 mL/min	UV, 254 nm	<i>Enhalus acroroides</i>	[99]
	ODS Hypersil C ₁₈	MeOH:ACN (1.25:1 v/v) (A), 0.5% AcOH:H ₂ O (B)	flow rate: 0.8 mL/min	MS	<i>Perilla frutescens</i>	[100]
	Zorbax SB-C ₁₈	PA:H ₂ O pH 4.0 (A), ACN (B)	injection volume: 50 µL; flow rate: 0.6 mL/min; 25 °C	DAD, 330 nm	<i>Vernonia condensata</i>	[101]
Luteolin	ODS C ₁₈	MeOH (A), 0.05% TFA:H ₂ O (B)	injection volume: 20 µL; flow rate: 1.0 mL/min	UV, 280 nm	<i>Corchorus olitorius</i>	[102]
	RP	0.5% PA:H ₂ O (A), ACN (B)	injection volume: 20 µL; flow rate: 0.8 mL/min; at 35 °C	Triple-TOF-MS	<i>Veronicastrum latifolium</i>	[103]
	RP C ₁₈	1% FA:H ₂ O (A), 40% solvent A:ACN (B)	flow rate: 0.5 mL/min; 25 °C	DAD-ESI-MS/MS	<i>Olea europaea</i> , olive oil	[104]
	Discovery HS C ₁₈	2% AcOH (A), ACN (B)	injection volume: 20 µL; flow rate: 0.8 mL/min	DAD	<i>Agastache foeniculum</i>	[105]
	Ultrasphere 5 C ₁₈	H ₂ O (A), ACN (B)	injection volume: 10 µL; flow rate: 1 mL/min; 25 °C	ESI-MS; 350 nm	<i>Rosa rugosa</i>	[106]
Luteolin 6-glucoside	Vydac RP C ₁₈	0.05% TFA:H ₂ O (A), 0.038% TFA:ACN (v/v) (B)	injection volume: 10 µL flow rate: 1 mL/min; 36 °C	UV, 342 nm	<i>Ficaria verna</i>	[107]
Luteolin 8-glucoside	RP C ₁₈	0.5% FA:H ₂ O (A), ACN (B)	injection volume: 20 µL; flow rate: 0.5 mL/min; 23 °C	DAD, 254, 340 nm	<i>Jatropha gossypifolia</i> , <i>J. mollissima</i>	[108]
	Hypersil gold C ₁₈	0.1% FA:H ₂ O (A), 0.1% FA:MeOH (B)	injection volume: 10 µL; flow rate: 0.35 mL/min; 38 °C	MS	<i>Rhodo discolor</i>	[109]
Luteolin 7-glucoside	Thermo C ₁₈	0.3% FA:H ₂ O (A), ACN (B)	injection volume: 10 µL; flow rate: 1.0 mL/min; 30 °C	DAD-Q-Orbitrap-MS	<i>Epimedium brevicornum</i> , <i>Anacyclus pyrethrum</i> , <i>Lycium barbarum</i> , <i>Cuscuta australis</i>	[110]

Table 4. Contd.

Luteolin	Eclipse XDB C ₁₈	0.025% AcOH:H ₂ O (A), 5% Ace:ACN (B)	30 °C	ESI-MS/MS	<i>Olea europaea</i> , olive oil	[111]
Luteolin 7-glucoside	Eclipse XDB C ₁₈	1% FA:H ₂ O (A), ACN (B)	injection volume: 10 µL; flow rate: 1 mL/min; 25 °C	DAD-ESI- QTOF-MS/MS	<i>Verbascum ovatifolium</i>	[112]
Luteolin 7-rutinoside	Eclipse XDB C ₁₈	ACN (A), 0.2% FA (B)	flow rate: 0.3 mL/min; 30 °C	DAD, 230, 254, 290, 334 nm; MS/MS; NMR	<i>Ligustrum vulgare</i>	[26]
Luteolin						
Luteolin 7-4-diglucoside						
Luteolin 7-rutinoside	Gemini C ₁₈	0.5% AcOH:H ₂ O (A), ACN (B)	25 °C	ESI-QTOF-MS	<i>Olea europaea</i>	[78]
Luteolin 4-glucoside						
Luteolin 3-glucoside						
Luteolin 7-glucoside						
Luteolin 6-glucoside						
Luteolin 7-rhamnoside	Spherisorb S5 ODS-2	5% FA:H ₂ O (A), MeOH (B)	flow rate: 1 mL/min	DAD, 280 nm	<i>Cymbopogon citratus</i>	[79]
Luteolin 6-glucosyl-8-arabinoside						
Luteolin 2'-feruloylhexosyl-6-hexoside	Spherisorb S3 ODS-2 C ₁₈	0.1% FA:H ₂ O (A), ACN (B)	flow rate: 0.5 mL/min; 35 °C	DAD-MS; 280, 370 nm	<i>Arenaria montana</i>	[66,67]
Luteolin 6-glucoside						
Luteolin						
Luteolin 7-rutinoside	Kinetex 100 C ₁₈	1% FA:H ₂ O (A), 1% FA:ACN (B)	flow rate: 1 mL/min; 30 °C	ESI-QTOF-MS;	<i>Rosmarinus officinalis</i>	[82]
Luteolin 3-glucuronide	Superschera 100 RP C ₁₈			DAD, 324 nm		
Luteolin 3-(2'-acetyl)-glucuronide						
Luteolin 6-hydroxy-7-glucoside						
Luteolin hexosyl-hexoside-malylester						
Luteolin 6-glucosyl-7-galactoside						
Luteolin 6-glucosyl-7-rutinoside	AquasilW C ₁₈	TFA solution (pH 2.8) (A), ACN (B)	flow rate: 1.0 mL/min; 15 °C	UV/DAD, 340 nm	<i>Dianthus versicolor</i>	[88]
Luteolin 6-glucosyl-7-rhamnosyl-galactoside						
Luteolin 7-apiofuranosyl (1→2)-glucopyranoside						
Luteolin 7-glucopyranoside	Eclipse Plus C ₁₈	0.1% FA:MeOH (A), 0.1% FA:H ₂ O (B)	injection volume: 10 µL; isocratic mixture flow rate: 0.3 mL/min	QTOF-MS/MS	<i>Apium graveolens</i>	[80]
Luteolin 7-[apiofuranosyl (1→2)-(6'-malonyl)]-glucopyranoside						

Table 4. Contd.

	Kinetex PFP	0.8% AcOH:H ₂ O (A), ACN (B)	injection volume: 10 µL; flow rate: 0.7 mL/min; 40 °C	UV/DAD, 330 nm	<i>Clinacanthus nutans</i>	[44]
Luteolin 8-glucoside						
Luteolin						
Luteolin 7-glucoside						
Luteolin 7-glucuronyl-3-glucoside						
Luteolin 6-glucoside	Eclipse XDB C ₁₈	MeOH (A), 0.2% FA:H ₂ O (B)	flow rate: 0.8 mL/min; 30 °C	DAD-MS/MS; UV; 254, 360 nm	<i>Securigera securidaca</i>	[75]
Luteolin 6-glucosyl-2''-rhamnoside						
Luteolin 6-glucosyl-4'-glucoside						
Luteolin 3'-glucoside						
Luteolin hexosyl-rhamnoside						
Luteolin 7-rutinoside	Spherisorb S3 ODS-2 C ₈	0.1% FA:H ₂ O (A), ACN (B)	flow rate: 0.5 mL/min; 35 °C	DAD-MS; 280, 370 nm	<i>Coriandrum sativum</i>	[77]
Luteolin 7-glucoside						
Luteolin						
Luteolin 6-glucosyl-8-arabinoside	XDB C ₁₈	1% FA:H ₂ O (A), ACN (B)	injection volume: 100 µL; flow rate: 4 mL/min	NMR; MS	<i>Casimiroa edulis</i>	[116,117]
Luteolin 7-glucoside						
Luteolin 6-arabinosyl-8-glucoside						
Luteolin 3-glucopyranoside						
Luteolin 7-glucofuranoside	PLRP-S 100Å	0.1% FA:H ₂ O (A), ACN (B)	injection volume: 100 µL; flow rate: 1.5 mL/min	MS	<i>Thymus alternans</i>	[93]
Luteolin 7-rutinoside						
Luteolin methoxy-hexoside						
Luteolin 4'-glucopyranoside	XDB C ₁₈	1% FA:H ₂ O (A), ACN (B),	injection volume: 100 µL; flow rate: 4 mL/min			
Luteolin 6-hydroxy-7-glucoside	Gemini C ₁₈	0.1% FA:H ₂ O (A), ACN (B)	flow rate: 0.8 mL/min	UV-VIS, 200-400 nm; MS; DAD; NMR		
Luteolin						
Luteolin 7-rhamnoside	Synchronis C ₁₈	0.1% AcOH:H ₂ O (A), ACN (B)	injection volume: 5 µL; flow rate: 0.3 mL/min	DAD-MS/MS	Honey	[86]
Luteolin						
Luteolin rhamnosyl hexoside	HSS T3	0.1% FA:H ₂ O (A), 0.1% FA:ACN (B)	injection volume: 3.1 µL; flow rate: 0.15 mL/min	PDA-MS	<i>Phoenix dactylifera</i>	[74]
Luteolin rhamnosyl dihexoside						
Luteolin diglucuronide						
Luteolin 7-glucuronide	S3 ODS-2 C ₁₈	0.1% FA:H ₂ O (A), ACN (B)	flow rate: 0.5 mL/min; 35 °C	DAD-ESI-MS; 370, 330 and 280 nm	<i>Thymus pallescens</i> , <i>Saccocalyx</i> <i>satureioides</i> ,	[119,120]
Luteolin 7-rutinoside						

Table 4. Contd.

Luteolin 7-glucoside					<i>Pythothis verticillata</i>
Luteolin 6-glucoside					<i>Coleostephus myconis</i>
Luteolin					
Luteolin rutinoside				injection volume: 10 µL; flow rate: 0.4 mL/min	<i>Lathyrus pratensis</i>
Luteolin hexoside		ACN (A), 0.1% FA:H ₂ O (B)	Kimetex C ₁₈		
Luteolin 6-hexoside					[121]
Luteolin 7-glucoside		5% FA:H ₂ O (A), MeOH (B)	Luna C ₁₈	injection volume: 100 µL; flow rate: 1 mL/min; 35 °C	<i>L. aureus</i>
Luteolin hexuronide		0.1% FA:H ₂ O (A), MeOH (B)		injection volume: 10 µL; flow rate: 0.5 mL/min; 40 °C	<i>Thymus pulegioides</i>
Luteolin					
Luteolin hexosyl-pentoside			Eclipse Plus C ₁₈	injection volume: 5 µL; flow rate: 0.5 mL/min	<i>Ficus carica</i>
Luteolin 6-glucoside		0.5% AcOH:H ₂ O (A), ACN (B)			[87]
Luteolin 8-glucoside					
Luteolin 7-glucoside					
Luteolin (3-hydroxy-3-methylglutaryl)-X''-deoxyhexosyl-hexoside			ODS-2 C ₁₈ with ODS-2 C ₁₈ guard cartridge	flow rate: 0.2 mL/min; 25 °C	<i>Urtica membranacea</i>
Luteolin 6-hexoside		1% FA:H ₂ O (A), MeOH (B)			[122]
Luteolin 6-rutinoside					
Luteolin dihexoside					
Luteolin					
Luteolin 6,8-dihexoside					
Luteolin 6-hexosyl-8-pentoside					
Luteolin 6-pentosyl-8-hexoside					
Luteolin 6-hexoside					
Luteolin 8-hexoside					
Luteolin 7-(2''-pentosyl-4''-hexosyl)hexoside					
Luteolin 7-(2''-pentosyl)hexoside		0.01% AcOH:H ₂ O (A), ACN (B)	Synchronis C ₁₈	injection volume: 5 µL; flow rate: 0.25 mL/min	<i>Capsicum annuum</i>
Luteolin 7-glucoside					[76]
Luteolin 7-[2''-(5'''-sinapoyl)pentosyl]hexoside					
Luteolin 7-(2''-pentosyl-4''-hexosyl-6''-malonyl)hexoside					

Table 4. Cont.

Luteolin 7-(2''-pentosyl)-6''-malonyl)hexoside	Purospher star C ₁₈	10% FA:H ₂ O (A), ACN (B)	25 °C	DAD-ESI-MS; 320-280 nm	<i>Citrus aurantifolia</i>	[123]
Luteolin 7-[2''-(5''-sinapoyl)pentosyl-6''-malonyl]hexoside	Zorbax SB-C ₁₈	AFNH ₄ :H ₂ O:ACN:FA (A), AFNH ₄ :H ₂ O:ACN:FA (B)	injection volume: 5 µL; flow rate: 1.0 mL/min	ESI-MS; 325 nm	<i>Caucalis platycarpus</i>	[124]
Luteolin	Beta-Basic C ₁₈	5% FA:ACN (A); 5% FA:H ₂ O (B)	injection volume: 20 µL; flow rate: 0.9 mL/min	UV, 280 nm	<i>Melissa officinalis</i> <i>Mentha piperita</i> , <i>Salvia officinalis</i>	[54]
Luteolin 6,8-diglucoside	UPLC BEH C ₁₈ and a Acquity	0.1% AcOH:H ₂ O (A), 0.1% AcOH:MeOH (B)	injection volume: 5 µL; flow rate: 0.5 mL/min	DAD-ESI- QTOF-MS; 370 nm	<i>Lactuca sativa</i>	[72]
Luteolin 8-glucoside	UPLC BEH C ₁₈ VanGuardTM pre-column					
Luteolin 7-glucoside	HSS T3	0.1% FA:H ₂ O (A), 0.1% FA:ACN (B)	injection volume: 3 µL; flow rate: 0.4 mL/min	IMS-QTOF-MS		[73]
Luteolin 7-glucuronide						
Luteolin 7-rutinoside						
Luteolin diglucoside						
Luteolin hexoside						
Luteolin hydroxy-glucuronide	Hypersil Gold C ₁₈	0.1% FA:H ₂ O (A), ACN (B)	flow rate: 0.2 mL/min	DAD-ESI-MS	<i>Salvia elegans</i> , <i>S. greggii</i> , <i>S. officinalis</i>	[125,126]
Luteolin 7-glucoside					<i>Thymus baronae</i> , <i>T. pseudolanuginosus</i> , <i>T. caespitosus</i>	
Luteolin 7-glucuronide						
Luteolin malonyl-hexoside						
Luteolin glucuronide						
Luteolin glucoside						
Luteolin rutinoside						
Luteolin 7-rhamnopyl-(1-6)galactoside	Eclipse XDB-C ₁₈	0.1% FA:H ₂ O (A), 0.1% FA:ACN (B)	flow rate: 0.5 mL/min; 25 °C	MS	<i>Filago germanica</i>	[91]

Table 4. Cont.

	C ₁₈ /t-Bondapak RP ₁₈	MeOH:H ₂ O (42:58 v/v)	flow rate: 2.0 mL/min	NMR	<i>Galactites elegans</i>	[90]
Luteolin 4'-glucuronide						
Luteolin						
Luteolin 3'-7-diglucoside			injection volume: 5 µL;	DAD, 340 nm		
Luteolin 7-glucoside			flow rate: 0.8 mL/min;	DAD-ESI-	<i>Allophylus africanus</i>	[83,127]
Luteolin 6-(2-rhamnosyl)-hexoside	Kinetex 100 A C ₁₈	1% FA:H ₂ O (A), ACN (B)	25 °C	MS/MS;		
Luteolin (pentosyl)-hexoside				280, 340 nm		
Luteolin hexoside						
Luteolin 6-glucoside	ODS2 C ₈	0.1% FA:H ₂ O (A), ACN (B)	flow rate: 0.5 mL/min;	DAD-ESI-MS;	<i>Achillea millefolium</i>	[68,69]
			35 °C	280, 370 nm		
Luteolin 6-hexosyl-8-pentoside						
Luteolin 2'-deoxyhexosyl-6-glucoside						
Luteolin 6-glucoside						
Luteolin 6-pentosyl-8-pentoside						
Luteolin-7-rhamnoside						
Luteolin 7-glucoside						
Luteolin 2''-deoxyhexosyl-pentoside	S3 ODS-2 C ₁₈	0.1% FA:H ₂ O (A), ACN (B)	flow rate: 0.5 mL/min;	DAD-MS;	<i>Cymbopogon citratus</i>	[70,71]
			35 °C	280, 370 nm		
Luteolin 6-pentoside						
Luteolin 2'-deoxyosyl-6-(6-deoxy-pento-hexosuloside						
Luteolin						
Luteolin 8-glucoside						
Luteolin 4'-glucoside	C ₁₈	0.005 % FA:H ₂ O (A), MeOH (B)	injection volume: 10 µL;	MS-Orbitrap	<i>Chrysanthemum trifurcatum</i>	[92]
Luteolin 7-glucoside			flow rate: 0.5 mL/min;			
Luteolin 6-glucoside			30 °C			
Luteolin 6-glucoside						
Luteolin 8-glucoside						
Luteolin 6-deoxyhexosyl-8-pentoside	HSS T3	0.1% FA:H ₂ O (A), 0.1% FA:ACN (B)	injection volume: 3.1 µL;	PDA-MS	<i>Passiflora edulis</i>	[128]
Luteolin 6-fucoside			flow rate: 0.15 mL/min			
Luteolin 8-deoxyhexoside						
Luteolin 6,8-diglucoside						
Luteolin 6,8-diglucoside						
Luteolin 8-glucosyl-7-glucoside isomer	Kinetex C ₁₈	0.05% FA:H ₂ O (A), 0.05% FA:ACN (B)	flow rate: 0.4 mL/min;	MS/MS	<i>Eragrostis tef</i>	[84]
Luteolin 6-glucosyl-7-glucoside isomer			40 °C			

Table 4. Cont.

Luteolin 8-glucosyl-7-rhamnoside	Nucleosil 100-3.5 C ₁₈	FA:H ₂ O (A), FA:ACN (B)	injection volume: 20 µL	MS	<i>Arum hygrophilum</i>	[129]
Luteolin 8-glucoside						
Luteolin 7-glucoside						
Luteolin 7-rhamnoside						
Luteolin 7-(6'-syringyl)glucosyl-6-glucoside	Eclipse Plus C ₁₈	0.2% FA:H ₂ O (A), 0.2% FA:ACN (B)	30 °C	PDA-ESI-MS/MS UV, 350 nm	<i>Triticum aestivum</i>	[130]
Luteolin 7-(2''-syringyl)arabinosyl-6-glucoside						
Luteolin 8-(6'-diacetyl)glucoside						
Luteolin						
Luteolin 6-glucoside						
Luteolin 6-[6'-glocosyl-caffeoyl]-glucopyranosyl(→2)-glucopyranoside						
Luteolin 6-glucopyranoside						
Luteolin 7-glucoside						
Luteolin 6-glucoside	Synchronis C ₁₈	0.1% FA:H ₂ O (A), ACN (B)	injection volume: 5 µL; flow rate: 0.25 mL/min	MS/MS	<i>Iris punctata</i> , <i>I. variegata</i> , <i>I. humilis</i>	[131]
Luteolin 7-(2''-p-coumaroyl)-rhamnoside						
Luteolin	Luna Omega Polar C ₁₈ with Polar C ₁₈ Security Guard cartridge	0.1% FA:H ₂ O (A), ACN (B)	flow rate: 0.4 mL/min	ESI-MS/MS; 320, 350 nm	<i>Parentucellia latifolia</i>	[132,133]
Luteolin hexoside						
Luteolin						
Luteolin glucoside						
Luteolin glucuronide	Intersil ODS	ACN:H ₂ O:FA (10:89:1 v/v/v) (A), ACN:H ₂ O:FA (89:10:1 v/v/v) (B)	injection volume: 10 µL; flow rate: 0.5 mL/min; 40 °C	DAD-MS/MS; 360 nm	<i>Verbascum eskischirensis</i>	[134]
Luteolin pentosyl-glucoside						
Luteolin 4'-glucoside	Kinetex RP C ₁₈	PA:H ₂ O pH 3 (A), PA:ACN pH 3 (B)	injection volume: 1 µL; flow rate: 1.2 mL/min; 35 °C	UV	<i>Matricaria recutita</i>	[135]
Luteolin 7-O-glucuronide	C ₁₈	0.02% TFA:H ₂ O (A), MeOH:ACN (3:7 v/v) (B)	injection volume: 2.5 µL; flow rate: 0.9 mL/min; 45 °C	DAD-ESI-MS 240, 254, 325 nm	<i>Lippia alba</i>	[136]
Luteolin glucoside						
Luteolin 7-O-β-glucoside						
Luteolin glucuronide	YMC-Triart C ₁₈	0.1% FA:H ₂ O (A), 0.1% FA:ACN (B)	injection volume: 10 µL; flow rate: 0.8 mL/min	DAD-ESI-MS 265, 280, 330, and 360 nm	<i>Chrysanthemum morifolium</i>	[137]
Luteolin malonylglucoside						
Luteolin						

Table 4. Cont.

Luteolin 7-diglucuronide	Eclipse XDB C ₁₈	0.03% PA:H ₂ O (A), solvent A:ACN (1:9 v/v) (B)	injection volume: 20 µL; flow rate: 0.8 mL/min; 25 °C	DAD, 210, 250, 320, 350 and 370 nm	<i>Thymus pannonicus</i>	[138]
Luteolin 7-O-glucuronide						

Abbreviations: Ace, acetone; AcOH, acetic acid; ACN, acetonitrile; AFNH₄, ammonium formate; BuOH, butanol; DAD, diode array detector; DAD-ESI-MS, diode array detector combined with electrospray ionization and mass spectrometry; DAD-ESI-QTOF-MS, diode array detector combined with electrospray ionization and tandem mass spectrometry; DAD-ESI-QTOF-MS, diode array detector combined with mass spectrometry; DAD-MS/MS, diode array detector combined with tandem mass spectrometry; DAD-QTOF-MS, diode array detector combined with quadrupole – time of flight mass spectrometry; ESI-IT-MS/MS, electrospray ionization combined with ion trap and tandem mass spectrometry; ESI-MS, electrospray ionization combined with mass spectrometry; ESI-MS/MS, electrospray ionization combined with tandem mass spectrometry; ESI-QTOF-MS, electrospray ionization combined with quadrupole – time of flight mass spectrometry; FA, formic acid; IMS-QTOF-MS, ion-mobility spectrometry combined with quadrupole – time of flight mass spectrometry; MeOH, methanol; MS/MS, tandem mass spectrometry; PA, phosphoric acid; PAD, pulsed amperometric detection; PDA-ESI-MS/MS, pulsed amperometric detection combined with electrospray ionization and tandem mass spectrometry; PDA-ESI-MS, pulsed amperometric detection combined with electrospray ionization and mass spectrometry; PDA-MS, pulsed amperometric detection combined with mass spectrometry; TFA, trifluoroacetic acid; UV/PAD-MS, UV/pulsed amperometric detection combined with mass spectrometry.

For example, the HPLC-PAD-MS technique was used in the analysis of aerial flowering parts of the Edelweiss alpine region (*Leontopodium alpinum*). This method allowed the basic separation of almost all components of the *L. alpinum* extract prepared by exhaustive dichloromethane (DCM) followed by MeOH extraction. In total, 14 compounds have been isolated from the extract, including several luteolin derivatives. The authors used a gradient as the mobile phase as follows: H₂O:0.9% FA:0.1% AcOH:1.5% BuOH (A) and ACN:30% MeOH:0.9% FA:0.1% AcOH (B) and MeOH (C). The structure of the isolated components was additionally confirmed using NMR spectroscopy [29].

2.3. Liquid Chromatography in the Analysis of Luteolin Derivatives

LC combined with tandem mass spectrometry (LC-MS/MS) (Table 5) is especially useful in the analysis of multicomponent mixtures, such as herbal extracts because it does not require a large amount of the sample or previous separation. To further reduce the influence of other factors on the analysis, more advanced techniques, involving the combination of more than one detection method, e.g., LC combined with NMR and MS (LC-NMR-MS), are increasingly used [139].

Research on ethanol extract from *Lophatherum gracile* stems and leaves was performed using LC coupled with MS/MS. Gradient elution was performed using 0.3% FA and MeOH. Analysis of the species revealed the presence of, among others, luteolin 7-O- β -D-glucoside, and luteolin 6-C-glucoside [140].

Another raw material containing luteolin and its derivatives is the cocoa seed (*Theobroma cacao*). In the analysis of the H₂O:MeOH extract, the following mobile phase was used: H₂O:0.1% FA and ACN:0.1% FA. The elution was carried out in a linear gradient, whereas LC combined with electrospray ionization and tandem mass spectrometry (LC-ESI-MS/MS) coupling allowed the identification of the tested compounds [141].

Lin and Harnly performed a water-methanol analysis of the flower extract of *Chrysanthemum morifolium* and distinguished many compounds, including numerous derivatives of luteolin. In this case, the mobile phase was a mixture of 0.1% FA:H₂O and 0.1% FA:ACN, in varying proportions. The qualitative determination of the analyzed substances was based on a comparison of retention times as well as mass and UV/Vis spectra [142].

Table 5. Liquid chromatography in the analysis of luteolin derivatives.

Luteolin derivative	Stationary phase	Mobile phase	Conditions	Detection	Analyzed species	Ref.
Luteolin	Zorbax SB C ₁₈ column with Security-Guard C ₁₈	MeOH (A), 0.5% AcOH:H ₂ O (B)	flow rate: 1.0 mL/min; injection volume: 20 µL	MS/MS	<i>Abri herba</i> , <i>A. mollis</i>	[143]
	Inertsil ODS-3	0.1% FA:H ₂ O (A), ACN (B)	flow rate: 0.5 mL/min; injection volume: 10 µL	MS/MS	<i>Castanea mollissima</i>	[144]
Luteolin 7-glucoside	RP C ₁₈	0.1% FA:H ₂ O (A), 0.1% FA:ACN (B)	injection volume: 5 µL; flow rate: 0.3 mL/min; 40 °C	ESI-MS/MS	<i>Centaurea cyanus</i>	[145]
	Eclipse XDB C ₁₈	1% FA:H ₂ O (A), MeOH (B)	injection volume: 5 mL; flow rate: 0.6 mL/min; 45 °C	MS/MS	<i>Plantago atrata</i> , <i>P. coronopus</i> , <i>P. holosteam</i> , <i>P. lanceolata</i> , <i>P. reniformis</i> , <i>P. schtaarzenbergiana</i>	[146]
Luteolin	Zorbax Plus C ₁₈	0.1% FA:H ₂ O (A), 0.1% FA:ACN (B)	injection volume: 1 µL; flow rate: 0.4 mL/min	MS	<i>Matricaria recutita</i> , <i>Achillea millefolium</i> , <i>Thymus vulgaris</i> , <i>Salvia officinalis</i>	[30]
Luteolin 7-apiosyl-glucoside	Eclipse XDB C ₁₈	0.05% FA:H ₂ O (A), MeOH (B)	flow rate: 1 mL/min	MS/MS	<i>Vitis vinifera</i>	[147]
Luteolin 7-glucoside				DAD-ESI-MS; DAD, 350, 310,		
Luteolin 7-malonyl-aptiosyl-glucoside	Symmetry C ₁₈	0.1% FA:H ₂ O (A), 0.1% FA:ACN (B)	flow rate: 1.0 mL/min; 25 °C	270 nm; UV, 190-650 nm	<i>Apium graveolens</i>	[148]
Luteolin 7-6'-malonyl-aptiosyl-glucoside						
Luteolin 3'-glucoside	Zorbax SB C ₁₈	0.1% FA:H ₂ O (A); 0.1% FA:ACN (B)	injection volume: 5 µL; flow rate: 0.3 mL/min; 25 °C	MS/MS; TQMS; ESI	<i>Phlomis persica</i>	[27]
Luteolin 6-glucoside						
Luteolin 6,8-dihexoside	XTerra MS C ₁₈	ACN (A), 0.05% AcOH:H ₂ O (B)	injection volume: 20 µL; flow rate: 1.0 mL/min	PDA-MS; NMR	<i>Ph. elliptica</i>	[149]
Luteolin 7-rutinoside						
Luteolin 7-glucopyranoside	Octadecyl silica gel ODS	H ₂ O:MeOH:FA (89:10:1 v/v/v) (A), MeOH:H ₂ O:FA (89:10:1 v/v/v) (B)	flow rate: 1 mL/min; 40 °C	MS/MS	<i>Nepeta cilicica</i>	[150]

Table 5. Contd.

Luteolin						
Luteolin dihexoside	Capcell Park C ₁₈	0.5% FA:H ₂ O (A), 0.5% FA:ACN (B)	flow rate: 0.5 mL/min; 25 °C	MS/MS	<i>Humulus japonicus</i>	[151]
Luteolin 7-rutinoside						
Luteolin glucoside						
Luteolin 7-acetylglucoside						
Luteolin 6-glucoside	Intersil ODS	ACN:H ₂ O:FA (10:89:1 <i>v/v/v</i>) (A), ACN:H ₂ O:FA (89:10:1 <i>v/v/v</i>) (B)	flow rate: 0.7 mL/min; 40 °C	MS/MS	<i>Achillea sinensis</i>	[152]
Luteolin glucoside						
Luteolin methoxy-2''-pentosyl-6-hexoside						
Luteolin 2''-rhamnosyl-6''-hexosyl-glucoside	ODS2 C ₈	0.1% FA:H ₂ O (A), ACN (B)	flow rate: 0.5 mL/min; 35 °C	DAD-ESI-MS; 280, 370 nm	<i>Geranium molle</i>	[68,70,153]
Luteolin 7-glucosyl-8-glucoside						
Luteolin 6-glucoside						
Luteolin 6-hexosyl-8-pentoside						
Luteolin acetylhexoside						
Luteolin 6-glucoside	Spherisorb S3 ODS2 C ₁₈	0.1% FA:H ₂ O (A), ACN (B)	flow rate: 0.5 mL/min; 35 °C	DAD-ESI-MS/MS	<i>Achillea millefolium</i> <i>Colostephus myconis</i> <i>Rosmarinus officinalis</i>	[120,154]
Luteolin 3-glucuronide						
Luteolin glucuronide						
Luteolin hexosyl-pentoside						
Luteolin 7-glucoside	Zorbax RP C ₁₈	0.1% FA:H ₂ O (A), 0.1% FA:ACN (B)	injection volume: 5 µL; flow rate: 0.4 mL/min; 35 °C	QTOF	<i>Ficus carica</i>	[156]
Luteolin 7-hexoside						
Luteolin 6-hexoside						
Luteolin 8-glucoside						
Luteolin 6-hexosyl-8-acetyl-hexoside						
Luteolin 8-glucosyl-7,3'-dimethoxy-2''-O-glycoside	ODS2	H ₂ O:ACN:FA	injection volume: 20 µL; flow rate: 0.8 mL/min	MS/MS	<i>Oxalis pes-caprae</i>	[157]
Luteolin 8-glucosyl-7,3'-dimethoxy-6-desoxyhexoside						
Luteolin 6-glucoside	Hydro RP	H ₂ O (A), MeOH (B), 5% AcOH:MeOH (C)	flow rate: 1 mL/min	MS/MS	<i>Passiflora morifolia</i>	[158]
Luteolin 8-glucoside						
Luteolin						
Luteolin 6-glucoside	Luna C ₁₈	0.1% FA:H ₂ O (A), 0.1% FA:ACN (B)	flow rate: 0.4 mL/min	DAD, 280, 320, 365 nm; MS; MS/MS	<i>Theobroma cacao</i>	[141]
Luteolin 8-glucoside						
Luteolin 7-glucoside						

Table 5. Cont.

Luteolin 6-glucoside	XBridge C ₁₈	0.3% FA:H ₂ O (A), MeOH (B)	injection volume: 1 µL; flow rate: 1 mL/min; 40 °C	MS/MS; ESI-MS	<i>Lophatherum gracile</i>	[140]
Luteolin 7-glucoside						
Luteolin						
Luteolin glucuronyl-hexoside						
Luteolin 7-pentosyl-hexoside						
Luteolin 7-rutinoside						
Luteolin 7-glucoside	Symmetry C ₁₈	0.1% FA:H ₂ O (A), 0.1% FA:ACN (B)	flow rate: 1.0 mL/min; 25 °C	DAD-ESI-MS; 350, 310, 270 and 520 nm	<i>Chrysanthemum morifolium</i>	[142]
Luteolin 7-glucuronide						
Luteolin glucoside						
Luteolin 7-malonyl-6''-glucoside						
Luteolin 7-acetyl-6''-glucoside						
Luteolin 7-dihexoside						
Luteolin						
Luteolin 7-glucuronide	Acquity BEH C ₁₈	0.1% FA:H ₂ O (A), 0.1% FA:ACN (B)	flow rate: 0.3 mL/min; 40 °C	QTOF-MS/MS	<i>Ageratum conyzoides</i>	[159]
Luteolin hexoside	Zorbax SB C ₁₈	0.5% FA:H ₂ O (A), ACN (B)	injection volume: 5 µL; flow rate: 0.4 mL/min	MS/MS	<i>Matricaria recutita</i>	[160]
Luteolin hexoside						
Luteolin hexosyl-deoxy-hexose	Hypersil gold C ₁₈	1% FA:H ₂ O (A), 0.1% FA:ACN (B)	flow rate: 1 mL/min	MS/MS	<i>Cecropia obtusa</i>	[161]
Luteolin dihexoside						
Luteolin pentosyl-hexoside	Spherisorb S3 ODS-2 C ₁₈	0.1% FA:H ₂ O (A), ACN (B)	flow rate: 0.5 mL/min; 35 °C	DAD-ESI-MS/MS	<i>Cofula cinerea</i>	[120,162]
Luteolin 7-glucoside						
Luteolin malonyl-hexoside						
Luteolin						
Luteolin 8-glucoside	Zorbax SB C ₁₈	0.1% FA:AFNH ₄ (A), 0.1% FA:ACN (B)	injection volume: 1 mL; flow rate: 0.2 mL/min	ESI-MS/MS	<i>Ocimum sanctum</i>	[163]
Luteolin 5-glucopyranoside						

Abbreviations: AcOH, acetic acid; ACN, acetonitrile; AFNH₄, ammonium formate; DAD-ESI-MS, diode array detector combined with electrospray ionization and mass spectrometry; DAD, diode array detector; DAD-ESI-MS/MS, diode array detector combined with electrospray ionization and tandem mass spectrometry; ESI, electrospray ionization; ESI-MS, electrospray ionization combined with mass spectrometry; FA, formic acid; MeOH, methanol; MS/MS, tandem mass spectrometry; PDA-MS, pulsed amperometric detection combined with mass spectrometry; QTOF, quadrupole time-of-flight; TQMS, triple quadrupole mass spectrometer.

2.4. Gas Chromatography in the Analysis of Luteolin and Its Derivatives

Gas chromatography (GC) is a technique used to analyze volatile as well as non-volatile compounds after their derivatization. GC is characterized by chromatographic distribution of either a gas mobile phase on a solid adsorbent (gas-solid chromatography) or a liquid on an inert support (gas-liquid chromatography). GC can be hyphenated with various detection techniques such as GC combined with mass spectrometry (GC-MS), GC combined with tandem mass spectrometry (GC-MS/MS) or GC combined with time of flight mass spectrometry (GC-TOF-MS), thus greatly increasing the versatility, sensitivity and accuracy of the method [164,165]. The analyzed substances should be thermally stable, and their boiling (or sublimation) temperature should not exceed 350–400°C. To achieve this, non-volatile substances are often derivatized. Polar functional groups are transformed into their less polar counterparts, thus increasing the volatility of the prepared compounds. The most common examples include substitution with a trimethylsilyl (TM) group, organic radicals or compounds such as trimethylchlorosilane (TMCS), hexamethyldisilazane (HMDS) or *N,O*-bis(trimethylsilyl)-trifluoroacetamide (BSTFA). Such an approach greatly increases the number of possible analytes [2,17]. For example, phenolic groups of flavonoids are often transformed into their less polar trimethylsilyl counterparts allowing for rapid and effective separation of complex mixtures [166].

In adsorption GC, a gas that is chemically inert to the stationary phase as well as the components being analyzed is used as the mobile phase. Most often hydrogen, nitrogen or argon is used. Helium is being used less often due to its higher cost than other gases and the implementation of the principles of chemical safety. The mobile phase must be properly selected for compatibility with the detector used. However, the carrier gas itself does not have a significant influence on the separation effects of the analyzed mixtures [17]. In the process of separation, the method of application of the sample to the chromatography column is very important. The sample should always have as small of a volume and the shortest dosing time as possible. This ensures better separation and narrower bands [17,164].

Gas chromatography uses open-ended columns, i.e., capillary columns and packed columns. Open-ended (OT-open tubular) columns are characterized by much higher efficiency than packed columns; therefore, they are chosen much more often [164]. Capillary columns are particularly useful in the separation of substances with significantly different boiling points. Ideally, the column should have a similar polarity to the analyzed components. However, due to the higher efficiency and greater durability of stationary phases with low polarity, so capillary columns are recommended for chromatographic analyses [17,164].

Another factor that influences the efficiency of the separation of the analyzed sample components, as well as the time of analysis, is temperature. The separation temperature should be selected depending on the stationary phase used and the boiling point of the analytes [17,164].

The analysis of luteolin derivatives has been carried out in accordance with the general procedure used for analysis of other flavonoids (Table 6) [165]. MS was used for detection of volatile derivatives of luteolin, while the use of a flame ionization detector (FID) was described only in two papers [167,168]. Most commonly, helium was used as a carrier gas (e.g., [169–171]), but the use of nitrogen was also recorded [167,168]. The derivatization of luteolin, which is necessary for chromatographic separation, was mostly achieved with BSTFA/TMCS [170–172]. For the analysis of lipophilic luteolin derivatives, such as 7,3',4'-trimethyl-luteolin in *Arnica alpina*, no derivatization was necessary [168].

2.5. Counter-Current Chromatography in the Analysis of Luteolin Derivatives

Counter-current chromatography (CCC) is a variation of liquid chromatography in which both the stationary and mobile phases are liquid. The separation of the constituents of the mixture is carried out in a system of immiscible liquids that are in equilibrium with each other. The method is simple and rapid, offering the possibility of introducing the raw sample to the column without need for previous clean-up [173]. Counter-current chromatography is mainly used for purification of natural compounds, while its use as an analytical technique is far less common. In CCC, various dividing techniques can be used, thus distinguishing centrifugal partition chromatography (CPC) and rapid- or high-speed CCC (HSCCC), often

referred to as hydrodynamic chromatography [174,175]. High-speed CCC is particularly often encountered in studies involving the separation of flavonoids [176]. Table 7 presents the conditions for the separation of mixtures containing luteolin and its derivatives using rapid counter-current chromatography. Separation of luteolin derivatives from mixtures of different phytochemicals is usually carried out with mixtures of EtOAc with one of alcohol (BuOH, EtOH or AcOH) and H₂O. Upon separation, structure determination by NMR is often necessary [173,177]. However, instead of NMR, high resolution mass spectrometry (HRMS) can also be employed for structure confirmation, as evidenced by the use of this technique for differentiation of various luteolin derivatives in *Lippia organoides* [178].

Table 6. Gas chromatography in the analysis of luteolin and its derivatives.

Luteolin derivative	Column	Derivatization	Conditions	Detection	Analyzed species	Ref.
	HP-5-MS	1% TMCS:BSTFA	carrier gas: He; injector temperature : 250 °C A: (column temperature) 5 min, 170°C; 3 °C/min, 170–255 °C; 1 min, 255 °C; 2 °C/min, 255–310 °C; flow rate: 0.5 mL/min; analysis time: 70 min; B: (column temperature) 5 min, 160°C; 3°C/min, 160–188°C; 1 min, 188 °C; 15 °C/min, 188–241 °C; 1 min, 241 °C; 2 °C/min, 241–282 °C; 5 °C/min, 282–310 °C; 5 min, 310 °C; flow rate : 1.0 mL/min; analysis time: 50 min	APCI-TOF-MS	Fruits of various olives species (<i>Olea</i> L.)	[170]
Luteolin	Capillary column Supelco SPBM-5	two- and three-phase transfer catalysis (PTC), methyl iodide	carrier gas: He; injector temperature: 260 °C; detector temperature: 280 °C; furnace temperature: 5 min, 50 °C; 5 °C/min, 50–150 °C; 10 °C/min, 150–210 °C; analysis time: 45 min	MS	<i>Mentha spicata</i> , <i>Hypericum perforatum</i>	[179]
	non-polar RSL 200 BP	0.2 M trimethylamine hydroxide (TMAH):H ₂ O-free MeOH Py:HMDS:TMCS	carrier gas: N ₂ ; linear speed of the carrier 17.5 cm/s; 0–2 min, 280 °C and 235 °C; 1 °C/min, 280–290 °C; flow rate: 30 mL/min	FID	different samples form AFRC Institute of Plant Science Research and John Innes Institute, Norwich, U.K.	[167]
	BPX5	Py:BSTFA:TMCS) (50:50:1 v/v/v)	carrier gas: He; injector temperature: 310 °C; 1 min, 100 °C; 30 °C/min, 100–210 °C; 2 °C/min, 210–240 °C; 4 °C/min, 240–270 °C; 5 °C/min, 270–310 °C; 5 min, 310 °C; flow rate: 1.5 mL/min	QMS	Propolis, <i>Chrysanthemum</i> sp, <i>Theobroma cacao</i> (bitter chocolate)	[171]

Table 6. Cont.

Capillary column Low-bleed CP-5il 8 CB-MS	TMCS (100 µL), BSTFA (200 µL) HMDS:TMCS:Py (3:1:9, v/v/v)	carrier gas: He; 2 °C/min, 70–135 °C; 10 min, 135 °C; 4 °C/min, 135–220 °C; 10 min, 220 °C; 3.5 °C/min, 220–270 °C; 20 min, 270 °C; injector temperature: 280 °C; detector temperature: 290 °C; flow rate: 1.9 mL/min	MS	<i>Teucrium polium</i>	[169]
Quartz capillary column	Py:BSTFA (1:1 v/v)	carrier gas: He; injector temperature 220 °C; detector temperature: 270 °C; 2.3 °C/min 200–270 °C; 30 min, 270 °C	MS	<i>Aspalathus linearis</i>	[172]
Capillary column Permabond OV-1 Capillary column OV-1	--- ---	carrier gas: N ₂ , He; injector temperature: 300 °C; column temperature: 270 °C (isothermal); flow rate: 1.3 mL/min	FID MS	<i>Arnica alpina</i>	[168]

Abbreviations: Py, pyridine, BSTFA, N,O-bis(trimethylsilyl)trifluoroacetamide; TMS, trimethylsilyl; HMDS, hexamethyldisilazane; TMCS, trimethylchlorosilane; APCL-TOF-MS, atmospheric pressure chemical ionization combined with quadrupole – time of flight mass spectrometry; FID, flame ionization detector; QMS, quadrupole mass spectrometry.

Table 7. Counter-current chromatography, as a preparative technique in the separation of luteolin derivatives.

Luteolin derivative	Solvent system	Conditions	Detection	Analyzed species	Ref.
Luteolin 6-glucoside	EtOAc:BuOH:H ₂ O (2:1:3 v/v/v)	rotation speed: 800 rpm; flow rate (lower phase): 2.4 mL/min	UV-VIS, 254 nm; NMR; MS	<i>Patrinia villosa</i>	[173]
Luteolin 7-glucoside	EtOAc:EtOH:AcOH:H ₂ O (4:1:0.25:5 v/v/v/v)	rotation speed: 800 rpm; flow rate (lower phase): 1.5 mL/min	UV, 254 nm; NMR; MS	<i>Paeonia suffruticosa</i>	[177]
Luteolin 6,8-dihexoside					
Luteolin 8-glucoside	Hx:EtOH:H ₂ O	rotation speed: 850 rpm;			
Luteolin 6-glucoside	(4:3:1 v/v/v)	flow rate (lower phase): 2 mL/min	TLC; HPLC-UV-HRMS	<i>Lippia origanoides</i>	[178]
Luteolin 7-glucoside					

Abbreviations: AcOH, acetic acid; BuOH, butanol; EtOAc, ethyl acetate; EtOH, ethanol; HRMS, high resolution mass spectrometry; Hx, hexane, rpm, revolutions per minute.

3. Conclusions

The presented comparison of chromatographic methods currently used to determine luteolin and its derivatives provides a systematic summary of the available knowledge. Without a doubt, chromatographic analysis may be successfully employed as an efficient method for both qualitative assessment (fingerprinting) and quantitative determination of luteolin derivatives. In tedious and time-consuming determinations of multi-ingredient plant extracts, including those that contain the most prevalent luteolin derivatives, combinations of large-scale chromatographic techniques with serially aligned detection modalities such as LC-MS/MS or LC/NMR/MS were found to be particularly useful. Such beneficial coupling of chromatography with other analytic techniques expands analytical capabilities while additionally improving the accuracy, sensitivity, and precision of assays. Despite the dominant position of LC in the analysis of natural compounds and the dynamic development of novel chromatographic methods, the TLC/HPTLC has not lost its important place in the phytochemical analysis of luteolin derivatives. The technique is relatively simple and inexpensive while facilitating rapid qualitative and quantitative analysis of test compounds. In addition, it facilitates large quantities of diluted samples being deposited in the stationary phase, allowing for a wider choice of mobile phase carriers. The technique is subject to continuous improvements and its range of applicability is expanding.

Effective chromatographic analysis in the determination of luteolin derivatives requires appropriately selected chromatographic separation conditions. The appropriate choice of stationary phase sorbent may significantly improve test conditions. Most TLC analyses of luteolin derivatives are carried out in normal phase systems featuring a polar (hydrophilic) sorbent phase. In HPLC, separation conditions can be chosen more arbitrarily as the technique allows for the use of stationary phases of varying polarity which is particularly advantageous in the analysis of compounds that are either insoluble or poorly soluble in water. In order to additionally improve the sensitivity of HPLC analyses, one should focus on the column parameters responsible for appropriate separation. Quite often, the fairly successful analyses are used as starting points for further modifications, including the development of preparative-scale analyses.

Of all chromatographic techniques, GC is the least applicable in the analysis of plant extracts, including those that contain luteolin derivatives. Despite its high sensitivity and efficiency when coupled with various detection techniques (MS, MS/MS, TOF-MS), the chromatographic separation process involves high temperatures and derivatization of analytes. Due to this important aspect, GC-MS is less frequently used in the analysis of polyphenolic compounds.

The complexity of plant matrices is unquestionably a significant problem in the chromatographic analysis of plant extracts. It has a negative impact on the efficacy of analyses and prevents complete identification of all components of the plant extract. However, chromatography remains the primary and most effective analytical technique available in the current state of the art for the determination of compounds of natural origin.

Author Contributions: Conceptualization, M.T. and M.Z.K.; literature investigation, A.M.J.; writing—original draft preparation, A.M.J., M.T., M.Z.K.; writing—review and editing, A.M.J., M.T.; supervision, M.T., M.Z.K.

Funding: The work was funded by the project № POWR.03.02.00-00-I051/16 from European Union funds, PO WER 2014-2020, grant №. 05/IMSD/G/2019.

Conflicts of Interest: All authors state that they are free of any conflicts of interest related to this paper.

References

1. López-Lázaro, M. Distribution and biological activities of the flavonoid luteolin. *Mini Rev. Med. Chem.* **2009**, *9*, 31–59.
2. Szultka, M.; Buszewski, B.; Papaj, K.; Szeja, W.; Rusin, A. Determination of flavonoids and their metabolites by chromatographic techniques. *Trends Anal. Chem.* **2013**, *47*, 47–67.
3. Nabavi, S.F.; Braidy, N.; Gortzi, O.; Sobarzo-Sanchez, E.; Daglia, M.; Skalicka-Woźniak, K.; Nabavi, S.M. Luteolin as an anti-inflammatory and neuroprotective agent: A brief review. *Brain Res. Bull.* **2015**, *119*, 1–

- 11.
4. Bravo, L. Polyphenols: Chemistry, dietary sources, metabolism, and nutritional significance. *Nutr. Rev.* **1998**, *56*, 317–333.
5. Lin, Y.; Shi, R.; Wang, X.; Shen, H.-M. Luteolin, a flavonoid with potential for cancer prevention and therapy. *Curr. Cancer Drug Targets* **2008**, *8*, 634–646.
6. Aziz, N.; Kim, M.-Y.; Cho, J.Y. Anti-inflammatory effects of luteolin: A review of in vitro, in vivo, and in silico studies. *J. Ethnopharmacol.* **2018**, *225*, 342–358.
7. Imran, M.; Rauf, A.; Abu-Izneid, T.; Nadeem, M.; Shariati, M.A.; Khan, I.A.; Imran, A.; Orhan, I.E.; Rizwan, M.; Atif, M.; et al. Luteolin, a flavonoid, as an anticancer agent: A review. *Biomed. Pharmacother.* **2019**, *112*, 108612.
8. Narayana, K.R.; Reddy, M.S.; Chaluvadi, M.R.; Krishna, D.R. Bioflavonoids classification, pharmacological, biochemical effects and therapeutic potential. *Indian J. Pharmacol.* **2001**, *33*, 2–16.
9. Harborne, J.B.; Baxter, H. *The Handbook of Natural Flavonoids*; Harborne, J.B., Baxter, H., Eds.; John Wiley & Sons, Inc.: Chichester, UK, 1999.
10. Lam, K.Y.; Ling, A.P.K.; Koh, R.Y.; Wong, Y.P.; Say, Y.H. A review on medicinal properties of orientin. *Adv. Pharmacol. Sci.* **2016**, *2016*, 4104595.
11. Zheng, H.; Zhang, M.; Luo, H.; Li, H. Isoorientin alleviates UVB-induced skin injury by regulating mitochondrial ROS and cellular autophagy. *Biochem. Biophys. Res. Commun.* **2019**, *514*, 1133–1139.
12. Wu, Q.-Y.; Wong, Z.C.-F.; Wang, C.; Fung, A.H.-Y.; Wong, E.O.-Y.; Chan, G.K.-L.; Dong, T.T.-X.; Chen, Y.; Tsim, K.W.-K. Isoorientin derived from *Gentiana veitchiorum* Hemsl. flowers inhibit melanogenesis by down-regulating MITF-induced tyrosinase expression. *Phytomedicine* **2019**, *57*, 129–136.
13. Fan, X.; Lv, H.; Wang, L.; Deng, X.; Ci, X. Isoorientin ameliorates APAP-induced hepatotoxicity via activation Nrf2 antioxidative pathway: The involvement of AMPK/Akt/GSK3 β . *Front. Pharmacol.* **2018**, *9*, 1334.
14. Anilkumar, K.; Reddy, G. V.; Azad, R.; Yarla, N.S.; Dharmapuri, G.; Srivastava, A.; Kamal, M.A.; Pallu, R. Evaluation of anti-inflammatory properties of isoorientin isolated from tubers of *Pueraria tuberosa*. *Oxid. Med. Cell. Longev.* **2017**, *2017*, 5498054.
15. Jo, B.-G.; Park, N.-J.; Jegal, J.; Choi, S.; Lee, S.W.; Yi, L.W.; Kim, S.-N.; Yang, M.H. *Stellera chamaejasme* and its main compound luteolin 7-O-glucoside alleviates skin lesions in oxazolone- and 2,4-dinitrochlorobenzene-stimulated murine models of atopic dermatitis. *Planta Med.* **2018**, *85*, 583–590.
16. Chen, S.; Yang, B.; Xu, Y.; Rong, Y.; Qiu, Y. Protection of luteolin-7-O-glucoside against apoptosis induced by hypoxia/reoxygenation through the MAPK pathways in H9c2 cells. *Mol. Med. Rep.* **2018**, *17*, 7156–7162.
17. McNair, H.M.; Miller, J.M. *Basic Gas Chromatography*, 2nd ed.; John Wiley & Sons, Inc.: Hoboken, NJ, USA, 2009.
18. Monteiro, M.L.G.; Marsico, E.; Lázaro, C.; Conte Júnior, C. Thin-layer chromatography applied to foods of animal origin: A tutorial review. *J. Anal. Chem.* **2016**, *71*, 459–470.
19. Kazakevich, Y.; LoBrutto, R. HPLC theory and practice. In *HPLC for Pharmaceutical Scientists*; Kazakevich, Y., LoBrutto, R., Eds.; John Wiley & Sons, Inc.: Hoboken, NJ, USA, 2007; pp. 3–13.
20. Medić-Šarić, M.; Jasprica, I.; Mornar, A.; Maleš, Ž. Application of TLC in the isolation and analysis of flavonoids. In *Thin Layer Chromatography in Phytochemistry*; Waksmundzka-Hajnos, M., Shrema, J., Kowalska, T., Eds.; CRC Press, Taylor & Francis Group: Boca Raton, FL, USA, 2008; pp. 405–423.
21. Fuchs, B.; Süß, R.; Teuber, K.; Eibisch, M.; Schiller, J. Lipid analysis by thin-layer chromatography—A review of the current state. *J. Chromatogr. A* **2011**, *1218*, 2754–2774.
22. Poole, C.F. Milestones, core concepts, and contrasts. In *Instrumental Thin-Layer Chromatography*; Poole, C.F., Ed.; Elsevier Inc.: Amsterdam, The Netherlands, 2015; pp. 1–3.
23. Santiago, M.; Strobel, S. Thin layer chromatography. *Methods Enzymol.* **2013**, *533*, 303–324.
24. Waksmundzka-Hajnos, M.; Hawrył, M.A.; Cieśla, Ł. Analysis of plant material. In *Instrumental Thin-Layer Chromatography*; Poole, C.F., Ed.; Elsevier Inc.: Amsterdam, The Netherlands, 2015; pp. 505–508.
25. Phadungrakwittaya, R. Identification of apigenin and luteolin in *Artemisia annua* L. for the quality control. *Siriraj Med. J.* **2019**, *71*, 240–245.
26. Mučaji, P.; Nagy, M.; Liptaj, T.; Prónayová, N.; Švajdlenka, E. Separation of a mixture of luteolin-7-rutinoside and luteolin-7-neohesperidoside isolated from *Ligustrum vulgare* L. *JPC J. Planar Chromatogr.* **2009**, *22*, 301–304.
27. Aghakhani, F.; Kharazian, N.; Lori Gooini, Z. Flavonoid constituents of *Phlomis* (Lamiaceae) species using

- liquid chromatography mass spectrometry. *Phytochem. Anal.* **2018**, *29*, 180–195.
28. Kozyra, M.; Głowniak, K.; Boguszewska, M. The analysis of flavonoids in the flowering herbs of *Carduus acanthoides* L. *Curr. Issues Pharm. Med. Sci.* **2013**, *26*, 10–15.
 29. Schwaiger, S.; Seger, C.; Wiesbauer, B.; Schneider, P.; Ellmerer, E.P.; Sturm, S.; Stuppner, H. Development of an HPLC-PAD-MS assay for the identification and quantification of major phenolic edelweiss (*Leontopodium alpinum* Cass.) constituents. *Phytochem. Anal.* **2006**, *17*, 291–298.
 30. Jesionek, W.; Majer-Dziedzic, B.; Choma, I. Separation, identification, and investigation of antioxidant ability of plant extract components using TLC, LC-MS, and TLC-DPPH. *J. Liq. Chromatogr. Relat. Technol.* **2015**, *38*, 1147–1153.
 31. Amirkhanova, A.; Ustenova, G.; Krauze, M.; Poblocka, L.; Shynykul, Z. Thin-layer chromatography analysis of extract *Oxytropis glabra* lam. dc. In Proceedings of the 18th International Multidisciplinary Scientific Geoconference (SGEM 2018), Albena, Bulgaria, 30 June–9 July 2018; pp. 775–782.
 32. Nile, S.; Park, S.W. HPTLC densitometry method for simultaneous determination of flavonoids in selected medicinal plants. *Front. Life Sci.* **2015**, *8*, 97–103.
 33. Kukkar, M.; Kukkar, R.; Saluja, A. Validation of HPTLC method for the analysis of luteolin in *Cardiospermum halicacabum* Linn. *Int. J. Green Pharm.* **2014**, *8*, 252–256.
 34. Hassanein, H.; Said-Al Ahl, H.; MM, A. Antioxidant polyphenolic constituents of *Satureja montana* L. Growing in Egypt. *Int. J. Pharm. Pharm. Sci.* **2014**, *6*, 578–581.
 35. Satpathy, S.; Patra, A.; Ahirwar, B. Development and validation of a novel high-performance thin-layer chromatography method for the simultaneous determination of apigenin and luteolin in *Hygrophila spinosa* T. Anders. *JPC J. Planar Chromatogr. Mod. TLC* **2018**, *31*, 437–443.
 36. Shawk, E.; Abou El Kheir, R.M. Rapid discrimination of different *Apiaceae* species based on HPTLC fingerprints and targeted flavonoids determination using multivariate image analysis. *Phytochem. Anal.* **2018**, *29*, 452–462.
 37. Swar, G.; Shailajan, S.; Menon, S. Activity based evaluation of a traditional Ayurvedic medicinal plant: *Saraca asoca* (Roxb.) de Wilde flowers as estrogenic agents using ovariectomized rat model. *J. Ethnopharmacol.* **2017**, *195*, 324–333.
 38. Patel, N.; Patel, K.; Patel, K.; Tejal, G. Validated HPTLC method for quantification of luteolin and apigenin in *Premna mucronata* Roxb., Verbenaceae. *Adv. Pharmacol. Sci.* **2015**, *2015*, 1–7.
 39. Gupta, N.; Lobo, R.; Kumar, N.; Bhagat, J.K.; Mathew, J.E. Identity-based High-performance thin layer chromatography fingerprinting profile and tumor inhibitory potential of *Anisochilus carnosus* (L.f.) wall against ehrlich ascites carcinoma. *Pharmacogn. Mag.* **2015**, *11*, 474–480.
 40. Bros, I.; Soran, M.-L.; Naşcu-Briciu, R.; Codruta, C. HPTLC quantification of some flavonoids in extracts of *Satureja hortensis* L. obtained by use of different techniques. *JPC J. Planar Chromatogr.* **2009**, *22*, 25–28.
 41. Ristivojevic, P.; Dimkic, I.; Trifkovic, J.; Beric, T.; Vovk, I.; Milojkovic-Opsenica, D.; Stankovic, S. Antimicrobial activity of Serbian propolis evaluated by means of MIC, HPTLC, bioautography and chemometrics. *PLoS ONE* **2016**, *11*, e0157097.
 42. Shaikh, F.; Sancheti, J.; Sathaye, S. Phytochemical and pharmacological investigations of *Eclipta alba* (Linn.) Hassak leaves for antiepileptic activity. *Int. J. Pharm. Pharm. Sci.* **2012**, *4*, 319–323.
 43. Margină, D.; Oлару, O.T.; Ilie, M.; Gradinaru, D.; GuTu, C.; Voicu, S.; Dinischiotu, A.; Spandidos, D.A.; Tsatsakis, A.M. Assessment of the potential health benefits of certain total extracts from *Vitis vinifera*, *Aesculus hippocastanum* and *Curcuma longa*. *Exp. Ther. Med.* **2015**, *10*, 1681–1688.
 44. Chelyn, J.L.; Omar, M.H.; Mohd Yousof, N.S.A.; Ranggasamy, R.; Wasiman, M.I.; Ismail, Z. Analysis of flavone C-glycosides in the leaves of *Clinacanthus nutans* (Burm. f.) Lindau by HPTLC and HPLC-UV/DAD. *Sci. World J.* **2014**, *2014*, 1–6.
 45. Pereira, C.A.M.; Yariwake, J.H.; Lancas, F.M.; Wauters, J.-N.; Tits, M.; Angenot, L. A HPTLC densitometric determination of flavonoids from *Passiflora alata*, *P. edulis*, *P. incarnata* and *P. caerulea* and comparison with HPLC method. *Phytochem. Anal.* **2004**, *15*, 241–248.
 46. Wang, J.; Tang, F.; Yue, Y.; Guo, X.; Yao, X. Development and validation of an HPTLC method for simultaneous quantitation of isoorientin, isovitexin, orientin, and vitexin in bamboo-leaf flavonoids. *J. AOAC Int.* **2010**, *93*, 1376–1383.
 47. Cook, R.; Hennell, J.R.; Lee, S.; Khoo, C.S.; Carles, M.C.; Higgins, V.J.; Govindaraghavan, S.; Sucher, N.J. The *Saccharomyces cerevisiae* transcriptome as a mirror of phytochemical variation in complex extracts of *Equisetum arvense* from America, China, Europe and India. *BMC Genomics* **2013**, *14*, 445.

48. Srinivas, P.; Reddy, S.R. Screening for antibacterial principle and activity of *Aerva javanica* (Burm .f) Juss. ex Schult. *Asian Pac. J. Trop. Biomed.* **2012**, *2*, S838–S845.
49. Guerrini, A.; Bruni, R.; Maietti, S.; Poli, F.; Rossi, D.; Paganetto, G.; Muzzoli, M.; Scalvenzi, L.; Sacchetti, G. Ecuadorian stingless bee (Meliponinae) honey: A chemical and functional profile of an ancient health product. *Food Chem.* **2009**, *114*, 1413–1420.
50. Bazytko, A.; Tomczyk, M.; Flazińska, A.; Łęgas, A. Chemical fingerprint of *Potentilla* species by using HPTLC method. *JPC J. Planar Chromatogr.* **2011**, *24*, 441–444.
51. Celep, E.; Akyüz, S.; İnan, Y.; Yesilada, E. Assessment of potential bioavailability of major phenolic compounds in *Lavandula stoechas* L. ssp. *stoechas*. *Ind. Crops Prod.* **2018**, *118*, 111–117.
52. Bilušić Vundać, V.; Maleš, Ž.; Plazibat, M.; Golja, P.; Cetina-Čizmek, B. HPTLC determination of flavonoids and phenolic acids in some Croatian *Stachys* taxa. *JPC J. Planar Chromatogr.* **2005**, *18*, 269–273.
53. Fecka, I.; Kowalczyk, A.; Cisowski, W. Optimization of the separation of flavonoid glycosides and rosmarinic acid from *Mentha piperita* on HPTLC plates. *JPC J. Planar Chromatogr.* **2004**, *17*, 22–25.
54. Fecka, I.; Turek, S. Determination of water-soluble polyphenolic compounds in commercial herbal teas from Lamiaceae: Peppermint, melissa, and sage. *J. Agric. Food Chem.* **2007**, *55*, 10908–10917.
55. Fecka, I.; Turek, S. Determination of polyphenolic compounds in commercial herbal drugs and spices from Lamiaceae: Thyme, wild thyme and sweet marjoram by chromatographic techniques. *Food Chem.* **2008**, *108*, 1039–1053.
56. Fecka, I.; Raj, D.; Krauze-Baranowska, M. Quantitative determination of four water-soluble compounds in herbal drugs from Lamiaceae using different chromatographic techniques. *Chromatographia* **2007**, *66*, 87–93.
57. Jug, U.; Glavnik, V.; Kranjc, E.; Vovk, I. HPTLC–densitometric and HPTLC–MS methods for analysis of flavonoids. *J. Liq. Chromatogr. Relat. Technol.* **2018**, *41*, 329–341.
58. Lebot, V.; Lawac, F.; Michalet, S.; Legendre, L. Characterization of taro [*Colocasia esculenta* (L.) Schott] germplasm for improved flavonoid composition and content. *Plant. Genet. Resour.* **2017**, *15*, 260–268.
59. Orsini, F.; Vovk, I.; Glavnik, V.; Jug, U.; Corradini, D. HPTLC, HPTLC-MS/MS and HPTLC-DPPH methods for analyses of flavonoids and their antioxidant activity in *Cyclanthera pedata* leaves, fruits and dietary supplement. *J. Liq. Chromatogr. Relat. Technol.* **2019**, *42*, 290–301.
60. Nile, S.H.; Park, S.W. HPTLC analysis, antioxidant and antigout activity of Indian plants. *Iran. J. Pharm. Res.* **2014**, *13*, 531–539.
61. Chisvert, A.; Benedé, J.L.; Salvador, A. Current trends on the determination of organic UV filters in environmental water samples based on microextraction techniques—A review. *Anal. Chim. Acta* **2018**, *1034*, 22–38.
62. Dias, I.H.K.; Wilson, S.R.; Roberg-Larsen, H. Chromatography of oxysterols. *Biochimie* **2018**, *153*, 3–12.
63. Pascual-Maté, A.; Osés, S.M.; Fernández-Muiño, M.A.; Sancho, M.T. Analysis of polyphenols in honey: Extraction, separation and quantification procedures. *Sep. Purif. Rev.* **2018**, *47*, 142–158.
64. Kazakevich, Y. HPLC theory. In *HPLC for Pharmaceutical Scientists*; Kazakevich, Y., LoBrutto, R., Eds.; John Wiley & Sons, Inc.: Hoboken, NJ, USA, 2007; pp. 40–70.
65. Kazakevich, Y.; LoBrutto, R. Stationary phases. In *HPLC for Pharmaceutical Scientists*; Kazakevich, Y., LoBrutto, R., Eds.; John Wiley & Sons, Inc.: Hoboken, NJ, USA, 2007; pp. 77–90.
66. Pereira, E.; Barros, L.; Calhella, R.C.; Dueñas, M.; Carvalho, A.M.; Santos-Buelga, C.; Ferreira, I.C.F.R. Bioactivity and phytochemical characterization of *Arenaria montana* L. *Food Funct.* **2014**, *5*, 1848–1855.
67. Barros, L.; Dueñas, M.; Carvalho, A.M.; Ferreira, I.C.F.R.; Santos-Buelga, C. Characterization of phenolic compounds in flowers of wild medicinal plants from Northeastern Portugal. *Food Chem. Toxicol.* **2012**, *50*, 1576–1582.
68. Dias, M.I.; Barros, L.; Dueñas, M.; Pereira, E.; Carvalho, A.M.; Alves, R.C.; Oliveira, M.B.P.P.; Santos-Buelga, C.; Ferreira, I.C.F.R. Chemical composition of wild and commercial *Achillea millefolium* L. and bioactivity of the methanolic extract, infusion and decoction. *Food Chem.* **2013**, *141*, 4152–4160.
69. Rodrigues, S.; Calhella, R.C.; Barreira, J.C.M.; Dueñas, M.; Carvalho, A.M.; Abreu, R.M.V.; Santos-Buelga, C.; Ferreira, I.C.F.R. *Crataegus monogyna* buds and fruits phenolic extracts: Growth inhibitory activity on human tumor cell lines and chemical characterization by HPLC–DAD–ESI/MS. *Food Res. Int.* **2012**, *49*, 516–523.
70. Roriz, C.L.; Barros, L.; Carvalho, A.M.; Santos-Buelga, C.; Ferreira, I.C.F.R. *Pterospartum tridentatum*, *Gomphrena globosa* and *Cymbopogon citratus*: A phytochemical study focused on antioxidant compounds. *Food Res. Int.* **2014**, *62*, 684–693.

71. Barros, L.; Pereira, E.; Calheta, R.C.; Dueñas, M.; Carvalho, A.M.; Santos-Buelga, C.; Ferreira, I.C.F.R. Bioactivity and chemical characterization in hydrophilic and lipophilic compounds of *Chenopodium ambrosioides* L. *J. Funct. Foods* **2013**, *5*, 1732–1740.
72. Viacava, G.E.; Roura, S.I.; López-Márquez, D.M.; Berrueta, L.A.; Gallo, B.; Alonso-Salces, R.M. Polyphenolic profile of butterhead lettuce cultivar by ultrahigh performance liquid chromatography coupled online to UV–visible spectrophotometry and quadrupole time-of-flight mass spectrometry. *Food Chem.* **2018**, *260*, 239–273.
73. Yang, X.; Cui, X.; Zhao, L.; Guo, D.; Feng, L.; Wei, S.; Zhao, C.; Huang, D. Exogenous glycine nitrogen enhances accumulation of glycosylated flavonoids and antioxidant activity in lettuce (*Lactuca sativa* L.). *Front. Plant. Sci.* **2017**, *8*, 2098.
74. Farag, M.A.; Handoussa, H.; Fekry, M.I.; Wessjohann, L.A. Metabolite profiling in 18 Saudi date palm fruit cultivars and their antioxidant potential *via* UPLC-QTOF-MS and multivariate data analyses. *Food Funct.* **2016**, *7*, 1077–1086.
75. Ibrahim, R.M.; El-Halawany, A.M.; Saleh, D.O.; Naggari, E.M.B. El; El-Shabrawy, A.E.-R.O.; El-Hawary, S.S. HPLC-DAD-MS/MS profiling of phenolics from *Securigera securidaca* flowers and its anti-hyperglycemic and anti-hyperlipidemic activities. *Rev. Bras. Farmacogn.* **2015**, *25*, 134–141.
76. Mudrić, S.Ž.; Gašić, U.M.; Dramićanin, A.M.; Ćirić, I.Ž.; Milojković-Opsenica, D.M.; Popović-Dorđević, J.B.; Momirović, N.M.; Tešić, Ž.L. The polyphenolics and carbohydrates as indicators of botanical and geographical origin of Serbian autochthonous clones of red spice paprika. *Food Chem.* **2017**, *217*, 705–715.
77. Barros, L.; Dueñas, M.; Dias, M.I.; Sousa, M.J.; Santos-Buelga, C.; Ferreira, I.C.F.R. Phenolic profiles of in vivo and in vitro grown *Coriandrum sativum* L. *Food Chem.* **2012**, *132*, 841–848.
78. Quirantes-Pine, R.; Lozano-Sanchez, J.; Herrero, M.; Ibanez, E.; Segura-Carretero, A.; Fernandez-Gutierrez, A. HPLC-ESI-QTOF-MS as a powerful analytical tool for characterising phenolic compounds in olive-leaf extracts. *Phytochem. Anal.* **2013**, *24*, 213–223.
79. Costa, G.; Nunes, F.; Vitorino, C.; Sousa, J.J.; Figueiredo, I. V.; Batista, M.T. Validation of a RP-HPLC method for quantitation of phenolic compounds in three different extracts from *Cymbopogon citratus*. *Res. J. Med. Plant.* **2015**, *9*, 331–339.
80. Liu, G.; Linwu, Z.; Song, D.; Lu, C.; Xu, X. Isolation, purification, and identification of the main phenolic compounds from leaves of celery (*Apium graveolens* L. var. dulce Mill./Pers.). *J. Sep. Sci.* **2016**, *40*, 472–479.
81. Taghouti, M.; Martins-Gomes, C.; Schäfer, J.; Félix, L.M.; Santos, J.A.; Bunzel, M.; Nunes, F.M.; Silva, A.M. *Thymus pulegioides* L. as a rich source of antioxidant, anti-proliferative and neuroprotective phenolic compounds. *Food Funct.* **2018**, *9*, 3617–3629.
82. Achour, M.; Mateos, R.; Ben Fredj, M.; Mtiraoui, A.; Bravo, L.; Saguem, S. A comprehensive characterisation of rosemary tea obtained from *Rosmarinus officinalis* L. collected in a sub-humid area of Tunisia. *Phytochem. Anal.* **2018**, *29*, 87–100.
83. Ferreres, F.; Gomes, N.G.M.; Valentão, P.; Pereira, D.M.; Gil-Izquierdo, A.; Araújo, L.; Silva, T.C.; Andrade, P.B. Leaves and stem bark from *Allophylus africanus* P. Beauv.: An approach to anti-inflammatory properties and characterization of their flavonoid profile. *Food Chem. Toxicol.* **2018**, *118*, 430–438.
84. Ravisankar, S.; Abegaz, K.; Awika, J.M. Structural profile of soluble and bound phenolic compounds in teff (*Eragrostis tef*) reveals abundance of distinctly different flavones in white and brown varieties. *Food Chem.* **2018**, *263*, 265–274.
85. Khallouki, F.; Breuer, A.; Merieme, E.; Ulrich, C.M.; Owen, R.W. Characterization and quantitation of the polyphenolic compounds detected in methanol extracts of *Pistacia atlantica* Desf. fruits from the Guelmim region of Morocco. *J. Pharm. Biomed. Anal.* **2017**, *134*, 310–318.
86. Vasić, V.; Gašić, U.; Stanković, D.; Lušić, D.; Vukić-Lušić, D.; Milojković-Opsenica, D.; Tešić, Ž.; Trifković, J. Towards better quality criteria of European honeydew honey: Phenolic profile and antioxidant capacity. *Food Chem.* **2019**, *274*, 629–641.
87. Ammar, S.; Contreras, M.d.M.; Belguith-Hadrich, O.; Bouaziz, M.; Segura-Carretero, A. New insights into the qualitative phenolic profile of *Ficus carica* L. fruits and leaves from Tunisia using ultra-high-performance liquid chromatography coupled to quadrupole-time-of-flight mass spectrometry and their antioxidant activity. *RSC Adv.* **2015**, *5*, 20035–20050.
88. Obmann, A.; Purevsuren, S.; Zehl, M.; Kletter, C.; Reznicek, G.; Narantuya, S.; Glas, S. HPLC determination of flavonoid glycosides in Mongolian *Dianthus versicolor* Fisch. (Caryophyllaceae) compared with quantification by UV spectrophotometry. *Phytochem. Anal.* **2012**, *23*, 254–259.

89. Chen, H.-J.; Inbaraj, B.S.; Chen, B.-H. Determination of phenolic acids and flavonoids in *Taraxacum formosanum* Kitam by liquid chromatography-tandem mass spectrometry coupled with a post-column derivatization technique. *Int. J. Mol. Sci.* **2012**, *13*, 260–285.
90. Tebboub, O.; Cotugno, R.; Oke-Altuntas, F.; Bouheroum, M.; Demirtas, Í.; D’Ambola, M.; Malafronte, N.; Vassallo, A. Antioxidant potential of herbal preparations and components from *Galactites elegans* (All.) Nyman ex soldano. *Evid. Based. Complement. Alternat. Med.* **2018**, *2018*, 9294358.
91. Saleem, H.; Htar, T.T.; Naidu, R.; Nawawi, N.S.; Ahmad, I.; Ashraf, M.; Ahemad, N. Biological, chemical and toxicological perspectives on aerial and roots of *Filago germanica* (L.) huds: Functional approaches for novel phyto-pharmaceuticals. *Food Chem. Toxicol.* **2019**, *123*, 363–373.
92. Tahri, W.; Chatti, A.; Romero-González, R.; López-Gutiérrez, N.; Frenich, A.G.; Landoulsi, A. Phenolic profiling of the aerial part of *Chrysanthemum trifurcatum* using ultra high-performance liquid chromatography coupled to Orbitrap high resolution mass spectrometry. *Anal. Methods* **2016**, *8*, 3517–3527.
93. Dall’Acqua, S.; Peron, G.; Ferrari, S.; Gandin, V.; Bramucci, M.; Quassinti, L.; Mártonfi, P.; Maggi, F. Phytochemical investigations and antiproliferative secondary metabolites from *Thymus alternans* growing in Slovakia. *Pharm. Biol.* **2017**, *55*, 1162–1170.
94. Abu-Reidah, I.M.; Gil-Izquierdo, Á.; Medina, S.; Ferreres, F. Phenolic composition profiling of different edible parts and by-products of date palm (*Phoenix dactylifera* L.) by using HPLC-DAD-ESI/MSn. *Food Res. Int.* **2017**, *100*, 494–500.
95. Vinayagam, A.; Sudha, P.N. Separation and identification of phenolic acid and flavonoids from *Nerium indicum* flowers. *Indian J. Pharm. Sci.* **2015**, *77*, 91–95.
96. Vitalini, S.; Madeo, M.; Tava, A.; Iriti, M.; Vallone, L.; Avato, P.; Cocuzza, C.E.; Simonetti, P.; Argentieri, M.P. Chemical profile, antioxidant and antibacterial activities of *Achillea moschata* Wulfen, an endemic species from the Alps. *Molecules* **2016**, *21*, 830.
97. Liu, H.; Zhang, M.; Guo, Y.; Qiu, H. Solid-phase extraction of flavonoids in honey samples using carbamate-embedded triacontyl-modified silica sorbent. *Food Chem.* **2016**, *204*, 56–61.
98. Li, L.; Jiang, H.; Wu, H.; Zeng, S. Simultaneous determination of luteolin and apigenin in dog plasma by RP-HPLC. *J. Pharm. Biomed. Anal.* **2005**, *37*, 615–620.
99. Klangprapun, S.; Buranrat, B.; Caichompoo, W.; Nualkaew, S. Pharmacognostical and physicochemical studies of *Enhalus acoroides* (L.F.) royle (rhizome). *Pharmacogn. J.* **2018**, *10*, s89–s94.
100. Song, T.; Liu, L. A strategy for quality control of the fruits of *Perilla frutescens* (L.) Britt based on antioxidant activity and fingerprint analysis. *Anal. Methods* **2016**, *8*, 295–302.
101. da Silva, J.B.; Temponi, V. dos S.; Gasparetto, C.M.; Fabri, R.L.; Aragão, D.M. de O.; Pinto, N. de C.C.; Ribeiro, A.; Scio, E.; Del-Vechio-Vieira, G.; de Sousa, O.V.; et al. *Vernonia condensata* Baker (Asteraceae): A promising source of antioxidants. *Oxid. Med. Cell. Longev.* **2013**, *2013*, 698018.
102. Hasan, H.T.; Kadhim, E.J. Phytochemical investigation of leaves and seeds of *Corchorus olitorius* L. Cultivated in Iraq. *Asian J. Pharm. Clin. Res.* **2018**, *11*, 408–417.
103. Yin, L.; Han, H.; Zheng, X.; Wang, G.; Li, Y.; Wang, W. Flavonoids analysis and antioxidant, antimicrobial, and anti-inflammatory activities of crude and purified extracts from *Veronicastrum latifolium*. *Ind. Crops Prod.* **2019**, *137*, 652–661.
104. Amanpour, A.; Kelebek, H.; Selli, S. LC-DAD-ESI-MS/MS-based phenolic profiling and antioxidant activity in Turkish cv. Nizip Yaglik olive oils from different maturity olives. *J. Mass Spectrom.* **2019**, *54*, 227–238.
105. Ivanov, I.; Vrancheva, R.; Petkova, N.; Tumbarski, Y.; Dincheva, I.; Badjakov, I. Phytochemical compounds of anise hyssop (*Agastache foeniculum*) and antibacterial, antioxidant, and acetylcholinesterase inhibitory properties of its essential oil. *J. Appl. Pharm. Sci.* **2019**, *9*, 72–78.
106. Ren, G.; Xue, P.; Sun, X.; Zhao, G. Determination of the volatile and polyphenol constituents and the antimicrobial, antioxidant, and tyrosinase inhibitory activities of the bioactive compounds from the by-product of *Rosa rugosa* Thunb. var. plena Regal tea. *BMC Complement. Altern. Med.* **2018**, *18*, 307.
107. Tomczyk, M.; Gudej, J. Quantitative analysis of flavonoids in the flowers and leaves of *Ficaria verna* Huds. *Z. Naturforsch. C.* **2003**, *58*, 762–764.
108. Félix-Silva, J.; Gomes, J.A.S.; Fernandes, J.M.; Moura, A.K.C.; Menezes, Y.A.S.; Santos, E.C.G.; Tambourgi, D.V.; Silva-Junior, A.A.; Zucolotto, S.M.; Fernandes-Pedrosa, M.F. Comparison of two *Jatropha* species (Euphorbiaceae) used popularly to treat snakebites in Northeastern Brazil: Chemical profile, inhibitory activity against *Bothrops erythromelas* venom and antibacterial activity. *J. Ethnopharmacol.* **2018**, *213*, 12–20.
109. Sánchez-Roque, Y.; Ayora-Talavera, G.; Rincón-Rosales, R.; Gutiérrez-Miceli, F.; Meza Gordillo, R.;

- Winkler, R.; Gamboa-Becerra, R.; Ayora, T.; Ruíz-Valdiviezo, V. The flavonoid fraction from *Rhoeo discolor* leaves acts antiviral against influenza A virus. *Rec. Nat. Prod.* **2017**, *11*, 532–546.
110. Rehemani, A.; Aisa, H.A.; Ma, Q.L.; Nijat, D.; Abdulla, R. Quality evaluation of the traditional medicine majun mupakhi ELA via chromatographic fingerprinting coupled with UHPLC-DAD-Quadrupole-Orbitrap-MS and the antioxidant activity in vitro. *Evid. Based. Complement. Alternat. Med.* **2018**, *2018*, 1035809.
111. Moreno-González, R.; Juan, M.E.; Planas, J.M. Table olive polyphenols: A simultaneous determination by liquid chromatography–mass spectrometry. *J. Chromatogr. A* **2019**, 460434.
112. Luca, S.V.; Miron, A.; Aprotosoae, A.C.; Mihai, C.-T.; Vochita, G.; Gherghel, D.; Ciocarlan, N.; Skalicka-Wozniak, K. HPLC-DAD-ESI-Q-TOF-MS/MS profiling of *Verbascum ovalifolium* Donn ex Sims and evaluation of its antioxidant and cytogenotoxic activities. *Phytochem. Anal.* **2019**, *30*, 34–45.
113. Quirantes-Piné, R.; Funes, L.; Micol, V.; Segura-Carretero, A.; Fernández-Gutiérrez, A. High-performance liquid chromatography with diode array detection coupled to electrospray time-of-flight and ion-trap tandem mass spectrometry to identify phenolic compounds from a *Lemon verbena* extract. *J. Chromatogr. A* **2009**, *1216*, 5391–5397.
114. Flores-Ocelotl, M.R.; Rosas-Murrieta, N.H.; Moreno, D.A.; Vallejo-Ruiz, V.; Reyes-Leyva, J.; Dominguez, F.; Santos-López, G. *Taraxacum officinale* and *Urtica dioica* extracts inhibit dengue virus serotype 2 replication in vitro. *BMC Complement. Altern. Med.* **2018**, *18*, 95.
115. Colombo, R.; Harumi Yariwake, J.; Queiroz, E.; Ndjoko, K.; Hostettmann, K. LC-MS/MS analysis of sugarcane extracts and differentiation of monosaccharides moieties of flavone C-glycosides. *J. Liq. Chromatogr. Relat. Technol.* **2013**, *36*, 239–258.
116. Elkady, W.M.; Ibrahim, E.A.; Gonaïd, M.H.; El Baz, F.K. Chemical profile and biological activity of *Casimiroa edulis* non-edible fruit's parts. *Adv. Pharm. Bull.* **2017**, *7*, 655–660.
117. Mattila, P.; Astola, J.; Kumpulainen, J. Determination of flavonoids in plant material by HPLC with diode-array and electro-array detections. *J. Agric. Food Chem.* **2000**, *48*, 5834–5841.
118. de Beer, D.; Joubert, E.; Malherbe, C.J.; Jacobus Brand, D. Use of countercurrent chromatography during isolation of 6-hydroxyluteolin-7-O- β -glucoside, a major antioxidant of *Athrixia phyllicoides*. *J. Chromatogr. A* **2011**, *1218*, 6179–6186.
119. Ziani, B.E.C.; Barros, L.; Boumehira, A.Z.; Bachari, K.; Heleno, S.A.; Alves, M.J.; Ferreira, I.C.F.R. Profiling polyphenol composition by HPLC-DAD-ESI/MSn and the antibacterial activity of infusion preparations obtained from four medicinal plants. *Food Funct.* **2018**, *9*, 149–159.
120. Bessada, S.M.F.; Barreira, J.C.M.; Barros, L.; Ferreira, I.C.F.R.; Oliveira, M.B.P.P. Phenolic profile and antioxidant activity of *Coleostephus myconis* (L.) Rchb.f.: An underexploited and highly disseminated species. *Ind. Crops Prod.* **2016**, *89*, 45–51.
121. Llorent-Martínez, E.J.; Ortega-Barrales, P.; Zengin, G.; Uysal, S.; Ceylan, R.; Guler, G.O.; Mocan, A.; Aktumsek, A. *Lathyrus aureus* and *Lathyrus pratensis*: Characterization of phytochemical profiles by liquid chromatography-mass spectrometry, and evaluation of their enzyme inhibitory and antioxidant activities. *RSC Adv.* **2016**, *6*, 88996–89006.
122. Carvalho, A.R.; Costa, G.; Figueirinha, A.; Liberal, J.; Prior, J.A.V.; Lopes, M.C.; Cruz, M.T.; Batista, M.T. *Urtica* spp.: Phenolic composition, safety, antioxidant and anti-inflammatory activities. *Food Res. Int.* **2017**, *99*, 485–494.
123. Brito, A.; Ramirez, J.E.; Areche, C.; Sepúlveda, B.; Simirgiotis, M.J. HPLC-UV-MS profiles of phenolic compounds and antioxidant activity of fruits from three citrus species consumed in Northern Chile. *Molecules* **2014**, *19*, 17400–17421.
124. Plazonić, A.; Bucar, F.; Maleš, Ž.; Mornar, A.; Nigović, B.; Kujundžić, N. Identification and quantification of flavonoids and phenolic acids in burr parsley (*Caucalis platycarpos* L.), using high-performance liquid chromatography with diode array detection and electrospray ionization mass spectrometry. *Molecules* **2009**, *14*, 2466–2490.
125. Pereira, O.R.; Catarino, M.D.; Afonso, A.F.; Silva, A.M.S.; Cardoso, S.M. *Salvia elegans*, *Salvia greggii* and *Salvia officinalis* decoctions: Antioxidant activities and inhibition of carbohydrate and lipid metabolic enzymes. *Molecules* **2018**, *23*, E3169.
126. Afonso, A.F.; Pereira, O.R.; Neto, R.T.; Silva, A.M.S.; Cardoso, S.M. Health-promoting effects of *Thymus herba-barona*, *Thymus pseudolanuginosus*, and *Thymus caespititius* decoctions. *Int. J. Mol. Sci.* **2017**, *18*, E1879.
127. Ferreres, F.; Grosso, C.; Gil-Izquierdo, A.; Fernandes, A.; Valentão, P.; Andrade, P. Comparing the phenolic

- profile of *Pilocarpus pennatifolius* Lem. by HPLC–DAD–ESI/MSn with respect to authentication and enzyme inhibition potential. *Ind. Crops Prod.* **2015**, *77*, 391–401.
128. Otify, A.; George, C.; Elsayed, A.; Farag, M.A. Mechanistic evidence of *Passiflora edulis* (Passifloraceae) anxiolytic activity in relation to its metabolite fingerprint as revealed *via* LC-MS and chemometrics. *Food Funct.* **2015**, *6*, 3807–3817.
 129. Afifi, F.U.; Kasabri, V.; Litescu, S.; Abaza, I.F.; Tawaha, K. Phytochemical and biological evaluations of *Arum hygrophilum* Boiss. (Araceae). *Pharmacogn. Mag.* **2017**, *13*, 275–280.
 130. Kowalska, I.; Pecio, L.; Ciesla, L.; Oleszek, W.; Stochmal, A. Isolation, chemical characterization, and free radical scavenging activity of phenolics from *Triticum aestivum* L. aerial parts. *J. Agric. Food Chem.* **2014**, *62*, 11200–11208.
 131. Kostic, A.Z.; Gasic, U.M.; Pesic, M.B.; Stanojevic, S.P.; Barac, M.B.; Macukanovic-Jocic, M.P.; Avramov, S.N.; Tesic, Z.L. Phytochemical analysis and total antioxidant capacity of rhizome, above-ground vegetative parts and flower of three *Iris* species. *Chem. Biodivers.* **2019**, *16*, e1800565.
 132. Llorent-Martínez, E.J.; Córdova, M.L.F.; Zengin, G.; Bahadori, M.B.; Aumeeruddy, M.Z.; Rengasamy, K.R.R.; Mahomoodally, M.F. *Parentucellia latifolia* subsp. *latifolia*: A potential source for loganin iridoids by HPLC-ESI-MSn technique. *J. Pharm. Biomed. Anal.* **2019**, *165*, 374–380.
 133. Llorent-Martínez, E.J.; Zengin, G.; Lobine, D.; Molina-García, L.; Mollica, A.; Mahomoodally, M.F. Phytochemical characterization, *in vitro* and *in silico* approaches for three *Hypericum* species. *New J. Chem.* **2018**, *42*, 5204–5214.
 134. Öztürk, G.; Aǧalar, H.G.; Yildiz, G.; Göger, F.; Kirimer, N. Biological activities and luteolin derivatives of *Verbascum eskisehirensis* Karavel., Ocak Ekici. *J. Res. Pharm.* **2019**, *23*, 532–542.
 135. Bączek, K.B.; Wiśniewska, M.; Przybył, J.L.; Kosakowska, O.; Węglarz, Z. Arbuscular mycorrhizal fungi in chamomile (*Matricaria recutita* L.) organic cultivation. *Ind. Crops Prod.* **2019**, *140*, 111562.
 136. Gomes, A.F.; Almeida, M.P.; Leite, M.F.; Schwaiger, S.; Stuppner, H.; Halabalaki, M.; Amaral, J.G.; David, J.M. Seasonal variation in the chemical composition of two chemotypes of *Lippia alba*. *Food Chem.* **2019**, *273*, 186–193.
 137. Han, A.-R.; Nam, B.; Kim, B.-R.; Lee, K.-C.; Song, B.-S.; Kim, S.H.; Kim, J.-B.; Jin, C.H. Phytochemical composition and antioxidant activities of two different color chrysanthemum flower teas. *Molecules* **2019**, *24*, 329.
 138. Arsenijević, J.; Drobac, M.; Šoštarić, I.; Ražić, S.; Milenković, M.; Couladis, M.; Maksimović, Z. Bioactivity of herbal tea of Hungarian thyme based on the composition of volatiles and polyphenolics. *Ind. Crops Prod.* **2016**, *89*, 14–20.
 139. Cheng, S.; Shiea, J. Advanced spectroscopic detectors for identification and quantification: Mass spectrometry. In *Instrumental Thin-Layer Chromatography*; Poole, C.F., Ed.; Elsevier Inc.: Amsterdam, The Netherlands, 2015; p. 251.
 140. Shao, Y.; Wu, Q.; Wen, H.; Chai, C.; Shan, C.; Yue, W.; Yan, S.; Xu, H. Determination of flavones in *Lophatherum gracile* by liquid chromatography tandem mass spectrometry. *Instrum. Sci. Technol.* **2014**, *42*, 173–183.
 141. Sánchez-Rabáneda, F.; Jauregui, O.; Casals, I.; Andres-Lacueva, C.; Izquierdo-Pulido, M.; Lamuela-Raventós, R.M. Liquid chromatographic/electrospray ionization tandem mass spectrometric study of the phenolic composition of cocoa (*Theobroma cacao*). *J. Mass Spectrom.* **2003**, *38*, 35–42.
 142. Lin, L.-Z.; Harnly, J.M. Identification of the phenolic components of chrysanthemum flower (*Chrysanthemum morifolium* Ramat). *Food Chem.* **2010**, *120*, 319–326.
 143. Liu, R.; Yan, W.; Han, Q.; Lv, T.; Wang, X.; Liu, X.; Fan, X.; Meng, C.; Wang, C. Simultaneous detection of four flavonoids and two alkaloids in rat plasma by LC-MS/MS and its application to a comparative study of the pharmacokinetics between *Abri Herba* and *Abri mollis Herba* extract after oral administration. *J. Sep. Sci.* **2019**, *42*, 1341–1350.
 144. Ye, Y.; Mo, S.; Feng, W.; Ye, X.; Shu, X.; Long, Y.; Guan, Y.; Huang, J.; Wang, J. The ethanol extract of *Involucrum castaneae* ameliorated ovalbumin-induced airway inflammation and smooth muscle thickening in guinea pigs. *J. Ethnopharmacol.* **2019**, *230*, 9–19.
 145. Escher, G.B.; Santos, J.S.; Rosso, N.D.; Marques, M.B.; Azevedo, L.; do Carmo, M.A.V.; Daguer, H.; Molognoni, L.; Prado-Silva, L.d.; Sant’Ana, A.S.; et al. Chemical study, antioxidant, anti-hypertensive, and cytotoxic/cytoprotective activities of *Centaurea cyanus* L. petals aqueous extract. *Food Chem. Toxicol.* **2018**, *118*, 439–453.

146. Janković, T.; Zdunić, G.; Beara, I.; Balog, K.; Pljevljakušić, D.; Stešević, D.; Šavikin, K. Comparative study of some polyphenols in *Plantago* species. *Biochem. Syst. Ecol.* **2012**, *42*, 69–74.
147. Pintać, D.; Četojević-Simin, D.; Berežni, S.; Orčić, D.; Mimica-Dukić, N.; Lesjak, M. Investigation of the chemical composition and biological activity of edible grapevine (*Vitis vinifera* L.) leaf varieties. *Food Chem.* **2019**, *286*, 686–695.
148. Lin, L.-Z.; Lu, S.; Harnly, J.M. Detection and quantification of glycosylated flavonoid malonates in celery, Chinese celery, and celery seed by LC-DAD-ESI/MS. *J. Agric. Food Chem.* **2007**, *55*, 1321–1326.
149. Siciliano, T.; De Tommasi, N.; Morelli, I.; Braca, A. Study of flavonoids of *Sechium edule* (Jacq) Swartz (Cucurbitaceae) different edible organs by liquid chromatography photodiode array mass spectrometry. *J. Agric. Food Chem.* **2004**, *52*, 6510–6515.
150. Işcan, G.; Göger, F.; Demirci, B.; Köse, Y.B. Chemical composition and biological activity of *Nepeta cilicica*. *Bangladesh J. Pharmacol.* **2017**, *12*, 204–209.
151. Choi, J.Y.; Desta, K.T.; Lee, S.J.; Kim, Y.-H.; Shin, S.C.; Kim, G.-S.; Lee, S.J.; Shim, J.-H.; Hacimüftüoğlu, A.; Abd El-Aty, A.M. LC-MS/MS profiling of polyphenol-enriched leaf, stem and root extracts of Korean *Humulus japonicus* Siebold & Zucc and determination of their antioxidant effects. *Biomed. Chromatogr.* **2018**, *32*, e4171.
152. Haliloglu, Y.; Ozek, T.; Tekin, M.; Goger, F.; Baser, K.H.C.; Ozek, G. Phytochemicals, antioxidant, and antityrosinase activities of *Achillea sivasica* Çelik and Akpulat. *Int. J. Food Prop.* **2017**, *20*, S693–S706.
153. Graça, V.C.; Dias, M.I.; Barros, L.; Calhelha, R.C.; Santos, P.F.; Ferreira, I.C.F.R. Fractionation of the more active extracts of *Geranium molle* L.: A relationship between their phenolic profile and biological activity. *Food Funct.* **2018**, *9*, 2032–2042.
154. Pereira, J.M.; Peixoto, V.; Teixeira, A.; Sousa, D.; Barros, L.; Ferreira, I.C.F.R.; Vasconcelos, M.H. *Achillea millefolium* L. hydroethanolic extract inhibits growth of human tumor cell lines by interfering with cell cycle and inducing apoptosis. *Food Chem. Toxicol.* **2018**, *118*, 635–644.
155. Gonçalves, G.A.; Corrêa, R.C.G.; Barros, L.; Dias, M.I.; Calhelha, R.C.; Correa, V.G.; Bracht, A.; Peralta, R.M.; Ferreira, I.C.F.R. Effects of in vitro gastrointestinal digestion and colonic fermentation on a rosemary (*Rosmarinus officinalis* L) extract rich in rosmarinic acid. *Food Chem.* **2019**, *271*, 393–400.
156. Soltana, H.; De Rosso, M.; Lazreg, H.; Vedova, A.D.; Hammami, M.; Flamini, R. LC-QTOF characterization of non-anthocyanic flavonoids in four Tunisian fig varieties. *J. Mass Spectrom.* **2018**, *53*, 817–823.
157. Gaspar, M.C.; Fonseca, D.A.; Antunes, M.J.; Frigerio, C.; Gomes, N.G.M.; Vieira, M.; Santos, A.E.; Cruz, M.T.; Cotrim, M.D.; Campos, M.G. Polyphenolic characterisation and bioactivity of an *Oxalis pes-caprae* L. leaf extract. *Nat. Prod. Res.* **2018**, *32*, 732–738.
158. Kite, G.C.; Porter, E.A.; Denison, F.C.; Grayer, R.J.; Veitch, N.C.; Butler, I.; Simmonds, M.S.J. Data-directed scan sequence for the general assignment of C-glycosylflavone O-glycosides in plant extracts by liquid chromatography-ion trap mass spectrometry. *J. Chromatogr. A* **2006**, *1104*, 123–131.
159. Paulina Tambunan, A.; Bahtiar, A.; Tjandrawinata, R. Influence of extraction parameters on the yield, phytochemical, TLC-densitometric quantification of quercetin, and LC-MS profile, and how to standardize different batches for long term from *Ageratum conyzoides* L. leaves. *Pharmacogn. J.* **2017**, *9*, 767–774.
160. Mincsovcics, E.; Ott, P.; Alberti, A.; Böszörményi, A.; Héthelyi, E.B.; Szoke, É.; Kery, A.; Lemberkovics, E.; Móricz, Á. In-situ clean-up and OPLC fractionation of chamomile flower extract to search active components by bioautography. *JPC J. Planar Chromatogr.* **2013**, *26*, 172–179.
161. Alves, G. de A.D.; Oliveira de Souza, R.; Ghislain Rogez, H.L.; Masaki, H.; Fonseca, M.J.V. *Cecropia obtusa* extract and chlorogenic acid exhibit anti aging effect in human fibroblasts and keratinocytes cells exposed to UV radiation. *PLoS ONE* **2019**, *14*, e0216501.
162. Ghouti, D.; Rached, W.; Abdallah, M.; Pires, T.C.S.P.; Calhelha, R.C.; Alves, M.J.; Abderrahmane, L.H.; Barros, L.; Ferreira, I.C.F.R. Phenolic profile and in vitro bioactive potential of Saharan *Juniperus phoenicea* L. and *Cotula cinerea* (Del) growing in Algeria. *Food Funct.* **2018**, *9*, 4664–4672.
163. Venuprasad, M.P.; Kandikattu, H.K.; Razack, S.; Amruta, N.; Khanum, F. Chemical composition of *Ocimum sanctum* by LC-ESI-MS/MS analysis and its protective effects against smoke induced lung and neuronal tissue damage in rats. *Biomed. Pharmacother.* **2017**, *91*, 1–12.
164. Majchrzak, T.; Wojnowski, W.; Lubinska-Szczygeł, M.; Różańska, A.; Namieśnik, J.; Dymerski, T. PTR-MS and GC-MS as complementary techniques for analysis of volatiles: A tutorial review. *Anal. Chim. Acta* **2018**, *1035*, 1–13.
165. Nolvachai, Y.; Marriott, P.J. GC for flavonoids analysis: Past, current, and prospective trends. *J. Sep. Sci.*

- 2013, 36, 20–36.
166. Zhang, K.; Zuo, Y. GC-MS determination of flavonoids and phenolic and benzoic acids in human plasma after consumption of cranberry juice. *J. Agric. Food Chem.* **2004**, *52*, 222–227.
167. Creaser, C.S.; Koupai-Abyazani, M.R.; Stephenson, G.R. Capillary column gas chromatography of methyl and trimethylsilyl derivatives of some naturally occurring flavonoid aglycones and other phenolics. *J. Chromatogr. A* **1989**, *478*, 415–421.
168. Schmidt, T.J.; Merfort, I.; Matthiesen, U. Resolution of complex mixtures of flavonoid aglycones by analysis of gas chromatographic-mass spectrometric data. *J. Chromatogr. A* **1993**, *634*, 350–355.
169. Proestos, C.; Sereli, D.; Komaitis, M. Determination of phenolic compounds in aromatic plants by RP-HPLC and GC-MS. *Food Chem.* **2006**, *95*, 44–52.
170. García-Villalba, R.; Pacchiarotta, T.; Carrasco-Pancorbo, A.; Segura-Carretero, A.; Fernández-Gutiérrez, A.; Deelder, A.M.; Mayboroda, O.A. Gas chromatography–atmospheric pressure chemical ionization-time of flight mass spectrometry for profiling of phenolic compounds in extra virgin olive oil. *J. Chromatogr. A* **2011**, *1218*, 959–971.
171. Gao, X.; Williams, S.J.; Woodman, O.L.; Marriott, P.J. Comprehensive two-dimensional gas chromatography, retention indices and time-of-flight mass spectra of flavonoids and chalcones. *J. Chromatogr. A* **2010**, *1217*, 8317–8326.
172. Krafczyk, N.; Glomb, M.A. Characterization of phenolic compounds in rooibos tea. *J. Agric. Food Chem.* **2008**, *56*, 3368–3376.
173. Peng, J.; Fan, G.; Hong, Z.; Chai, Y.; Wu, Y. Preparative separation of isovitexin and isoorientin from *Patrinia villosa* Juss by high-speed counter-current chromatography. *J. Chromatogr. A* **2005**, *1074*, 111–115.
174. Waksmundzka-Hajnos, M.; Sherma, J.; Kowalska, T. Overview of the field of TLC in phytochemistry and the structure of the book. In *Thin Layer Chromatography in Phytochemistry*; Waksmundzka-Hajnos, M., Sherma, J., Kowalska, T., Eds.; CRC Press, Taylor & Francis Group: Boca Raton, FL, USA, 2008; p. 5.
175. Skalicka-Woźniak, K.; Mroczek, T.; Koziol, E. High-performance countercurrent chromatography separation of *Peucedanum cervaria* fruit extract for the isolation of rare coumarin derivatives. *J. Sep. Sci.* **2015**, *38*, 179–186.
176. Sieniawska, E.; Skalicka-Woźniak, K. Isolation of chlorogenic acid from *Mutellina purpurea* L. herb using high-performance counter-current chromatography. *Nat. Prod. Res.* **2014**, *28*, 1936–1939.
177. Wang, X.; Cheng, C.; Sun, Q.; Li, F.; Liu, J.; Zheng, C. Isolation and purification of four flavonoid constituents from the flowers of *Paeonia suffruticosa* by high-speed counter-current chromatography. *J. Chromatogr. A* **2005**, *1075*, 127–131.
178. Leitão, S.G.; Leitão, G.G.; Vicco, D.K.T.; Pereira, J.P.B.; de Moraes Simão, G.; Oliveira, D.R.; Celano, R.; Campone, L.; Piccinelli, A.L.; Rastrelli, L. Counter-current chromatography with off-line detection by ultra high performance liquid chromatography/high resolution mass spectrometry in the study of the phenolic profile of *Lippia organoides*. *J. Chromatogr. A* **2017**, *1520*, 83–90.
179. Fiamegos, Y.C.; Nanos, C.G.; Vervoort, J.; Stalikas, C.D. Analytical procedure for the in-vial derivatization–extraction of phenolic acids and flavonoids in methanolic and aqueous plant extracts followed by gas chromatography with mass-selective detection. *J. Chromatogr. A* **2004**, *1041*, 11–18.



© 2019 by the authors. Licensee MDPI, Basel, Switzerland. This article is an open access article distributed under the terms and conditions of the Creative Commons Attribution (CC BY) license (<http://creativecommons.org/licenses/by/4.0/>).

Publication IV

Juszczak A.M., Wöelfle U., Zovko Končić M., Tomczyk M.: Skin cancer, including related pathways and therapy and the role of luteolin derivatives as potential therapeutics. *Medicinal Research Reviews* Vol. n/a, n/a , 2022, 40 pages.
DOI: 10.1002/med.21880

Skin cancer, including related pathways and therapy and the role of luteolin derivatives as potential therapeutics

Aleksandra M. Juszczak¹ | Ute Wöelfle² |
 Marijana Zovko Končić³ | Michał Tomczyk¹

¹Department of Pharmacognosy, Faculty of Pharmacy with the Division of Laboratory Medicine, Medical University of Białystok, Białystok, Poland

²Department of Dermatology and Venereology, Research Center Skinital, Medical Center, Faculty of Medicine, University of Freiburg, Freiburg, Germany

Abstract

Cutaneous malignant melanoma is the fastest growing and the most aggressive form of skin cancer that is diagnosed. However, its incidence is relatively scarce compared to the highest mortality rate of all skin cancers. The much more common skin cancers include nonmelanoma malignant

Abbreviations: ADAMTS, a disintegrin and metalloproteinase with thrombospondin motifs; AhR, aryl hydrocarbon receptors; AIDS, acquired immunodeficiency syndrome; AK, actinic keratoses; AKT, protein kinase B; AP-1, activator protein-1; ATP, adenosine triphosphate; Bax, Bcl-2-associated X; BCC, basal cell carcinoma; Bcl-2, B-cell lymphoma 2; BRAF, v-raf murine sarcoma viral oncogene homolog B; cAMP, cyclic adenosine monophosphate; CDK4, cyclin-dependent kinase 4; CDKN2A, cyclin-dependent kinase inhibitor 2A; CDKN2B, cyclin-dependent kinase inhibitor 2B; CHOP, CCAAT/enhancer-binding protein-homologous protein; CMM, cutaneous malignant melanoma; COX-2, cyclooxygenase-2; CREB, cAMP response element-binding protein; CTLA-4, cytotoxic T-lymphocyte-associated protein 4; CTS, cathepsins; c-KIT, tyrosine-protein kinase Kit; DCT, dopachrome tautomerase; DDB2, damage specific DNA binding protein 2; DNMTs, DNA methyltransferases; DTIC, dacarbazine; ECM, extracellular matrix; EDF, European Dermatology Forum; EGF, epidermal growth factor; EGFR, EGF receptor; EMT, epithelial-mesenchymal transition; ER, endoplasmic reticulum; ERK, extracellularly-regulated kinase; EZH2, enhancer of zeste homolog 2; FAK, focal adhesion kinase; FDA, U.S. Food and Drug Administration; FGF10, fibroblast growth factor 10; FN1, fibronectin 1; GANAB, glucosidase II alpha subunit; GDP, guanosine diphosphate; GM-CSF, granulocyte macrophage colony-stimulating factor; GTP, guanosine triphosphate; H3K27me3, trimethylation in histone H3 at lysine 27; HPV, β human papillomavirus; IARC, International Agency for Research on Cancer; ICAM1, intercellular adhesion molecule-1; IFN- α , interferon- α ; IFN- γ , interferon- γ ; IKK, inhibitory- κ B kinase; IL-1 α , interleukin 1 α ; IL-1 β , interleukin 1 β ; IL-2, interleukin 2; IL-3 β , interleukin 3 β ; IL-6, interleukin 6; ITGa2B, integrin α 2B; ITG β 3, integrin β 3; JNK, c-Jun N-terminal kinase; KIT, type III transmembrane receptor tyrosine kinase; KSR2, kinase suppressor of RAS 2; LAMA1, laminin subunit alpha 1; MAPK, the mitogen-activated protein kinase; MC1R, melanocortin-1-receptor; MEK, mitogen-activated protein kinase; MHC, major histocompatibility complex; MITF, microphthalmia-associated transcription factor; MMP, matrix metalloproteinase; MTT, 3-(4,5-dimethylthiazol-2-yl)-2,5-diphenyltetrazolium bromide; NDPK, nucleoside diphosphate kinase; NF1, neurofibromin type 1; NF- κ B, nuclear factor kappa-light-chain-enhancer of activated B; NMSC, non-melanoma malignant skin cancers; NRAS, neuroblastoma RAS viral oncogene homolog; Nrf2, nuclear factor 2 associated erythroid 2; PDIA3, protein disulfide-isomerase A3; PD-1, programmed death-1; PD-L1, programmed death ligand-1; PI3K, phosphoinositol-3-kinase; PKCe, protein kinase C ϵ ; PTEN, phosphatase and tensin homolog; RAF, rapidly accelerated fibrosarcoma; RAS, rat sarcoma viral oncogene; ROS, reactive oxygen species; RTK, tyrosine kinase receptors; SAR, structure-activity relationship; SCC, squamous cell carcinoma; SHH, sonic hedgehog; SRB, sulforhodamine B; Src, steroid receptor coactivator; STAT1, signal transducer and activator of transcription 1; STAT3, signal transducer and activator of transcription 3; TET1, ten-eleven translocation-1; TGF, tumor growth factor; TIMP, tissue inhibitor of MMP; TLR, toll-like receptor; TNF, tumor necrosis factor; TNF- α , tumor necrosis factor α ; TRAIL, TNF- α -related apoptosis-inducing ligand; TRP, transient receptor potential; TYR, tyrosinase; UV, ultraviolet; VEGF, vascular endothelial growth factor; XTT, 2,3-bis-(2-methoxy-4-nitro-5-sulphophenyl)-2H-tetrazolium-5-carboxanilide.; α -MSH, α -melanocyte stimulating hormone.

This is an open access article under the terms of the Creative Commons Attribution-NonCommercial License, which permits use, distribution and reproduction in any medium, provided the original work is properly cited and is not used for commercial purposes. © 2022 The Authors. *Medicinal Research Reviews* published by Wiley Periodicals LLC

³Department of Pharmacognosy, Faculty of Pharmacy and Biochemistry, University of Zagreb, Zagreb, Croatia

Correspondence

Michał Tomczyk, Department of Pharmacognosy, Faculty of Pharmacy with the Division of Laboratory Medicine, Medical University of Białystok, ul Mickiewicza 2a, 15-230 Białystok, Poland.
Email: michal.tomczyk@umb.edu.pl

Funding information

European Union funds, POWER 2014-2020, Grant/Award Numbers: POWR.03.02.00-00-1051/16, 05/IMSD/G/2019

skin cancers. Moreover, over the past several decades, the frequency of all skin cancers has increased much more dynamically than that of almost any other type of cancer. Among the available therapeutic options for skin cancers, chemotherapy used immediately after the surgical intervention has been an essential element. Unfortunately, the main problem with conventional chemopreventive regimens involves the lack of response to treatment and the associated side effects. Hence, there is a need for much more effective anticancer drugs. Correspondingly, the targeted alternatives have involved phytochemicals, which are safer chemotherapeutic agents and exhibit competitive anticancer activity with high therapeutic efficacy. Among polyphenolic compounds, some flavonoids and their derivatives, which are mostly found in medicinal plants, have been demonstrated to influence the modulation of signaling pathways at each stage of the carcinogenesis process, which is also important in the context of skin cancers. Hence, this review focuses on an exhaustive overview of the therapeutic effects of luteolin and its derivatives in the treatment and prevention of skin cancers. The bioavailability and structure–activity relationships of luteolin derivatives are also discussed. This review is the first such complete account of all of the scientific reports concerning this particular group of natural compounds that target a specific area of neoplastic diseases.

KEYWORDS

luteolin, melanoma, phytotherapy, skin cancer

1 | INTRODUCTION

Cutaneous malignant melanoma (CMM) is the fastest growing cancer in the fair-skinned Caucasian population and the most aggressive form of diagnosed skin cancer. Its incidence is less than 5% per year, which is relatively low compared to its high mortality rate, which is the highest of all skin cancers. However, over the past several decades, the incidence of CMM has increased much more rapidly than that of almost any other cancer.¹ According to the GLOBOCAN 2020 database (<https://gco.iarc.fr/today/home>) published by the International Agency for Research on Cancer (IARC), non-melanoma malignant skin cancers (NMSCs) are the most common skin cancers, accounting for 30% of the cancer burden, with an estimated incidence of over 350,000 cases per year only in Europe, making them the most common malignant neoplasms in white populations each year. The term NMSC encompasses basal cell carcinoma (BCC) and squamous cell carcinoma (SCC), which account for

90% of the tumors of this type.^{2,3} The term is also used in reference to adnexal tumors, cutaneous lymphomas, Merkel cell carcinoma, and other rare primary skin cancers. The incidence of NMSC (BCC and SCC) is 18- to 20-fold higher than that of malignant melanoma.⁴⁻⁸

The reported dramatic increase in skin cancer incidence is mainly attributed to chronic ultraviolet (UV) exposure and to skin type, which are the dominant risk factors. Additionally, personal factors such as age, sex, and genetic background contribute to CMM susceptibility and are mainly attributed to the melanin content in skin layers. Another important aspect is the inheritance of skin cancer susceptibility associated with low and high penetrance genes described in the following sections.³ The incidence of melanoma increases with age, as evidenced by the data showing that the average age of diagnosis is approximately 60 years. The risk of occurrence is also closely related to sex. The incidence of melanoma in men is 1.5-fold greater than it is in women. The relationship between incidence and age becomes very clear in people older than 75 years, when the incident coefficient increases twofold. Additionally, geographic zone, common or atypical nevi, and chronic sun exposure, especially in childhood, are suggested to be major environmental risk factors for melanoma.^{6,9,10} The relationship is evident in the correlation between the risk of BCC and the "history" of UV ray overexposure, particularly sunburn, especially in childhood. However, these factors do not translate into SCC, the risk of which is closely related to long-term UV exposure.¹¹ In contrast to that of melanoma, the incidence of NMSC has been proven to be closely related to age. At an early age, people of either sex show a similar prevalence for acquiring either NMSC. The situation changes for men older than 45 years, because NMSC affects this group of men 2- to 3-fold more frequently than women.^{3,5,6,12-15}

Among the available therapeutic options for skin cancer, chemotherapy administered immediately after surgical intervention has been an essential element of the available anticancer therapies for decades. Unfortunately, the main problem with conventional chemopreventive regimens is the lack of response to treatment. Hence, there is a need for much more effective anticancer drugs. Moreover, inherent side effects are other problems with currently available chemotherapeutics. Therefore, alternatives based on phytochemicals have been used because they are safer than traditional chemotherapeutic agents and exhibit competitive anticancer activity with high therapeutic efficacy.¹⁶ Currently, of all cancer therapeutics approved by the U.S. Food and Drug Administration (FDA), as many as 40% are directly or indirectly related to natural sources.¹⁷ Notably, cytostatic compounds including vincristine, vinblastine, vinorelbine, paclitaxel, docetaxel, topotecan, irinotecan, and others are only some examples of the anticancer drugs and plant-derived agents approved for clinical use.¹⁸⁻²⁰ The current state of knowledge supports evidence of the beneficial effects of combination therapies consisting of conventional anticancer drugs and natural compounds.²¹ Medicinal plants and their bioactive compounds have been successfully used for years as complementary therapies. In addition, the research performed with multiple cancer cell lines and animal models including skin cancer proves that these combinations can suppress many stages of development and progression of cancer cells by influencing a number of mechanisms, such as the cell cycle, and by inhibiting angiogenesis and proliferation or activating proapoptotic and pro-survival proteins.²²⁻²⁵ Currently, various formulations in the market contain compounds of natural origin for use in skin cancer or precancerous conditions such as *Birch Bark ointment*, *Curaderm*[®], or *Cansema*[®].²⁶ Among the groups of phytochemicals studied thus far, flavonoids constitute a class of secondary plant metabolites showing potent anticancer activity, particularly in the context of skin cancer, by modulating signaling pathways at each stage of carcinogenesis.^{18,27} However, in a search of literature published worldwide, only general reviews of the broadly understood anticancer activity of flavonoids can be found. Contrary to similar manuscripts, our review describes the therapeutic effects of luteolin²² and its derivatives in treating and preventing skin cancers, both NMSCs and melanoma, which significantly distinguishes our review from others. The bioavailability and structure-activity relationships (SARs) of luteolin and its derivatives are described, making this report the

first comprehensive and complete account of all scientific reports concerning this particular group of natural compounds targeting specific neoplastic diseases.

2 | METHODOLOGY/SEARCH STRATEGY

A comprehensive search analysis was performed to identify relevant scientific literature on the basis of an appropriate search string entered in relevant subject databases. The electronic databases of SCOPUS, Google Scholar, PubMed/MEDLINE, Web of Science (SCI-EXPANDED), Taylor & Francis Online, Wiley Online Library, EBSCO Discovery Service (EDS), REAXYS Database, and Science Direct/ELSEVIER were extensively searched in the preparation of this review. Clinical trial information was retrieved from the [ClinicalTrials.gov](https://www.clinicaltrials.gov) database. Chemical structures were confirmed with entries in the PubChem and REAXYS databases. Titles, abstracts, and keywords (TITLE-ABS-KEY) contained in these databases were searched using the following terms separately or in various combinations taking into account the requirements or limitations of the databases searched in the first screening step: "luteolin," OR "luteolin derivatives," OR "natural compounds," OR "flavonoids," OR "melanoma," OR "skin cancer," OR "cutaneous melanoma," OR "skin melanoma," OR "non-melanoma malignant skin cancers," OR "basal cell carcinoma," OR "squamous cell carcinoma," OR "skin basal cell carcinoma," OR "skin squamous cell carcinoma," OR "SCC," OR "BCC," OR "anticancer activity," OR "chemopreventive activity." The search was restricted to studies written in the English language. Only articles published between 1994 and 2021, which includes the first scientific report on the activity of the tested group of compounds in the context of skin cancer therapy or prevention, were retained. The second screening was based on full texts. Additional papers were identified from the review articles and reference lists identified in the initial literature searches.

2.1 | Inclusion and exclusion criteria

Studies conducted on models of skin melanoma and other skin neoplasms treated with luteolin and/or its derivatives and that included an evaluation of the preventive and/or antitumor effects of these natural compounds were retained. The inclusion criteria of the published studies were (1) research model criteria were adopted with in vitro and/or in vivo models and/or clinical trials of skin cancer treatments, (2) preventive and/or antitumor effects of pure compounds (luteolin and/or its derivatives) and/or plant extracts rich in luteolin and/or its derivatives were administered to the adopted models, (3) the criteria for the antitumor response were defined for each documented experiment (with an IC_{50} value above the concentration of the tested compounds) affecting the proliferation of cancer cells, (4) the research was reported in full, (5) the paper was published in the English language, and (6) the article was published after the first scientific report on the activity of the tested group of compounds and/or plant extracts containing the tested compounds on an adopted research model and before July 2021.

The exclusion criteria for the published articles were (1) studies on melanoma but not skin melanoma, (2) studies on cancers such as squamous cell carcinoma, SCC or basal cell carcinoma, or BCC but not in skin, (3) studies that reported preventive and/or antitumor activity of natural compounds on the adopted models but not of luteolin or a luteolin derivative, (4) studies that reported preventive and/or antitumor activity of flavonoids on the adopted models but not luteolin or a luteolin derivative, (5) studies that reported preventive and/or antitumor activity of synthetic drugs on the adopted models, (6) papers not published in the English language, and (7) study results presented in the form of a letter to the editor, a commentary, a preface, an abstract without full accompanying paper, a conference paper or a book review.

3 | SKIN CANCERS

3.1 | Non-melanoma malignant skin cancers

3.1.1 | Basal cell carcinomas

BCC, the most common skin cancer, is characterized by low malignancy and limited local invasiveness.^{3,28} However, the term semi-malignant appears in the context of BCC, particular with respect to rare metastases, occasional aggressive growth with tissue destruction, and involvement of lymph nodes.^{29,30} BCC develops de novo from cutaneous keratinocytes and is caused by UV-induced mutations in basal layer cells of the epidermis and its appendages.

Most often, BCC is located in areas exposed to direct sunlight, such as facial skin, especially above the line connecting the angle of the mouth with the opening of the external auditory canals, as well as the backs of the hands; however, it can occur anywhere on the body. Early cases of BCC usually appear as a translucent or pearly small papule, sometimes with visible telangiectasia. The BCC growth rate is slow, and its metastasis is sporadic. BCC consists of the following subtypes, which are distinguished on the basis of physical characteristics and histological findings: nodular, superficial, and morphea forms, accounting for 60%, 30%, and 5%–10% of cases, respectively.^{5,7,8,31}

3.1.2 | Squamous cell carcinomas

SCC is caused by malignant neoplasia of epidermal keratinocytes with variable squamous differentiation, local infiltration, and invasion into surrounding tissues.^{3,28} In contrast to BCC, SCC can arise from precursor lesions, including actinic keratoses (AKs) and SCC in situ, a condition called Bowen's disease, which is much more invasive and metastatic than BCC, mainly spreading to lymph nodes. SCC metastasis is the result of a complex process leading to the migration of cancer cells through the extracellular matrix (ECM), which is also degraded by proteases. AKs progress to SCC in 1%–10% of cases, a percentage that increases with the number of lesions on the patient, and the incidence of Bowen's disease derived from AKs is 3%–5%.

SCC lesions are most often located on sun-exposed skin areas, such as the back of the hands, ears, scalp, and central part of the face, which results in photodamage of the skin. Only in rare cases, they develop elsewhere on the body.² Characteristic SCC lesions are erythematous papules with well-limited edges. The first symptom of malignancy is induration, which is common to all SCCs.^{5,8,32}

3.2 | Melanoma

The European Dermatology Forum (EDF) Society defines melanoma as the most malignant skin cancer arising from pigmented nevi, mainly in atypical or unchanged skin, and tends toward early metastasis.^{1,33,34} The melanocytes located in the basal layer of the epidermis break away, causing uncontrolled malignant proliferation.

The clinicopathological classification of invasive melanoma is based on Clark and McGovern's proposal: superficial, lentigo maligna, nodular, and acral lentiginous melanoma.^{28,35} The most common type, accounting for 75% of all malignant melanomas, is superficial melanoma. A characteristic histological feature is the radial growth of the plaque into deeper layers of tissue past the papillary dermis and the dermal layer via single-cell dispersion. The most common localization of superficial melanoma is the surface of the back in men and the lower extremities in women and manifest, where the lesions feature irregular borders and asymmetrical shapes. In addition, the lesions have no characteristic color; melanoma can present as white, gray, blue, red, brown, and black.^{4,36,37} Lentigo

maligna melanoma is the second most common type. Most often, this form develops in areas exposed to direct sunlight, showing itself as a small macule with an asymmetric shape with an irregular border. Its size and color change as the tumor grows. Nodular melanoma constitutes 15%–30% of aggressive melanomas. It manifests as dark polypoid or pedunculated nodules with a rather small surface area because it grows rapidly deep into the skin layers and relatively slowly in width on the exposed layer. This growth pattern makes late diagnosis likely. The least common melanoma is acral lentiginous melanoma, accounting for only 5% of cases. Acral lentiginous lesions most often appear on the back of the hands, on the palmar side, and in subungual areas, where it appears as a change in pigmentation in the nail plate to dark brown or black.^{5,38,39} Despite the information obtained through the continuous development of clinical, histological, and biochemical methods, the course of melanoma remains very unpredictable. Melanoma is an aggressive malignant neoplasm that, despite favorable survival rates upon detection at an early stage, metastasizes beyond the primary site. In cases of metastases, the therapy options are quite limited because of the resistance to treatment, and the prognosis for patients is bleak.^{1,30,40–42}

4 | CAUSATIVE FACTORS AND PATHOGENESIS OF SKIN CANCERS

The complex process of skin carcinogenesis resulting from the clonal spread of mutated cells begins with neoplasm initiation and continues with the promotion and progression of neoplastic cells. In the irreversible stage of initiation, genotoxic effects influence normal cells, and in the next stage, the proliferation of initiated cells is reversible, but these cells ultimately progress through a subsequent stage of irreversible malignant transformation characterized by specific karyotypic instability; id est, the distinct stages involve promotion and progression of the malignancy, respectively.⁴³ Cells that undergo malignant transformation during cancer progression are predisposed to angiogenic responses and unlimited proliferation with the involvement of surrounding tissues and metastases, simultaneously triggering protective mechanisms against therapeutic proliferation-limiting pathways.^{44,45} This process is induced via complicated interactions between genetic and environmental factors such as UV radiation, genetic mutations, oncogene activation, malignancy suppressor gene deactivation, and DNA repair process disorder (Figure 1).^{3,5} In addition to UV radiation, many triggers are associated with skin cancers. Melanoma is defined

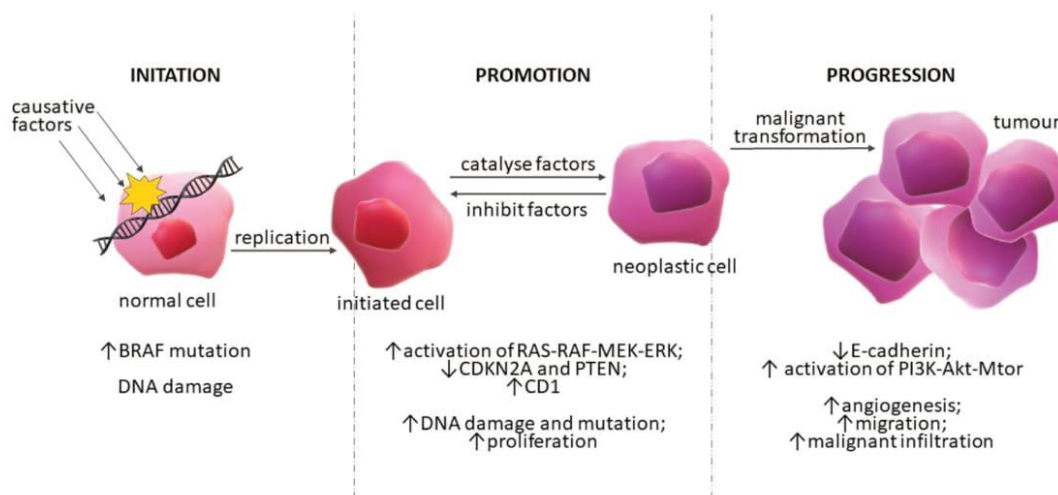


FIGURE 1 Skin carcinogenesis. Schematic representation of three steps in the process of carcinogenesis initiated by causative factors and a proposed mechanism of melanoma progression. Each stage of the depicted process includes associated mutations in key genes, changes in the cells, and the reversibility of the process [Color figure can be viewed at wileyonlinelibrary.com]

as an immunogenic neoplasm, as evidenced by the high morbidity in people with treatment-induced immunosuppression or with acquired immunodeficiency syndrome (AIDS). Additionally, patients taking immunosuppressants are also at high risk for developing SCC. In the case of BCC, chronic exposure to arsenic or a diagnosis of basal cell nevus syndrome (Gorlin syndrome) is a factor, and in the case of SCC, epidermolysis bullosa syndromes, chronic inflammation caused by damage to the skin, and mechanical irritation such as burn scars are factors. SCCs located within genital organs are often associated with the presence of the potentially oncogenic β human papillomavirus (HPV). HPV impairs the DNA repair process, driving carcinogenesis.^{4,5,46-51}

The multifactorial pathogenesis of skin cancers in the greatest number of cases begins with UV radiation exposure, resulting in a cascade of direct and indirect effects, such as DNA damage, gene mutations, immunosuppression, formation of cyclobutane pyrimidine dimers, oxidative stress, and inflammation. Chronic inflammation is characteristic of the pathogenesis of neoplasms, including skin cancers. Inflammation caused by exposure to UV radiation occurs through several mechanisms. In one mechanism, the levels of reactive oxygen species (ROS); cytokines, such as tumor necrosis factor α (TNF- α), interleukin 6 (IL-6), interleukin 1 β (IL-1 β), cyclooxygenase-2 (COX-2); and prostaglandin metabolites are increased.⁵²⁻⁵⁴ In another mechanism aryl hydrocarbon receptors (AhR) in keratinocytes and melanocytes are activated after binding of polycyclic aromatic hydrocarbons and organic environmental pollutants, leading to AhR-mediated induction of monooxygenases cytochrome P450 (CYP), CYP1A1 and CYP1A2, important enzymes in the metabolism of xenobiotics and often results in excessive generation of ROS, causing oxidative stress, inflammation, and carcinogenesis.⁵⁵⁻⁵⁷ Moreover, it has been shown that UV radiation exposure influences the course of all the above-mentioned stages of skin carcinogenesis, although the exact mechanism of action in the promotion and progression stages is unclear.^{45,58} UV rays degrade keratinocytes and melanocytes, causing malignant mutations, which are especially prevalent in fair skin, which has a low level of dark pigment (eumelanin) to block UV radiation. A correlation has been found between the occurrence of melanoma and increased melanogenesis and overexpression of melanogenic enzymes such as tyrosinase (TYR).^{59,60} Hence, blood TYR is measured as a marker in the diagnosis of melanoma.^{61,62} In addition to skin complexion, the harmful mutational UV effect is exacerbated by ozone depletion, latitude, and other factors.^{54,63,64} UVB radiation is much more mutagenic than UVA radiation; it induces changes in adjacent pyrimidines, contributing to the formation of mutagenic cyclopurimidine dimers and pyrimidine-pyrimidine adducts. UVA changes DNA through oxidative stress.^{8,65,66} As mentioned, low- and high-risk genes are essential in the process of skin cancer formation. The former includes the melanocortin-1-receptor (MC1R), which is closely related to the repair of UV-damaged DNA and the adaptive pigmentation response by encoding the α -melanocyte-stimulating hormone (α -MSH) receptor critical for melanin synthesis.⁶³ Key elements in skin cancer and its clinical evaluation are apoptotic pathways such as the tumor suppressors p53, tumor necrosis factor (TNF)-related apoptosis-inducing ligand (TRAIL), COX-2, nuclear factor kappa-light-chain-enhancer of activated B (NF- κ B), epidermal growth factor (EGF) receptor (EGFR), mitogen-activated protein kinase (MAPK) pathways and the sonic hedgehog (SHH) signaling.^{8,63,64,67}

A significant portion of NMSC cases, as many as 90% SCC and 50% BCC cases, present with mutation in the p53 suppressor gene inherently involved in cell cycle regulation, apoptosis, and DNA repair through its effect on genes such as p21, Fas, and damage specific DNA binding protein 2 (DDB2).^{68,69} p53 mutation is rarely found in melanoma. UV ray-induced mutation results in the induction of NMSC through resistance to apoptosis and clonal keratinocyte expression. Additionally, in SCC and melanoma, p53 has been observed to upregulate Fas/FasL pathway component expression, inducing apoptosis after binding of the Fas receptor to the FasL under physiological conditions. UV radiation exposure inhibits the expression of the death receptor characteristic in TRAIL, as observed in AK and SCC.^{8,63,70} Equally important in the pathogenesis of skin cancers, specific binding of EGFR, belonging to the tyrosine kinase receptor (RTK) family, and involved in most cell signaling processes, such as growth, proliferation, migration, differentiation and cell apoptosis, is changed in a manner measurable by immunohistochemistry. EGFR changes are detected in most cases of NMSC. Overexpression of EGFR in SCC cells contributes to the acquisition of the aggressive phenotype. Activation of EGFR is mediated not only by EGF but also by heparin binding and is a consequence of tumor growth factor (TGF) and amphiregulin activation. Active EGFR forms complexes with signaling proteins including Shc, steroid receptor coactivator (Src), leading to activation of

MAPK and the phosphoinositol-3-kinase (PI3K) pathways, ultimately leading to cell proliferation, apoptosis, tumor development, cancer cell migration, and metastasis.^{63,71–74}

Other RTKs in NMSC are also associated with disruptions to the signaling of the complex NF- κ B pathway induced directly by free radicals, carcinogens, X-rays, and UV radiation or indirectly by binding of cytokines to plasma membrane receptors under the influence of UV radiation.⁶⁸ NF- κ B controls many physiological processes and cell proliferation by regulating the cell cycle, apoptosis, and inflammation. As a result of a cascade of mechanisms, activated NF- κ B is translocated to the nucleus, where it promotes the transcription of apoptotic pro-inflammatory genes and genes targeting cytokine, including interferon, production pathways.^{63,75,76}

Activation of the NF- κ B pathway, as well as the MAPK and PI3K pathways, may also be a consequence of the overexpression of COX-2 induced by UVB radiation. COX-2 induces in this way inflammation, and cancer cell grows by induction of IL-6 and catalyzation of the formation of Prostaglandin E2 (PGE2) that is known to bind and activate its G protein-coupled receptors, prostaglandin E2 receptors (EPs) 1–4 (known as EP₁, EP₂, EP₃, and EP₄). The relationship between premalignant lesions and NMSC development and COX-2 activity has been proven repeatedly, and inhibition of the EP receptors pathways has the potential to prevent cutaneous SCCs⁷⁷; in addition, COX-2 inhibitors have been used in the therapy of SCC and BCC.^{63,78–80} Additionally, the SHH signaling pathway, consisting of transmembrane proteins Ptch1, Smo, and Shh, is important for sporadic and hereditary BCC. However, it is not associated with SCC. Activation of SHH is an underlying mechanism of BCC triggered by point mutation-induced inactivation of the Ptch1 component.^{30,63}

4.1 | The role of microbiome in skin cancers

The microbiome is another aspect correlated with skin cancer, changes to which may relate to mechanisms that increase or decrease the risk of skin cancer. As already mentioned, tissue damage and chronic skin inflammation are closely related to the occurrence of skin cancer. Modulation of inflammatory and immunological processes in the skin occurs through diverse external microbiome environments. Disruption of the normal skin microflora occurs due to environmental exposure, UV radiation, the influence of antibiotics as well as immunosuppressive drugs. Commensal skin bacteria have been shown to reduce inflammation during wound healing by regulating the inflammation-dependent toll-like receptors (TLRs) expressed in skin cells directly involved in neoplastic transformation (keratinocytes and melanocytes). Uncontrolled activation of TLRs is closely associated with chronic inflammation and increased likelihood of skin cancer. Hence, a strong correlation between a normal skin microbiome, adequate TLR receptor signaling, and the process of carcinogenesis is noted.⁸¹ Additionally, some commensal HPVs protect against UV-induced carcinogenesis. On the other hand, *Staphylococcus aureus* is strongly associated with both AK and SCC, implicating the carcinogenic process by inducing the release of pro-inflammatory cytokines (interleukin 1 α (IL-1 α), and interleukin 36 (IL-36)) in keratinocytes and thus promoting chronic inflammation. Furthermore, other pro-inflammatory cytokine-dependent cytokines regulate the cutaneous colonization of these microorganisms, maintaining the inflammatory loop and ultimately triggering tumor progression. In addition to *S. aureus*, other bacteria such as *S. epidermidis*, *Escherichia coli*, and *Pseudomonas aeruginosa* modulate inflammatory processes in keratinocytes that underlie oncogenesis. However, another strain, *Malassezia* reduces excessive colonization of *S. aureus* while preventing SCC.⁸² Moreover, the gut microbiome, in addition to its well-documented effects on gastrointestinal cancers, also influences dermatoses such as acne vulgaris, atopic dermatitis, psoriasis as well as skin cancers by modulating immune function. The cutaneous immunomodulatory effects of *Lactobacillus paracasei* have been documented.^{81,83,84} Although there are direct indications linking the skin microbiota and the immune system, the role of the skin microflora both in direct skin carcinogenesis and in modulating the immune system still needs to be clarified.

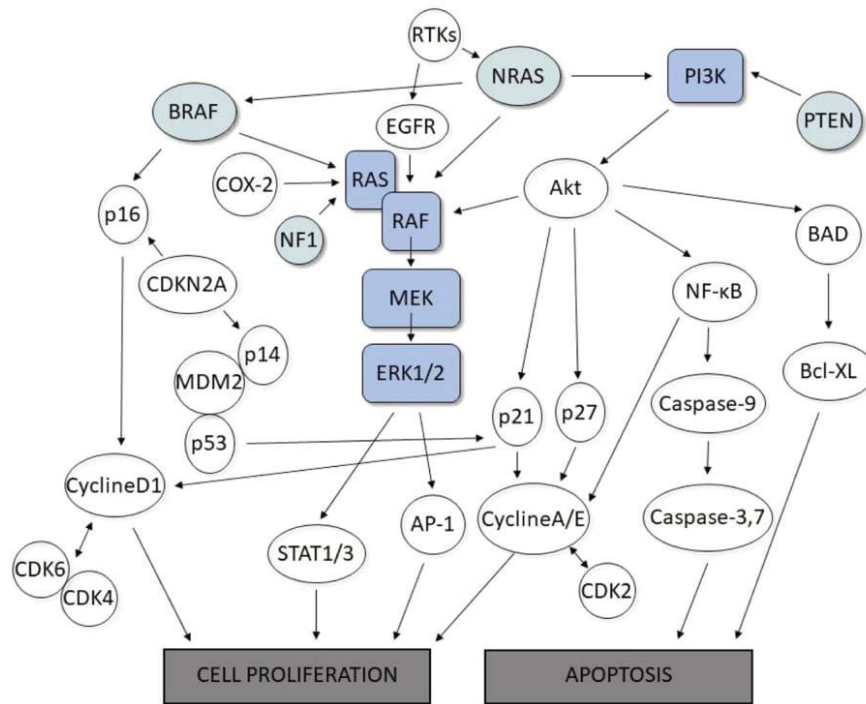


FIGURE 2 The molecular pathways in skin cancers. Objects highlighted in blue color symbolize RAS/RAF/MEK/ERK signaling cascade, also known as the mitogen-activated protein kinase (MAPK) pathway. The oncogenes outlined in the green have been identified as the most common oncogenes with somatic mutations in skin cancer, especially melanoma. Presented pathways and steps, connected by arrows showing interdependencies, represent complex signaling pathways leading to cell proliferation or apoptosis [Color figure can be viewed at wileyonlinelibrary.com]

5 | MOLECULAR PATHOGENETIC PATHWAYS IN THE GENESIS OF SKIN CANCER ESPECIALLY MELANOMA

5.1 | The mitogen-activated protein kinase pathway

Currently, many molecular pathways that accompany the transformation of normal melanocytes into benign or melanoma cells, as well as the progression and malignancy of melanomas, are known. Compared to many other human cancers, melanoma is more closely associated with somatic alterations.⁸⁵ The most common somatic mutations involve oncogenes neuroblastoma rat sarcoma viral (RAS) viral oncogene homolog (NRAS), v-raf murine sarcoma viral oncogene homolog B (BRAF), and neurofibromin type 1 (NF1) and suppressor genes phosphatase and tensin homolog (PTEN), p53 and others. These mutations affect cellular processes such as cell proliferation, growth and metabolism, apoptosis, and the cell cycle. The genomic changes induce impairments to the activation of fundamental signaling pathways, namely, the PI3K pathway and the RAS/rapidly accelerated fibrosarcoma (RAF)/mitogen-activated protein kinase (MEK)/extracellular-regulated kinase (ERK) signaling cascade, also known as the MAPK pathway (Figure 2). Mutations in the MAPK protein kinase pathway are the most frequently observed, and they have been found in 75%–90% of melanoma cases. The primary mutations affect BRAF (in 60%–80% of cases) and NRAS (in 15%–30% of cases), which are in the same pathway, although they are infrequently mutated at the same time.^{86–89}

The intracellular MAPK pathway transmits extracellular signals to the nucleus, thereby regulating proliferation, differentiation, and apoptosis. In addition, it is the central platform for the development of melanoma and may enable its initiation or propagation. The mechanism underlying dysregulated signaling involves somatic BRAF mutations, a proto-oncogene encoding a serine-threonine protein kinase in the MAPK pro-growth signaling pathway. These mutations induce genomic instability, enhance cell replicative potential and angiogenesis, inhibit apoptosis, and drive uncontrolled cell proliferation, which plays an important role in the development of melanoma.^{31,88} Typically, BRAF mutants are results of missense mutations, particularly an amino acid substitution at valine 600, such as V600E, V600K, and V600D, leading to abrogated encoded valine and increased glutamic acid, lysine, aspartic acid, and arginine residues, respectively.^{86,90,91} The BRAF protein has three domains, with two regulatory and one catalytic, involved in the phosphorylation of MEK and adenosine triphosphate (ATP) binding through a hydrophobic interaction with the “glycine-rich” loop and the activation segment of the catalytic domain in MEK. BRAF mutations generate the replacement of hydrophobic valine with polar and hydrophilic glutamic acid, BRAFV600E. This abnormal domain inversion results in a constitutively active conformation with very high kinase activity, driving melanoma progression.^{86,92} BRAF mutations are observed not only in cases of metastatic melanomas but also in more than one-half of benign nevi. They are crucial elements not only in the formation of melanocytic neoplasm but also in cancer progression.^{88,93–95}

The second source of molecular changes related to the activation of the RAS-RAF-mitogen in the MAPK pathway is the NRAS oncogene, which is associated with guanosine triphosphate (GTP) binding and regulation of the cellular response to soluble growth factors. NRAS mutations are reported in 15%–30% of melanoma cases, most of which are missense changes in codons 12/13 or 60/61, leading to prolonged NRAS signaling along with activated MAPK and PI3K pathways.^{31,86,88,89} As in the case of BRAF mutations, NRAS mutations are observed in patients with metastatic melanomas but also with benign nevi. Both of the described mutations in the MAPK pathway are associated with uncontrolled proliferation and metastatic development of primary melanoma, but these mutants may be used as targets for the development of anti-melanoma drugs.^{88,93,96,97}

The least common MAPK mutations include those correlated with suppressor gene NF1. The NF1 protein inhibits RAS signaling by inactivating RAS-GTP to RAS-guanosine diphosphate (RAS-GDP). Ultimately, the NF1 mutation leads to increased activity of NRAS and hence activated MAPK and PI3K pathways. Moreover, the integral cellular component tyrosine-protein kinase Kit (c-KIT) receptor, belonging to the previously mentioned RTK family, is also involved in these pathways due to multiple docking sites for proteins such as PI3K, leading to the activation of MAPK signaling pathway.^{74,98} c-KIT receptor activation leads to the proliferation and migration of melanoma cells or melanocytes, contributing to melanogenesis and the formation of tumors.^{72,74,86,88,99,100}

5.2 | The PI3K pathway

A distinct phosphoinositol-3-kinase (PI3K) pathway is involved in melanoma cell proliferation and metastasis. Overactivation of the PI3K pathway may be an indirect result of NRAS mutation, as described above, or loss of PTEN function. The PI3K pathway plays a role in inhibiting apoptosis, and in melanoma cells, its increased activity is associated with acquired resistance in melanoma treated with BRAF inhibitors.^{101,102} Under physiological conditions, PTEN, a suppressor gene, is closely related to the progression of the cell cycle. Additionally, as a protein subject to dephosphorylation and able to regulate cell-to-cell adhesion, PTEN deactivates the PI3K pathway and suppresses MAPK signaling. Detectable changes in the PI3K pathway and in PTEN expression are results of chromosomal deletions, missense point mutations, epigenetic mechanisms, or microRNA action.^{31,86,88,103}

5.3 | Oncogenes CDK4 and CDKN2A

Oncogene cyclin-dependent kinase 4 (CDK4) and the cyclin-dependent kinase inhibitor 2A (CDKN2A), which encodes p16INK4A, which is expressed in a cyclin-dependent kinase-dependent manner, are not only involved in the development of in situ melanoma (familial melanoma) but are also correlated with other malignancies, such as breast and pancreatic cancer.^{31,97,104,105} Both CDK4 and CDKN2A participate in the regulation of the cell cycle and regulate the transition of tumor cells from the G1 to S phase and thus can cause uncontrolled proliferation (Figure 2). Cyclin D1 activates the proto-oncogene CDK4, while p16INK4a has the opposite effect by inhibiting abnormal melanoma cell division.^{45,86,88,106} In addition, mutations in a tumor suppressor gene cyclin-dependent kinase inhibitor 2B (CDKN2B) in benign melanocytic nevi can lead to melanoma development.^{31,107}

6 | AVAILABLE THERAPY FOR SKIN CANCERS

As stated by the EDF Society, the mainstay of NMSC treatment is surgery followed by the histological examination of tumor margins, which is required to ensure treatment success and complete removal of the NMSC lesion.^{8,108} For radical excision intervention, the size, and depth of the infiltrating neoplastic lesion should be taken into consideration.³ In the case of high-risk tumors, in addition to surgical excision, Mohs micrographic surgery and radiotherapy are performed.⁶³ Mohs micrographic surgery is a highly efficient procedure for complete resection of both primary and recurrent BCC and SCC lesions, enabling the identification and complete removal of the tumor. Radiation therapy is used as complementary and palliative therapy in NMSC, but its effectiveness is limited by the inability to introduce it into the therapeutic management of recurrent BCC.⁸ Ablative techniques such as electrodesiccation, curettage, and cryotherapy are also recommended for low-risk NMSC.⁶³ Electrodesiccation with curettage is a frequent therapeutic method characterized by high effectiveness but limited to use in poorly defined BCC and SCC tumors posing increased risk and presenting with a recurrent nature.⁸ Therefore, in the case of SCC with an increased risk of metastases, surgical excision or Mohs surgery, not electrodesiccation or curettage, is recommended.⁵ Liquid nitrogen cryotherapy involving cold-induced NMSC destruction and precise CO₂ laser ablation are effective methods for the treatment of low-risk SCC and BCC. However, tumor removal using a CO₂ laser is a rarely used method.⁸ For all of the abovementioned methods, it is suggested that chemotherapy and/or immunotherapy be used as supplementary treatment or monotherapy.^{63,109} Topical therapy with 5% imiquimod is acceptable for application in BCC and Bowen's disease when used with 5-fluorouracil for regulating key cell receptors.^{3,5}

Primary melanomas detected in the early stages may respond effectively to local therapy involving surgical excision of the neoplastic skin lesion, with a 92% overall survival rate, with marginal cases depending on the pathological staging of the melanoma on the basis of Breslow classification.^{3,5,110,111} Additionally, sentinel lymph node dissection and radical removal of surrounding lymph nodes are recommended.^{95,112,113} The use of these methods of treatment at an early stage ensures a high survival rate. However, the prognosis becomes less encouraging with nodal involvement or metastasis, declining to only a 10% chance of 5-year survival. In the treatment of inoperable melanoma in the advanced stage of this disease, radiotherapy has also been ineffective.^{5,88,114} In recent years, the therapeutic options for metastatic melanoma have significantly expanded and include chemotherapy, immunotherapy, and targeted therapy.^{95,108,115}

6.1 | Chemotherapy

In the treatment of metastatic melanoma, chemotherapy has been the "standard" for more than 40 years, targeting the pathological pathways of apoptosis or their absence in cancer cells. Monotherapy of melanoma with

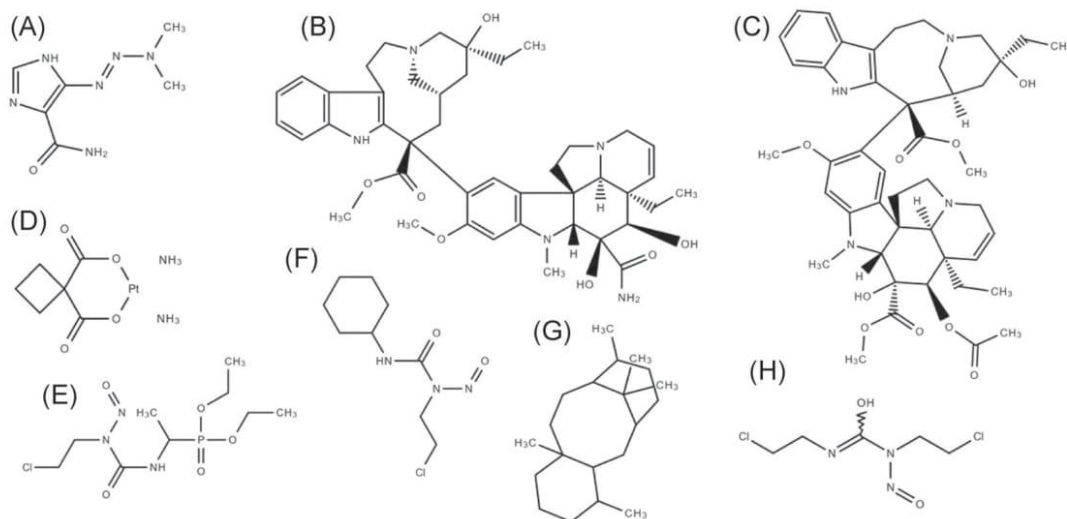


FIGURE 3 Chemical structures of clinical chemotherapeutics used in skin cancer treatment: dacarbazine (A), vindesine (B), vinblastine (C), carboplatin (D), fotemustine (E), lomustine (F), taxane (G), and carmustine (H)

dacarbazine (DTIC) is mainly a palliative therapy. DTIC is converted to the active alkylating metabolite 3-methyl-[triazene-1-yl]-imidazole-4-carboxamide. Although DTIC, the first chemotherapeutic treatment approved by the FDA for metastatic melanoma,¹¹⁶ is the most effective of all available methods of chemotherapy, it is largely ineffective, often inducing no therapeutic response. As a result, DTIC is recommended for use in combination therapy with other cytostatics: vindesine, vinblastine, cisplatin, carboplatin, taxane, carboplatin, or nitrosoureas, such as carmustine, lomustine, or fotemustine. These chemotherapeutic agents exhibit little effect when used as a single chemotherapeutic agent, with the exception of nitrosourea, whose activity is comparable to that of DTIC. However, combination therapy produces a slightly better response but with significant side effects. Currently, chemotherapy is considered a treatment of last resort for patients with resistance to more effective therapies (immunotherapies and targeted therapies) or in countries where access to new more-effective drugs is limited^{3,63,108,114} (Figure 3).

6.2 | Immunotherapy

Immunological treatment, which is one of the basic systemic therapies, is based on the manipulation of targeted immune system responses to melanoma cells. Upon immunostimulation of interleukin 2 (IL-2) through receptors composed of IL-2R α , IL-2R β , and IL-2R γ subunits, proliferation and the function of T lymphocytes and natural killer cells are activated; these cells search for melanoma cells expressing a major histocompatibility complex (MHC) molecule absent in all but melanoma cells and then lysing them, inhibiting tumor growth and immune checkpoints.^{88,114} Despite its effectiveness, IL-2 therapy is associated with numerous undesirable side effects. Inflammatory reactions, nausea, diarrhea, and capillary leak syndrome are observed in 16%–17% of patients receiving an intravenous infusion of IL-2.^{3,117} Interferon- α (IFN- α) administered after surgical excision as an adjunct therapy in patients with metastatic melanoma to inhibit the proliferation of residual melanoma cells continuously stimulates the activity of lymphocytes such as CD4⁺ and the secretion of interferon- γ (IFN- γ) and IL-2, leading to a long-term immune response.¹¹⁸ Unfortunately, patients in greatly advanced stages of melanoma show a low response to this therapy and, similar to IL-2 therapy, IFN- α induces cytotoxicity, especially during long-term treatment. IFN- α and

IL-2 constitute the main immunotherapies used with melanoma patients. The response rate to these treatments increases after biochemotherapy administration because of the combination of both immunotherapeutic agents and cytotoxic chemotherapeutic agents, such as DTIC, which is the third element of this therapy.^{88,114} A breakthrough in the development of novel immunotherapies has led to a therapy based on suppressing the immune response to the tumor microenvironment. Monoclonal antibodies, such as ipilimumab, nivolumab, and pembrolizumab, against the programmed death-1 (PD-1)/programmed death ligand-1 (PD-L1) inhibitory pathway that exists in the immune system to prevent the immune cells destroy normal host cells (autoimmunity), resulting in modulation of T lymphocyte activity and consequently to the immune-mediated tumor destruction and thus improving the overall survival time, even for people with advanced melanoma.^{3,63,86} In summary, IL-2 immunostimulation, tumor-blockades of T cell proliferation, and immune checkpoints are major targets of the immune response in melanoma immunotherapy.^{95,108,119,120}

6.3 | Targeted therapy

According to The European Interdisciplinary Guideline developed by the EDF society, targeted therapy takes advantage of the frequent mutations in MAPK pathway genes in melanoma patients by introducing highly selective BRAFV600 inhibitors, such as vemurafenib and dabrafenib.^{3,95,108} Despite previous results of clinical trials confirming high efficacy of vemurafenib and dabrafenib treatment, improved survival, and high tolerance, a large proportion of the patients developed resistance to treatment with BRAF inhibitors, which in turn caused reactivation of the MAPK pathway. Hence, regimens of combination therapies that include MEK inhibitors important in the MAPK cascade, such as cobimetinib and trametinib, are being explored.^{3,86,95,119,121} The effectiveness of targeting this therapeutic route has been confirmed in preclinical studies proving increased apoptosis and delayed onset of treatment resistance.^{3,121} The combination of BRAF inhibitors and MEK inhibitors administered to melanoma patients with an activating BRAFV600E mutation resulted in a significant improvement in survival and responses.^{86,122} Despite the success of novel therapies based on MAPK pathway inhibitors, a number of undesirable effects have also been revealed. Notably, therapies that include vemurafenib and dabrafenib can lead to SCC.^{3,86,88} In cases of some melanomas with an activating type III transmembrane receptor tyrosine kinase (KIT) mutation, a different targeted therapy may be an alternative approach. However, KIT therapy with imatinib is considered controversial and is still undergoing improvements.^{3,63}

7 | BIOACTIVITY OF LUTEOLIN AND ITS DERIVATIVES ON SKIN CANCER

The antitumor activity of flavonoids, in general, has been extensively described and documented thus far.^{74,80,123–128} Therefore, we present in detail our findings on the modulation of oncogenic skin cancer pathways by luteolin and its derivatives. Luteolin, a natural flavonoid commonly found in many plant raw materials, exhibits multiple biological effects, including anti-inflammatory, antioxidant, antiallergic, and anticancer properties. Therefore, it seems to be a promising source with preventive and therapeutic potential for the treatment of various cancers, including skin cancers.^{22,58,129–134} Moreover, because luteolin increases the therapeutic response of cancer cells, luteolin can be used as a complementary therapy.^{45,135,136}

The antitumor activity of luteolin has been found as a result of inhibited induction of apoptosis, disruption of the cell cycle, inhibition of cell proliferation and/or migration, and/or angiogenesis associated with increased invasiveness and tumor development. Notably, the proliferation and development of neoplastic cells *in vitro* are inhibited through a number of different pathways and the expression of many diverse genes.^{45,123,134,137–145} Furthermore, another important aspect is the ability of luteolin to multidimensionally regulate epigenetics layers in

the case of cancers, affecting the apoptotic effect. This occurs via inhibition of DNA methylation and trimethylation in histone H3 at lysine 27 (H3K27me3), activation of nuclear factor 2 associated erythroid 2 (Nrf2) demethylation, as well as inhibition of DNA methyltransferases (DNMTs), enhancer of zeste homolog 2 (EZH2), p53 and expression of key genes in cell cycle.^{24,146,147} In addition to reducing methylation of the Nrf2 promoter region, binding of (ten-eleven translocation-1) TET1 to the Nrf2 promoter and formation of a complex between p53 and Nrf2, are determined as the subsequent molecular mechanism underlying such proapoptotic activity of luteolin.¹⁴⁸ Luteolin induced both intracellular and extracellular apoptosis of C32 human amelanotic melanoma cells, which was confirmed by its effect on mitochondrial potential and the activity of caspase-3, caspase-8, caspase-9, and caspase-10 while stimulating autophagy.¹⁴⁹ It was also reported to downregulate the PI3K/protein kinase B (AKT) axis through downregulation of oncogenes fibroblast growth factor 10 (FGF10) and fibronectin 1 (FN1), and matrix metalloproteinases (MMPs) MMP-2 and MMP-9, and upregulation of tissue inhibitors of MMPs (TIMPs) TIMP-1 and TIMP-2, thereby inhibiting migration, inducing apoptosis, disrupting cell integrity and reducing the invasive potential of A375 human malignant melanoma cells. Furthermore, its inhibitory effect was also reported in an in vivo model.^{150–153} However, in vivo, the tumor showed adaptation and acquired resistance to luteolin treatment. Changes in A375 cells under the influence of luteolin, particularly FGF10 and FN1 genes, strongly influenced the expression of kinase suppressor of RAS 2 (KSR2), suggesting inhibition of the RAS pathway and downregulation of a number of components involved in ECM modifications (intercellular adhesion molecule-1 (ICAM1), laminin subunit alpha 1 (LAMA1), integrin alpha 2b (ITGA2B), and FN1) and proteinases such as a disintegrin and metalloproteinase with thrombospondin motifs (ADAMTSs) ADAMTS1 and ADAMTS18, MMP-1, MMP-10, cathepsins (CTS) CTSG, CTSK, and CTSV). Luteolin exerts a significant influence on the proliferation and invasion of melanoma cells by disrupting the ECM pathway by suppressing, for instance, MMP-1, MMP-2, or MMP-10 expression in other human malignant melanoma lines (SK-MEL-2, SK-MEL-28, and WM3211 cells), regardless of whether or not BRAF was mutated. In the case of the WM3211 cell line (wild-type for NRAS and BRAF), luteolin induced the rather rare downregulation of KIT expression, which was crucial for inhibiting the growth of these cells.¹⁵¹ Moreover, strong cytotoxicity and proapoptotic activity induced in these cells through arrest to the cell cycle and an accumulated number of these cells in the G0/G1 phase were demonstrated.¹⁶ It has been documented that luteolin can inhibit cell proliferation through cell cycle arrest in the G1 phase as a result of the inhibition of CDK2 activity, enhanced expression of CDKN1A, and regulation of CDK inhibitors in A375 and C32 cells.^{149,151}

Luteolin can have both anti- or pro-oxidant activity, which is at least partly determined by the cellular milieu. In malignant cells, which often contain already an increased oxidative stress level because of their upregulated metabolism, luteolin induces apoptosis by endoplasmic reticulum (ER) stress via increasing ROS levels. However, in healthy cells, luteolin shows antioxidative effects are described.¹⁵⁴ The relationship between cell proliferation, apoptosis, and the induction of luteolin-induced ROS levels, expression of ER stress, and CCAAT/enhancer-binding protein-homologous protein (CHOP) protein has been demonstrated in A2058 human metastatic melanoma cells.¹⁵⁵ On the other hand, Schomberg and co-authors examining four different melanoma lines, SK-MEL-2, SK-MEL-28, A375, and WM3211 cells, led to diametrically opposed conclusions. They hypothesized that it was not the increase in luteolin-induced ROS production that directly caused the inhibition of cell growth but it was probably the synergism of simultaneous modifying effects on multiple pathways, including aforementioned pathways associated with the ECM, the oncogenic signaling pathway, and immune response pathways.¹⁵¹ Interestingly, according to the results of studies comparing the effects of luteolin on two different melanoma lines, the SK-MEL-1 human metastatic melanoma cell line shows greater resistance to treatment than the B16F10 mouse primary melanoma cell line; however, the differences are insignificant, and it would be appropriate to further investigate the resistance of cells according to their origin.^{156,157}

Luteolin inhibited the invasive epithelial–mesenchymal transition (EMT) process, which induces morphological changes in melanoma cells and is involved in melanoma progression.^{158,159} This effect is a result of the reduced expression of MMP-9, reversed cadherin switching (downregulated N-cadherin and upregulated E-cadherin) in human epidermoid carcinoma and melanoma cells (A431-III, A431, A375, and B16F10 cells),^{160–163} and reduced

expression of the E-cadherin gene in WM3211 cells,¹⁵¹ contributing to the reduction in the invasive abilities of these cells, as well as inhibited tumor growth and progression. Moreover, integrin β 3 (ITG β 3) inhibition, changes in EMT signaling, and suppressed metastasis caused by luteolin treatment were also observed in an in vivo C57BL/6 mouse model established with B16F10 cells.^{153,161} The S100A7 protein may mediate EMT activation, leading to the emergence of additional neoplastic lesions. Luteolin decreased the signaling of Src/focal adhesion kinase (FAK), Src/signal transducer and activator of transcription 3 (STAT3), and S100A7 protein, thereby reducing the migratory abilities of A431-III cells.^{164–166} High invasiveness is a particular feature of A431-III cells that overexpress MMP-9 that is not evident in primary A431 cells. The effect of luteolin on MMP-9 may result from inhibition of Akt phosphorylation, while inhibition of N-cadherin expression may result in inhibition of the expression of the MAPK-ERK pathway.¹⁶⁰ It has been observed that luteolin induces apoptosis by regulating B-cell lymphoma 2 (Bcl-2) and Bcl-2-associated X (Bax) proteins in B16F10 cells,¹⁶⁷ inhibiting the secretion of MMP-2 and MMP-9 and changing the phosphorylation level of components of the EGFR signaling pathway in A431 cells, and the metastatic potential of these cells may be realized upon EGFR inhibition.¹⁶² Luteolin also exerts a strong chemopreventive effect against melanoma by targeting protein kinase C ϵ (PKC ϵ) and Src. It has been proven that treatment of the JB6 P+ mouse melanoma cell line that this flavone leads to suppressed expression of PKC ϵ and Src kinase and inhibition of the UVB-induced activity of COX-2, activator protein-1 (AP-1) and NF- κ B.¹⁵²

The process of melanogenesis can be described in two ways. Melanogenesis is a physiological mechanism conferring protection against the harmful effects of UV radiation. Hence, it prevents the malignant transformation causing skin cancer.¹⁶⁸ On the other hand, excessive melanogenesis, melanin deposition, and the related potential cytotoxic risk are associated with melanogenesis and, hence, melanoma.^{169,170} Hence, melanogenesis can be considered a target for therapy aimed at the elimination of malignant melanocytes and, at the same time, a target for chemopreventive action.^{60,61}

It has been documented that luteolin inhibits melanogenesis in B16F10 cells but not by reducing the level of TYR protein, as might be expected because luteolin exerts the opposite effect in the absence and presence of α -MSH. The antimelanogenic activity is attributed to the ability of luteolin to inhibit the catalytic activity of TYR and the expression of exogenous human TYR regulated through a pathway-dependent cyclic adenosine monophosphate (cAMP).^{171,172} However, in HMV-II human vaginal melanoma cells, the antimelanogenic effect was based on the opposing mechanism: Luteolin promoted melanin production by stimulating the activity of intracellular TYR.¹⁷³ Yamauchi et al. compared the proliferation of B16F10 cells and the extent of melanogenesis inhibition under the influence of luteolin and concluded that luteolin exhibits inhibitory activity only on extracellular melanogenesis and not on intracellular melanogenesis, as previously expected.^{174,175} Melanogenesis is related to the microphthalmia-associated transcription factor (MITF) a transcription factor of melanogenic enzymes, that is influenced by c-Jun N-terminal kinase (JNK), which together with p53 activates the apoptotic pathway; hence, the inhibition of B16F10 cell melanogenesis confirms the previously described proapoptotic effect of luteolin.^{176,177}

The ability to inhibit the melanogenesis of melanoma precursor cells has also been documented in the case of luteolin derivatives. The inhibitory potential of eight luteolin derivatives on extracellular melanogenesis and B16F10 cell proliferation was compared, with the results demonstrating the dependence of the antitumor effect on the length of the hydrocarbon 7-O- substitution. Hence, luteolin showed the lowest activity of the compounds tested, followed by 7-O-methyluteolin, 7-O-ethyluteolin, 7-O-propyluteolin, 7-O-butyluteolin, 7-O-pentyluteolin, and 7-O-hexyluteolin, which showed the highest activity. However, the bulkiness of the substituent at position 7 did not have a significant effect on the inhibition of the compared process; that is, 7-O-(1-methyl)propyluteolin and 7-O-methylcyclohexyluteolin showed activity similar to that of 7-O-ethyluteolin, 7-O-propyluteolin, 7-O-butyluteolin, and 7-O-pentyluteolin.¹⁷⁴ Another notable derivative in the context of melanogenesis inhibition is luteolin 7-sulfate, which simultaneously inhibited the synthesis of new TYR proteins and the catalytic activity of existing TYR proteins in B16F10 cells. The inhibition of TYR gene expression was related to the signaling pathway mediated by cAMP response element-binding protein (CREB) and MITF, which in this case, may explain the antimelanogenic activity of luteolin 7-sulfate; its antimelanogenic action is several dozen folds greater than that of

the known melanogenesis inhibitor arbutin and higher than the activity of luteolin itself.^{178,179} The results of the antitumor effects of luteolin and its derivatives are summarized in Table 1.

7.1 | Chemoprevention action

Skin cancer prevention is based on several schemes based on primary and secondary prevention. According to the National Cancer Institute, both schemes are based on public education: The primary prevention effort is based on the principles of photoprotection and the effects of increased exposure to sunlight, and secondary effort for skin cancer prevention is based on screening precancerous lesions for early diagnosis and detection.^{23,193–195} Chemopreventive agents for melanoma are used not only to prevent the occurrence of neoplastic lesions but also to inhibit their development and promote remission. However, because of the complexity of the transformation of melanocytes under the influence of UV radiation and the poor patient response to chemopreventive agents in clinical trials, chemoprevention of melanoma is a purely perfunctory scheme.^{58,196,197}

A large body of evidence suggests that luteolin, due to its antioxidant and anti-inflammatory properties, may also play an important role in the reduction of skin cancer progression and photocarcinogenesis and thus has a significant impact on the prevention of skin cancer. As described in the previous sections, oxidative stress is inextricably linked to the processes of tumor formation. Luteolin, due to its structure of 3-OH, 4'-OH, and the double bond between carbons C2-C3 and a carbonyl group on C4, removes ROS through its own oxidation, which has been confirmed by studies on cell-free systems.^{198,199} Moreover, it blocks ROS-producing oxidases, which are components in the lipoxygenase reaction involving the chelation of transition metal ions, and protects endogenous antioxidants, thus enhancing their action.²⁰⁰ These antioxidant abilities distinguish the ability of luteolin and its derivatives to protect against ROS-induced activation of MAPK, NF- κ B, and COX-2, as well as damage to lipids, DNA, and proteins, as confirmed not only through studies of cell-free systems but also *in vitro* and *in vivo* experiments,^{137,172,201–203} thus preventing the development of cancer.^{131,204,205} Moreover, the ability to induce the apoptosis of neoplastic cells, including melanoma cells, has been attributed to the pro-oxidative property of this flavone.¹⁵⁵ However, as previously mentioned, Schomberg et al.,¹⁴¹ examining five lines of cutaneous melanoma, came to the opposite conclusion, suggesting that the induction of ROS is a negligible side effect of luteolin treatment of melanoma while confirming its proapoptotic effect.¹⁵¹ ROS-related apoptosis is most likely due to cytotoxicity-related suppression of the NF- κ B pathway and activation of JNK, and this activation relationship has been confirmed in lung cancer; however, in melanoma, this relationship is based only on speculation.^{45,174,206} Indeed, the antioxidant activity may be correlated with NF- κ B, as confirmed with studies of the JB6 P+ melanoma cell line showing the potential of luteolin to suppress UVB radiation-induced NF- κ B, COX-2, and AP-1 expression, mainly by targeting PKC ϵ and Src.¹⁵²

Additionally, luteolin has been shown to directly inhibit PKC ϵ /Src activity and prevent UVB-induced DNA damage in keratinocyte cells. There is evidence for the preventive potential of luteolin in skin cancers associated with, *inter alia* skin photodamage as well as Nrf2 activity, closely related to oxidative stress. Luteolin suppresses the expression of COX-2, AP-1, and NF- κ B, regulates antioxidant enzymes, and prevents ROS accumulation and activation of MAPK and NF- κ B signaling pathways.²⁰⁷ The antioxidant activity of luteolin is a partial contribution to its anti-inflammatory effect, which is also related to the prevention of the carcinogenesis process due to the convergence of chronic inflammation and cancer.^{45,56} This luteolin effect is mediated by cells such as neutrophils and lymphocytes; TNF- α and IL-6 release-related inhibition; and signaling pathways involving these factors as previously described. Luteolin also blocks the production of the aforementioned cytokines due to the inhibition of NF- κ B and kinases involved in the MAPK signaling pathways and activation of inhibitory- κ B kinase (IKK).^{208–210} Furthermore, luteolin was found to inhibit UVB radiation-induced MMP-1 expression in the human keratinocyte cell line HaCaT, as well as UVB radiation-induced activation of AP-1, a well-known transcription factor mediating inflammation and proliferation, as well as the MMP-1 promoter, c-Fos and c-Jun, which make up the AP-1

TABLE 1 Antitumor activities of luteolin derivatives in relation to skin cancer

Luteolin derivative	Cell line	Inhibition of proliferation		Effect of action	Molecular target	Refs.
		IC ₅₀ (µg/ml)	Incubation time			
Luteolin	B16F10	0.7	72 h	↓Proliferation	Not evaluated	140
		>14.3	24 h	↓Proliferation	Not evaluated	180
		>14.3	72 h			
		Not detected		↑Melanogenesis	↑TYR, ↑ CREB	175
		>28.6	72 h	↓Proliferation, ↓melanogenesis	↓TYR, ↓ cAMP	172
		Not detected		↓Metastasis, ↓invasion, ↓progression, ↓EMT	↓FAK, ↓ N-cadherin, ↑E-cadherin	161
		>14.3	24 h	↓Proliferation	Not evaluated	157
		>14.3	72 h			
		>14.3	24 h	↓Proliferation	Not evaluated	156
		>14.3	72 h			
		>57.3	48 h	↓Melanogenesis	↓TYR	171
		>28.6	24 h	↓Melanogenesis	↓TYR	181
		3.5	24 h	↓Proliferation	Not evaluated	182
		9.8	72 h	↓Extracellular melanogenesis, ↓proliferation	Not evaluated	174
	1.6	48 h	↓Melanogenesis, ↓proliferation	Not evaluated	141	
	5	48 h	↓Melanogenesis, ↓proliferation	Not evaluated	178	
	6	-	↓Proliferation	Not evaluated	142	

(Continues)

TABLE 1 (Continued)

Luteolin derivative	Cell line	Inhibition of proliferation		Effect of action	Molecular target	Refs.
		IC ₅₀ (µg/ml)	Incubation time			
8.1			24 h	↓Melanogenesis, ↓proliferation	Not evaluated	143
4.3			48 h	↓Proliferation	Not evaluated	183
7			48 h	↓Melanogenesis, ↓proliferation	↓TYR	179
41.2			24 h	↓Proliferation, ↓migration, ↓invasion, ↓adhesion, ↓metastasis, ↓EMT	↓N-cadherin, ↑E-cadherin, ↓MMP-2, ↓MMP-9, ↓p-Akt, ↓HIF-1α, ↓VEGF-A, ↓p-VEGFR-2	163
18.4			48 h			
15.8			72 h			
40.3	A375		24 h	↓Proliferation, ↓migration, ↓invasion, ↓adhesion, ↓metastasis, ↓EMT	↓N-cadherin, ↑E-cadherin, ↓MMP-2, ↓MMP-9, ↓p-Akt, ↓HIF-1α, ↓VEGF-A, ↓p-VEGFR-2	163
18.6			48 h			
12.7			72 h			
10.4			24 h	↓Proliferation, ↑apoptosis, ↓migration, ↓invasion	↓MMP-2, ↓MMP-9, ↑TIMP-1, ↑TIMP-2, ↓pAkt1, ↓PI3K, ↓PI3K/Akt	150
5.3			48 h			
32.9			24 h	↓Proliferation, ↑apoptosis, ↑G0/G1 phase	Not evaluated	16
3.6			72 h	↓Proliferation, ↑apoptosis, ↓invasion, ↑G1 phase	↓CSF2RA, ↓ANGPT1, ↓FGF10, ↓FN1, ↓MAPK, ↓ PI3K, ↑KSR2, ↓RAS, ↑CDKN1A, ↓KRAS, ↓BRAF, ↓ MAP2K2 (MEK2), ↓CD274, ↓IL24, ↓CXCL8, ↓NGFR, ↓MMP- 1, ↓MMP-10, ↓JECM	151

TABLE 1 (Continued)

Luteolin derivative	Cell line	Inhibition of proliferation		Effect of action	Molecular target	Refs.
		IC ₅₀ (μg/ml)	Incubation time			
		5.2	24 h	↓Proliferation	Not evaluated	139
		9.7	24 h	↓Proliferation	Not evaluated	144
		6.5	48 h			
		5.8	72 h			
	C32	95.1	24 h	↓Proliferation, ↑autophagy, ↑apoptosis, ↓mitochondrial membrane potential, ↑G2/M phase, ↑S phase, ↓ G1 phase	↑Caspase-3, ↑caspase-8, ↑caspase-9, ↑caspase-10	149
		2.4	48 h	↓Proliferation	Not evaluated	139
	A2058	35	48 h	↓Proliferation, ↑apoptosis, ↑ER stress, ↑chemopreventive effect, ↑intracellular ROS	↑Phospho PERK, ↑ phospho eIF2α, ↑ATF6, ↑ CHOP, ↑ caspase-12	155
	Colo829	2.1	72 h	↓Proliferation	Not evaluated	151
	SK-MEL-1	>14.3	24 h	↓Proliferation	Not evaluated	157
		>14.3	72 h			
		>14.3	24 h	↓Proliferation	Not evaluated	156
		>14.3	72 h			
	SK-MEL-2	4.8	72 h	↓Proliferation, ↑apoptosis, ↓invasion	↓BRAF, ↓ HBEGF, ↓ Src, ↓NF1, ↓ NRTN, ↓ SPRED, ↓ MAPK, ↓ JAK3, ↓ MMP- 1, ↓ MMP-2, ↓ MMP-10, ↓ ECM, ↓ CDH1	151

(Continues)

TABLE 1 (Continued)

Luteolin derivative	Cell line	Inhibition of proliferation		Effect of action	Molecular target	Refs.
		IC ₅₀ (µg/ml)	Incubation time			
SK-MEL-28	SK-MEL-28	3.4	72 h	↓Proliferation, ↑apoptosis, ↓invasion, ↑chemopreventive effect, ↑intracellular ROS	↓GDNF, ↓MAPK, ↓SHC2, ↓DIC1, ↓RASAL1, ↓JAK3, ↓MMP-1, ↓MMP-2, ↓ECM	184
		9.2	48 h	↓Proliferation	Not evaluated	185
		>14.3	72 h	↓Proliferation	Not evaluated	162
		5.4	24 h	↓Proliferation, ↑apoptosis, ↓metastasis	↓EGFR, ↓EGF, ↓MMP-2, ↓MMP-9	182
A431	A431	25.6	24 h	↓Proliferation	Not evaluated	160
		Not detected		↓Migration, ↓invasion, ↓progression, ↓EMT	↓MMP-9, ↓EGFR	
		Not detected		↓Migration, ↓invasion, ↓progression, ↓EMT	↓N-cadherin, ↑E-cadherin, ↓MMP-9	
		7.5	24 h	↓Proliferation, ↓metastasis, ↓migration, ↓invasion, ↓EMT	↓p-Src, ↓pSTAT3, ↓S100A7, ↓Src/FAK ↓Src/STAT3/ S100A7, ↓ECM, ↓MMP, ↓RPS12, ↓RPS19, ↓Akt/ mTOR/c-Myc	164 186
WM3211	WM3211	15.9	24 h	↓invasion, ↓EMT		187
		Not detected				165
WM3211	WM3211	1.9	72 h	↓Proliferation, ↑apoptosis, ↓invasion, ↑chemopreventive	↓KIT, ↑NRAS, ↓MAP2K2, ↓IL24, ↓NGFR, ↓MMP-1, ↓MMP-2, ↓MMP-10, ↓ECM	151
		Not detected				

TABLE 1 (Continued)

Luteolin derivative	Cell line	Inhibition of proliferation		Effect of action	Molecular target	Refs.
		IC ₅₀ (µg/ml)	Incubation time			
	MDA-MB-435	8.7	48 h	effect, ↑intracellular ROS ↓Proliferation	Not evaluated	145
	HMV-II	Not detected		↑Intracellular melanogenesis	↑Intracellular TYR	173
	HMB-2	7	24 h	↑Chemopreventive effect, ↓proliferation, ↓ROS	Not evaluated	137
	JB6 P+	Not detected		↑Chemopreventive effect	↓PKCε, ↓Src, ↓COX-2, ↓AP-1, ↓NF-κB	152
	UACC-62	2.9	48 h	↓Proliferation	Not evaluated	188
Luteolin 6-glucoside	B16F10	>44.8	48 h	↓Invasion, ↓melanogenesis	Not evaluated	141
Luteolin 7-sulfate		>89.7	48 h	↓Melanogenesis	↓TYR, ↓TRP1, ↓DCT, ↓MITF, ↓CREB, ↓cAMP	170
		43.5	48 h	↓Melanogenesis, ↓proliferation	↓TYR, ↓MITF, ↓CREB	178
		69.1	48 h	↓Melanogenesis, ↓proliferation	↓TYR	179
Luteolin 7-methyl ether		8.4	72 h	↓Extracellular melanogenesis, ↓proliferation, ↑apoptosis	Not evaluated	174
Luteolin 7-ethyl ether		>15.7	72 h			

(Continues)

TABLE 1 (Continued)

Luteolin derivative	Cell line	Inhibition of proliferation		Effect of action	Molecular target	Refs.
		IC ₅₀ (µg/ml)	Incubation time			
Luteolin 7-propyl ether		5.3	72 h			
Luteolin 7-butyl ether		4.6	72 h			
Luteolin 7-pentyl ether		3.6	72 h			
Luteolin 7-hexyl ether		2.4	72 h			
Luteolin 7-(1-methylpropyl) ether		4.4	72 h			
Luteolin 7-methylcyclohexyl ether		5.2	72 h			
Ugonin J		>21.1	72 h	↓Extracellular melanogenesis, ↓proliferation	↓TYR	189
Ugonin K		>21.8	72 h			
Ugonin L		>21.8	72 h	Not demonstrated	Not demonstrated	
Luteolin 3'-methyl ether	B16F10	17	24 h	↓Proliferation	Not demonstrated	182
	A431	15.4	24 h	↓Proliferation	Not demonstrated	
Luteolin 4'-methyl ether	B16F10	>20	24 h	↓Proliferation, ↑apoptosis, ↓invasion	↑Caspase-3	190
Luteolin 4',5,7-trimethyl ether	UACC-62	>250	48 h	Not demonstrated	Not evaluated	138

TABLE 1 (Continued)

Luteolin derivative	Cell line	Inhibition of proliferation		Effect of action	Molecular target	Refs.
		IC ₅₀ (µg/ml)	Incubation time			
Luteolin 7-sambubioside	C32	>300	24 h	↓Proliferation	Not evaluated	149
Luteolin 7-glucoside		>300	24 h			
		12.5	48 h	↓Proliferation	Not evaluated	139
	A375	13.1	48 h		Not evaluated	
	UACC-62	9.4	48 h	↓Proliferation	Not evaluated	188
	B16F10	>31.4	48 h	↓Proliferation	Not evaluated	191
		>100	24 h	↓Melanogenesis	Not evaluated	192

complex.^{45,76,211} The photoprotective effect of luteolin on keratinocytes was also demonstrated by Verschooten and co-authors, proving an increase in the resistance of normal cells to UVB radiation-induced apoptosis, with an adverse effect on malignant keratinocytes.²¹² In an *in vivo* model, the anti-inflammatory effect of luteolin 7-O-glucoside was demonstrated by inhibiting the synthesis of COX-2, IL-1 β , and TNF- α , which are closely related to inflammation upon exposure to UVB radiation.^{213,214}

7.2 | The structure–activity relationship of luteolin derivatives

SAR analysis offers the possibility to isolate the chemical groups and structures critical for induced biological response and to correlate structural features to their activity. Unfortunately, due to the use of different cell lines, different analysis conditions, and measurement methods, it is not possible to carry out SAR analysis on the basis of documented IC₅₀ values obtained through heterogeneous techniques and the many accidents. Reports on the growth inhibitory effects against different skin cancer cell lines have not always been the same, indicating differences in the sensitivity of melanoma cells to the tested compounds. Despite these difficulties, a correlation between the position, number, and nature of substituents in the structure of luteolin and its derivatives and their antiproliferative activity has been identified.

The high antiproliferative activity of luteolin was first identified with the presence of a C2–C3 double bond in the C ring, the presence of hydroxyl groups at C5 and C7 in the A ring, and a catechol group containing two adjacent phenolic OH groups (3',4'-di-OH). Moreover, it has been shown that the C ring with an oxo group function at position C4 contributes to the high activity of compounds in this class. All the described structural elements determine and are required for high anticancer activity.^{140,142,156,157,162,215} However, certain kinds of structural modifications improve or eliminate this activity. Special attention has been directed to the number and O-methylation, and O-glycosylation status of the free hydroxyl groups at the C7 position in the A ring.

During the comparison of the cytotoxic and/or antiproliferative activity of flavonoids, it was documented that, in addition to the saturation of the C2–C3 bond, the presence of a methyl group in the structure of these compounds significantly enhances their effect. In particular, the 7-O-methoxyl group on the A ring of luteolin is associated with this effect. Moreover, the length of the linear hydrocarbon substituent at the C7 position of the A ring has a directly proportional effect on the antiproliferative activity (Figure 4). Additionally, it has been hypothesized that a group of these substituents attached to luteolin may stimulate the activation of JNK, which is strongly involved in melanogenesis, in addition to apoptosis, as confirmed by Yamauchi et al.¹⁷⁴ However, the mass of the substituent at position C7 has no significant effect on the inhibitory effect of the compound on proliferation

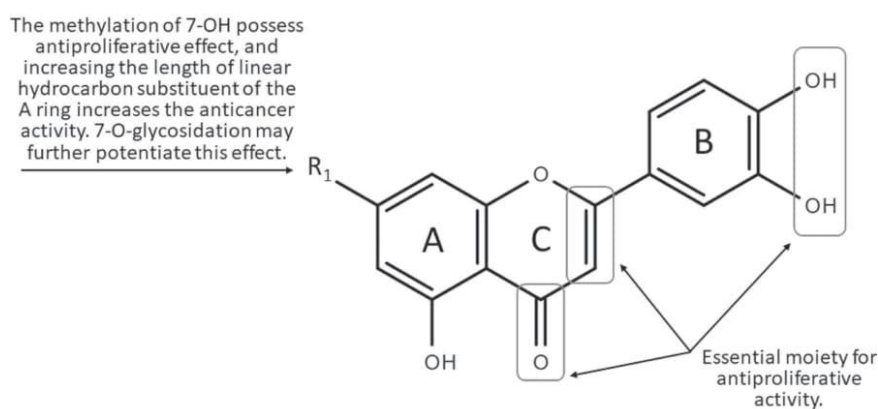


FIGURE 4 Chemical groups responsible for luteolin derivatives activity (SAR)

or melanogenesis.^{174,175} The location of the *O*-methyl substituent is substantial. The attachment of a methyl group at C3' reduces the antiproliferative activity compared to the occupation of the C7 position, which confirms that 3'-OH moiety in the structure of luteolin plays a vital role in determining high anticancer activity. The analogous situation with the participation of the *O*-methylation of 4'-OH results in a deepening of the abolition of the discussed antitumor activity. Moreover, simultaneous attachment of methyl groups at positions 5 and 7 of the A ring and at position 4' of the B ring significantly attenuates the antiproliferative effect, suggesting that the introduction of a higher number of methoxyl groups in the B ring (C4') and A ring (C5) leads to decreased antitumor activity. Hence, the *O*-methylation of 7-OH seems to be crucial, and increasing the length of the linear hydrocarbon substituent in the A ring increases the activity. Although the 7-*O*-methoxy group in the A ring of luteolin shows satisfactory activity, the attachment of other functional groups at C7, such as a sulfo group, abolishes the antiproliferative effect.

As previously mentioned, the presence of hydroxyl groups at C7 in the A ring significantly affects the antiproliferative activity of luteolin. *O*-glycosylation at this position may further potentiate this effect.^{139,188} However, *C*-glycosylation at the C6 position significantly reduces cytotoxicity induced in melanoma cells with concomitant inhibited melanogenesis, as observed for luteolin 6-*C*-glucoside (isoorientin) in the B16F10 cell line.^{141,170} Moreover, not only *C*-glycosylation of 6-OH result in a lack of antiproliferative activity, as observed for ugonins J, K, and L.¹⁸⁹

The lack of -OH substitution on C3 in the structure of luteolin creates the possibility of competitive binding of luteolin to the ATP-binding site important to the activity of kinases (including PKC ϵ , EGFR, and FAK), which may play an essential role in skin tumors, and more specifically, in the case of luteolin treatment, inhibiting kinase action.¹²⁶

The influence of substituents in the B ring is not sufficiently understood. It has been suggested that the 3'-OH moiety in the structure of luteolin, which, among other actions, determines the high anticancer activity of the compound, probably influences cell cycle arrest to a critical level.²¹⁵ However, in the case of modification to the structure of luteolin, we have data only in the case of *O*-methyl group introduction, instead of 4'-OH, with simultaneous attachment of 5,7-di-OH. The antiproliferative activity of 4',5,7-trimethoxyluteolin is not significant, but it is not possible to state clearly what aspect of the structure determines this activity.

8 | ROLE OF LUTEOLIN AND ITS DERIVATIVE-RICH EXTRACTS IN SKIN CANCER TREATMENTS

It has been reported that the hydroalcoholic extract of *Rosmarinus officinalis*, of which luteolin is one of the main compounds present at 0.2%, has an antiproliferative effect through cytotoxic and cytostatic mechanisms resulting in the induction of apoptosis and cell cycle arrest of A375 cells. The accumulation of apoptotic cells in the sub-G0 phase and arrest in the G0/G1 and G2/M phases was observed, which is consistent with the action of known anticancer substances.¹⁴⁴ A similar effect of *Jasione montana* diethyl ether extract in the C32 cell line has been described, and the main component critical for the activity was presumed to be luteolin, which was confirmed by studies on the activity of this compound alone.¹⁴⁹ Studies on both *J. montana* or *Phyllodium elegans* extracts in the C32 and A375 lines, respectively, proved the apoptotic potential of the extracts on the reduction mitochondria membrane potential as well as the increase of caspase-3 and caspase-9 activation.²¹⁶ It has been established that the antioxidant activity of natural compounds is not correlated with their antiproliferative activity in cancer cell lines; their pro-oxidative properties are critical for their effects.²¹⁷ However, Cattaneo and co-authors found that the pro-oxidative effect of rosemary extract does not directly mediate its cytotoxic activity. The inhibition of the expression of proteins crucial for maintaining cellular homeostases, such as protein disulfide-isomerase A3 (PDIA3), glucosidase II alpha subunit (GANAB), PCB1, and PCB2, causing ER stress, was identified as the molecular mechanism underlying the induced cytotoxicity. Although luteolin is one of the main components of this extract, it did

not directly influence the antiproliferative activity but probably had a synergistic effect in the multicomponent activity.¹⁴⁴

The effects of *Petroselinum crispum* and *Matricaria chamomilla* extracts, which are abundant in polyphenols and flavonoids, including luteolin and its 7-O-glucoside, were tested in A375 cells. Despite the negligible antiproliferative activity and minor effect on the cell cycle distribution, *P. crispum* extract showed proapoptotic potential by increasing the expression of caspase-3, which is the executioner caspase in the process of apoptosis and DNA damage,^{218,219} and caspase-2, as confirmed by staining with Annexin V-PI. The *M. chamomilla* extract, containing 8% of the content of luteolin and its derivative, was found to have slightly weaker activity. However, these dominant compounds in both extracts were apigenin and its glycosidic forms, with a predominance of apigenin glucoside in the *M. chamomilla* extract. The content of luteolin and its derivative was only 5% of the polyphenol content in the *P. crispum* extract.²²⁰ However, in the case of the *J. montana* extract, the effect on caspase-3 activation as well as on caspase-8, caspase-9, and caspase-10 is attributed to luteolin, the predominant component in the extract.¹⁴⁹ The aqueous extract of *Olea europaea* leaves also was found to be proapoptotic in B16F10 cells, with its effect mediated via ERK1/2 and p53 activating pathways. However, Majumder and co-authors suggested that the underlying mechanism of ERK1/2 receptor interference is most likely triggered by oleuropein, which is one of the main components of this extract, not luteolin. However, due to the wide range of plant matrices, it can be assumed that this effect may be caused by multicomponent synergism in this fraction.²⁵

In the B16F10 line, an apoptosis-stimulating effect was also shown by the hydromethanolic extract of *Biophytum sensitivum*, participating in the regulation of Bcl-2 and p53 genes and catalyzing the expression of the aforementioned caspase-3. In addition, Guruvayoorappan and co-authors reported that an extract rich in flavonoids is characterized by an antimetastatic nature and the inhibition of pro-inflammatory cytokines that play a significant role in chemoprevention, such as TNF- α , IL-1 β , IL-6, and granulocyte-macrophage colony-stimulating factor (GM-CSF).²²¹ In addition, it has been proven that the extract of *B. sensitivum* as well as *Daphne gnidium* reduces the invasion and mobility of B16F10 cells in models of C57BL/6 and Balb/C mice in vivo.¹⁹¹ Furthermore, it activates the expression of the tissue metalloproteinase inhibitors TIMP-1 and TIMP-2 and subsequently limiting the expression of MMP-2 and MMP-9. Changes in pro-inflammatory cytokines had been tested in an in vitro model,²²¹ as well as ERK1/2 and signal transducer and activator of transcription-1 (STAT1) pathway expression, and prolyl hydroxylase, lysyl oxidase, nucleoside diphosphate kinase (NDPK), and vascular endothelial growth factor (VEGF) levels. It can be assumed that a number of flavonoids, including luteolin 7-methyl ester and isoorientin, are critical for the antimetastatic and anti-malignant activity in neoplastic cells.^{222,223}

It has been suggested that the biological activity of the water extract of *Gentiana veitchiorum* flowers is caused by isoorientin, a main flavonoid constituting 0.4% of this extract. Due to the presence of this derivative, the extract significantly suppresses the melanin content of B16F10 cells by inhibiting the mRNA expression of TYR, transient receptor potential (TRP), and dopachrome tautomerase (DCT), as well as inhibiting MITF transcription and CREB phosphorylation. Additionally, it is suspected that the activity of isoorientin causes the arrest of the intracellular cAMP pathway.¹⁷⁰ A similar outcome has been observed with *Phyllospadix watensis* extract, except that luteolin 7-sulfate was critical for its antimelanogenic activity.¹⁷⁹ Moreover, high activity of TYR inhibition and melanogenesis, correlating with the high content of luteolin and its derivatives, is observed in the case of *Asphodelus microcarpus* extracts.²²⁴ The results of the antitumor effects of species-rich in luteolin and its derivatives are summarized in Table 2.

9 | LIMITATIONS AND CHALLENGES

When comparing the IC₅₀ values of luteolin and its derivatives on the viability of cells in the same line, the method used, and incubation time, significant discrepancies between the extreme values can be observed. Therefore, the authors of this review analyzed the conditions of the experiments performed and the criteria of the methods used

TABLE 2 Antitumor activities of luteolin and its derivative-rich species in relation to skin cancer

Species	Cell line	Inhibition of proliferation		Effect of action	Molecular target	Refs.
		IC ₅₀ (μ g/ml)	Incubation time			
<i>Ailanthus excelsa</i>	C32	36.5	48 h	↓ Proliferation	Not evaluated	139
	A375	78.4	5 48 h			
<i>Ajuga chamaepitys</i>	B16F10	406.7	24 h	↓ Proliferation	↓ NF- κ B	225
	B16F10	741.4	24 h			
<i>Ajuga genevensis</i>	B16F10	236.8	24 h			
<i>Ajuga laxmannii</i>	B16F10	Not detected				
<i>Anastatica hierochuntica</i>	B16F10	Not detected		↓ Melanogenesis	Not evaluated	181
<i>Artemisia princeps</i>	B16F10	80.6	48 h	↓ Melanogenesis, ↓ proliferation	Not evaluated	141
	(MM)					
<i>Arthrophytum scoparium</i>	B16F10	>100	48 h	↓ Melanogenesis	Not evaluated	226
<i>Asphodelus microcarpus</i>	B16F10	400	48 h	↓ Melanogenesis, ↓ proliferation	↓ TYR	224
	B16F10	>10	24 h	↓ Metastasis, ↓ invasion, ↑ apoptosis, ↓ proliferation	↓ MMP-2, ↓ MMP-9, ↓ ERK-1, ↓ ERK-2, ↓ VEGF, ↓ IL-1 β , ↓ TNF- α , ↓ IL-6, ↓ GM-CSF, ↓ Bcl-2, ↑ p53, ↑ caspase-3	221,222
<i>Citrus volkameriana</i>	UACC62	>100	48 h	↓ Proliferation	Not evaluated	227
<i>Daphne gnidium</i>	B16F10	Not detected		↑ Apoptosis	↓ CTL	191
<i>Gentiana veitchiorum</i>	B16F10	>2 000	48 h	↓ Melanogenesis	↓ TYR, ↓ TRP1, ↓ DCT, ↓ MITF, ↓ CREB, ↓ cAMP	170
<i>Hyssopus seravshanicus</i>	B16F10	Not detected		↑ Melanogenesis	Not evaluated	228

(Continues)

TABLE 2 (Continued)

Species	Cell line	IC ₅₀ (μ g/ml)	Inhibition of proliferation Incubation time	Effect of action	Molecular target	Refs.
<i>Jasione montana</i>	C32	119.7	24 h	↓ Proliferation, ↑ autophagy, ↑ apoptosis, ↓ mitochondrial membrane potential, ↑ G2/M phase, ↑ S phase, ↓ G1 phase	↑ Caspase-3, ↑ caspase-8, ↑ caspase-9, ↑ caspase-10	149
<i>Jatropha tanjorensis</i>	A431	58.5	48 h	↓ Proliferation	Not evaluated	229
<i>Matricaria chamomilla</i>	A375	>60	72 h	↑ Apoptosis, ↑ G1 phase	↑ Caspase-2, ↑ caspase-3	220
<i>Olea europaea</i>	B16F10	91.8	24 h	↓ Proliferation, ↑ apoptosis	↑ ERK1/2, ↑ p53	25
	HTB-140	>50	24 h	Not evaluated	Not evaluated	230
	WM793	>50	24 h			
	A375	>100	24 h	↓ Proliferation	Not evaluated	231
<i>Penthorum chinense</i>	B16F10	>100	24 h	↓ Proliferation, ↓ melanogenesis, ↑ autophagy	↓ TYR, ↓ MITF, ↑ LC3B	232
<i>Petroselinum crispum</i>	A375	>60	72 h	↑ Apoptosis, ↑ sub-G1 phase	↑ Caspase-2, ↑ caspase-3	220
<i>Phyllocladum elegans</i>	A375	117.2	24 h	↓ Proliferation, ↓ metastasis, ↑ apoptosis, ↓ mitochondrial membrane potential	↑ Caspase-3, ↑ caspase-9, ↑ MuD	216
<i>Phyllospadix iwatensis</i>	B16F10	>300	48 h	↓ Melanogenesis	↓ TYR	179
<i>Pinus koraiensis</i>	A375	>1000	48 h	Not demonstrated	Not evaluated	233

TABLE 2 (Continued)

Species	Cell line	IC ₅₀ (µg/ml)	Inhibition of proliferation Incubation time	Effect of action	Molecular target	Refs.
<i>Plantago lagopus</i>	UACC-62	66.1	48 h	↓ Proliferation	Not evaluated	188
<i>Rosmarinus officinalis</i>	A375	63.0	72 h	↓ Proliferation, ↑ apoptosis, ↑ sub-G0 and ↓ G0/G1 phases, ↓ intracellular ROS	↓ PDIA3, ↓ GANAB, ↓ PCB1, ↓ PCB2	144
<i>Sonneratia caseolaris</i>	B16F10	>100	24 h	↓ Melanogenesis	Not evaluated	192,234

for determining the IC_{50} values for the compounds shown in Table 1. For example, the difference between IC_{50} values in the range of 5.2–32.9 $\mu\text{g/ml}$ in studies describing the activity of luteolin in the A375 cell line after 24-h incubation seems to be related to the use of different methods for assessing cell viability. The sulforhodamine B (SRB) assay used by Said et al. ($IC_{50} = 5.2 \mu\text{g/ml}$) is widely used to test cytotoxicity in cell-based studies but is not based on measurement of metabolic activity, in contrast to the 2,3-bis-(2-methoxy-4-nitro-5-sulfophenyl)-2H-tetrazolium-5-carboxanilide (XTT) assay used by George et al. ($IC_{50} = 32.9 \mu\text{g/ml}$), in which XTT was metabolically reduced by the enzyme mitochondrial dehydrogenase in living cells to the water-soluble product formazan. In both of these cases, the same type of medium (DMEM) was used, which differed from that used in other studies with the same cell line, such as the studies performed by Yao and co-authors as well as Cattaneo and co-authors, who used RPMI medium. The results of the studies by Yao and co-authors and by Cattaneo and co-authors were evaluated by another tetrazolium salt, substitute for XTT, 3-(4,5-dimethylthiazol-2-yl)-2,5-diphenyltetrazolium bromide (MTT) assay performed under the same analysis conditions and showed very similar IC_{50} values of 10.4 and 9.7 $\mu\text{g/ml}$, respectively. Hence, the choice of not only the method to determine activity level but also of the culture medium seems to be important. Moreover, in many cases, it has been observed that the incubation time plays a critical role in determining the IC_{50} value, as shown in the results from luteolin treatment of, for example, C32 cells (Table 1). Notably, cell proliferation involves many biochemical processes, many of which depend on each other, and the studied natural compounds can influence the processes at different stages or in different ways. Moreover, the proven antiproliferative potential of luteolin definitively varies according to the diversity and complexity of the gene expressed in different cell lines. Therefore, certain mutations in different *in vitro* cell models can render a cell line resistant to the action of this flavone, as perfectly illustrated by the differences in the B16F10 and A375 cell lines shown in Table 1. It can be assumed that the differences between these extreme results are due to the use of different solvents with the test compound or the use of different cell media enriched with various substances. In these cases, it is difficult to standardize and compare IC_{50} values reflecting a proliferation-depressing effect, as additional factors appear to influence the outcomes. In addition, cell lines should not be passaged too many times or cultured for too long, and the test substances, despite their high purity, are subject to degradation, especially when dissolved in solvent and stored under unsuitable conditions.

In vitro and *in vivo*, luteolin and its derivatives exhibit a diverse antitumor response depending on the model adopted. Although encouraging results render luteolin and its derivatives as potential anticancer agents for the treatment of skin cancer, the effects of these natural compounds in therapeutic intervention are quite complex due to the genetically related mechanisms underlying their activity. Therefore, the molecular mechanisms in each cell need to be understood, and the selectivity, efficacy, pharmacological and toxicological properties of luteolin and its derivatives need to be analyzed, which will be crucial in translating them from laboratory studies to clinical trials. Extensive clinical studies are needed to determine whether luteolin, as well as its derivatives, can act in a manner similar to that described in various *in vitro* and *in vivo* models. Currently, only 16 studies are listed in the ClinicalTrials.gov database (<http://www.clinicaltrials.gov>), of which none is addressing the use of luteolin in skin cancer. However, clinical trials of luteolin intervention for tongue SCC can be found, offering potential hope for topical application in skin cancer as well. Considering the low bioavailability of natural compounds in general and of luteolin and its derivatives in particular and because oral administration is challenging, topical administration seems to be an alternative.²³⁵ Due to its lipophilicity, luteolin is able to penetrate deep into human skin. This effect has been confirmed with *in vivo* studies demonstrating its ability not only to absorb into the skin surface but also to penetrate deeper skin layers, thus providing potential for use in topical therapy of skin cancer.^{131,132} However, there is still a need to develop a suitable formulation. The hope is for new pharmaceutical systems that provide, in addition to higher drug solubility, increased biochemical stability, and bioavailability, as well as controlled release of the drug in the target tissue. Particularly noteworthy are nanosystems such as liposomes, polyerosomes, dendrimers, nanotubes, quantum dots, nano micelles, nanogels, polymer nanoparticles, nanospheres, magnetic nanoparticles, solid lipid nanoparticles, nanostructured lipid carriers, which provide impressive advances in skin cancer therapy by efficiently transporting the therapeutic agent through the stratum corneum and delivering it to deeper

skin layers. They have been proven to have high skin penetration, controlled reaching to the specific tumor site, bioavailability, and their efficacy and specificity. Moreover, recent research is focused on developing new proper nanotechnology-based forms of skin cancer therapy.²³⁶⁻²³⁹ Additionally, the therapeutic efficacy of nanoparticles like liposomes has also been confirmed for other cancers as potential drug delivery systems also approved for clinical use.²⁴⁰⁻²⁴² However, a prerequisite for a therapeutic effect are realistic conditions with effective concentrations at the target site, for which quantitative studies are necessary. Although the dermal penetration of luteolin offers hope for its use in topical therapy, further scientific study on luteolin and its derivatives is still needed to obtain a clear description of its dermal penetration, dosing strategies, development of a suitable pharmaceutical formulation, prolongation of topical drug release, stability, and optimal dose. In addition, it is crucial to determine the full safety and bioavailability of these compounds in patient studies because, despite their relative safety and use in children with autism,^{151,243} cases of exacerbated chemical colitis in mice have been reported after oral administration.²⁴⁴

The anticancer efficacy of luteolin and its derivatives supports further research aimed at the development of new treatment options for skin cancer. Further work is needed to evaluate their use in preclinical and clinical studies to obtain a clear picture of the effects of these natural compounds from a biochemical point of view.

ACKNOWLEDGMENT

The study was funded by Project no. POWR.03.02.00-00-I051/16 from European Union funds, POWER 2014-2020, Grant no. 05/IMSD/G/2019.

CONFLICT OF INTERESTS

The authors declare that there are no conflict of interests.

DATA AVAILABILITY STATEMENT

Data sharing is not applicable to this article as no new data were created or analyzed in this study.

ORCID

Aleksandra M. Juszcak  <https://orcid.org/0000-0002-3072-9869>

Ute Wölfle  <http://orcid.org/0000-0003-0093-560X>

Marijana Zovko Končić  <http://orcid.org/0000-0002-8787-6667>

Michał Tomczyk  <http://orcid.org/0000-0002-4063-1048>

REFERENCES

1. Matthews NH, Li W-Q, Qureshi AA, Weinstock MA, Cho E. Epidemiology of melanoma. In: Ward WH, Farma JM, eds. *Cutaneous Melanoma: Etiology and Therapy*. Codon Publications; 2017:3-23.
2. Girschik J, Fritschl L, Threlfall T, Slevin T. Deaths from non-melanoma skin cancer in Western Australia. *Cancer Causes Control*. 2008;19(8):879-885.
3. Orthaber K, Pristovnik M, Skok K, Perić B, Maver U. Skin cancer and its treatment: novel treatment approaches with emphasis on nanotechnology. *J Nanomater*. 2017;2017(2):1-20.
4. Diepgen TL, Mahler V. The epidemiology of skin cancer. *Br J Dermatol*. 2002;146(s61):S1-S6.
5. Linares MA, Zakaria A, Nizran P. Skin cancer. *Prim Care*. 2015;42(4):645-659.
6. Apalla Z, Lallas A, Sotiriou E, Lazaridou E, Ioannides D. Epidemiological trends in skin cancer. *Dermatol Pract Concept*. 2017;7(2):1-6.
7. Katalinic A, Kunze U, Schafer T. Epidemiology of cutaneous melanoma and non-melanoma skin cancer in Schleswig-Holstein, Germany: incidence, clinical subtypes. *Br J Dermatol*. 2003;149(6):1200-1206.
8. Madan V, Lear JT, Szeimies RM. Non-melanoma skin cancer. *Lancet*. 2010;375(9715):673-685.
9. Rastrelli M, Tropea S, Rossi CR, Alaibac M. Melanoma: epidemiology, risk factors, pathogenesis, diagnosis and classification. *In Vivo*. 2014;28(6):1005-1011.
10. Chen ST, Geller AC, Tsao H. Update on the epidemiology of melanoma. *Curr Dermatol Rep*. 2013;2(1):24-34.

11. Reichrath J, Rass K. Ultraviolet damage, DNA repair and vitamin D in nonmelanoma skin cancer and in malignant melanoma: an update. In: Reichrath J, ed. *Sunlight, Vitamin D and Skin Cancer*. Springer; 2014:208-233.
12. Leiter U, Garbe C. Epidemiology of melanoma and nonmelanoma skin cancer—the role of sunlight. *Adv Exp Med Biol*. 2008;624:89-103.
13. Fransen M, Karahalios A, Sharma N, English DR, Giles GG, Sinclair RD. Non-melanoma skin cancer in Australia. *Med J Aust*. 2012;197(10):565-568.
14. Rubin AI, Chen EH, Ratner D. Basal-cell carcinoma. *N Engl J Med*. 2005;353(21):2262-2269.
15. Apalla Z, Calzavara-Pinton P, Lallas A, et al. Histopathological study of perilesional skin in patients diagnosed with nonmelanoma skin cancer. *Clin Exp Dermatol*. 2016;41(1):21-25.
16. George VC, Kumar DRN, Suresh PK, Kumar S, Kumar RA. Comparative studies to evaluate relative *in vitro* potency of luteolin in inducing cell cycle arrest and apoptosis in HaCat and A375 cells. *Asian Pac J Cancer Prev*. 2013;14(2): 631-637.
17. Newman DJ, Cragg GM. Natural products as sources of new drugs over the 30 years from 1981 to 2010. *J Nat Prod*. 2012;75(3):311-335.
18. Chinembiri TN, Du Plessis LH, Gerber M, Hamman JH, Du Plessis J. Review of natural compounds for potential skin cancer treatment. *Molecules*. 2014;19(8):11679-11721.
19. da Rocha AB, Lopes RM, Schwartzmann G. Natural products in anticancer therapy. *Curr Opin Pharmacol*. 2001;1(4): 364-369.
20. Cragg GM, Newman DJ. Plants as a source of anti-cancer agents. *J Ethnopharmacol*. 2005;100(1-2):72-79.
21. Aumeeruddy MZ, Mahomoodally MF. Combating breast cancer using combination therapy with 3 phytochemicals: piperine, sulforaphane, and thymoquinone. *Cancer*. 2019;125(10):1600-1611.
22. Imran M, Rauf A, Abu-Izneid T, et al. Luteolin, a flavonoid, as an anticancer agent: a review. *Biomed Pharmacother*. 2019;112:108612.
23. Iqbal J, Abbasi BA, Ahmad R, et al. Potential phytochemicals in the fight against skin cancer: current landscape and future perspectives. *Biomed Pharmacother*. 2019;109:1381-1393.
24. Penta D, Somashekar BS, Meeran SM. Epigenetics of skin cancer: interventions by selected bioactive phytochemicals. *Photodermatol Photoimmunol Photomed*. 2018;34(1):42-49.
25. Majumder D, Debnath M, Libin Kumar KV, et al. Metabolic profiling and investigations on crude extract of *Olea europaea* L. leaves as a potential therapeutic agent against skin cancer. *J Funct Foods*. 2019;58:266-274.
26. Ijaz S, Akhtar N, Khan MS, et al. Plant derived anticancer agents: a green approach towards skin cancers. *Biomed Pharmacother*. 2018;103:1643-1651.
27. Chahar MK, Sharma N, Dobhal MP, Joshi YC. Flavonoids: a versatile source of anticancer drugs. *Pharmacogn Rev*. 2011;5(9):1-12.
28. Müller CSL, Reichrath J. Histology of melanoma and nonmelanoma skin cancer. In: Reichrath J, ed. *Sunlight, Vitamin D and Skin Cancer*. Springer; 2014:215-226.
29. Emmert S, Schön MP, Haenssle A. Molecular biology of basal and squamous cell carcinomas. In: Reichrath J, ed. *Sunlight, Vitamin D and Skin Cancer*. Springer; 2014:171-191.
30. Khavari PA. Modelling cancer in human skin tissue. *Nat Rev Cancer*. 2006;6(4):270-280.
31. Pal HC, Hunt KM, Diamond A, Elmets A, Afaq C, F. Phytochemicals for the management of melanoma. *Mini Rev Med Chem*. 2016;16(12):953-979.
32. Röwert-Huber J, Patel MJ, Forschner T, et al. Actinic keratosis is an early *in situ* squamous cell carcinoma: a proposal for reclassification. *Br J Dermatol*. 2007;156(s3):8-12.
33. Tsatmali M, Ancans J, Thody AJ. Melanocyte function and its control by melanocortin peptides. *J Histochem Cytochem*. 2002;50(2):125-133.
34. Garbe C, Amaral T, Peris K, et al. European consensus-based interdisciplinary guideline for melanoma. Part 1: diagnostics – update 2019. *Eur J Cancer*. 2020;126:141-158.
35. Goyanna R, Torres ET, Broders AC. Histological grading of malignant tumors: Broder's method. *Hospital*. 1951;39(6): 791-818.
36. Abbasi NR, Shaw HM, Rigel DS, et al. Early diagnosis of cutaneous melanoma: revisiting the ABCD criteria. *JAMA*. 2004;292(22):2771-2776.
37. Vestergaard ME, Macaskill P, Holt PE, Menzies SW. Dermoscopy compared with naked eye examination for the diagnosis of primary melanoma: a meta-analysis of studies performed in a clinical setting. *Br J Dermatol*. 2008;159(3): 669-676.
38. Park HS, Cho KH. Acral lentiginous melanoma *in situ*: a diagnostic and management challenge. *Cancers*. 2010;2(2): 642-652.
39. Ward WH, Lambreton F, Goel N, Yu JQ, Farma JM. Clinical presentation and staging of melanoma. In: Ward WH, Farma JM, eds. *Cutaneous Melanoma: Etiology and Therapy*. Codon Publications; 2017:79-91.

40. Belter B, Haase-Kohn C, Pietzsch J. Biomarkers in malignant melanoma: recent trends and critical perspective. In: Ward WH, Farma JM, eds. *Cutaneous Melanoma: Etiology and Therapy*. Codon Publications; 2017:39-57.
41. Erdei E, Torres SM. A new understanding in the epidemiology of melanoma. *Expert Rev Anticancer Ther*. 2010;10(11):1811-1823.
42. Califano J, Nance M. Malignant melanoma. *Facial Plast Surg Clin North Am*. 2009;17(3):337-348.
43. Pitot HC. Multistage carcinogenesis – genetic and epigenetic mechanisms in relation to cancer prevention. *Cancer Detect Prev*. 1993;17(6):567-573.
44. Hanahan D, Weinberg RA. The hallmarks of cancer. *Cell*. 2000;100(1):57-70.
45. Lin Y, Shi R, Wang X, Shen H-M. Luteolin, a flavonoid with potentials for cancer prevention and therapy. *Curr Cancer Drug Targets*. 2008;8(7):634-646.
46. Walter SD, King WD, Marrett LD. Association of cutaneous malignant melanoma with intermittent exposure to ultraviolet radiation: results of a case-control study in Ontario, Canada. *Int J Epidemiol*. 1999;28(3):418-427.
47. Gilchrist BA, Eller MS, Geller AC, Yaar M. The pathogenesis of melanoma induced by ultraviolet radiation. *N Engl J Med*. 1999;340(17):1341-1348.
48. National Cancer Institute (NIH) Skin Cancer Treatment (PDQ®)–Health Professional Version. Accessed July 13, 2021. <https://www.cancer.gov/types/skin/hp/skin-treatment-pdq>
49. Koh HK. Cutaneous melanoma. *N Engl J Med*. 1991;325(3):171-182.
50. Preston DS, Stern RS. Nonmelanoma cancers of the skin. *N Engl J Med*. 1992;327(23):1649-1662.
51. English DR, Armstrong BK, Kricger A, Winter MG, Heenan PJ, Randell PL. Case-control study of sun exposure and squamous cell carcinoma of the skin. *Int J Cancer*. 1998;77(3):347-353.
52. Hensler S, Mueller MM. Inflammation and skin cancer: old pals telling new stories. *Cancer J*. 2013;19(6):517-524.
53. Jiao J, Mikulec C, Ishikawa T, et al. Cell-type-specific roles for COX-2 in UVB-induced skin cancer. *Carcinogenesis*. 2014;35(6):1310-1319.
54. D'Orazio J, Jarrett S, Amaro-Ortiz A, Scott T. UV Radiation and the skin. *Int J Mol Sci*. 2013;14(6):12222-12248.
55. Dupont E, Gomez J, Bilodeau D. Beyond UV radiation: a skin under challenge. *Int J Cosmet Sci*. 2013;35(3):224-232.
56. George VC, Vijesh VV, Amararathna DIM, et al. Mechanism of action of flavonoids in prevention of inflammation-associated skin cancer. *Curr Med Chem*. 2016;23(32):3697-3716.
57. Vogel CFA, Van Winkle LS, Esser C, Haarmann-Stemmann T. The aryl hydrocarbon receptor as a target of environmental stressors – implications for pollution mediated stress and inflammatory responses. *Redox Biol*. 2020;34:101530.
58. Chhabra G, Ndiaye MA, Garcia-Peterson LM, Ahmad N. Melanoma chemoprevention: current status and future prospects. *Photochem Photobiol*. 2017;93(4):975-989.
59. Hara H, Lee MH, Chen H, Luo D, Jimbow K. Role of gene expression and protein synthesis of tyrosinase, TRP-1, lamp-1, and CD63 in UVB-induced melanogenesis in human melanomas. *J Invest Dermatol*. 1994;102(4):495-500.
60. Riley PA. Melanogenesis: a realistic target for antimelanoma therapy? *Eur J Cancer*. 1991;27(9):1172-1177.
61. Riley PA. Melanogenesis and melanoma. *Pigment Cell Res*. 2003;16(5):548-552.
62. Prichard RS, Dijkstra B, McDermott EW, Hill ADK, O'Higgins NJ. The role of molecular staging in malignant melanoma. *Eur J Surg Oncol*. 2003;29(4):306-314.
63. Simões MCF, Sousa JJS, Pais AACC. Skin cancer and new treatment perspectives: a review. *Cancer Lett*. 2015;357(1):8-42.
64. Nikolaou V, Stratigos AJ. Emerging trends in the epidemiology of melanoma. *Br J Dermatol*. 2014;170(1):11-19.
65. Rütger TM. How different wavelengths of the ultraviolet spectrum contribute to skin carcinogenesis: the role of cellular damage responses. *J Invest Dermatol*. 2007;127(9):2103-2105.
66. Ridley AJ, Whiteside JR, McMillan TJ, Allinson SL. Cellular and sub-cellular responses to UVA in relation to carcinogenesis. *Int J Radiat Biol*. 2009;85(3):177-195.
67. Bouwes JNB, Plasmeijer EI, Feltkamp MCW. Beta-papillomavirus infection and skin cancer. *J Invest Dermatol*. 2008;128(6):1355-1358.
68. Amin ARMR, Kucuk O, Khuri FR, Shin DM. Perspectives for cancer prevention with natural compounds. *J Clin Oncol*. 2009;27(16):2712-2725.
69. Bode AM, Dong Z. Post-translational modification of p53 in tumorigenesis. *Nat Rev Cancer*. 2004;4(10):793-805.
70. Nickoloff BJ, Qin J-Z, Chaturvedi V, Bacon P, Panella J, Denning MF. Life and death signaling pathways contributing to skin cancer. *J Invest Dermatol Symp Proc*. 2002;7(1):27-35.
71. Uribe P, Gonzalez S. Epidermal growth factor receptor (EGFR) and squamous cell carcinoma of the skin: molecular bases for EGFR-targeted therapy. *Pathol Res Pract*. 2011;207(6):337-342.
72. Hubbard SR, Miller WT. Receptor tyrosine kinases: mechanisms of activation and signaling. *Curr Opin Cell Biol*. 2007;19(2):117-123.

73. Oda K, Matsuoka Y, Funahashi A, Kitano H. A comprehensive pathway map of epidermal growth factor receptor signaling. *Mol Syst Biol.* 2005;1:2005.0010.
74. Teillet F, Boumendjel A, Boutonnat J, Ronot X. Flavonoids as RTK inhibitors and potential anticancer agents. *Med Res Rev.* 2008;28(6):715-745.
75. Feehan RP, Shantz LM. Molecular signaling cascades involved in nonmelanoma skin carcinogenesis. *Biochem J.* 2016;473(19):2973-2994.
76. Oeckinghaus A, Ghosh S. The NF-kappaB family of transcription factors and its regulation. *Cold Spring Harb Perspect Biol.* 2009;1(4):a000034.
77. Moon H, White AC, Borowsky AD. New insights into the functions of COX-2 in skin and esophageal malignancies. *Exp Mol Med.* 2020;52(4):538-547.
78. Maglio DHG, Paz M, Cela E, Leoni J. Cyclooxygenase-2 overexpression in non-melanoma skin cancer: molecular pathways involved as targets for prevention and treatment. In: La Porta C, ed. *Skin Cancers – Risk Factors, Prevention and Therapy.* IntechOpen Limited; 2011:272.
79. Buckman SY, Gresham A, Hale P, et al. COX-2 expression is induced by UVB exposure in human skin: implications for the development of skin cancer. *Carcinogenesis.* 1998;19(5):723-729.
80. Nichols JA, Katiyar SK. Skin photoprotection by natural polyphenols: anti-inflammatory, antioxidant and DNA repair mechanisms. *Arch Dermatol Res.* 2010;302(2):71-83.
81. Sherwani MA, Tufail S, Muzaffar AF, Yusuf N. The skin microbiome and immune system: potential target for chemoprevention? *Photodermatol Photoimmunol Photomed.* 2018;34(1):25-34.
82. Squarzanti DF, Zavattaro E, Pizzimenti S, Amoroso A, Savoia P, Azzimonti B. Non-melanoma skin cancer: news from microbiota research. *Crit Rev Microbiol.* 2020;46(4):433-449.
83. Yu Y, Champer J, Beynet D, Kim J, Friedman AJ. The role of the cutaneous microbiome in skin cancer: lessons learned from the gut. *J Drugs Dermatol.* 2015;14(5):461-465.
84. Rodríguez-Daza MC, Pulido-Mateos EC, Lupien-Meilleur J, Guyonnet D, Desjardins Y, Roy D. Polyphenol-mediated gut microbiota modulation: toward prebiotics and further. *Front Nutr.* 2021;8:689456.
85. Akbani R, Akdemir KC, Aksoy BA, et al. Genomic classification of cutaneous melanoma. *Cell.* 2015;161(7):1681-1696.
86. Leonardi GC, Falzone L, Salemi R, et al. Cutaneous melanoma: from pathogenesis to therapy (Review). *Int J Oncol.* 2018;52(4):1071-1080.
87. Chappell WH, Steelman LS, Long JM, et al. Ras/Raf/MEK/ERK and PI3K/PTEN/Akt/mTOR inhibitors: rationale and importance to inhibiting these pathways in human health. *Oncotarget.* 2011;2(3):135-164.
88. Liu Y, Sheikh MS. Melanoma: molecular pathogenesis and therapeutic management. *Mol Cell Pharmacol.* 2014;6(3):228.
89. Fedorenko IV, Gibney GT, Smalley KSM. NRAS mutant melanoma: biological behavior and future strategies for therapeutic management. *Oncogene.* 2013;32(25):3009-3018.
90. Rubinstein JC, Sznol M, Pavlick AC, et al. Incidence of the V600K mutation among melanoma patients with BRAF mutations, and potential therapeutic response to the specific BRAF inhibitor PLX4032. *J Transl Med.* 2010;8:67.
91. Lovly CM, Dahlman KB, Fohn LE, et al. Routine multiplex mutational profiling of melanomas enables enrollment in genotype-driven therapeutic trials. *PLOS One.* 2012;7(4):e35309.
92. Davies H, Bignell GR, Cox C, et al. Mutations of the BRAF gene in human cancer. *Nature.* 2002;417(6892):949-954.
93. Pollock PM, Harper UL, Hansen KS, et al. High frequency of BRAF mutations in nevi. *Nat Genet.* 2003;33(1):19-20.
94. Dong J, Phelps RG, Qiao R, et al. BRAF oncogenic mutations correlate with progression rather than initiation of human melanoma. *Cancer Res.* 2003;63(14):3883-3885.
95. Oliveira Júnior R, Ferraz C, Silva M, et al. Flavonoids: promising natural products for treatment of skin cancer (melanoma). In: Koehn FE, ed. *Natural Products and Cancer Drug Discovery.* IntechOpen Limited; 2017:161-210.
96. Houben R, Becker JC, Kappel A, et al. Constitutive activation of the Ras-Raf signaling pathway in metastatic melanoma is associated with poor prognosis. *J Carcinog.* 2004;3:6.
97. Platz A, Eghyazi S, Ringborg U, Hansson J. Human cutaneous melanoma: a review of NRAS and BRAF mutation frequencies in relation to histogenetic subclass and body site. *Mol Oncol.* 2008;1(4):395-405.
98. Roskoski RJ. Structure and regulation of Kit protein-tyrosine kinase – the stem cell factor receptor. *Biochem Biophys Res Commun.* 2005;338(3):1307-1315.
99. Nissan MH, Pratilas CA, Jones AM, et al. Loss of NF1 in cutaneous melanoma is associated with RAS activation and MEK dependence. *Cancer Res.* 2014;74(8):2340-2350.
100. Handolias D, Salemi R, Murray W, et al. Mutations in KIT occur at low frequency in melanomas arising from anatomical sites associated with chronic and intermittent sun exposure. *Pigment Cell Melanoma Res.* 2010;23(2):210-215.

101. Shi H, Hugo W, Kong X, et al. Acquired resistance and clonal evolution in melanoma during BRAF inhibitor therapy. *Cancer Discov.* 2014;4(1):80-93.
102. Hennessy BT, Smith DL, Ram PT, Lu Y, Mills GB. Exploiting the PI3K/AKT pathway for cancer drug discovery. *Nat Rev Drug Discov.* 2005;4(12):988-1004.
103. Mirmohammadsadegh A, Marini A, Nambiar S, et al. Epigenetic silencing of the PTEN gene in melanoma. *Cancer Res.* 2006;66(13):6546-6552.
104. Liu L, Dilworth D, Gao L, et al. Mutation of the CDKN2A 5' UTR creates an aberrant initiation codon and predisposes to melanoma. *Nat Genet.* 1999;21(1):128-132.
105. Shain AH, Yeh I, Kovalyshyn I, et al. The genetic evolution of melanoma from precursor lesions. *N Engl J Med.* 2015; 373(20):1926-1936.
106. Massagué J. G1 cell-cycle control and cancer. *Nature.* 2004;432(7015):298-306.
107. McNeal AS, Liu K, Nakhate V, et al. CDKN2B loss promotes progression from benign melanocytic nevus to melanoma. *Cancer Discov.* 2015;5(10):1072-1085.
108. Garbe C, Amaral T, Peris K, et al. European consensus-based interdisciplinary guideline for melanoma. Part 2: treatment – update 2019. *Eur J Cancer.* 2020;126:141-177.
109. Martinez JC, Otley CC. The management of melanoma and nonmelanoma skin cancer: a review for the primary care physician. *Mayo Clin Proc.* 2001;76(12):1253-1265.
110. Joyce KM. Surgical management of melanoma. In: Ward WH, Farma JM, eds. *Cutaneous Melanoma: Etiology and Therapy.* Codon Publications; 2017:91-101.
111. Torre LA, Bray F, Siegel RL, Ferlay J, Lortet-Tieulent J, Jemal A. Global cancer statistics, 2012. *CA Cancer J Clin.* 2015; 65(2):87-108.
112. Garbe C, Peris K, Hauschild A, et al. Diagnosis and treatment of melanoma. European consensus-based interdisciplinary guideline – update 2012. *Eur J Cancer.* 2012;48(15):2375-2390.
113. Harries M, Malvey J, Lebbe C, et al. Treatment patterns of advanced malignant melanoma (stage III-IV) – A review of current standards in Europe. *Eur J Cancer.* 2016;60:179-189.
114. Bhatia S, Tykodi SS, Thompson JA. Treatment of metastatic melanoma: an overview. *Oncology.* 2009;23(6):488-496.
115. Bilir SP, Ma Q, Zhao Z, Wehler E, Munakata J, Barber B. Economic burden of toxicities associated with treating metastatic melanoma in the United States. *Am Health Drug Benefits.* 2016;9(4):203-213.
116. Kim T, Amaria RN, Spencer C, Reuben A, Cooper ZA, Wargo JA. Combining targeted therapy and immune checkpoint inhibitors in the treatment of metastatic melanoma. *Cancer Biol Med.* 2014;11(4):237-246.
117. Millet A, Martin AR, Ronco C, Rocchi S, Benhida R. Metastatic melanoma: insights into the evolution of the treatments and future challenges. *Med Res Rev.* 2017;37(1):98-148.
118. Bajetta E, Del Vecchio M, Bernard-Marty C, et al. Metastatic melanoma: chemotherapy. *Semin Oncol.* 2002;29(5): 427-445.
119. Su MY, Fisher DE. Immunotherapy in the precision medicine era: melanoma and beyond. *PLoS Med.* 2016;13(12): e1002196.
120. Tang T, Eldabaje R, Yang L. Current status of biological therapies for the treatment of metastatic melanoma. *Anticancer Res.* 2016;36(7):3229-3241.
121. Singh BP, Salama AKS. Updates in therapy for advanced melanoma. *Cancers.* 2016;8(1):17.
122. Ascierto PA, McArthur GA, Dréno B, et al. Cobimetinib combined with vemurafenib in advanced BRAF(V600)-mutant melanoma (coBRIM): updated efficacy results from a randomised, double-blind, phase 3 trial. *Lancet Oncol.* 2016;17(9):1248-1260.
123. Chae HS, Xu R, Won JY, Chin YW, Yim H. Molecular targets of genistein and its related flavonoids to exert anticancer effects. *Int J Mol Sci.* 2019;20(10):1-18.
124. Liskova A, Koklesova L, Samec M, et al. Flavonoids in cancer metastasis. *Cancers.* 2020;12(6):1-29.
125. Scheau C, Mihai LG, Bădărău IA, Căruntu C. Emerging applications of some important natural compounds in the field of oncology. *Farmacia.* 2020;68(6):992-998.
126. Kanadaswami C, Lee LT, Lee PPH, et al. The antitumor activities of flavonoids. *In Vivo.* 2005;19(5):895-910.
127. Lotha R, Sivasubramanian A. Flavonoids nutraceuticals in prevention and treatment of cancer: a review. *Asian J Pharm Clin Res.* 2018;11(1):42-47.
128. Chirumbolo S, Bjørklund G, Lysiuk R, Vella A, Lenchyk L, Upyr T. Targeting cancer with phytochemicals via their fine tuning of the cell survival signaling pathways. *Int J Mol Sci.* 2018;19(11):3568.
129. Ombra MN, Paliogiannis P, Stucci LS, et al. Dietary compounds and cutaneous malignant melanoma: recent advances from a biological perspective. *Nutr Metab.* 2019;16(1):1-15.
130. Momtaz S, Niaz K, Maqbool F, Abdollahi M, Rastrelli L, Nabavi SM. STAT3 targeting by polyphenols: novel therapeutic strategy for melanoma. *Biofactors.* 2017;43(3):347-370.

131. Seelinger G, Merfort I, Wölfle U, Schempp CM. Anti-carcinogenic effects of the flavonoid luteolin. *Molecules*. 2008;13(10):2628-2651.
132. González-Vallinas M, González-Castejón M, Rodríguez-Casado A, Ramírez, de Molina A. Dietary phytochemicals in cancer prevention and therapy: a complementary approach with promising perspectives. *Nutr Rev*. 2013;71(9):585-599.
133. Pan M-H, Lai C-S, Wu J-C, Ho C-T. Epigenetic and disease targets by polyphenols. *Curr Pharm Des*. 2013;19(34):6156-6185.
134. Ganai SA, Sheikh FA, Baba ZA, Mir MA, Mantoo MA, Yattoo MA. Anticancer activity of the plant flavonoid luteolin against preclinical models of various cancers and insights on different signalling mechanisms modulated. *Phytother Res*. 2021;35(7):3509-3532.
135. Islam SU, Ahmed MB, Ahsan H, et al. An update on the role of dietary phytochemicals in human skin cancer: new insights into molecular mechanisms. *Antioxidants*. 2020;9(10):1-30.
136. López-Lázaro M. Distribution and biological activities of the flavonoid luteolin. *Mini Rev Med Chem*. 2009;9(1):31-59.
137. Horváthová K, Chalupa I, Šebová L, Tóthová D, Vachálková A. Protective effect of quercetin and luteolin in human melanoma HMB-2 cells. *Mutat Res - Genet Toxicol Environ Mutagen*. 2005;565(2):105-112.
138. Seito LN, Ruiz ALTG, Vendramini-Costa D, et al. Antiproliferative activity of three methoxylated flavonoids isolated from *Zeyheria montana* Mart. (Bignoniaceae) leaves. *Phyther Res*. 2011;25(10):1447-1450.
139. Said A, Tundis R, Hawas UW, et al. *In vitro* antioxidant and antiproliferative activities of flavonoids from *Ailanthus excelsa* (Roxb.) (Simaroubaceae) leaves. *Z Naturforsch C*. 2010;65(3-4):180-186.
140. Kawaii S, Tomono Y, Katase E, Ogawa K, Yano M. Antiproliferative activity of flavonoids on several cancer cell lines. *Biosci Biotechnol Biochem*. 1999;63(5):896-899.
141. Akihisa T, Kawashima K, Orido M, et al. Antioxidative and melanogenesis-inhibitory activities of caffeoylquinic acids and other compounds from moxa. *Chem Biodivers*. 2013;10(3):313-327.
142. Nagao T, Abe F, Kinjo J, Okabe H. Antiproliferative constituents in plants 10. Flavones from the leaves of *Lantana montevidensis* Briq. and consideration of structure-activity relationship. *Biol Pharm Bull*. 2002;25(7):875-879.
143. Meng TX, Irino N, Kondo R. Melanin biosynthesis inhibitory activity of a compound isolated from young green barley (*Hordeum vulgare* L.) in B16 melanoma cells. *J Nat Med*. 2015;69(3):427-431.
144. Cattaneo L, Cicconi R, Mignogna G, et al. Anti-proliferative effect of *Rosmarinus officinalis* L. Extract on human melanoma A375 cells. *PLOS One*. 2015;10(7):1-18.
145. Dar AA, Dangroo NA, Raina A, et al. Biologically active xanthenes from *Codonopsis ovata*. *Phytochemistry*. 2016;132:102-108.
146. Jiang W, Xia T, Liu C, Li J, Zhang W, Sun C. Remodeling the epigenetic landscape of cancer-application potential of flavonoids in the prevention and treatment of cancer. *Front Oncol*. 2021;11:705903.
147. Arora I, Sharma M, Tollefsbol TO. Combinatorial epigenetics impact of polyphenols and phytochemicals in cancer prevention and therapy. *Int J Mol Sci*. 2019;20(18):4567.
148. Kang KA, Piao MJ, Hyun YJ, et al. Luteolin promotes apoptotic cell death via upregulation of Nrf2 expression by DNA demethylase and the interaction of Nrf2 with p53 in human colon cancer cells. *Exp Mol Med*. 2019;51(4):1-14.
149. Juszcak AM, Czarnomys R, Strawa JW, Zovko Končić M, Bielawski K, Tomczyk M. *In vitro* anticancer potential of *Jasione montana* and its main components against human amelanotic melanoma cells. *Int J Mol Sci*. 2021;22(7):3345.
150. Yao X, Jiang W, Yu D, Yan Z. Luteolin inhibits proliferation and induces apoptosis of human melanoma cells: *in vivo* and *in vitro* by suppressing MMP-2 and MMP-9 through the PI3K/AKT pathway. *Food Funct*. 2019;10(2):703-712.
151. Schomberg J, Wang Z, Farhat A, et al. Luteolin inhibits melanoma growth *in vitro* and *in vivo* via regulating ECM and oncogenic pathways but not ROS. *Biochem Pharmacol*. 2020;177:114025.
152. Byun S, Lee KW, Jung SK, et al. Luteolin inhibits protein kinase C ϵ and c-Src activities and UVB-induced skin cancer. *Cancer Res*. 2010;70(6):2415-2423.
153. Tian L, Wang S, Jiang S, et al. Luteolin as an adjuvant effectively enhances CTL anti-tumor response in B16F10 mouse model. *Int Immunopharmacol*. 2021;94:107441.
154. Ralph SJ, Rodríguez-Enríquez S, Neuzil J, Saavedra E, Moreno-Sánchez R. The causes of cancer revisited: "mitochondrial malignancy" and ROS-induced oncogenic transformation – why mitochondria are targets for cancer therapy. *Mol Aspects Med*. 2010;31(2):145-170.
155. Kim JK, Kang KA, Ryu YS, et al. Induction of endoplasmic reticulum stress *via* reactive oxygen species mediated by luteolin in melanoma cells. *Anticancer Res*. 2016;36(5):2281-2289.
156. Rodríguez J, Yáñez J, Vicente V, et al. Effects of several flavonoids on the growth of B16F10 and SK-MEL-1 melanoma cell lines: relationship between structure and activity. *Melanoma Res*. 2002;12(2):99-107.
157. Yáñez J, Vicente V, Alcaraz M, et al. Cytotoxicity and antiproliferative activities of several phenolic compounds against three melanocytes cell lines: relationship between structure and activity. *Nutr Cancer*. 2004;49(2):191-199.

158. Kushiro K, Chu RA, Verma A, Núñez NP. Adipocytes promote B16BL6 melanoma cell invasion and the epithelial-to-mesenchymal transition. *Cancer Microenviron*. 2012;5(1):73-82.
159. Hussain Y, Cui JH, Khan H, Aschner M, Batiha GES, Jeandet P. Luteolin and cancer metastasis suppression: focus on the role of epithelial to mesenchymal transition. *Med Oncol*. 2021;38(6):1-12.
160. Lin Y, Tsai P, Kandaswami CC, et al. Effects of dietary flavonoids, luteolin, and quercetin on the reversal of epithelial-mesenchymal transition in A431 epidermal cancer cells. *Cancer Sci*. 2011;102(10):1829-1839.
161. Ruan JS, Liu YP, Zhang L, et al. Luteolin reduces the invasive potential of malignant melanoma cells by targeting β 3 integrin and the epithelial-mesenchymal transition. *Acta Pharmacol Sin*. 2012;33(10):1325-1331.
162. Huang YT, Hwang JJ, Lee PP, et al. Effects of luteolin and quercetin, inhibitors of tyrosine kinase, on cell growth and metastasis-associated properties in A431 cells overexpressing epidermal growth factor receptor. *Br J Pharmacol*. 1999;128(5):999-1010.
163. Li C, Wang Q, Shen S, Wei X, Li G. HIF-1 α /VEGF signaling-mediated epithelial-mesenchymal transition and angiogenesis is critically involved in anti-metastasis effect of luteolin in melanoma cells. *Phyther Res*. 2019;33(3):798-807.
164. Fan JJ, Hsu WH, Lee KH, et al. Dietary flavonoids luteolin and quercetin inhibit migration and invasion of squamous carcinoma through reduction of Src/Stat3/S100A7 signaling. *Antioxidants*. 2019;8(11):557.
165. Lin YC, Tsai PH, Lin CY, et al. Impact of flavonoids on matrix metalloproteinase secretion and invadopodia formation in highly invasive A431-III cancer cells. *PLoS One*. 2013;8(8):e71903.
166. Lee L-T, Huang Y-T, Hwang J-J, et al. Transinactivation of the epidermal growth factor receptor tyrosine kinase and focal adhesion kinase phosphorylation by dietary flavonoids: effect on invasive potential of human carcinoma cells. *Biochem Pharmacol*. 2004;67(11):2103-2114.
167. Iwashita K, Kobori M, Yamaki K, Tsushida T. Flavonoids inhibit cell growth and induce apoptosis in B16 melanoma 4A5 cells. *Biosci Biotechnol Biochem*. 2000;64(9):1813-1820.
168. Gilchrist BA, Eller MS. DNA photodamage stimulates melanogenesis and other photoprotective responses. *J Invest Dermatol*. 1999;4(1):35-40.
169. Parvez S, Kang M, Chung H-S, et al. Survey and mechanism of skin depigmenting and lightening agents. *Phytother Res*. 2006;20(11):921-934.
170. Wu QY, Wong ZCF, Wang C, et al. Isoorientin derived from *Gentiana veitchiorum* Hemsl. flowers inhibits melanogenesis by down-regulating MITF-induced tyrosinase expression. *Phytomedicine*. 2019;57:129-136.
171. An SM, Kim HJ, Kim J-E, Boo YC. Flavonoids, taxifolin and luteolin attenuate cellular melanogenesis despite increasing tyrosinase protein levels. *Phytother Res*. 2008;22(9):1200-1207.
172. Choi MY, Song HS, Hur HS, Sim SS. Whitening activity of luteolin related to the inhibition of cAMP pathway in α -MSH-stimulated B16 melanoma cells. *Arch Pharm Res*. 2008;31(9):1166-1171.
173. Takekoshi S, Nagata H, Kitatani K. Flavonoids enhance melanogenesis in human melanoma cells. *Tokai J Exp Clin Med*. 2014;39(3):116-121.
174. Yamauchi K, Fujieda A, Mitsunaga T. Selective synthesis of 7-O-substituted luteolin derivatives and their melanogenesis and proliferation inhibitory activity in B16 melanoma cells. *Bioorganic Med Chem Lett*. 2018;28(14):2518-2522.
175. Horibe I, Satoh Y, Shiota Y, et al. Induction of melanogenesis by 4'-O-methylated flavonoids in B16F10 melanoma cells. *J Nat Med*. 2013;67(4):705-710.
176. Shi R, Huang Q, Zhu X, et al. Luteolin sensitizes the anticancer effect of cisplatin via c-Jun NH2-terminal kinase-mediated p53 phosphorylation and stabilization. *Mol Cancer Ther*. 2007;6(4):1338-1347.
177. Bu J, Ma PC, Chen ZQ, et al. Inhibition of MITF and tyrosinase by paeonol-stimulated JNK/SAPK to reduction of phosphorylated CREB. *Am J Chin Med*. 2008;36(2):245-263.
178. Lee SW, Kim JH, Song H, Seok JK, Hong SS, Boo YC. Luteolin 7-sulfate attenuates melanin synthesis through inhibition of CREB- and MITF-mediated tyrosinase expression. *Antioxidants*. 2019;8(4):87.
179. Kwak JY, Seok JK, Suh H-J, et al. Antimelanogenic effects of luteolin 7-sulfate isolated from *Phyllospadix iwatensis* Makino. *Br J Dermatol*. 2016;175(3):501-511.
180. Martínez C, Yáñez J, Vicente V, et al. Effects of several polyhydroxylated flavonoids on the growth of B16F10 melanoma and Melan-a melanocyte cell lines: influence of the sequential oxidation state of the flavonoid skeleton. *Melanoma Res*. 2003;13(1):3-9.
181. Nakashima S, Matsuda H, Oda Y, Nakamura S, Xu F, Yoshikawa M. Melanogenesis inhibitors from the desert plant *Anastatica hierochuntica* in B16 melanoma cells. *Bioorg Med Chem*. 2010;18(6):2337-2345.
182. Dar AA, Rath SK, Qaudri A, et al. Isolation, cytotoxic evaluation, and simultaneous quantification of eight bioactive secondary metabolites from *Cicer microphyllum* by high-performance thin-layer chromatography. *J Sep Sci*. 2015;38(23):4021-4028.
183. Touil YS, Fellous A, Scherman D, Chabot GG. Flavonoid-induced morphological modifications of endothelial cells through microtubule stabilization. *Nutr Cancer*. 2009;61(3):310-321.

184. Manthey JA, Guthrie N. Antiproliferative activities of citrus flavonoids against six human cancer cell lines. *J Agr Food Chem*. 2002;50(21):5837-5843.
185. Peng H, Xing Y, Gao L, Zhang L, Zhang G. Simultaneous separation of apigenin, luteolin and rosmarinic acid from the aerial parts of the copper-tolerant plant *Elsholtzia splendens*. *Environ Sci Pollut Res Int*. 2014;21(13):8124-8132.
186. Chen KC, Hsu WH, Ho JY, et al. Flavonoids luteolin and quercetin inhibit RPS19 and contributes to metastasis of cancer cells through c-Myc reduction. *J Food Drug Anal*. 2018;26(3):1180-1191.
187. Lin CW, Lai GM, Chen KC, et al. RPS12 increases the invasiveness in cervical cancer activated by c-Myc and inhibited by the dietary flavonoids luteolin and quercetin. *J Funct Foods*. 2015;19:19236-19247.
188. Gálvez M, Martín-Cordero C, López-Lázaro M, Cortés F, Ayuso MJ. Cytotoxic effect of *Plantago* spp. on cancer cell lines. *J Ethnopharmacol*. 2003;88(2-3):125-130.
189. Yamauchi K, Mitsunaga T, Itakura Y, Batubara I. Extracellular melanogenesis inhibitory activity and the structure-activity relationships of ugonins from *Helminthostachys zeylanica* roots. *Fitoterapia*. 2015;104:10469-10474.
190. Choi J, Lee D-H, Park S-Y, Seol J-W. Diosmetin inhibits tumor development and block tumor angiogenesis in skin cancer. *Biomed Pharmacother*. 2019;117:109091.
191. Chaabane F, Mustapha N, Mokdad-Bzeouich I, et al. *In vitro* and *in vivo* anti-melanoma effects of *Daphne gnidium* aqueous extract via activation of the immune system. *Tumour Biol*. 2016;37(5):6511-6517.
192. Arung E, Kuspradini H, Kusuma I, et al. Effects of isolated compound from *Sonneratia caseolaris* leaf: a validation of traditional utilization by melanin biosynthesis and antioxidant assays. *J Appl Pharm Sci*. 2015;5(10):39-43.
193. Apalla Z, Nashan D, Weller RB, Castellsagué X. Skin cancer: epidemiology, disease burden, pathophysiology, diagnosis, and therapeutic approaches. *Dermatol Ther*. 2017;7:5-19.
194. Olson AL, Gaffney CA, Starr P, Dietrich AJ. The impact of an appearance-based educational intervention on adolescent intention to use sunscreen. *Health Educ Res*. 2008;23(5):763-769.
195. National Cancer Institute (NIH). Skin Cancer Prevention (PDQ®)—Health Professional Version. Accessed July 13, 2021.
196. Demierre M-F, Nathanson L. Chemoprevention of melanoma: an unexplored strategy. *J Clin Oncol*. 2003;21(1):158-165.
197. Lao CD, Demierre M-F, Sondak VK. Targeting events in melanoma carcinogenesis for the prevention of melanoma. *Expert Rev Anticancer Ther*. 2006;6(11):1559-1568.
198. Lien EJ, Ren S, Bui HH, Wang R. Quantitative structure-activity relationship analysis of phenolic antioxidants. *Free Radic Biol Med*. 1999;26(3-4):285-294.
199. Romanova D, Vachálková A, Čipák L, Ovesná Z, Rauko P. Study of antioxidant effect of apigenin, luteolin and quercetin by DNA protective method. *Neoplasma*. 2001;48(2):104-107.
200. Ross JA, Kasum CM. Dietary flavonoids: bioavailability, metabolic effects, and safety. *Annu Rev Nutr*. 2002;22:2219-2234.
201. Horváthová K, Novotny L, Vachalkova A. The free radical scavenging activity of four flavonoids determined by the comet assay. *Neoplasma*. 2003;50(4):291-295.
202. Shimoi K, Masuda S, Furugori M, Esaki S, Kinae N. Radioprotective effect of antioxidative flavonoids in gamma-ray irradiated mice. *Carcinogenesis*. 1994;15(11):2669-2672.
203. Gendrisch F, Esser PR, Schempp CM, Wölflle U. Luteolin as a modulator of skin aging and inflammation. *Biofactors*. 2021;47(2):170-180.
204. Brown JE, Rice-Evans CA. Luteolin-rich artichoke extract protects low density lipoprotein from oxidation *in vitro*. *Free Radic Res*. 1998;29(3):247-255.
205. Wölflle U, Esser PR, Simon-Haarhaus B, Martin SF, Lademann J, Schempp CM. UVB-induced DNA damage, generation of reactive oxygen species, and inflammation are effectively attenuated by the flavonoid luteolin *in vitro* and *in vivo*. *Free Radic Biol Med*. 2011;50(9):1081-1093.
206. Ju W, Wang X, Shi H, Chen W, Belinsky SA, Lin Y. A critical role of luteolin-induced reactive oxygen species in blockage of tumor necrosis factor-activated nuclear factor- κ B pathway and sensitization of apoptosis in lung cancer cells. *Mol Pharmacol*. 2007;71(5):1381-1388.
207. Xian D, Guo M, Xu J, Yang Y, Zhao Y, Zhong J. Current evidence to support the therapeutic potential of flavonoids in oxidative stress-related dermatoses. *Redox Rep*. 2021;26(1):134-146.
208. Xagorari A, Papapetropoulos A, Mauromatis A, Economou M, Fotsis T, Roussos C. Luteolin inhibits an endotoxin-stimulated phosphorylation cascade and proinflammatory cytokine production in macrophages. *J Pharmacol Exp Ther*. 2001;296(1):181-187.
209. Kumazawa Y, Kawaguchi K, Takimoto H. Immunomodulating effects of flavonoids on acute and chronic inflammatory responses caused by tumor necrosis factor alpha. *Curr Pharm Des*. 2006;12(32):4271-4279.
210. Hayden MS, Ghosh S. Signaling to NF- κ B. *Genes Dev*. 2004;18(18):2195-2224.

211. Lim SH, Jung SK, Byun S, et al. Luteolin suppresses UVB-induced photoageing by targeting JNK1 and p90RSK2. *J Cell Mol Med*. 2013;17(5):672-680.
212. Verschooten L, Smaers K, Van Kelst S, et al. The flavonoid luteolin increases the resistance of normal, but not malignant keratinocytes, against UVB-induced apoptosis. *J Invest Dermatol*. 2010;130(9):2277-2285.
213. Szekalska M, Sosnowska K, Tomczykowa M, Winnicka K, Kasacka I, Tomczyk M. *In vivo* anti-inflammatory and anti-allergic activities of cynaroside evaluated by using hydrogel formulations. *Biomed Pharmacother*. 2020;121:109681.
214. Yi YS. Regulatory roles of flavonoids on inflammasome activation during inflammatory responses. *Mol Nutr Food Res*. 2018;62(13):1-45.
215. Casagrande F, Darbon JM. Effects of structurally related flavonoids on cell cycle progression of human melanoma cells: regulation of cyclin-dependent kinases CDK2 and CDK1. *Biochem Pharmacol*. 2001;61(10):1205-1215.
216. Jung S, Shin J, Oh J, et al. Cytotoxic and apoptotic potential of *Phyllodium elegans* extracts on human cancer cell lines. *Bioengineered*. 2019;10(1):501-512.
217. Ullah MF, Ahmad A, Khan HY, Zubair H, Sarkar FH, Hadi SM. The prooxidant action of dietary antioxidants leading to cellular DNA breakage and anticancer effects: implications for chemotherapeutic action against cancer. *Cell Biochem Biophys*. 2013;67(2):431-438.
218. Denault J-B, Salvesen G. Caspases: keys in the ignition of cell death. *Chem Rev*. 2003;34:1024489-1024500.
219. Porter AG, Jänicke RU. Emerging roles of caspase-3 in apoptosis. *Cell Death Differ*. 1999;6(2):99-104.
220. Danciu C, Zupko I, Bor A, et al. Botanical therapeutics: phytochemical screening and biological assessment of chamomile, parsley and celery extracts against A375 human melanoma and dendritic cells. *Int J Mol Sci*. 2018;19(11):1-20.
221. Guruvayoorappan C, Kuttan G. Apoptotic effect of *Biophytum sensitivum* on B16F-10 cells and its regulatory effects on nitric oxide and cytokine production on tumor-associated macrophages. *Integr Cancer Ther*. 2007;6(4):373-380.
222. Guruvayoorappan C, Girija K. *Biophytum sensitivum* (L.) DC inhibits tumor cell invasion and metastasis through a mechanism involving regulation of MMPs, prolyl hydroxylase, lysyl oxidase, nm23, ERK-1, ERK-2, STAT-1, and proinflammatory cytokine gene expression in metastatic lung tissue. *Integr Cancer Ther*. 2008;7(1):42-50.
223. Lin YL, Wang WY. Chemical constituents of *Biophytum sensitivum*. *Chinese Pharm J*. 2003;55:71-75.
224. Di Petrillo A, González-Paramás AM, Era B, et al. Tyrosinase inhibition and antioxidant properties of *Asphodelus microcarpus* extracts. *BMC Complement Altern Med*. 2016;16(1):453.
225. Rauca V-F, Vlase L, Casian T, et al. Biologically active *Ajuga* species extracts modulate supportive processes for cancer cell development. *Front Pharmacol*. 2019;10:334.
226. Chao HC, Najjaa H, Villareal MO, et al. *Arthrophytum scoparium* inhibits melanogenesis through the down-regulation of tyrosinase and melanogenic gene expressions in B16 melanoma cells. *Exp Dermatol*. 2013;22(2):131-136.
227. Said A, El-Fiky NM, Rashed K, et al. Anticancer, anti HIV-1 and antimicrobial potentials of methanol extract and non polar fractions of *Citrus volkameriana* leaves and phytochemical composition. *Res J Med Plant*. 2015;9(5):201-214.
228. Shomirzoeva O, Li J, Numonov S, et al. Chemical components of *Hyssopus seravshanicus*: antioxidant activity, activations of melanogenesis and tyrosinase, and quantitative determination by UPLC-DAD. *Nat Prod Res*. 2019;33(6):866-870.
229. Arun KP, Brindha P. Investigations into phenolic and alkaloid constituents of *Jatropha tanjorensis* by LC-MS/MS and evaluating its bioactive property. *Asian J Chem*. 2015;27(9):3249-3253.
230. Makowska-Wąs J, Galanty A, Gdula-Argasińska J, et al. Identification of predominant phytochemical compounds and cytotoxic activity of wild Olive leaves (*Olea europaea* L. ssp. *sylvestris*) harvested in South Portugal. *Chem Biodivers*. 2017;14(3):1-10.
231. Boruga M, Enatescu V, Pinzaru J, et al. Assessment of olive leaves extract - cytotoxicity *in vitro* and angiogenesis *in ovo*. *Farmacia*. 2021;69(1):38-43.
232. Jeong D, Lee J, Park SH, et al. Antiphotodaging and antimelanogenic effects of *Penthorum chinense* pursh ethanol extract due to antioxidant - and autophagy-inducing properties. *Oxid Med Cell Longev*. 2019;2019:9679731.
233. Yi J, Wang Z, Bai H, Yu X, Jing J, Zuo L. Optimization of purification, identification and evaluation of the *in vitro* antitumor activity of polyphenols from *Pinus koraiensis* pinecones. *Molecules*. 2015;20(6):10450-10467.
234. Sadhu SK, Ahmed F, Ohtsuki T, Ishibashi M. Flavonoids from *Sonneratia caseolaris*. *J Nat Med*. 2006;60(3):264-265.
235. Manzoor MF, Ahmad N, Ahmed Z, et al. Novel extraction techniques and pharmaceutical activities of luteolin and its derivatives. *J Food Biochem*. 2019;43(9):e12974.
236. Sabir F, Barani M, Rahdar A, et al. How to face skin cancer with nanomaterials: a review. *Biointerface Res Appl Chem*. 2021;11(4):11931-11955.
237. Padya BS, Pandey A, Pisay M, et al. Stimuli-responsive and cellular targeted nanoplatfoms for multimodal therapy of skin cancer. *Eur J Pharmacol*. 2021;890:173633.
238. Dasari S, Yedjou CG, Brodell RT, Cruse AR, Tchounwou PB. Therapeutic strategies and potential implications of silver nanoparticles in the management of skin cancer. *Nanotechnol Rev*. 2020;9(1):1500-1521.

239. Gupta S, Bansal R, Gupta S, Jindal N, Jindal A. Nanocarriers and nanoparticles for skin care and dermatological treatments. *Indian Dermatol Online J.* 2013;4(4):267-272.
240. Wu G, Li J, Yue J, Zhang S, Yunusi K. Liposome encapsulated luteolin showed enhanced antitumor efficacy to colorectal carcinoma. *Mol Med Rep.* 2018;17(2):2456-2464.
241. Koudelka S, Turanek Knotigova P, Masek J, et al. Liposomal delivery systems for anti-cancer analogues of vitamin E. *J Control Release.* 2015;207:59-69.
242. Dianzani C, Zara GP, Maina G, et al. Drug delivery nanoparticles in skin cancers. *BioMed Res Int.* 2014;2014:895986.
243. Tsilioni I, Taliou A, Francis K, Theoharides TC. Children with autism spectrum disorders, who improved with a luteolin-containing dietary formulation, show reduced serum levels of TNF and IL-6. *Transl Psychiatry.* 2015; 5(9):e647.
244. Karrasch T, Kim J-S, Jang BI, Jobin C. The flavonoid luteolin worsens chemical-induced colitis in NF- κ BEGFP transgenic mice through blockade of NF- κ B-dependent protective molecules. *PLOS One.* 2007;2(7):1-15.

How to cite this article: Juszcak AM, Wöelfle U, Končić MZ, Tomczyk M. Skin cancer, including related pathways and therapy and the role of luteolin derivatives as potential therapeutics. *Med Res Rev.* 2022;1-40. doi:10.1002/med.21880

Chapter 10. Declarations of the author of the doctoral dissertation

Białystok, May 10, 2022

Aleksandra Maria Juszcak

.....
Author's name (first, middle, last)

Medical University of Białystok, POLAND

.....
Employment/affiliation

Author's declaration

I hereby declare that my participation in the preparation of the publication:

1. Juszcak A.M., Zovko Končić M., Tomczyk M. Recent trends in the application of chromatographic techniques in the analysis of luteolin and its derivatives. *Biomolecules*, 2019, Vol. 9, ID 731, 38 pages. DOI: 10.3390/biom9110731

included in my doctoral dissertation consisted of the literature investigation, participation in the writing of the original manuscript, elaboration of a compilation of chromatographic techniques for the analysis of luteolin and its derivatives, elaboration of the discussion, which I define as **70 %** of participation in the preparation of the above-mentioned publication.

2. Juszcak A.M., Czarnomysy R., Strawa J.W., Zovko Končić M., Bielawski K., Tomczyk M. *In vitro* anticancer potential of *Jasione montana* and its main components against human amelanotic melanoma cells. *International Journal of Molecular Sciences*, 2021, Vol. 22, ID 3345, 25 pages. DOI: 10.3390/ijms22073345

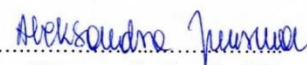
included in my doctoral dissertation consisted of the co-conceptualizing, co-preparation of research assumptions, performing biological assays in the cell culture model and analyzing and interpreting the results obtained from them, elaboration of statistical analysis, participation in the writing of the original manuscript, preparation of schemes and figures, elaboration of the discussion, which I define as **65 %** of participation in the preparation of the above-mentioned publication.

3. Juszcak A.M., Wöelfle U., Zovko Končić M., Tomczyk M. Skin cancer, including related pathways and therapy and the role of luteolin derivatives as potential therapeutics. *Medicinal Research Reviews*, 2022, 40 pages. DOI: 10.1002/med.21880

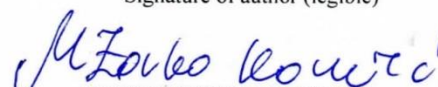
included in my doctoral dissertation consisted of the co-conceptualizing, preparation of the scheme of work, literature investigation, participation in the writing of the original manuscript, elaboration of the description of molecular pathogenetic pathways, available therapy and the part referring to the activity of luteolin and its derivatives against skin cancers, preparation of schemes and figures, elaboration of the discussion, which I define as **80 %** of participation in the preparation of the above-mentioned publication.

4. Juszcak A.M., Jakimiuk K., Czarnomysy R., Strawa J.W., Zovko Končić M., Bielawski K., Tomczyk M. The wound healing property of *Jasione montana* extracts and its main secondary metabolites. *Frontiers in Pharmacology*, 2022, Vol. 13, ID 894233, 13 pages. DOI: 10.3389/fphar.2022.894233

included in my doctoral dissertation consisted of the co-designing the concept, co-preparation of research assumptions, performing biological assays in the cell culture model and analyzing and interpreting the results obtained from them, elaboration of statistical analysis, participation in the writing of the original manuscript, preparation of schemes and figures, elaboration of the discussion, which I define as **60 %** of participation in the preparation of the above-mentioned publication.


.....
Signature of author (legible)


.....
Signature of supervisor (legible)


.....
Signature of supervisor (legible)

Chapter 11. Declarations of the co-authors of the doctoral dissertation

Białystok, May 9, 2022

Michał Tomczyk

.....
Co-author's name (first, middle, last)

Medical University of Białystok, POLAND

.....
Employment/affiliation

Co-author's declaration

I hereby declare that my participation in the preparation of the publication:

1. Juszczak A.M., Zovko Končić M., Tomczyk M. Recent trends in the application of chromatographic techniques in the analysis of luteolin and its derivatives. *Biomolecules*, 2019, Vol. 9, ID 731, 38 pages. DOI: 10.3390/biom9110731

Comprising a part of the doctoral dissertation of Ms Aleksandra Maria Juszczak, MSc, consisted in * conceptualization, methodology, formal analysis, writing – original draft preparation, writing – review and editing, supervision, project administration, corresponding author.

2. Juszczak A.M., Czarnomysy R., Strawa J.W., Zovko Končić M., Bielawski K., Tomczyk M. *In vitro* anticancer potential of *Jasione montana* and its main components against human amelanotic melanoma cells. *International Journal of Molecular Sciences*, 2021, Vol. 22, ID 3345, 25 pages. DOI: 10.3390/ijms22073345

Comprising a part of the doctoral dissertation of Ms Aleksandra Maria Juszczak, MSc, consisted in * co-conceptualizing, methodology, formal analysis, writing – original draft preparation, writing – review and editing, supervision, project administration, corresponding author.

3. Juszczak A.M., Wöelfle U., Zovko Končić M., Tomczyk M. Skin cancer, including related pathways and therapy and the role of luteolin derivatives as potential therapeutics. *Medicinal Research Reviews*, 2022, 40 pages. DOI: 10.1002/med.21880

Comprising a part of the doctoral dissertation of Ms Aleksandra Maria Juszczak, MSc, consisted in * co-conceptualization, formal analysis, writing – review and editing, supervision, project administration, corresponding author.

4. Juszczak A.M., Jakimiuk K., Czarnomysy R., Strawa J.W., Zovko Končić M., Bielawski K., Tomczyk M. Wound healing properties of *Jasione montana* extracts and their main secondary metabolites. *Frontiers in Pharmacology*, 2022, Vol. 13, ID 894233, 13 pages. DOI: 10.3389/fphar.2022.894233

Comprising a part of the doctoral dissertation of Ms Aleksandra Maria Juszczak, MSc, consisted in * co-conceptualization, formal analysis, writing – review and editing, supervision, project administration, corresponding author.

I also agree that Ms Aleksandra Maria Juszczak, MSc present the aforementioned work as part of their doctoral dissertation comprising of a series of single-subject articles published peer-reviewed scientific journal.


.....
Signature (legible)

* for co-authored works included in the publication series, it is recommended that **the co-author** declares their material (NOT percentage) work [e.g. formulation of study hypothesis, initiation of the study, specific study tasks (e.g. specific experiments, data collection and processing, statistical summaries, etc.), analysis of the results, preparation of the manuscript, etc.]. Identification of the co-author's contribution should be sufficiently precise for an accurate assessment of their participation and role in each of the listed studies.

Zagreb, May 6, 2022

Professor Marijana Zovko Končić

.....
Co-author's name (first, middle, last)

University of Zagreb, CROATIA

.....
Employment/affiliation

Co-author's declaration

I hereby declare that my participation in the preparation of the publication:

1. Juszczak A.M., Zovko Končić M., Tomczyk M. Recent trends in the application of chromatographic techniques in the analysis of luteolin and its derivatives. *Biomolecules*, 2019, Vol. 9, ID 731, 38 pages. DOI: 10.3390/biom9110731

Comprising a part of the doctoral dissertation of Ms Aleksandra Maria Juszczak, MSc, consisted in * co-designing the concept, reviewing, editing and formal analyzing the manuscript.

2. Juszczak A.M., Czarnomysy R., Strawa J.W., Zovko Končić M., Bielawski K., Tomczyk M. *In vitro* anticancer potential of *Jasione montana* and its main components against human amelanotic melanoma cells. *International Journal of Molecular Sciences*, 2021, Vol. 22, ID 3345, 25 pages. DOI: 10.3390/ijms22073345

Comprising a part of the doctoral dissertation of Ms Aleksandra Maria Juszczak, MSc, consisted in * co-conceptualizing, reviewing, editing and formal analyzing the manuscript.

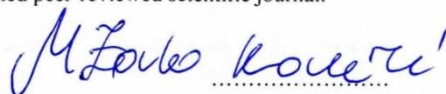
3. Juszczak A.M., Wöelfle U., Zovko Končić M., Tomczyk M. Skin cancer, including related pathways and therapy and the role of luteolin derivatives as potential therapeutics. *Medicinal Research Reviews*, 2022, 40 pages. DOI: 10.1002/med.21880

Comprising a part of the doctoral dissertation of Ms Aleksandra Maria Juszczak, MSc, consisted in * reviewing and editing the final version of manuscript.

4. Juszczak A.M., Jakimiuk K., Czarnomysy R., Strawa J.W., Zovko Končić M., Bielawski K., Tomczyk M. Wound healing properties of *Jasione montana* extracts and their main secondary metabolites. *Frontiers in Pharmacology*, 2022, Vol. 13, ID 894233, 13 pages. DOI: 10.3389/fphar.2022.894233

Comprising a part of the doctoral dissertation of Ms Aleksandra Maria Juszczak, MSc, consisted in * co-conceptualizing, reviewing, editing and formal analyzing the manuscript.

I also agree that Ms Aleksandra Maria Juszczak, MSc present the aforementioned work as part of their doctoral dissertation comprising of a series of single-subject articles published peer-reviewed scientific journal.



.....
Signature (legible)

*for co-authored works included in the publication series, it is recommended that **the co-author** declares their material (NOT percentage) work [e.g. formulation of study hypothesis, initiation of the study, specific study tasks (e.g. specific experiments, data collection and processing, statistical summaries, etc.), analysis of the results, preparation of the manuscript, etc.]. Identification of the co-author's contribution should be sufficiently precise for an accurate assessment of their participation and role in each of the listed studies.

Białystok, May 10, 2022

Professor Krzysztof Bielawski

.....
Co-author's name (first, middle, last)

Medical University of Białystok, POLAND

.....
Employment/affiliation

Co-author's declaration

I hereby declare that my participation in the preparation of the publication:

1. Juszczak A.M., Czarnomysy R., Strawa J.W., Zovko Končić M., Bielawski K., Tomczyk M. *In vitro* anticancer potential of *Jasione montana* and its main components against human amelanotic melanoma cells. *International Journal of Molecular Sciences*, 2021, Vol. 22, ID 3345, 25 pages.
DOI: 10.3390/ijms22073345

Comprising a part of the doctoral dissertation of Ms Aleksandra Maria Juszczak, MSc, consisted in * reviewing and editing the final version of manuscript.

2. Juszczak A.M., Jakimiuk K., Czarnomysy R., Strawa J.W., Zovko Končić M., Bielawski K., Tomczyk M. Wound healing properties of *Jasione montana* extracts and their main secondary metabolites. *Frontiers in Pharmacology*, 2022, Vol. 13, ID 894233, 13 pages.
DOI: 10.3389/fphar.2022.894233

Comprising a part of the doctoral dissertation of Ms Aleksandra Maria Juszczak, MSc, consisted in * reviewing and editing the final version of manuscript.

I also agree that Ms Aleksandra Maria Juszczak, MSc present the aforementioned work as part of their doctoral dissertation comprising of a series of single-subject articles published peer-reviewed scientific journal.


.....
Signature (legible)

* for co-authored works included in the publication series, it is recommended that **the co-author** declares their material (NOT percentage) work [e.g. formulation of study hypothesis, initiation of the study, specific study tasks (e.g. specific experiments, data collection and processing, statistical summaries, etc.), analysis of the results, preparation of the manuscript, etc.]. Identification of the co-author's contribution should be sufficiently precise for an accurate assessment of their participation and role in each of the listed studies.

Freiburg, April 12, 2022

Dr. Ute Wölfle

.....
Co-author's name (first, middle, last)

University of Freiburg, GERMANY

.....
Employment/affiliation

Co-author's declaration

I hereby declare that my participation in the preparation of the publication:

Juszczak A.M., Wölfle U., Zovko Končić M., Tomczyk M. Skin cancer, including related pathways and therapy and the role of luteolin derivatives as potential therapeutics. *Medicinal Research Reviews*, 2022, 40 pages.

DOI: 10.1002/med.21880

Comprising a part of the doctoral dissertation of Ms Aleksandra Maria Juszczak, MSc, consisted in * reviewing and editing the manuscript.

I also agree that Ms Aleksandra Maria Juszczak, MSc, present the aforementioned work as part of their doctoral dissertation comprising of a series of single-subject articles published peer-reviewed scientific journal.



.....
Signature (legible)

** for co-authored works included in the publication series, it is recommended that **the co-author** declares their material (NOT percentage) work [e.g. formulation of study hypothesis, initiation of the study, specific study tasks (e.g. specific experiments, data collection and processing, statistical summaries, etc.), analysis of the results, preparation of the manuscript, etc.]. Identification of the co-author's contribution should be sufficiently precise for an accurate assessment of their participation and role in each of the listed studies.*

Białystok, May 10, 2022

Robert Czarnomysy

.....
Co-author's name (first, middle, last)

Medical University of Białystok, POLAND

.....
Employment/affiliation

Co-author's declaration

I hereby declare that my participation in the preparation of the publication:

1. Juszczak A.M., Czarnomysy R., Strawa J.W., Zovko Končić M., Bielawski K., Tomczyk M. *In vitro* anticancer potential of *Jasione montana* and its main components against human amelanotic melanoma cells. *International Journal of Molecular Sciences*, 2021, Vol. 22, ID 3345, 25 pages.
DOI: 10.3390/ijms22073345

Comprising a part of the doctoral dissertation of Ms Aleksandra Maria Juszczak, MSc, consisted in * designing and co-preparing of *in vitro* assays on the melanoma cell line.

2. Juszczak A.M., Jakimiuk K., Czarnomysy R., Strawa J.W., Zovko Končić M., Bielawski K., Tomczyk M. Wound healing properties of *Jasione montana* extracts and their main secondary metabolites. *Frontiers in Pharmacology*, 2022, Vol. 13, ID 894233, 13 pages.
DOI: 10.3389/fphar.2022.894233

Comprising a part of the doctoral dissertation of Ms Aleksandra Maria Juszczak, MSc, consisted in * co-designing and co-preparing of *in vitro* assays on the fibroblast cell line.

I also agree that Ms Aleksandra Maria Juszczak, MSc present the aforementioned work as part of their doctoral dissertation comprising of a series of single-subject articles published peer-reviewed scientific journal.


.....
Signature (legible)

* for co-authored works included in the publication series, it is recommended that **the co-author** declares their material (NOT percentage) work [e.g. formulation of study hypothesis, initiation of the study, specific study tasks (e.g. specific experiments, data collection and processing, statistical summaries, etc.), analysis of the results, preparation of the manuscript, etc.]. Identification of the co-author's contribution should be sufficiently precise for an accurate assessment of their participation and role in each of the listed studies.

Białystok, May 10, 2022

Katarzyna Jakimiuk

.....
Co-author's name (first, middle, last)

Medical University of Białystok, POLAND

.....
Employment/affiliation

Co-author's declaration

I hereby declare that my participation in the preparation of the publication:

Juszczak A.M., Jakimiuk K., Czarnomysy R., Strawa J.W., Zovko Končić M., Bielawski K., Tomczyk M. Wound healing properties of *Jasione montana* extracts and their main secondary metabolites. *Frontiers in Pharmacology*, 2022, Vol. 13, ID 894233, 13 pages.
DOI: 10.3389/fphar.2022.894233

Comprising a part of the doctoral dissertation of Ms Aleksandra Maria Juszczak, MSc, consisted in * co-conducting studies on antioxidant and anti-enzymatic activities of extracts and isolated compounds and co-preparing the original manuscript.

I also agree that Ms Aleksandra Maria Juszczak, MSc present the aforementioned work as part of their doctoral dissertation comprising of a series of single-subject articles published peer-reviewed scientific journal.

Katarzyna Jakimiuk

.....
Signature (legible)

** for co-authored works included in the publication series, it is recommended that **the co-author** declares their material (NOT percentage) work [e.g. formulation of study hypothesis, initiation of the study, specific study tasks (e.g. specific experiments, data collection and processing, statistical summaries, etc.), analysis of the results, preparation of the manuscript, etc.]. Identification of the co-author's contribution should be sufficiently precise for an accurate assessment of their participation and role in each of the listed studies.*

Białystok, May 10, 2022

Jakub Władysław Strawa

.....
Co-author's name (first, middle, last)

Medical University of Białystok, POLAND

.....
Employment/affiliation

Co-author's declaration

I hereby declare that my participation in the preparation of the publication:

1. Juszczak A.M., Czarnomysy R., Strawa J.W., Zovko Končić M., Bielawski K., Tomczyk M. *In vitro* anticancer potential of *Jasione montana* and its main components against human amelanotic melanoma cells. *International Journal of Molecular Sciences*, 2021, Vol. 22, ID 3345, 25 pages.
DOI: 10.3390/ijms22073345

Comprising a part of the doctoral dissertation of Ms Aleksandra Maria Juszczak, MSc, consisted in * preparation of chromatographic analysis of obtained extracts and isolated compounds and co-writing of the original manuscript.

2. Juszczak A.M., Jakimiuk K., Czarnomysy R., Strawa J.W., Zovko Končić M., Bielawski K., Tomczyk M. Wound healing properties of *Jasione montana* extracts and their main secondary metabolites. *Frontiers in Pharmacology*, 2022, Vol. 13, ID 894233, 13 pages.
DOI: 10.3389/fphar.2022.894233

Comprising a part of the doctoral dissertation of Ms Aleksandra Maria Juszczak, MSc, consisted in * co-preparation of chromatographic analysis of obtained extracts and isolated compounds and co-writing of the original manuscript.

I also agree that Ms Aleksandra Maria Juszczak, MSc present the aforementioned work as part of their doctoral dissertation comprising of a series of single-subject articles published peer-reviewed scientific journal.

Strawa Jakub.....
Signature (legible)

* for co-authored works included in the publication series, it is recommended that **the co-author** declares their material (NOT percentage) work [e.g. formulation of study hypothesis, initiation of the study, specific study tasks (e.g. specific experiments, data collection and processing, statistical summaries, etc.), analysis of the results, preparation of the manuscript, etc.]. Identification of the co-author's contribution should be sufficiently precise for an accurate assessment of their participation and role in each of the listed studies.

Chapter 12. List of scientific accomplishments

List of publications comprising the doctoral dissertation:

1. **Juszczak A.M.**, Czarnomysy R., Strawa J.W., Zovko Končić M., Bielawski K., Tomczyk M.: *In vitro* anticancer potential of *Jasione montana* and its main components against human amelanotic melanoma cells. *International Journal of Molecular Sciences* Vol. 22, ID 3345, 2021, 25 pages.
DOI: 10.3390/ijms22073345
IF₂₀₂₀ = 5.923, MES score = 140
2. **Juszczak A.M.**, Jakimiuk K., Czarnomysy R., Strawa J.W., Zovko Končić M., Bielawski K., Tomczyk M.: Wound healing properties of *Jasione montana* extracts and their main secondary metabolites. *Frontiers in Pharmacology* Vol. 13, ID 894233, 2022, 13 pages.
DOI: 10.3389/fphar.2022.894233
IF₂₀₂₀ = 5.810, MES score = 100
3. **Juszczak A.M.**, Zovko Končić M., Tomczyk M.: Recent trends in the application of chromatographic techniques in the analysis of luteolin and its derivatives. *Biomolecules* Vol. 9, ID 731, 2019, 38 pages.
DOI: 10.3390/biom9110731
IF₂₀₁₉ = 4.879, MES score = 100
4. **Juszczak A.M.**, Woelfle U., Zovko Končić M., Tomczyk M.: Skin cancer, including related pathways and therapy and the role of luteolin derivatives as potential therapeutics. *Medicinal Research Reviews* 2022, 40 pages.
DOI: 10.1002/med.21880
IF₂₀₂₀ = 12.944, MES score = 140

List of other scientific publications:

1. Augustynowicz D., Jakimiuk K., Uysal S., Strawa J.W., **Juszczak A.M.**, Zengin G., Tomczyk M.: LC-ESI-MS profiling of *Potentilla norvegica* and evaluation of its biological activities. *South African Journal of Botany* Vol. 142, 259-265, 2021, 7 pages.
DOI: 10.1016/j.sajb.2021.06.042
IF₂₀₂₀ = 2.315, MEiN = 100
2. Sarikurkcü C., Locatelli M., Tartaglia A., Ferrone V., **Juszczak A.M.**, Ozer M.S., Tepe B., Tomczyk M.: Enzyme inhibition and antioxidant activity of the water extracts from the plants *Aesculus hippocastanum*, *Olea europaea* and *Hypericum perforatum* that are used as folk remedies in Turkey. *Molecules* Vol. 25, ID 1202, 2020, 14 pages.
DOI: 10.3390/molecules25051202
IF₂₀₁₉ = 4.412, MEiN = 140

Summary Impact Factor (IF) = **36.283**
Summary number of MES scores = **720 points**
h-index (Web of Science/SCOPUS) = **2/3**

List of conference communications:

1. **Juszczak A.M.**, Jakupović L., Marijan M., Zovko Končić M., Tomczyk M.: Assessment of anti-ageing activity of glycerol extracts from *Jasione montana* L. 1st Joint meeting on Natural Products Pharmacology SIF - SIPHAR - IMGNPP, Naples, Italy, February 24-26, 2022.
2. **Juszczak A.M.**, Czarnomysy R., Strawa J.W., Zovko Končić M., Bielawski K., Tomczyk M.: Apoptosis induction in C32 human melanoma cells by *Jasione montana* and its main phytoconstituents. GA - 69th Annual Meeting 2021, Virtual Conference, Bonn, Germany, September 5-8, 2021, Book of Abstracts p. 133, doi:10.1055/s-0041-1736896.

3. **Juszczak A.M.**, Czarnomysy R., Strawa J.W., Zovko Končić M., Bielawski K., Tomczyk M.: *In vitro* evaluation of *Jasione montana* and its main flavonoids on human melanoma cells. PSE e-Congress "Plant Derived Natural Products as Pharmacological and Nutraceutical Tools", Chieti-Pescara, Italy, September 15-25, October 6-16, 2020, Book of Abstracts p. 82.
4. Augustynowicz D., Uysal S., Zengin G., Jakimiuk K., Strawa J.W., **Juszczak A.M.**, Tomczyk M.: LC-MS determination of marker metabolites and biological activities of *Potentilla norvegica*. PSE e-Congress "Plant Derived Natural Products as Pharmacological and Nutraceutical Tools", Chieti-Pescara, Italy, September 15-25, October 6-16, 2020, Book of Abstracts p. 83.
5. **Juszczak A.M.**, Czarnomysy R., Strawa J.W., Zovko Končić M., Bielawski K., Tomczyk M.: LC-MS characterization and cytotoxic activities of selected extracts and their main compounds from *Jasione montana*. T20 PSE Conference Liverpool 2020 on "Contemporary Natural Products Discovery Research", Liverpool, United Kingdom, 6 March, 2020.

List of other scientific accomplishments:

Scientific internships:

1. "Extraction according to green chemistry principles, extraction optimization and techniques for evaluation of antioxidant, anti-tyrosinase and anti-inflammatory potential in an *in vitro* model of glycerol plant extracts" under the supervision of Prof. Marijana Zovko Končić in the Department of Pharmacognosy, Faculty of Pharmacy and Biochemistry, University of Zagreb, 20 September – 17 October, 2021.
2. "Techniques for evaluation of anti-inflammatory activity and cytotoxicity of plant extracts and compounds" under the supervision of Prof. Sebastian Granica in the Center for Preclinical Studies, Microbiota Lab, Department of Pharmacognosy and Molecular Basis of Phytotherapy, Faculty of Pharmacy, Medical University of Warsaw, 14 November – 4 December, 2020.
3. "Organic synthesis, purification and characterization of compounds with antimalarial activity" under the supervision of Prof. Zrinka Rajić in the Department of Medicinal Chemistry, Faculty of Pharmacy and Biochemistry, University of Zagreb, 4 April – 9 July, 2018.

Scientific projects/grants:

1. Principal investigator of the scientific project no. SUB/2/DN/22/004/2212 „Optimization of the extraction process and evaluation of the anti-aging activity of *Jasione montana* L.” (in Polish „Optymalizacja procesu ekstrakcji oraz ocena aktywności przeciwstarzeniowej *Jasione montana* L.”) for the year 2022.
2. Principal investigator of the scientific grant for International Doctoral Studies in Medical and Pharmaceutical Sciences no. 02/IMSD/G/2021 „Optimization of the extraction process and evaluation of the anti-aging activity of *Jasione montana* L.” (in Polish „Optymalizacja procesu ekstrakcji oraz ocena aktywności przeciwstarzeniowej *Jasione montana* L.”) for the years 2021/2022.
3. Principal investigator of the scientific project no. SUB/2/DN/21/004/2212 „Assessment of the chemical composition and biological activity of selected extracts and isolated compounds from the aerial parts of *Jasione montana* L.” (in Polish „Ocena składu chemicznego oraz aktywności biologicznej wybranych ekstraktów oraz wyizolowanych związków z nadziemnych części *Jasione montana* L.”) for the year 2021.
4. Principal investigator of the scientific project no. SUB/2/DN/20/003/2212 „Assessment of the phytochemical profile and biological activity of selected extracts and flavonoid compounds from the *Jasione montana* herb” (in Polish „Ocena profilu fitochemicznego

- oraz aktywności biologicznej wybranych ekstraktów i związków flawonoidowych z ziela *Jasione montana*") for the year 2020.
5. Principal investigator of the scientific project no. SUB/2/DN/19/002/2212 „Assessment of cytotoxic activity of selected extracts and compounds from *Jasione montana* L.” (in Polish „Ocena aktywności cytotoksycznej wybranych ekstraktów i związków z *Jasione montana* L.”) for the year 2019.
 6. Principal investigator of the scientific grant for International Doctoral Studies in Medical and Pharmaceutical Sciences no. 05/IMSD/G/2019 „Assessment of the phytochemical profile and cytotoxic activity of selected extracts and isolated compounds from the aerial parts of *Jasione montana* L. (Campanulaceae)” (in Polish „Ocena profilu fitochemicznego oraz aktywności cytotoksycznej wybranych ekstraktów i związków wyizolowanych z części nadziemnych *Jasione montana* L. (Campanulaceae)”) for the years 2019/2021.

The didactics activity:

1. Auxiliary superintendence of students as part of the master's theses in the field of pharmacy studies of the Medical University of Białystok in the academic years 2019–2020, and 2020–2021.
2. Co-conducting practical classes in the subject of *Natural cosmetic products* (in Polish *Naturalne produkty kosmetyczne*) in the field of cosmetology studies of the Medical University of Białystok in the academic years 2019–2020, 2020–2021, and 2021–2022.